

Adsorption of 3,7-dimethyl-1-octanol in single and binary mixtures using Selexsorb CD[®]

by

Anke Louw

Thesis presented in partial fulfilment
of the requirements for the Degree

of

MASTER OF ENGINEERING
(CHEMICAL ENGINEERING)

in the Faculty of Engineering

at Stellenbosch University

Supervisor

(Professor C.E. Schwarz)

March 2023

DECLARATION

By submitting this thesis electronically, I declare that the entirety of the work contained therein is my own, original work, that I am the sole author thereof (save to the extent explicitly otherwise stated), that reproduction and publication thereof by Stellenbosch University will not infringe any third party rights and that I have not previously in its entirety or in part submitted it for obtaining any qualification.

Date: March 2023

Copyright © 2023 Stellenbosch University

All rights reserved

ABSTRACT

The petrochemical industry is considered to be one of the large contributors to the global economy. The hydrocarbons produced by it are readily used as fuels. The product streams engendered by hydrocarbon production can contain low concentrations of by-products such as alcohols, which have inherent industrial value.

Adsorption is a favoured method of separating 1-alcohols from an n-decane stream, as it is the most versatile, economic, and environmentally friendly among separation methods. It is a three-step process consisting of an external mass transfer, an internal mass transfer and adsorption onto active sites. The process typically occurs by means of physisorption or chemisorption. The aim of this study is to expand the limited 1-alcohol adsorption database by investigating the adsorption of 3,7-dimethyl-1-octanol (3,7-DMO), 1-octanol&3,7-DMO and 1-decanol&3,7-DMO from n-decane while using Selexsorb CD® (SCD). The project scope includes the investigation of these systems at different temperatures and initial concentrations and adsorbate ratios for the binary component systems through experimental work and kinetic and equilibrium modelling.

The experimental work was conducted using a bench-scale water bath batch-adsorption system. Mesh baskets were filled with 10 g adsorbent and fully submerged in beakers containing a solution of 0.5-3.3 alcohol and the remainder n-decane. Kinetic and equilibrium studies were conducted along with displacement tests for the two binary systems. Kinetic and equilibrium isotherm models were fitted to the datasets by using nonlinear regression.

Certain project shortcomings were identified when it was consistently seen that the kinetic data generated for 3,7-DMO, 1-decanol&3,7-DMO and 1-octanol&3,7-DMO adsorption onto SCD was accompanied by a drop in adsorbate loading from 7 h to 24 h. The major project shortcoming was the primary batch experimental setup which had beakers open to atmosphere that facilitated evaporation of the water in the water bath and subsequent condensation of said water vapour dripping into the solution. Additionally, solution evaporation also took place which meant that the assumption of constant volume of solution throughout the 24 h experiment was incorrect. A secondary batch experimental setup, where the feed stock was submerged in a sealed Schott bottle, minimised the potential of evaporation or condensate droplets forming in the solution and the kinetic profiles generated at 45 °C approached equilibrium with no drop in adsorbate loading between 7 to 24 h.

For the adsorption of 3,7-dimethyl-1-octanol, it was found that an increase in initial concentration increased the equilibrium adsorbent loading achieved but that it plateaued beyond 1.5 mass%. An increase in temperature increased the adsorbent loading achievable for the first 7 h.

The maximum adsorbate loading achievable for 3,7-DMO onto SCD was found to be approximately 114 mg.g⁻¹. The pseudo-second-order model ($R^2 = 0.98$) was the best fitting kinetic model and the Langmuir and Redlich-Peterson equilibrium isotherm models ($R^2 = 0.9$) fitted the single equilibrium data best.

In the case of the two binary component systems, it was found that temperature had no discernible effect on the adsorbent loading. An increase in overall initial concentration increased the adsorbent loading for the first 7 h, but the equilibrium adsorbent loading appeared to fluctuate with no discernible trend.

The binary component systems both indicated that the Elovich model fitted the data well at 25 °C and the pseudo-second-order model fitted best at 45 °C. The rate constant and maximum loading were higher at 45 °C as compared to 25 °C. The binary component isotherm models that fit the two binary component systems best were the extended Freundlich and modified competitive Langmuir model indicating that both systems were heterogeneous in nature and interaction does occur between adsorbate molecules. could not predict the binary component adsorbate loadings as accurately as the single component models.

Displacement tests showed that linear, smaller molecules are preferentially adsorbed when compared to branched, larger molecules. The displacement potential ranked from largest to smallest was 1-octanol, 1-decanol and 3,7-DMO.

Recommendations for future studies include quantifying through experimental work some thermodynamic properties such Gibbs free energy and entropy of adsorption. All future batch adsorption tests are recommended to be performed on experimental setups that seal the adsorption system and prevents water ingress or solution evaporation. Lastly, semi-continuous experiments can be performed to obtain 3,7-DMO adsorption data when the solution is allowed to flow through a packed bed rather than stirred.

OPSOMMING

Die petrochemiese industrie word beskou as een van die grootste bydraers tot die globale ekonomie. Die koolwaterstof geproduseer word gereedelik gebruik as brandstowwe. Die produkstrome wat volg uit koolwaterstofproduksie kan lae konsentrasies byprodukte bevat, soos alkohole wat inherente industriële waarde het.

Adsorpsie is 'n gunsteling skeidingsmetode van oksigeneerde byprodukte uit 'n paraffienstroom omdat dit baie veelsydig, ekonomies, en omgewingsvriendelik is. Dit is 'n drie-stap-proses wat bestaan uit eksterne massa-oordrag, interne massa-oordrag en poriediffusie. Die proses neem tipies plaas via fisisorpsie of chemisorpsie. Die doel van hierdie studie is om die beperkte 1-alkohol-adsorpsiedatabasis te vergroot deur die adsorpsie van 3,7-dimetiel-1-octanol, 1-oktanol & 3,7-dimetiel-1-oktanol en 1-dekanol & 3,7-dimetiel-1-oktanol van n-dekaan te ondersoek deur Selexsorb CD[®] te gebruik. Die projekbestek sluit in die ondersoek van hierdie sisteme by verskillende temperature en aanvanklike konsentrasies en adsorbaatverhoudings vir die binêre komponentsisteme deur eksperimentele werk en kinetiese en ekwilibriummodellering.

Die eksperimentele werk is uitgevoer deur 'n banktoetskaal, waterbad, lot adsorpsiesisteam te gebruik. Maasmandjies is gevul met 10 g adsorbeermiddel en heeltemal onderdompel in die bekere wat 'n oplossing van 0.5 – 3.3 massa% alkohol en die res n-dekaan bevat. Kinetiese en ekwilibriumstudies is uitgevoer saam met verplasingtoetse vir die twee binêre sisteme. Kinetiese en ekwilibrium isotermiese modelle is gepas op die datastelle deur nie-liniêre regressie.

Sekere tekortkominge in die projek is geïdentifiseer toe dit konsekwent gesien is dat die kinetiese data wat gegenereer is vir 3,7-DMO, 1-dekanol&3,7-DMO en 1-oktanol&3,7-DMO adsorpsie op SCD, gepaard gegaan het met 'n daling in die adsorbaat lading vanaf 7 uur tot 24 uur. Die grootste tekortkoming van die projek was die primêre lot eksperimentele opset wat bekere oop aan die atmosfeer gehad het, wat verdamping van die water in die waterbad moontlik gemaak het en gevolglike kondensasie van die genoemde waterdamp wat in die oplossing gedrup het. Daarbenewens het oplossing verdamping ook plaasgevind, wat beteken dat die aanname van 'n konstante volume oplossing gedurende die 24 uur eksperiment onjuis was. 'n Sekondêre lot eksperimentele opset, waar die toevoer in 'n verseëlde Schott-bottel ondergedompel was, het die potensiaal van verdamping of kondensaatdruppels wat in die oplossing vorm, geminimaliseer en die kinetiese profiele wat by 45 °C gegenereer is, het die ewewig benader sonder dat daar 'n daling in adsorbaat lading tussen 7 en 24 uur was.

Vir die adsorpsie van 3,7-dimetiel-1-oktanol, is dit gevind dat 'n verhoging in aanvanklike konsentrasie die ekwilibrium adsorbeermiddellading bereik, verhoog het, maar afgeplat het bo 1.5 massa%. 'n Verhoging in temperatuur het die adsorbeermiddellading wat bereik kan word vir die eerste sewe ure verhoog.

Die maksimum adsorpsielading bereikbaar vir 3,7-dimetiel-1-oktanol op Selexsorb CD[®] was ongeveer 114 mg.g⁻¹. Die pseudo-2^{de}-orde model ($R^2=0.98$) en die Langmuir en Redlich-Peterson-ekwilibrium isotermiese modelle ($R^2=0.9$) het die enkel komponent adsorpsiesisteam die beste gepas.

Vir die twee binêre komponentsisteme is dit gevind dat temperature geen waarneembare effek op die adsorbeermiddellading gehad het nie. 'n Verhoging in algehele aanvanklike konsentrasie het die adsorbeermiddellading verhoog vir die eerste sewe ure maar dit het voorgekom asof die ewilibrum adsorbeermiddellading varieer het sonder 'n waarneembare tendens .

Die binêre komponentsisteme het beide aangedui dat die Elovich-model die data goed pas by 25 °C en die pseudo 2de-orde model die beste by 45 °C pas. Die tempokonstante en maksimum lading was hoër by 45 °C in vergelyking met 25 °C. Die binêre komponent isotermitesse modelle wat die twee binêre komponent stelsels die beste pas, was die uitgebreide Freundlich en gewysigde kompeterende Langmuir-modelle, wat aandui dat beide stelsels heterogeen van aard is en dat daar interaksie tussen adsorbaat molekules plaasvind.

Die verplasingtoetse het gewys dat liniêre, kleiner molekules voorkeurig geadsorbeer het in vergelyking met vertakte, groter molekules. Die verplasingpotensiaal van grootste tot kleinste gerangskik was 1-oktanol, 1-dekanol en 3,7-dimetiel-1-oktanol.

Aanbevelings vir toekomstige studies sluit kwantifisering deur middel van eksperimentele werk van sommige termodinamiese eienskappe soos Gibbs vrye energie en entropie van adsorpsie in. Daar word aanbeveel dat alle toekomstige lot-adsorpsietoetse uitgevoer word op eksperimentele opsetstukke wat die adsorpsiestelsel seël en waterinvoer of oplossingsverdamping voorkom. Laastens kan semi-deurlopende eksperimente uitgevoer word om 3,7-DMO adsorpsiedata te verkry wanneer die oplossing toegelaat word om deur 'n gepakte bed te vloei eerder as omgeroer te word.

TABLE OF CONTENTS

CHAPTER 1	INTRODUCTION.....	1
1.1	BACKGROUND	1
1.2	PROBLEM STATEMENT DEVELOPMENT	2
1.3	AIMS AND OBJECTIVES	6
1.4	PROJECT SCOPE.....	7
1.5	THESIS OUTLINE	8
CHAPTER 2	LITERATURE REVIEW	10
2.1	ADSORPTION FUNDAMENTALS.....	10
2.1.1	Adsorption mechanism.....	10
2.1.2	Physisorption	12
2.1.3	Chemisorption	13
2.1.4	Parameters affecting adsorption.....	14
2.2	ADSORBENTS.....	14
2.2.1	Physiochemical properties	15
2.2.2	Variations of activated alumina.....	18
2.2.3	Adsorbent selection.....	21
2.3	ADSORBATE	22
2.3.1	Molecular properties of adsorbate	22
2.3.2	Linear versus branched molecules	23
2.3.3	Adsorbate selection.....	24
2.4	MULTICOMPONENT ADSORBATE SYSTEM.....	25
2.4.1	Multicomponent adsorptive mechanisms.....	26
2.4.2	Displacement effects	27
2.4.3	Interaction effects	28
2.5	EFFECTS OF TEMPERATURE ON ADSORPTION	28
2.6	ADSORPTION QUANTIFICATION.....	29
2.6.1	Equilibrium versus maximum capacity.....	30
2.7	ADSORPTION KINETIC MODELS.....	31
2.7.1	Pseudo-first-order	32

2.7.2	Pseudo-second order.....	32
2.7.3	Elovich.....	32
2.7.4	Weber and Morris	33
2.8	ADSORPTION EQUILIBRIUM ISOTHERM MODELS	34
2.8.1	Single-component equilibrium isotherm models.....	36
2.8.2	Binary-component equilibrium-isotherm models.....	38
2.9	MODEL FITTING	41
2.10	CHAPTER SUMMARY	43
CHAPTER 3	EXPERIMENTAL DESIGN AND METHODOLOGY.....	45
3.1	CHAPTER OVERVIEW	45
3.2	SELECTION OF EXPERIMENTAL PARAMETER RANGE	45
3.2.1	Temperature.....	45
3.2.2	Initial adsorbate concentration	46
3.2.3	Mixing speed	47
3.3	EXPERIMENTAL SETUP	47
3.4	EXPERIMENTAL PLAN	48
3.5	MATERIALS	50
3.6	METHODOLOGY.....	50
3.6.1	Phases 1 & 2	50
3.6.2	Phase 3	51
3.6.3	GC sample preparation & analysis.....	52
3.7	VALIDATION OF EXPERIMENTAL PROCEDURES.....	52
3.8	SECONDARY BATCH ADSORPTION EXPERIMENTAL SETUP.....	54
3.8.1	Repeatability.....	57
3.9	CHAPTER OUTCOME	57
CHAPTER 4	EVALUATION OF PROJECT SHORTCOMINGS	59
4.1	CHAPTER OVERVIEW	59
4.2	COMPARISON OF PRIMARY BAES AND SECONDARY BAES.....	59
4.2.1	Binary system comparison at different temperatures	59

4.2.2	Comparison of results achieved using Primary versus Secondary BAES 45 °C for single component and binary systems	62
4.2.3	Volume Assumption	64
4.2.4	Presence of water.....	67
4.3	CHAPTER OUTCOME.....	69
CHAPTER 5	SINGLE COMPONENT ADSORPTION	70
5.1	EFFECT OF TEMPERATURE.....	70
5.2	EFFECT OF INITIAL ADSORBATE CONCENTRATION.....	73
5.2.1	Effect of initial concentration at 25 °C	73
5.2.2	Effect of initial concentration at 35 °C	75
5.2.3	Effect of initial concentration at 45 °C	77
5.2.4	Summary of the effect of initial concentration	78
5.3	SINGLE-COMPONENT MODELLING	80
5.3.1	Single Kinetic Models.....	80
5.3.2	Single Isotherm Models.....	85
5.4	CHAPTER OUTCOMES	88
CHAPTER 6	BINARY COMPONENT ADSORPTION.....	90
6.1	EFFECT OF TEMPERATURE	90
6.1.1	1-decanol&3,7-DMO.....	91
6.1.2	1-octanol&3,7-DMO	92
6.2	EFFECT OF COMPOSITION	93
6.2.1	Overall initial concentration.....	93
6.2.2	Adsorbate ratio.....	100
6.3	BINARY COMPONENT MODELLING	101
6.3.1	Binary Kinetic Modelling.....	102
6.3.2	Binary Isotherm Modelling.....	106
6.4	CHAPTER OUTCOMES	111
CHAPTER 7	EVALUATION OF DISPLACEMENT POTENTIAL	112
7.1	1-OCTANOL&1-DECANOL.....	113
7.2	1-OCTANOL&3,7-DMO	115
7.3	1-DECANOL&3,7-DMO	116

7.4	CHAPTER OUTCOMES	117
CHAPTER 8 CONCLUSION AND RECOMMENDATIONS		118
8.1	3,7-DMO ADSORPTION FROM N-DECANE SOLUTION ON SCD	118
8.2	1-OCTANOL&3,7-DMO AND 1-DECANOL&3,7-DMO ADSORPTION FROM N-DECANE SOLUTION ON SCD.....	118
8.3	RECOMMENDATIONS	120
REFERENCES 121		
	Appendix A Methodology.....	130
	Appendix B Processed and Raw data	152
	Appendix C Additional Graphical Experimental results.....	181
	Appendix D Additional kinetic modelling results	195

NOMENCLATURE LIST

Symbols		
a_{ij}	competition coefficient for extended Freundlich isotherm model	Dimensionless
a_{RP}	Redlich-Peterson isotherm model constant	$\text{ml}\cdot\text{mg}^{-1}$
b_{ij}	adsorption constants of extended Freundlich isotherm model	Dimensionless
C	Weber & Morris model parameter	$\text{mg}\cdot\text{g}^{-1}$
C_{BET}	energy of surface interaction constant	$\text{L}\cdot\text{mg}^{-1}$
C_e	equilibrium concentration	$\text{mg}\cdot\text{l}^{-1}$
C_s	adsorbate monolayer saturation concentration	$\text{mg}\cdot\text{l}^{-1}$
g	Redlich-Peterson isotherm exponent	Dimensionless
k_1	pseudo-first-order rate constant	min^{-1}
k_2	pseudo-second order rate constant	min^{-1}
k_{ip}	Weber & Morris model rate constant	$\text{mg}\cdot\text{g}^{-1}\text{min}^{-1/2}$
K_f	Freundlich isotherm constant	$(\text{mg}\cdot\text{g}^{-1})\cdot(\text{ml}\cdot\text{mg}^{-1})^{-1/n}$
K_L	Langmuir isotherm constant	$\text{ml}\cdot\text{mg}^{-1}$
K_s	Sips equilibrium isotherm constant	$(\text{mg}\cdot\text{ml}^{-1})^{-1/m}$
k_{rp}	Redlich-Peterson isotherm constant	$\text{ml}\cdot\text{g}^{-1}$
m	Sips isotherm constant	Dimensionless
N	constant related to adsorbent-adsorbate system	Dimensionless

n	Freundlich constant related to non-competitive heterogeneity	Dimensionless
q	mass adsorbate loaded on adsorbent	mg.g ⁻¹
q_{calc}	calculated mass of adsorbate loaded on adsorbent	mg.g ⁻¹
q_e	equilibrium adsorption loading: mass of adsorbate (mg) adsorbed per mass of adsorbent (g).	mg.g ⁻¹
q_{e,meas}	experimentally determined equilibrium adsorption loading	mg.g ⁻¹
q_t	mass of adsorbate loaded on adsorbent at any time during the experiment	mg.g ⁻¹
Q_i	equilibrium adsorbate loading of component i when present in a single component system	mg.g ⁻¹
q_m	maximum adsorption capacity	mg.g ⁻¹
q_{m,i}	maximum adsorption capacity for single component in a binary mixture	mg.g ⁻¹
Q_m	equilibrium adsorbate loading of component i when present in a multicomponent system	mg.g ⁻¹
q_s	theoretical isotherm saturation capacity	mg.g ⁻¹
R	universal gas constant	8.314 J.mol ⁻¹ K ⁻¹
R²	coefficient of determination	Dimensionless
R²_{adj}	adjusted coefficient of determination	Dimensionless
R_{binary}	ratio of %removal of component A to %removal of component B	mass%.mass% ⁻¹
R_L	dimensionless Langmuir constant	Dimensionless
SD	standard deviation	expressed in same units as original value

S_n	standard error	Dimensionless
t	time	min
T	absolute adsorbate temperature	K
v	volume	ml
w	mass	g

Greek Symbols

α	Elovich model initial adsorption rate	mg.g ⁻¹ min ⁻¹
β	Elovich model parameter	g.mg ⁻¹
η	interaction factor	Dimensionless
ρ	density	kg.m ⁻³

Subscripts and superscripts

e	At equilibrium	-
compA	adsorbate A in a binary mixture	-
compB	adsorbate B in a binary mixture	-
e	equilibrium conditions	-
t	at any time (t) during the experimental run	-
m	maximum conditions (e.g. capacity)	-
o	at initial time/start of experiment	-

Acronyms

AA	activated alumina	-
ARE	average relative error	-

BAES	batch-adsorption experimental setup	-
BET	Brunauer-Emmett-Teller	-
DMO	dimethyl-1-octanol	-
DOM	dissolved organic matter	-
EABS	sum of absolute errors	-
EDX	energy-dispersive X-ray	-
EMT	external mass transfer	-
FTIR	Fourier transform infrared	-
GC	gas chromatography	-
GC-MS	gas chromatography mass spectrometry	-
HYBRID	hybrid fractional error function	-
IPD	intraparticle diffusion	-
LM	Langmuir model	-
MET	MacMillan-Teller	-
MOF	metal organic frameworks	-
MPSD	Marquardt's percent standard deviation	-
OMP	organic micro-pollutants	-
PSD	pore size distribution	-
RMSE	root mean square error	-
SCD	Selexsorb CD [®]	-
SCDx	Selexsorb CDx [®]	-

SEM	scanning electron microscope	-
SNE	sum of normalised errors	-
SSA	specific surface area	-
WMM	Weber & Morris Model	-
XRD	X-Ray Diffraction	-

Chapter 1 Introduction

1.1 Background

The petrochemical industry contributes greatly to economic growth (Bondarenko *et al.*, 2020). It is responsible for the production of basic chemicals and plastics that are key elements in the manufacture of a variety of consumer goods (Abdullahi and Galadima, 2014). Both hydrocarbons and various alcohols form part of these basic chemicals. Hydrocarbons are compounds that contain a mixture of hydrogen and carbon atoms and are readily used as fuels. The type of fuel is dependent on the carbon chain length: liquefied petroleum gas (C₃₋₄), gasoline (C₅₋₁₂), diesel fuel (C₁₃₋₂₂) and light waxes (C₂₃₋₃₃) (Li *et al.*, 2014). During the production of these hydrocarbons, it is possible to obtain by-products such as alcohols in the product stream.

According to Li *et al.* (2014), primary alcohols that contain more than six carbon atoms (such as 1-decanol, 1-octanol and 3,7-DMO) have many industrial applications. These include synthesising surfactants, washing agents and plasticizers (Li *et al.*, 2014). Derivatives of long chain alcohols can be used in the agricultural, papermaking, food processing and pharmaceuticals industry and in the manufacturing of construction materials and machinery (Li *et al.*, 2014). In the case of surfactants, the process involves passing petrochemical feedstock through different processes. The feedstock (containing alcohols) can be processed or reacted through alkylation or ethoxylation to produce surfactants (Li *et al.*, 2014). Alkylation is the mechanism involved in reacting primary alcohols with alkyl halides. This alkylation reaction takes place by means of a chemical catalyst under specific system temperatures and pressures. Often, this reaction fails to reach 100% conversion, which engenders residual alcohols in the intermediate alkane stream. These residual alcohols may pose problems downstream and should thus be removed (Li *et al.*, 2014). The alkylation reaction can fail to reach 100% conversion for several reasons: inadequate mixing, side reactions, the reaction reaches equilibrium (forward and reverse reaction rate is equal) or the operating conditions are not optimal (Hu *et al.*, 2015).

Different techniques have been employed to separate alcohols and alkanes, including supercritical fluid extraction (Bonthuys *et al.*, 2011), extraction combined with azeotropic distillation (Li *et al.*, 2014) and complex fluid fractionation (Zamudio, 2014). These methods possess significant advantages such as high recovery rates and product purity. However, a considerable number of them are not viable for use in industry, either for economic reasons or process complexities or with a view to capacity limitations (Li *et al.*, 2014).

Traditional chemical engineering methods of separation (that are more suitable for industry) include distillation, adsorption, membrane processes, absorption, stripping and extraction (Maghsoudi, Abdi and Aidani, 2020). Each of these methods involves advantages and disadvantages, and the method of separation is chosen based on system-specific requirements. Some of these methods, including distillation, have large energy requirements and, in the case of two molecules with similar boiling points, it is difficult to achieve a high degree of separation (Bhatta *et al.*, 2015). In the case of certain alcohol/alkane systems where the boiling points are similar, the degree of separation achieved from distillation

would be lower than if adsorption was used. If distillation is used to separate two arbitrary alcohols of similar carbon chain lengths and boiling points (A and B), product stream A would still contain high levels of B and vice versa. However, if an alkane of shorter carbon chain length (8-10) is in a solution with an alcohol of long carbon chain length (22-27), then the boiling points would be considerably different and distillation would be a more plausible method of separation (Li *et al.*, 2014). Li *et al.* (2014) compares the different boiling points of alkanes versus alcohols of varying carbon chain lengths and presents the similarity in boiling point of 1-decanol compared to n-decane (195 °C and 174 °C respectively) versus the difference in boiling point of arachidyl alcohol compared to n-decane (372 °C and 174 °C respectively). Li *et al.* (2014) propose separating the former by using a complex three-step process of fractional distillation and azeotropic distillation. This is a more complicated and costly process than adsorption. In recent years, the petrochemical industry has been trying to minimise the costs of operation by using less energy-intensive separation processes (Maghsoudi, Abdi and Aidani, 2020). Adsorption is an advantageous method of separation because of its low energy consumption, low toxicity and low corrosion (Bhatta *et al.*, 2015). It is a surface phenomenon process that occurs when molecules are transported from the bulk phase to a phase interface where they are bound by chemical or physical forces (Marais, 2008; Mouelhi *et al.*, 2016). Industrial applications of adsorption generally focus on solid-gas or solid-liquid interfaces (Dąbrowski, 2001). It is considered an advantageous process within industry, due to its simple design and low investment and operating costs (Nageeb, 2013). Adsorbents can be used to treat industrial wastewater, industrial effluent or agricultural waste; it can be used further to purify product streams and are commonly used in reaction, petrochemical and environmental engineering (Kulkarni, 2016; Patel, 2019).

Given this, the use of adsorption principles to remove oxygenates has been applied in the petrochemical industry (Milestone and Bibby, 1981). Although it is a widely used process and several research projects have focused on it, the database related to alcohol/ alkane separation using adsorbents is limited.

1.2 Problem statement development

To the author's knowledge, the availability of open literature, that is, publicly available literature that is accessed for free or by means of an institution, is limited when it comes to the adsorption of 1-alcohols from n-alkanes on activated alumina (AA). Some literature that focuses on the adsorption of alcohols is accessible, including foci on the adsorption of water and ethanol on H152 alumina (Rao and Sircar, 1993), ethanol and methanol adsorption on γ -alumina (DeCanio, Nero and Bruno, 1992) and isobutyl alcohol adsorption on η - and γ -alumina (Knözinger and Stübner, 1978). These studies present research pertaining to short chain alcohol (C_1 - C_4) adsorption. However, the investigation of long chain alcohol (C_6 - C_{10}) adsorption has been studied only twice (Bosman, 2019; Groenewald, 2019).

Single and binary component systems will be investigated in this study and the analyses of the binary component adsorption results would require single component adsorption data of all adsorbate types. During the problem statement development phase of this study it was therefore decided to use the single component adsorption data generated by Bosman (2019) and Groenewald (2019) to expand on the 1-alcohol binary component adsorption database. This section will focus on outlining the work done by

these two researchers, and describe the critical review that was used to identify a lacuna in extant literature and how this thesis aims to address it.

Groenewald (2019) investigated the removal of 1-octanol, 1-hexanol and 1-decanol from an n-decane solution by using various forms of AA. Groenewald (2019) also examined the regeneration of these AA adsorbents, whereas the current study is focused solely on adsorption. The objectives and critical outcomes of Groenewald's research pertaining to adsorption are outlined in Table 1.

Table 1 Summary of the research objectives and main outcomes of Groenewald (2019). Reworded from the thesis of Groenewald (2019).

Research objective	Main outcome
Design and construct a bench-scale batch-adsorption setup.	A heated water bath setup was designed and built.
Perform equilibrium and kinetic adsorption tests to identify the effect of adsorbate type, temperature and adsorbent type on the adsorption process.	<p>Operating conditions:</p> <ul style="list-style-type: none"> • Adsorbents investigated: activated alumina F220 (AA F220), Selexsorb CD[®] (SCD), Selexsorb CDx[®] (SCDx) • Alkanes used: n-decane • Alcohols/Adsorbates used: 1-decanol, 1-hexanol and 1-octanol (range: 0.5-1.5 mass%) • Only single component systems used • Operating temperatures: 25, 30 and 35 °C <p>For all three adsorbates F220 performed the best at 35 °C.</p>
Model the experimentally determined equilibrium and kinetic models using existing model.	<p>Models used:</p> <ul style="list-style-type: none"> • Kinetic models: Weber-Morris, pseudo-first and second orders • Equilibrium isotherm models: Langmuir, Freundlich and Dubinin-Radushkevich <p>The adsorbate-adsorbent bonding was found by means of physisorption. The rate-limiting step of most of the systems appeared diffusion rate limited.</p>

Table 1 indicates lacunae in Groenewald's work. These are listed below and were used to develop the problem statement of the present project.

- Multicomponent adsorption systems

- Temperatures above 35 °C
- A larger range of initial adsorbate concentrations (that is, > 1.5 mass%)
- Broader range of pre-existing kinetic and equilibrium models

Bosman's research followed on that of Groenewald's and as such addressed some of these lacunae. Bosman's overarching aim was to investigate the adsorption of 1-hexanol, 1-octanol and 1-decanol in single and binary component systems from an n-decane solution onto various forms of AA (2019). The main objectives and outcomes are summarised in Table 2. As indicated, it is clear that Bosman addressed some of the lacunae in Groenewald's work, and this is reflected in the table.

Table 2 Summary of main objectives and outcomes used to identify the problem statement for the current study. Based on the thesis of Bosman (2019).

Research objective	Main outcome
Experimentally investigate the adsorption of single and binary 1-alcohol systems onto different types of AA.	<p data-bbox="956 338 1246 367">Single 1-alcohol system</p> <p data-bbox="756 398 1015 427">Operating conditions:</p> <ul data-bbox="804 459 1449 658" style="list-style-type: none"> <li data-bbox="804 459 1394 488">• Adsorbents investigated: AA F220, SCD, SCDx <li data-bbox="804 501 1134 530">• Alkanes used: n-decane <li data-bbox="804 544 1449 613">• Alcohols/Adsorbates used: 1-decanol, 1-hexanol and 1-octanol (range: 0.5-1.5 mass%) <li data-bbox="804 627 1211 656">• Operating temperature: 45 °C <p data-bbox="956 687 1246 716">Binary 1-alcohol system</p> <p data-bbox="756 748 1015 777">Operating conditions:</p> <ul data-bbox="804 808 1449 1093" style="list-style-type: none"> <li data-bbox="804 808 1394 837">• Adsorbents investigated: AA F220, SCD, SCDx <li data-bbox="804 851 1134 880">• Alkanes used: n-decane <li data-bbox="804 893 1449 1048">• Binary 1-alcohol systems: 1-decanol&1-hexanol, 1-hexanol&1-octanol and 1-decanol&1-octanol (equimass mixtures with overall initial concentration: 0.3-3 mass%) <li data-bbox="804 1061 1294 1090">• Operating temperature: 25 and 45°C <p data-bbox="756 1122 1449 1196">For both systems SCD and SCDx marginally outperformed F220 (except for the adsorption of 1-decanol)</p>
Model experimentally determined equilibrium and kinetic data for single and binary 1-alcohol systems.	<p data-bbox="756 1328 919 1357">Models used:</p> <ul data-bbox="804 1388 1449 1588" style="list-style-type: none"> <li data-bbox="804 1388 1449 1458">• Kinetic models: Weber-Morris, pseudo-first, second and nth orders <li data-bbox="804 1471 1449 1588">• Equilibrium isotherm models with multicomponent modifications: Langmuir, Freundlich, Sips and Redlich-Peterson. <p data-bbox="756 1619 1449 1778">The adsorbate-adsorbent bonding was found to be a form of chemisorption. The rate-limiting step of most of the systems appeared to be limited in terms of diffusion and external mass transfer rate.</p>

Bosman (2019) and Groenewald (2019) concluded that 1-hexanol, 1-octanol and 1-decanol can be adsorbed from an n-decane solution using variations of AA. They studied the effect of varying molecular sizes on single and binary 1-alcohol adsorption (Bosman, 2019; Groenewald, 2019). However, the study

of adsorbing a branched 1-alcohol (with a less cylindrical shape) from n-decane on AA in a competitive or non-competitive adsorption system was not studied.

Examining branched 1-alcohol adsorption in a non-competitive system provides the necessary data to proceed with a study where the branched 1-alcohol is present in a competitive adsorption system. This is of interest because, in the industry, a solution would have multiple impurities present; in this case, 1-alcohols. The first key aspect of a competitive adsorption study would be to determine how two 1-alcohol isomers would interact with each other and the adsorbent at different system conditions. The second would be to determine how a linear 1-alcohol molecule interacts with a branched, larger 1-alcohol molecule, where both have an identical carbon chain backbone. The effect of different adsorbate ratios used for these binary component systems is also of importance, as industrial application calls for a broad understanding of how adsorbate ratios affect system performance.

The investigation of these two binary component systems can be improved by investigating whether any displacement or interaction effects occurs, as these would be of particular interest when designing multicomponent adsorption systems in industry (Padilla-Ortega, Leyva-Ramos and Flores-Cano, 2013). Bosman (2019) did evaluate the interactive effects of binary component adsorption systems. However, experimental studies focused on the displacement potential of two different components in a binary component adsorption system have not been performed. Such investigations would improve the understanding of multicomponent adsorption.

Prior to stipulating the objectives of the present project, the reasons for focusing on 3,7-DMO for single and binary component adsorption will be briefly outlined. Firstly, 3,7-DMO is readily available and is used in several industrial applications. Secondly, 3,7-DMO satisfied all the needs for the study in terms of matching the main carbon chain length of 1-octanol and being an isomer of 1-decanol. Thirdly, limited research has been done on the adsorption of 3,7-DMO in terms of using a porous adsorbent. Only the production of 3,7-DMO from citronellal using catalysts has been investigated (Krishna *et al.*, 2016; Sudiarmanto *et al.*, 2017). Sudiarmanto *et al.* (2017) investigated the production of 3,7-DMO because of its value in the petroleum industry. Since petroleum is derived from a non-renewable energy source, gasoline fuel is augmented with additives to increase the octane numbers and in turn the oxygen levels. Frequently, 3,7-DMO is used for this purpose (Sudiarmanto *et al.*, 2017). 3,7The substance is furthermore frequently employed in the fragrance industry in sprays and other household items (Krishna *et al.*, 2016).

1.3 Aims and objectives

The main aim of this project is to characterise the single component adsorption of 3,7-DMO and the binary component adsorption of 1-decanol&3,7-DMO and 1-octanol&3,7-DMO from an n-decane stream onto SCD through experimentally executed kinetic and equilibrium studies. A secondary aim will be to fit kinetic and equilibrium isotherm models to selected single and binary component systems.

The main aim will be achieved by adhering to the following objectives:

1. Perform kinetic and equilibrium experiments to determine the removal of 3,7-DMO from an n-decane stream by using SCD and investigate the effect of temperature and initial concentration.
 - a. Collect kinetic and equilibrium data at different temperatures and a range of initial adsorbate concentrations.
2. Perform kinetic and equilibrium experiments to determine the removal of 1-alcohols from two different binary systems (1-decanol&3,7-DMO and 1-octanol&3,7-DMO) from an n-decane stream by using SCD.
 - a. Collect kinetic and equilibrium data at different temperatures within a range of initial adsorbate concentrations and adsorbate ratios and investigate the effect of these three parameters on binary component adsorption.
 - b. Investigate the effect of molecular shape and size on the adsorption of 1-alcohols present in a binary system.
3. Determine how 1-decanol, 1-octanol and 3,7-DMO perform in a competitive adsorption binary system.
 - a. Determine the interaction parameters for each 1-alcohol.
 - b. Perform displacement tests on three binary systems.

The secondary aim of the project will be achieved by adhering to the following (fourth and final) project objective:

4. Fit two- and three-parameter kinetic and equilibrium models per component to the results generated by experimental studies on the single component and binary component adsorption systems. Identify best fit and deduce the adsorption mechanisms and system characteristics based on the model assumptions.

1.4 Project scope

The problem statement is used to define the project scope. The importance of the latter is to define the project's boundaries and stipulate that, although areas of improvement or further research will be identified, they will not be covered in this study.

The scope will be limited to one porous adsorbent, a form of AA. The latter is considered to be an industrially relevant adsorbent. The extant database on single and binary component 1-alcohol adsorption is limited: thus, generating more adsorption data for a specific AA type adsorbent was prioritised here. Greater insight into the performance of a specific adsorbent (when contacted with a variety of adsorbates) was considered to be more valuable. During alkane production through alkylation or ethoxylation 100% conversion of primary alcohols is not always achieved (Lorenzen *et al.*, 2009). Thus, alkane production product stream sometimes have low concentrations of primary alcohols present (Lorenzen *et al.*, 2009). Preliminary tests were performed using AA F200, SCD and SCDx to determine those adsorbents that yielded higher loadings of 3,7-DMO. It was found that the Selexsorb series outperformed AA F200, while SCD marginally outperformed SCDx. Therefore, the decision was taken to focus this study on SCD.

The project will focus on the removal of the following three adsorbate systems from an n-decane stream using SCD.

- Single component system: 3,7-DMO.
- Binary component system: 1-octanol&3,7-DMO.
- Binary component system: 1-decanol&3,7-DMO.

1-Octanol and 1-decanol were selected for the two binary components systems for two reasons. Firstly, the study aims to determine whether SCD is suitable for the removal of 3,7-DMO, while this measure is, to an extent, a comparative one, as the degree of success is also related to how well other 1-alcohols are adsorbed. Secondly, for binary component adsorption isotherm modelling, single component data were required, thus it made sense to build on the work of Bosman (2019) and use equilibrium isotherm model parameters of the single component adsorption studies performed on 1-octanol and 1-decanol.

Experiments will be conducted using bench-scale apparatus at 3 different temperatures for the single component study (25 °C, 35 °C and 45 °C) a within a range of 0.5-3.3 mass% adsorbate concentration. The binary component systems will be investigated at two different system temperatures (25 °C and 45 °C) within a range of 1–3.3 mass% combined initial adsorbate concentration. The combined initial adsorbate concentration embodies the total concentration of the two adsorbates in the binary component system.

Selected kinetic and equilibrium isotherm models will be fitted to the single and binary component adsorption data generated experimentally. Regardless of whether the single or binary component system is involved, only models with two or three parameters (per adsorbate component present) will be investigated. The theoretical model assumptions will be used to draw conclusions regarding the characteristics of the adsorbate, adsorbent, adsorbate-adsorbent interactions and adsorbate-adsorbate interactions. Conclusions regarding the adsorption of adsorbate in a non-competitive (3,7-DMO) and competitive system (3,7-DMO, 1-decanol and 1-octanol) will be drawn solely from the results collected in this project. Any shortcomings in the experimental setup used will be identified and the repercussions assessed, but these will not be further investigated.

Adsorption data (kinetic profiles, adsorbate loading, adsorption capacity and so forth) can be expressed in terms of moles of mass, while the units used is left to the discretion of the researcher (Parhi *et al.*, 2009). This study will primarily report all experimentally determined data and model parameters in terms of mass.

1.5 Thesis outline

Figure 1 outlines the structure of this thesis, providing clarity on its layout and where each objective will be addressed. Figure 1 should be considered in conjunction with Section 1.3.

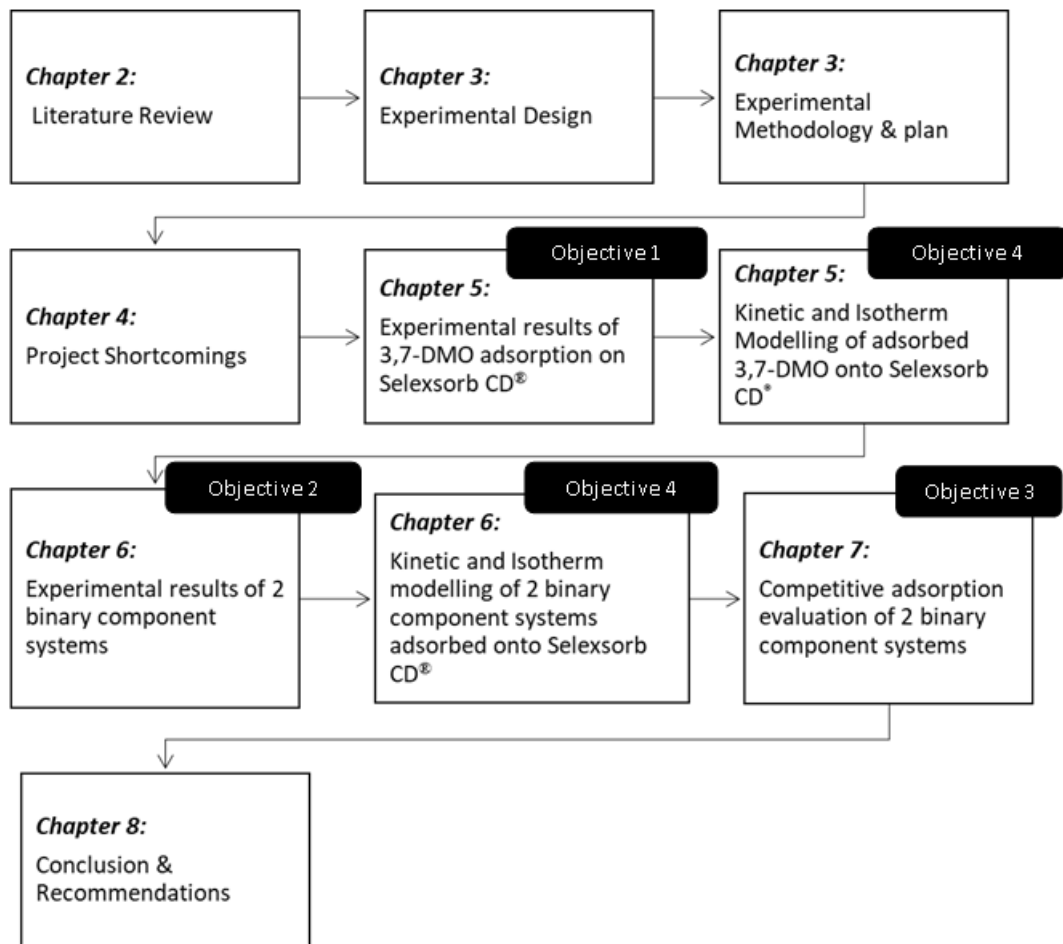


Figure 1 Outline of the thesis flow and structure and where each objective will be addressed.

Chapter 2 Literature review

This chapter aims to give the necessary background to successfully address all objectives provided in Section 1.3. It will also incorporate a critical review of the literature available to support the development of a sound experimental methodology, which will enable an in-depth result review to be used to draw critical conclusions.

2.1 Adsorption fundamentals

Adsorption is a surface phenomenon involving molecules, atoms or ions in a liquid or gaseous state that attach to a surface (Binnie, Kimber and Thomas, 2017). This study exclusively considers porous adsorbents and, although it is recognised that adsorption is not limited only to porous mediums, non-porous adsorbents will not be covered in this study.

Adsorption exploits the difference in the affinity of a porous medium to one solute in contrast with another. The adsorption process results in interphase accumulation at the surface between two phases. Thus, adsorption can be said to shift the high concentration of solute from the bulk phase to the adsorbed layer (interphase accumulation) and ultimately into the pores. Throughout the present argument, the substance that is adsorbed will be referred to as 'the adsorbate,' while the surface onto which the substance is adsorbed will be referred to as 'the adsorbent' or 'the surface.' The amount of adsorbate adsorbed onto the adsorbent at a time will be referred to as 'the adsorbate loading.'

2.1.1 Adsorption mechanism

Adsorbate material (gaseous or liquid phase) accumulates on active sites in the pores of the adsorbent (Binnie, Kimber and Thomas, 2017). This phenomenon occurs when the attractive energy of the adsorbate to the adsorbent surface is stronger than the energy between the adsorbate and the bulk solution (Binnie, Kimber and Thomas, 2017), while the energy available is sufficient to move adsorbate molecules from a comparatively high entropy state to a stable adsorbed state (Budi, Stipp and Andersson, 2018). The adsorbate molecules possess free energy (entropy), which enables interaction of the molecules with the adsorbent surface (Budi, Stipp and Andersson, 2018). The entropy of adsorbate molecules in the bulk phase increases with increasing adsorbate concentration; under equilibrium conditions less energy is required to adsorb molecules from a low entropy state in contrast with a high entropy state (Kumar *et al.*, 2019).

Adsorption is considered to be a three-step process including external mass transfer (film diffusion), internal mass transfer (intraparticle diffusion) and adsorption (Figure 2) (Patel, 2019). The final step refers to the adsorbate uptake of a molecule that lies within a pore volume onto an adsorption/ active site. External mass transfer is the movement of molecules from the bulk fluid phase through the liquid film that forms around the adsorbent bead (Worch, 2012; Patel, 2019). The driving force for this step is the difference in concentration between the bulk solution and the adsorbent surface (Wang and Guo, 2020). If the initial adsorbate concentration (albeit within the ambit of a binary or single component system) is

low, the external mass transfer will become progressively slower. As more of the adsorbate moves onto the surface of the adsorbent, less will be in solution and, if the adsorbate is not in excess, the driving force will be reduced. The effect of mass transfer limitations can be experimentally determined by comparing the adsorption achieved when no mixing takes place against different speeds of mixing. Furthermore, a single adsorbent bead can be used rather than a whole bed of adsorbents.

Once inside the boundary layer, internal mass transfer transports the adsorbate molecule through a pore opening on the surface of the adsorbent by means of intraparticle diffusion (Worch, 2012). Upon reaching an active site, the final step is the adsorption/ diffusion of the adsorbate molecule onto an active site of the adsorbent (Patel, 2019; Wang and Guo, 2020). Typically, external mass transfer (EMT) is considered the rate-limiting step (Patel, 2019). To minimise the resistance to EMT, the mixing speed or flowrate in a batch or continuous adsorption setup should be increased so as to reduce the thickness of the stagnant film surrounding the adsorbent particle (Binnie, Kimber and Thomas, 2017).

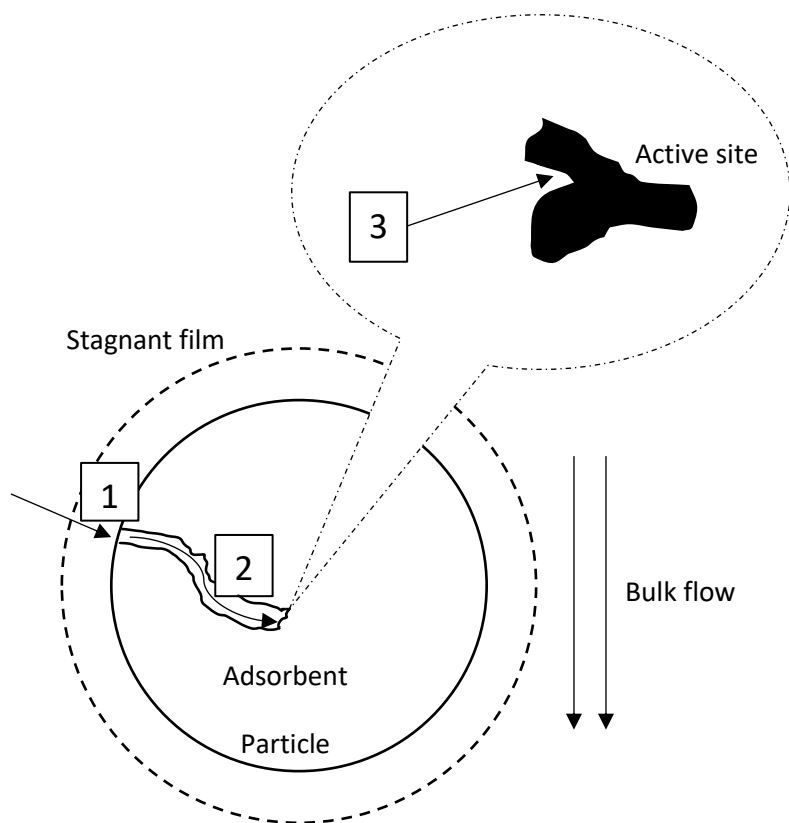


Figure 2 Graphic depiction of the three-step adsorption process where (1) represents the region of external mass transfer (film diffusion), (2) region of internal mass transfer (intraparticle diffusion), (3) adsorption onto an active site. Redrawn from Patel (2019).

The adsorption process involves the principles of potential and kinetic energy in which the former is not temperature-dependent while the latter is (Ebelegi, Ayawei and Wankasi, 2020). Potential energy exists between an adsorbate molecule and a specific active site relative to the distance of the molecule to the active site (Kumar *et al.*, 2019). This potential energy can be thought of as interaction energy that draws a specific adsorbate molecule to a specific active site (Kumar *et al.*, 2019). The adsorptive uptake (third step as shown in Figure 2) occurs at an active site on the adsorbent surface which is capable of bringing

a specific adsorbate molecule from the bulk fluid phase (high energy state) to an adsorbed state (local minimum energy state) by means of relatively weaker physical forces or stronger chemical forces (Rabia, Ibrahim and Zulkepli, 2018; Kumar *et al.*, 2019).

Adsorption energy is defined by Kumar *et al.* (2019) as the difference between the system energy and the sum of the adsorbate and adsorbent energy. The adsorbate molecules in the bulk fluid phase possess kinetic energy that is temperature dependent, while the distance from a specific adsorption site is classified as the potential energy of the adsorbate molecule (Zhou *et al.*, 2020). Adsorbate molecules transition from being in a state of moving randomly in the bulk fluid phase to being in a local energy minimum state when adsorbed onto an active site (Kumar *et al.*, 2019). At this local energy minimum, the translational and vibrational energy is at a local minimum (Kumar *et al.*, 2019). During the adsorption process, a loss of potential and kinetic energy occurs, but the total energy is conserved, which corresponds to the heat of adsorption. The latter is the energy required to overcome the attractive forces that exist between adsorbate molecules in the bulk phase and the entropy of the free molecule (Zhou *et al.*, 2020). Additional energy is needed for an adsorbed molecule to overcome the potential energy that exists between the adsorbate molecule and the active site and the kinetic energy of the adsorbate molecule in the bulk fluid phase. This is referred to as the binding energy required for the uptake of an adsorbate molecule onto an active site (Kumar *et al.*, 2019).

The active sites on the adsorbent surface possess what is known as surface energy (Zhou *et al.*, 2020). An active site with a high surface energy always works towards being in its lowest and most stable energy state. This stable energy state can be achieved by adsorbing an adsorbate molecule with lower energy onto its surface (Zhou *et al.*, 2020).

2.1.2 Physisorption

As mentioned, physical adsorption is a direct result of London-Van der Waals force's forming between the adsorbent surface and adsorbate particle (Webb, 2003). It can be said that physical adsorption involves a secondary binding mechanism whereby electrons are shared between adsorbate and adsorbent (Rabia, Ibrahim and Zulkepli, 2018). Physisorption can take place, provided that the system has the correct temperature and adsorbate concentration in the bulk fluid (Webb, 2003). Although a mechanism may be considered dominant, both mechanisms of adsorption can be at play in an adsorption system (Webb, 2003).

The attractive forces between the adsorbed molecule and surface may be dipole-dipole interactions, dispersion interactions or hydrogen bonding (Patel, 2019). These are generally weaker forces, a recognition that supports the notion that molecules can be released and are then free to travel over the surface, where they are not bound to one location (Webb, 2003). If physisorption is the predominant mechanism for the binary component systems in this study (1-decanol&3,7-DMO and 1-octanol&3,7-DMO), some displacement may occur alongside competitive adsorption (Rabia, Ibrahim and Zulkepli, 2018). Due to this, physical adsorption can be reversed by altering the concentration gradient between the adsorbed phase and bulk liquid phase (Binnie, Kimber and Thomas, 2017). The process is reversible

due to the low enthalpy requirements (20 kJ/mol), and this favours the application of regeneration processes, which is appealing to industry (Rabia, Ibrahim and Zulkepli, 2018). This does not form part of the scope of the present project, but the easily reversible nature of physisorption may affect the success of the adsorption of the 1-octanol, 1-decanol and 3,7-DMO in a binary system.

2.1.3 Chemisorption

Chemical adsorption, unlike physisorption, involves the transfer of electrons from the adsorbate to the adsorbent surface (Binnie, Kimber and Thomas, 2017). This form of adsorption occurs by means of a chemical reaction at the surface of the material and results in a redistribution of electrons between the adsorbed atoms and adsorbent surface (Alturki and Simonetti, 2017). Considering the redistribution of electrons, chemisorption typically occurs in mono-layer fashion, as adsorption can only occur when in direct contact with the chemically active surface (Webb, 2003).

Chemisorption results in the formation of a type of surface compound and, because of the bond that thus forms between adsorbate and adsorbent, it is more difficult to reverse chemisorption than in the case of physisorption (Webb, 2003). The typical enthalpy of adsorption is considerably higher (200 kJ/mol), the bond length is shorter and the bond strength is greater than that of physisorption (Patiha *et al.*, 2016). Stronger electrostatic forces are present in the adsorbate-adsorbent system and consist of covalent or electrostatic chemical bonds (Patel, 2019). Some studies indicate that short and long chain alcohols are often primarily adsorbed by means of chemisorption (Panja, Saliba and Koel, 1998; Okhrimenko *et al.*, 2013; Bosman, 2019), while others indicate a mixed complex between physisorption and chemisorption for C₁-C₄ alcohols (Nguyen, Reyniers and Marin, 2010). The characteristics of the alcohol being adsorbed influence the mechanism of adsorption (Nguyen, Reyniers and Marin, 2010).

In certain cases, it has been found that the chemical adsorption mechanism is related to surface phenomena. In other words, the reaction rate is controlled by the surface reaction, which implies the importance of considering specific surface area in the design of experimental setups and the selection of the adsorbent. The total surface area of adsorbents available typically range from 500-2000 m².g⁻¹ depending on the pore class (2.2.1.3). Chemisorption is of a more selective nature, in contrast with physisorption, and the possibility of such adsorption is dependent on the adsorbent and adsorbate type (Webb, 2003).

Webb (2003) also found that physisorption and chemisorption can occur simultaneously on a given surface. This happens when adsorbate molecules are adsorbed by means of chemisorption directly onto the surface, while a layer of physisorbed adsorbate molecules forms on top of the chemisorbed layer (Webb, 2003). The temperature of the system (assuming the temperature of the bulk solution is the same as the adsorbent surface) influences whether physical or chemical adsorption takes place. A change in temperature can change the predominant mechanism of adsorption (Webb, 2003). At an increased system temperature, the energy level is sometimes too high for physical adsorption, but nonetheless it will favour the initial high energy demands of chemical adsorption.

2.1.4 Parameters affecting adsorption

Adsorption is considered to be a complex phenomenon that, although extensively researched, is not yet fully understood. However, certain parameters have been identified as factors that affect it. These include adsorbent type, adsorbate type, adsorbent affinity and operating conditions (Patel, 2019).

The physical and chemical factors related to the adsorbate include molecular weight, size, functional group, polarity, hydrophobicity and solubility (Kose, 2010). The physical and chemical factors related to the adsorbent include surface area, pore size, pore size distribution and surface chemistry (Kose, 2010). The adsorbate-adsorbent affinity system implies that the properties of the target compound as well as the bulk solution significantly affect the extent of adsorption (Binnie, Kimber and Thomas, 2017). The properties of the bulk solution should also be considered, namely pH, ionic strength and competitive solutes (Kose, 2010). In this study, pH and ionic strength are not considered. The project scope focuses mainly on molecular structure, shape and size. The operating conditions that affect adsorption capacity and performance include temperature, mixing speed, contact time and the question as to whether the operation is of a batch or continuous nature (Bansal and Goyal, 2005). These considerations evidence that adsorption is a complex mechanism involving several parameters that will affect the performance of the system. The present project therefore selects among these, and will focus on the composition and temperature of the bulk solution and how this affects the adsorption process.

2.2 Adsorbents

As mentioned in Section 2.1.4, the adsorbent type is an important parameter and care should be taken when selecting a system-specific one. The physical and chemical characteristics of adsorbents can provide useful information regarding potential adsorption behaviour. However, the behaviour and response to various operating conditions is system-specific and can be defined with greater accuracy by means of experimental work (Bansal and Goyal, 2005). Extant studies focused mainly on the adsorption of long chain alcohols onto various AA adsorbents to establish that the differences in results were minor (Bosman, 2019). The adsorbent type plays a key role in the adsorbate-adsorbent interaction, but it should not be considered in isolation. The degree of success of an adsorption system lies in how well the adsorbate interacts with the adsorbent. Therefore, the choice of adsorbent is not purely focused on its favourable properties (quality, durability and corrosion resistance and so forth): the ambit of the focus includes the matter of compatibility with the adsorbate.

Adsorbents can be divided into three classes: synthetic, natural and semi-synthetic (Rabia, Ibrahim and Zulkepli, 2018). Synthetic adsorbents are porous materials typically produced in a laboratory. These adsorbents have a high adsorption capacity, but they incur high manufacturing costs. Natural adsorbents are naturally occurring and consist of plant root, leaf and agricultural waste that are dried, crushed and sieved. These are typically used in wastewater treatment. The advantage of using natural adsorbents is low manufacturing costs. However, the adsorption capacity of these is often low. Semi-synthetic adsorbents are natural materials that undergo certain chemical and physical activation processes to develop highly porous surfaces. Adsorbents that are fundamentally variations of AA are considered to be

semi-synthetic (Rabia, Ibrahim and Zulkepli, 2018). The major advantages associated with the use of semi-synthetic adsorbents is low cost and high efficiency of the material. Synthetic and semi-synthetic adsorbents have considerable advantages such as stability at high temperatures and corrosion resistance (Yamaguchi *et al.*, 2002). AA possesses said advantages and can also be regenerated and re-used for a few cycles (Yamaguchi *et al.*, 2002; Rabia, Ibrahim and Zulkepli, 2018).

Industrial adsorbents can be further divided into oxygen-containing, carbon-based or polymer-based categories. The properties of adsorbents are readily identified by using FTIR, SEM, XRD or BET analysis. FTIR determines the chemical composition, SEM investigates morphology and XRD provides information relating to crystallographic structure (Kurniawan *et al.*, 2011). The scope of the present project includes one adsorbent rather than comparing several different adsorbents. Although all analyses could be beneficial for the project, detailed information is not critical for its aims. The parameter considered to be most important is the pore structure of the solid. Such adsorbents are typically highly porous in nature as it directly influences its adsorption capacity on account of the increased surface area. These larger surface areas of such adsorbents cause a large mass of adsorbate to be collected relative to the mass of adsorbent used (Yi *et al.*, 2015).

The selection of the adsorbent used in this study involves the investigation of certain key parameters such as pore size distribution, average pore diameter, specific surface area and specific pore volume (Unger, 1972). BET analysis techniques may be employed to determine these parameters from gas adsorption and desorption measurements (Unger, 1972; Xavier and Banda, 2016).

2.2.1 Physiochemical properties

Each of the parameters deemed to be most important (as determined briefly above) will be unpacked here. It should be noted that the properties associated with the parameters are considered to be interlinked (Choma and Jaroniec, 2001).

2.2.1.1 Heterogeneous versus homogeneous surfaces

Adsorbent surfaces can be homogeneous and heterogeneous in nature (Choon Ng *et al.*, 2017). Homogeneous adsorbents exhibit limited variation in its chemical and structural properties. The energy of the active sites on the adsorbent are the same, no impurities or variations occur in the functional groups on the active sites and the pore size distribution is minimal. Homogeneous surface energy means that each active site possesses the same surface energy and will target adsorbate molecules of a specific lower energy level.

Adsorbents are considered to be heterogeneous when different types of binding/ active sites are present on the surface with different adsorbate uptake/ binding energies at these sites (Kumar *et al.*, 2019). Most porous materials contain more than two types of adsorption sites (Kumar *et al.*, 2019). Heterogeneous surfaces involve the coexistence of different chemical and structural properties on an adsorbent surface (Chiang *et al.*, 2018). In other words, physical curvature of the adsorbent and variation in pore sizes all introduce surface heterogeneity. Impurities on the adsorbent surface or different functional groups bound to the surface introduce chemical heterogeneity. Heterogeneous surface energy means that the

active sites of the adsorbent possess a distribution of surface energies. The adsorbent will try to adsorb lower energy molecules onto the highest surface energy active sites first. This means that, for energetically heterogeneous surfaces, adsorbate molecules of different energy levels will be targeted.

2.2.1.2 *Surface area*

The range of pore sizes determines the specific surface area available. The following surface areas are typically found (Unger, 1972).

- Microporous adsorbents – $SSA > 500 \text{ m}^2.\text{g}^{-1}$
- Mesoporous adsorbents – $10 < SSA < 500 \text{ m}^2.\text{g}^{-1}$
- Macroporous adsorbents – $SSA < 10 \text{ m}^2.\text{g}^{-1}$

This suggests that the pore size is inversely proportional to specific surface area, which supports the school of thought that the active sites in macroporous regions are limited along with the adsorption potential (Unger, 1972).

The surface area includes both the internal and external surface (Worch, 2012). The external surface area (where macropores are mostly found) determines the rate of adsorption. The internal surface area generally exceeds the external one. It effects the adsorbate loading and adsorbent capacity, as most adsorption sites are found internally. It can be said that a large internal surface area is proportional to the number of micropores and volume of these pores (Worch, 2012).

2.2.1.3 *Pore classes and porosity*

In a study of organic adsorption systems, the pore structure was found to greatly influence the interaction effects in multi-adsorbate systems (Aschermann, Zietzschmann and Jekel, 2018). The width of the pores control the rate at which matter is transported to the active sites in the centre of the adsorbent bead (Unger, 1972). This is due to pore size variation where three major pore size classifications have been made: macro, meso and micropores. The respective sizes of these pores are found in Table 3.

Table 3 Range of pore radius for three different pore classes (International Union of Pure and Applied Chemistry, 1994)

Pore class	Pore radius (nm)
Macropores	$R > 50$
Mesopores	$2 < R < 50$
Micropores	$R < 2$

The characterisation of pores is useful, as the average pore size influences the shape of the adsorption isotherm (Dubinin, 1974). Macropores are known to provide access to smaller pores, thus controlling the rate of diffusion which, in turn, facilitates adsorption—however, it contributes minimally to its extent (Unger, 1972).

Porosity is defined as the ratio of volume of pores to total volume. A large porosity is desirable, as this increases the space available for adsorbate molecules to diffuse into. However, the average pore

diameter relative to the size of the adsorbate molecule is of importance (Unger, 1972). Although a higher micropore volume is desirable, it is important to consider the possibility of size exclusion in the event of narrow pores relative to molecules with a larger aperture (Worch, 2012). This is often found in high molecular weight organic matter contacted with microporous adsorbents (Worch, 2012).

Adsorption strength increases with decreasing pore size (Kose, 2010). A decrease in pore size increases the contact points between the adsorbate and adsorbent, which results in adsorption potential between opposing pore walls overlapping (Kose, 2010). If opposing pore walls are separated by little more than the particle diameter, the adsorption forces in the micropores increase and stronger binding occurs (Kose, 2010). This is because the adsorption potential comes from various locations surrounding the particle. This is significant for the current study, as there is a difference in molecular shape and diameter of 3,7-DMO when compared to 1-octanol and 1-decanol.

The adsorption potential is said to decrease from micro to macropore classes. Larger pores reduce available surface area and overlapping of adsorption potential but allow for more particles to enter the pore channel. Hence, macropores contribute to the rate of diffusion to a greater extent than the adsorption capacity. For molecules such as 3,7-DMO that have a larger diameter, this may result in some adsorption in the macropores, while it could also lead to an increased chance of displacement.

2.2.1.4 *Pore size distribution and layout*

Adsorbents are said to have pore size distribution when two or all three of the pore size ranges are present. The pore system directly influences the adsorption kinetics and equilibrium, which emphasizes the importance of understanding the unique pore size distribution of the adsorbents under consideration (Worch, 2012). With the exception of naturally occurring adsorbents, most are known to exhibit a large internal surface area with pore size distribution of at least two of the three pore size ranges or classes present (Unger, 1972; Worch, 2012). If it is found that the adsorbent structure of the adsorbents under consideration is similar across the board, and has a limited effect on the adsorptive capacity. This justifies a restriction of focus on investigating one adsorbent.

In conjunction with PSD (particle size distribution), the layout of pores should also be considered. Pores are classified according to volume, radial range and shape (Lim, Kim and Lee, 2019). They are further classified as open or closed (Wang and Yang, 2004). Closed pores involve macroscopic properties such as bulk density, but they are inaccessible to external fluids. Therefore, they do not aid adsorption or desorption and, as such, will not be considered in this study. Open pores have at least one channel open to the external surface of the solid and are thus accessible to a fluid (Figure 3). As evidenced in Figure 3, a variety of pore channels exist.

A more detailed and accurate description may prove useful for understanding exactly how adsorption takes place and through which channels. However, the more pressing issue is to determine whether the pore and particle size correspond with adsorption. This is important especially in terms of multicomponent adsorption. In the event of varying adsorbate size, pore blockage may occur, which would then make it more likely to determine whether competitive adsorption take place. In a multicomponent system, where all adsorbate sizes are compatible with the average pore size, and if

reduced adsorbate loading occurs in a binary versus single component system it is indicative of adsorbate interactions and competitive adsorption (Wang and LeVan, 2010).

Another important factor (other than the radial range of the pore) is its entry shape. The three that occur most include slit-shaped, square and rectangular ones. This should be considered, as certain adsorbate molecules may have a shape that is incompatible with that of the pore. The entry shape, pore type and class are of importance, as pore filling is the main mechanism of adsorption in micropores (Kose, 2010).

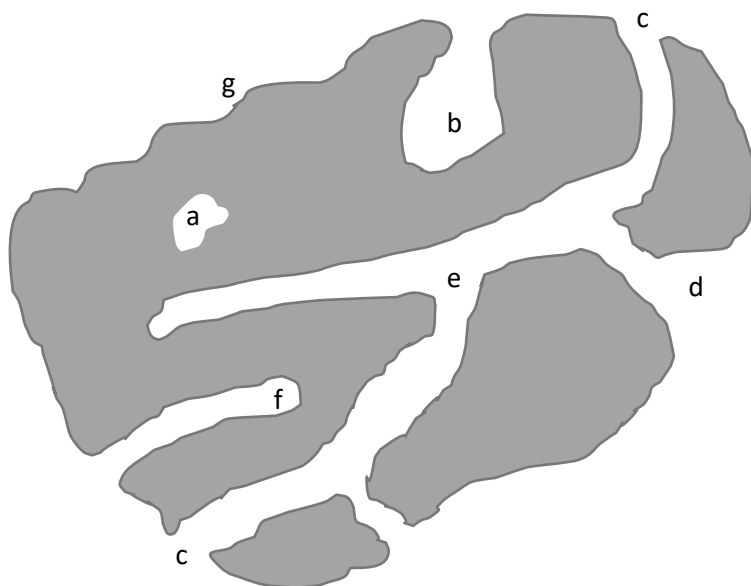


Figure 3 Schematic cross-section of a porous solid. (a) closed pore, (b) ink-bottle shaped pore, (c) cylindrical open, (d) slit-shaped, (e) through pore, (f) cylindrical blind pore, (g) roughness on the external surface. Redrawn from (Wang and Yang, 2004).

A closed pore (Figure 3(a)) is inaccessible to an adsorbate molecule and can thus not participate in adsorbing it from the bulk fluid phase. Closed pores only affect the mechanical properties of the adsorbent material, which is not the focus of this project. In contrast, the pores represented in Figure 3(b-f) are accessible for adsorbate molecules to interact with active sites in the pore volume.

It is important to note that the research done by Groenewald (2019) and Bosman (2019) investigated different types of AA. Given that they established that all three adsorbents performed similarly, while some marginally outperformed others, the aim of the present study is to focus on one type of AA adsorbent, as indicated. The objectives are to expand the 1-alcohol adsorption database and understand the adsorbate-adsorbent interactions. Therefore, it is necessary to ensure a good understanding of the adsorbent structure around selecting the adsorbent to be investigated.

2.2.2 Variations of activated alumina

Many different adsorbents are available for the removal of volatile organic compounds, including activated carbon, silica gel, zeolites and AA (Díaz *et al.*, 2004). The results presented in Bosman's work indicated that variations of AA (F220, SCD and SCDx) are most suitable for the adsorption of alcohols (1-

decanol, 1-octanol and 1-hexanol) from an alkane (n-decane) solution (2019). Given this, it was decided to focus the review of adsorbents here solely on AA.

Aluminium and aluminium-based materials are considered to be valuable for industrial adsorbent synthesis, due to their low molecular weight, high quality, durability and corrosion resistance (Rabia, Ibrahim and Zulkepli, 2018). The adsorbent is available in sustainable quantities, as it can be manufactured with minimal effort. The production of AA typically involves four major steps: production of aluminium hydroxide, pre-shaping (if necessary), heat treatment at high temperatures and final shaping (if necessary) (Saridede, Çizmecioglu and Değerli, 2005; Gautam *et al.*, 2014).

Adsorbate-adsorbent interactions such as 1-alcohol with AA are dependent on the physiochemical properties and specific variations of adsorbent used (Kose, 2010). This engenders a need for a review of the structural and physiochemical properties of the different AA variants. Physical, chemical and (in some cases) electrostatic interactions are the main interactions found between adsorbates and adsorbents (Kose, 2010). The surface of AA is considered strongly polar and consequently has a higher affinity for polar or semi-polar molecules, in contrast with nonpolar molecules (Ruthven, 1984).

AA typically possesses a heterogenous pore structure and is classified as a type IV mesoporous material with broad size distribution and open pores (Mouelhi *et al.*, 2016). Its physiochemical properties, such as surface chemistry, are related to the functional groups found on the adsorbent surface. These determine the acidic or basic nature of the adsorbent surface. In the presence of oxygen-containing functional groups, the surface is considered acidic, while nitrogen-containing functional groups produce basic conditions. Extant work investigated the physical factors affecting the adsorption of synthetic organic molecules onto activated carbon. It was found that surface chemistry played a significant role in adsorption (Kose, 2010). It is assumed here that, although the adsorbent type is different, these findings will suit other adsorbent surfaces such as AA. The amphoteric nature of the AA and the successful adsorption of alcohols in single and binary component systems as demonstrated by Bosman (2019), suggests the surface chemistry is acceptable.

AA has attracted increased interest in industry due to low associated costs and its water filtration capabilities (Chen *et al.*, 2015). It is a favoured adsorbent due to its large surface area, pore volume and subsequent high adsorptive capacity. The adsorption performance is dependent on the available surface area and available adsorption sites for physisorption and chemisorption. It is known to adsorb gases and liquids while maintaining its structural integrity. Its application in industry includes the removal of impurities from gaseous or liquid streams and the concentration and purification of effluent (Rabia, Ibrahim and Zulkepli, 2018), while $\gamma\text{-Al}_2\text{O}_3$ has been applied to hydrocarbon adsorption (Díaz *et al.*, 2004). It has been widely used in wastewater treatment, removal of organic acids and surfactants from aqueous solutions (the alcohols considered in this project would be classified as such) (Chen *et al.*, 2015). AA has also been used successfully for the adsorption of fluorine, phosphates, arsenic, colloidal silica, mercury and selenium (Saridede, Çizmecioglu and Değerli, 2005). The application of AA is therefore clearly diverse. However, despite extensive studies relating to the different uses of AA, little data is available for 1-alcohol

removal. As mentioned, the work done by Groenewald (2019) and Bosman (2019) were identified to be the two major sources of alcohol adsorption studies and will be referenced frequently in the text.

Various types of AA are available on the industrial market. Two series will be considered in this literature review, including F200 and SCDx. The F-200 series comprises a smooth uniform sphere (BASF, 2009). This uniformity and sphericity are considered to be valuable properties, as they prevent adsorbent segregation and minimise channelling resulting in more efficient use of the entire desiccant (BASF, 2009). This brand of AA is known for high crush strength, which allows for the use of taller towers; it is highly resistant to amine attack and is particularly useful for the dehydration of acid containing liquid and gases (BASF, 2009). Additional beneficial properties include low abrasion, which results in less dust collection during transport while minimising pressure drops and downstream issues because of plugging. It is known for its use in acid removal, adsorption of highly polar compounds such as alcohols and hydrocarbon adsorption (BASF, 2009). The F-200 series contains F220 adsorbents, of which the structural properties are presented in Table 4.

The Selexsorb series consists of smooth, spherical adsorbents deemed to be appropriate for the removal of polar molecules such as water, oxygenated hydrocarbons, ketones, aldehydes, oxygenates mercaptans, sulphides and nitrogen-based molecules. It is typically available in three nominal sizes: spheres that measure 1/16', 1/8' and 3/16' (Silva *et al.*, 2007). Within the Selexsorb series one finds SCDx and SCDx of which the structural properties are compared in Table 4 (BASF, 2014).

Table 4 BET results for adsorbent types taken under consideration. These were determined using laboratory BET analysis techniques at the analytical laboratory of Stellenbosch University.

Specific adsorbent type	BET surface area (m ² .g ⁻¹)	Pore volume (cm ³ .g ⁻¹)	Pore size (Å)
F220 1/8' (3 mm)	306	0.424	55
SCDx 1/8' (3 mm)	410	0.46	45
SCDx 1/8' (3 mm)	448	0.493	44

Table 5 illustrates a comparison of the elemental composition of SCD, SCDx and F-200. The data were obtained by means of EDX analysis by Bosman (2019). Given that the same adsorbent manufacturer will be used in the present work, the composition is assumed to be similar with negligible differences. The study is focused on building upon and filling the gaps in the work of Groenewald (2019) and Bosman (2019), as indicated, and this approach is therefore considered to be sound. The differences in composition between all three variants are of greater importance than their absolute composition. Table 5 shows that F220 comprises only carbon and aluminium oxide, whereas the Selexsorb series contains additional sodium and silica. F220 possesses a higher crush strength and bulk density, in contrast with the Selexsorb series. However, the Selexsorb series has a larger surface area. Upon comparison of the BET surface area (Table 4) and that provided by the BASF manufacturers (Table 5), the absolute surface areas are found to differ, but the trend observed is similar.

Table 5 Comparison of SCD, SCDx and F220 manufactured and supplied by BASF (BASF, 2009, 2014; Bosman, 2019).

Properties	SCD	SCDx	F220
Chemical composition (mass%)			
Aluminium (mass%)	43.7	41.9	47.5
Oxygen (mass%)	46.1	43.3	49.5
Sodium (mass%)	1.30	1.70	-
Carbon (mass%)	2.30	2.80	3.00
Silica (mass%)	6.60	10.3	-
Surface area 1/8' (m ² .g ⁻¹)	410	450	350
Crush strength (kg)	11	11	14
Bulk density (kg.m ⁻³)	697	665	769

2.2.3 Adsorbent selection

As discussed in Section 2.2.2, the adsorbents to be considered here are as follows.

- AA F220
- SCD 1/8'
- SCDx 1/8'

All three adsorbents are known to have a high affinity for organic molecules. Extant literature regarding the adsorption of alcohols in these adsorbents is limited. However, the overall consensus is that AA displays high capacities for long and short chain alcohols (Bosman, 2019; Groenewald, 2019; Meshcheryakov *et al.*, 2021). According to Groenewald (2019), all three adsorbents successfully removed 1-hexanol, 1-decanol and 1-octanol from an n-decane solution (Groenewald, 2019). Although AA F220 marginally outperformed the other two adsorbents, Groenewald (2019) and Bosman (2019) found that all three adsorbents were able to remove 1-hexanol, 1-decanol and 1-octanol in binary component systems. In these systems, SCDx and SCD marginally outperformed AA F220 (Bosman, 2019).

The differences in adsorption capacity and adsorption efficiency achieved by using these adsorbents in single component and binary component systems appears minimal. An aim of the present study is therefore to characterise the adsorption behaviour of 3,7-DMO in a single component system and 1-octanol&3,7-DMO and 1-decanol&3,7-DMO in a binary component one. The focus of the study on a single adsorbent is further justified by the similarities in performance.

In light of the findings of these two researchers, it was decided to focus on a single adsorbent and the most industrially relevant adsorbents. SCD is the more recent adsorbent to feature on the market. According to the BET results it has a larger surface area than F220. Its pore volume is also larger, although its pore size is smaller. However, it is hypothesised that the combination of a larger surface area and smaller pore size may be more favourable. Bosman found that, for binary systems, Selexsorb was

favourable, and the bulk of this study is related to binary systems. As mentioned in Section 2.4.3, SCD and SCDx present 'slit-shaped' pores which have not been studied extensively (Harrison *et al.*, 2014). Given the consideration of the lacuna in extant literature in addition to an effort to ensure industrial relevancy, it was decided to focus solely on SCD. This decision was supported by a preliminary experiment conducted at 25 °C and an initial concentration of 3.3 mass% of 3,7-DMO which was contacted with SCD, AA F200 and SCDx, as shown in Appendix A.1. The difference in adsorbate loadings for the Selexsorb range was found to be minor but SCD achieved higher adsorbate loadings and was thus established as the most suitable adsorbent for this study.

2.3 Adsorbate

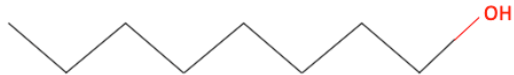
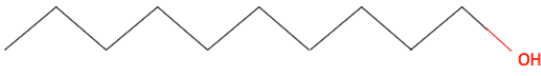
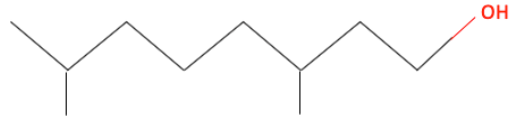
The affinity of an adsorbent to a certain adsorbate is dependent on its physical and chemical characteristics, including molecular weight, size, shape and polarity (Gautam *et al.*, 2014). It is important to assess the physiochemical properties of the adsorbate molecules, as this has a direct effect on the capacity and rate of adsorption (Zotov *et al.*, 2018).

2.3.1 Molecular properties of adsorbate

The molecular dimension and conformation of the adsorbate control accessibility to pores and dictate how well the adsorbate interacts with the adsorbent (Vlugt, Krishna and Smit, 1999). It has been established that the adsorption rate decreased with increasing molecular size (Kose, 2010; Bosman, 2019). Vlugt, Krishna and Smit (1999) investigated the adsorption of hydrocarbons and found that most linear alkanes displayed Langmuir adsorption isotherm behaviour, while certain larger alkanes (hexane & heptane) showed inflection points. This underscores the importance of reviewing the molecular weight and chemical structure of the three alcohols considered in this project, as illustrated in Table 6 (see Abrams *et al.*, 1984; USDA, 2016).

Alcohol chain length and molecular weight are linked and influence the interactions of the molecule with the adsorbent. Bosman (2019) found that, albeit only marginally so, short chain alcohols (1-hexanol & 1-octanol) adsorption was better than that of long chain alcohols such as 1-decanol. This indicates that shorter molecules are favoured over longer molecules, but this finding does not speak to the effect of nonlinear or branched molecules. It is suspected that the rate of adsorption in a single 3,7-DMO system is slower than that of 1-octanol, which will be confirmed through kinetic studies (Zotov *et al.*, 2018). The molecular properties directly influence the adsorption capacity: if the interaction between the adsorbent surface and adsorbate molecule is not favourable or pore sizes do not correspond to adsorbate sizes, the adsorbate loading will be limited (Pfnür, Feulner and Menzel, 1983).

Table 6 Molecular properties of 1-octanol, 1-decanol and 3,7-DMO.

Chemical	Formula	Molecular weight (g.mol ⁻¹)	CAS number	Chemical structure
1-octanol	C ₈ H ₁₈ O	130.23	111-87-5	
1-decanol	C ₁₀ H ₂₂ O	158.28	112-30-1	
3,7-DMO	C ₁₀ H ₂₂ O	158.28	106-21-8	

A study that reviewed the adsorption of VOCs (volatile organic compounds) onto AA found that the exact structure and functional groups of the adsorbate can result in specific interactions with a given adsorbent (Díaz *et al.*, 2004). AA interacts well with polar molecules. Due to the (-OH) functional group attached to each alcohol, 1-decanol, 3,7-DMO and 1-octanol are all considered to be somewhat polar. According to extant research (Bosman, 2019), AA has a high affinity for both 1-octanol and 1-decanol. No studies however evaluate the adsorption capacity of AA for 3,7-DMO. It should be noted that more than 75 isomers of 1-decanol exist. This isomer was chosen in the present study on account of its two branches and its backbone similarity to 1-octanol, its industrial application and the fact that it is readily sourced at low cost. These alcohols will be present (in low concentrations) in an alkane solution. Alkanes are nonpolar molecules and, although all three AA variations are capable of adsorbing hydrocarbons, it is suspected that polar molecules will be favoured and negligible amounts of alkane will be adsorbed. The aim of the present study in this regard is to purify the n-decane solution so that disregarding small amounts of adsorbed alkane is considered acceptable.

Alcohols have higher boiling points than their alkane counterparts. This is due to the intermolecular forces associated with hydrogen bonds which are stronger than the Van der Waals forces present in alkanes. This gives rise to the question as to why adsorption was used instead of distillation. However, distillation processes have high energy requirements and subsequent high operating costs. If the concentration of alcohols in an alkane stream are low enough to use adsorption methods and the adsorption capacity complies with the concentration of alcohols present, adsorption is preferred.

2.3.2 Linear versus branched molecules

As discussed in Section 2.4.1, the rate and adsorption capacity of short chain alcohols was faster and better than that of long chain alcohols. To expand on this, cases where alcohol chain length or molecular

weight is equal, while one component is branched and another linear should be considered. This is the case for 1-decanol and 3,7-DMO (as shown in Table 6 above). Bosman (2019) speculated that the reason for better adsorption of short chain alcohols was due to the fact that smaller molecules diffuse with greater ease (Bosman, 2019). Assuming that the size of molecules affects adsorption, it may be concluded that the shape/ configuration of adsorbate molecules will also influence adsorption. The chemical structure provided in Table 6 shows that 1-decanol is linear and long, while 3,7-DMO is shorter but wider due to the branched nature of the molecule.

Kose (2010) investigated the adsorption of synthetic organic compounds onto activated carbon and found the adsorption uptake increased with decreasing molecular size. In the case of a binary system containing 1-octanol and 3,7-DMO, the former is of lower molecular weight, linear and more cylindrically shaped than the latter compound (Maccallum and Tieleman, 2002). The adsorption capacity of 1-octanol in a single component system is anticipated to be greater than that of 3,7-DMO. However, in a binary system, 3,7-DMO may block pores, thus reducing the 1-octanol uptake. A binary system containing 1-decanol and 3,7-DMO is more complex, as the molecular weights are equal while the shape different. It is suspected that molecular shape and pore compatibility play significant roles in the adsorption process.

It has been found that nonplanar molecules have an advantage over planar molecules, as they are generally more flexible and can thus access deeper regions of the pores, in contrast with molecules of a greater rigidity (Kose, 2010). Alcohols are described as nonplanar, as they are sp³-hybridised. Properties of sp³ hybridised molecules include a tetrahedral geometric shape, 109.5° bond angle and single bonds. The presence of single bonds is suspected to aid the flexibility of compounds (Wick, Martin and Siepmann, 2000). Bosman (2019) investigated the pore shapes of AA F220, SCD and SCDx and, since the same adsorbent from the same manufacturer, the results are considered suitable for the present study. These indicated that the pore size and shape of AA F220 were not well-defined, while those of SCD and SCDx could be classified as 'slit-shaped pores' (Wang and Yang, 2004; Bosman, 2019; Wang and Guo, 2020). For this reason, 1-decanol (which is linear and more cylindrically shaped) may be more compatible with the pore shape of SCD and SCDx compared to 3,7-DMO. However, a study of branched versus linear alkanes found that, in some cases, the branched alkane loading was higher due to more efficient packing within the pores (Harrison *et al.*, 2014).

2.3.3 Adsorbate selection

Groenewald (2019) focused on three different alcohols (1-hexanol, 1-octanol and 1-decanol) and one alkane (n-decane), and performed kinetic and equilibrium studies on single component systems. Bosman (2019) considered the same three alcohols and alkane and performed largely binary component studies. In view of the limited data available around these issues, it was decided to also focus on n-decane and similar alcohols within the ambit of the present project. It is considered here to be more beneficial to have a detailed understanding of how different types of 1-alcohols interact with SCD, instead of attempting to understand a multitude of different systems. 3,7-DMO was selected to this end, as it is a product commonly used as a fragrance ingredient in shampoos, deodorants, soaps and other toiletries

as well as in common household items such as cleaning materials and detergents (Lapczynski *et al.*, 2008)—as indicated.

It was further decided to examine two different systems, since Bosman (2019) investigated the binary systems comprised of 1-octanol and 1-decanol (. As mentioned in Section 2.4, molecular properties and characteristics (such as functional groups or branched versus unbranched) play a key role in the affinity and adsorption capacity of one component versus another. Therefore, these alcohol combinations were selected to gain insight into the effect of these properties as indicated in Table 7. The common denominators in the two systems include the solvent (1-decane) and the 3,7-DMO.

Table 7 Two systems to be considered with justification of selection.

Alkane	Alcohol, alcohol	Justification
n-decane	3,7-DMO, 1-octanol	Effect of two alcohols, an unbranched mixed with a branched alcohol of different molecular weight. Both have the 1-octanol backbone, but 3,7-DMO has two additional branches.
n-decane	3,7-DMO, 1-decanol	Effect of two alcohols of equal molecular weight (isomers) that differ in shape: 1-decanol is a linear molecule while 3,7-DMO takes on an L-shape with two protrusions.

The analysis and interpretation of binary component information requires single component data of each adsorbate present. Single system data for 1-octanol and 1-decanol in an n-decane solution was collected by Groenewald (2019) and Bosman (2019), and these results will be used with a view to fitting the binary component isotherm models. However, single component system data for 3,7-DMO were lacking, and were thus generated here. Generating single component data is useful, as it increases understanding of adsorbate-adsorbent interactions while it also determines interaction effects, as mentioned in Section 2.5.3.

2.4 Multicomponent adsorbate system

It should be noted that some molecules, although small enough, may still not adsorb or diffuse into the pores of the adsorbent. The adsorption of one solute as opposed to another may be due to surface charge, different functional groups, size and structure as well as the adsorbent surface porosity and active sites available (Girish, 2017). Multicomponent adsorption involves a more complex adsorption mechanism than single component adsorption.

A study investigating the adsorption of multicomponent heavy metal systems found that the adsorption capacity for each component in a single versus multicomponent system varied (Padilla-Ortega, Leyva-Ramos and Flores-Cano, 2013). Adsorption sites are occupied sequentially filling the highest energy sites first and then progressing to the lowest energy sites with increasing adsorbed solute concentration (Chiou, 2003). It is known that the surface site of a solid cannot be shared by two or more different kinds of adsorbates: thus, competitive adsorption is a common occurrence (Chiou, 2003). Competitive adsorption is a broad term that encompasses different phenomena that occur in a multicomponent system. These phenomena include displacement effects and the two main multicomponent adsorption mechanisms known as pore blockage and direct site adsorption (Mouelhi *et al.*, 2016).

2.4.1 Multicomponent adsorptive mechanisms

Competitive adsorption often occurs when one component competes with another by reducing the sorption rate or the equilibrium capacity of the second compound (Mouelhi *et al.*, 2016). Three main competitive adsorption mechanisms exist: direct site competition, pore blockage and hydrophobic interactions. A secondary component may tend to preferentially adsorb despite the initial concentration of a primary component exceeding the former as a consequence of these mechanisms individually or in combination. This would imply that the secondary component has a higher intrinsic affinity for the adsorbent in question (Lin *et al.*, 2015). A good reason therefore exists for evaluating different mixture ratios for binary component systems (see Section 3.4).

Direct competition entails that adsorbate molecules compete for active sites within the micropore system (Mouelhi *et al.*, 2016). Site competition between adsorbates typically occurs in the presence of low weight molecules (Lin *et al.*, 2015). It is speculated that the most prominent adsorptive mechanism in a binary system consisting of two adsorbates of equal molecular weight (as is the case for 1-decanol and 3,7-DMO), would be direct site competition. The strength of the competition between adsorbate components is dependent on their relative concentration (Lin *et al.*, 2015).

In multicomponent adsorbate systems it is highly probable that parallel adsorption of both components will be encountered, which results in pore blockage (Aschermann, Zietzschmann and Jekel, 2018). Parallel adsorption is a phenomenon that occurs when different adsorbates are not adsorbed sequentially in a multicomponent system but, instead, both adsorbates interact with the adsorbent at the same time. One adsorbate (e.g. 3,7-DMO) is not adsorbed to capacity first. The second adsorbate (e.g. 1-decanol) is not adsorbed only after this. Instead, both 1-decanol and 3,7-DMO start to fill the adsorbent active sites in parallel. Intraparticle pore blockage generally occurs in high molecular weight adsorptive systems. The mechanism relies on the existence of pore size distribution and variation in adsorbate size (Mouelhi *et al.*, 2016). The larger molecule typically accumulates in the pore systems, particularly in the mesopores, and hinders the diffusion of smaller particles to the adsorption sites located in the micropores (Mouelhi *et al.*, 2016). In the case of adsorbates of different sizes and shapes, parallel adsorption may result in a larger adsorbate molecule moving through the pores that hinders the diffusion of smaller molecules into

the micropores. This is of concern if larger molecules cling to all the surrounding walls reducing the chances of smaller molecules to move through and attach to other wall surfaces.

It has been established, for instance, that parallel adsorption caused DOM resulted in increased OMP desorption (Aschermann, Zietzschmann and Jekel, 2018). It is speculated that the larger molecules (DOM) blocked pores and prevented desorption of smaller molecules and essentially prevented displacement. Aschermann, Zietzschmann and Jekel (2018) speculated that, in some cases, pore blocking compounds could decrease desorption kinetics, while direct competing compounds could increase kinetics (Aschermann, Zietzschmann and Jekel, 2018). This encourages investigation into the primary competitive adsorption mechanism that takes place in a system.

Desorption is known to occur mainly for the following reasons: the displacement of adsorbate from an adsorption site within the pore (Section 2.5.2) or the reverse of adsorption potential (driving force). The reversed adsorption potential would occur when the concentration of the adsorbate on the adsorbent surface is substantially greater than that of the bulk solution engendering a driving force that encourages desorption. The former is defined as competitive adsorption (Aschermann, Zietzschmann and Jekel, 2018). The latter can occur in continuous flow and batch setups, but will where the adsorbate has a high adsorbed concentration versus adsorbate bulk concentration. Desorption as a result of reversed adsorption potential is not investigated in this study, but should be considered in future projects (Bayuo *et al.*, 2020).

2.4.2 Displacement effects

In a multicomponent system, if an adsorbent has a higher affinity for one adsorbate than another, it may be adsorbed by displacing the latter (Chiou, 2003). Mouelhi *et al.* (2016) investigated displacement effects by allowing a single component system containing adsorbate A and the required solution to approach equilibrium. This is termed 'preloading' the adsorbent. Once equilibrated, a given amount of component B was added to achieve the desired initial concentration and the new solution once again allowed to reach equilibrium. The change in the concentration of component A in the bulk solution was monitored (Mouelhi *et al.*, 2016). The macropore system of the adsorbent is typically used to aid displacement (Aschermann, Zietzschmann and Jekel, 2018).

This method can also be used to compare the adsorption curves of component B when exposed to preloaded adsorbent contrasted with a mixture of component A & B exposed to fresh adsorbent (Mouelhi *et al.*, 2016). Direct competition is said to occur when the mixture is contacted with fresh adsorbent. However, in the event of preloaded adsorbent, pore blockage and/ or displacement may occur. This happens when active sites are still available while the pathways are blocked by the pre-loaded adsorbent, which could skew the true displacement potential. Displacement occurs when the pre-loaded adsorbent is knocked off its adsorbed site and replaced with the secondary component. To quantitatively understand the competitive mechanism a ratio system may be used (Mouelhi *et al.*, 2016)—Equation 1:

$$R = \frac{\% \text{removal}_{\text{compA}}}{\% \text{removal}_{\text{compB}}} \quad (1)$$

This is monitored with time (in conjunction with kinetic studies). A spike and then gradual decrease in the R-value would indicate that component A is adsorbed faster than component B.

2.4.3 Interaction effects

These effects and mechanisms all stem from the interaction of adsorbates in a multicomponent system (Girish, 2017). The interactions among adsorbate molecules can be best described as a function of the adsorption capacity of a specific adsorbate when found in a multicomponent system (Q_m) relative to its adsorption capacity in a single component system (Q_i). Three possible interactions are said to occur (Girish, 2017):

- Synergistic interaction ($\frac{Q_m}{Q_i} > 1$): The adsorption capacity of an adsorbent for a specific adsorbate is enhanced in the presence of a multicomponent system.
- Non-interaction ($\frac{Q_m}{Q_i} = 1$): The adsorption capacity remains the same regardless of whether the adsorbate is in a single or multicomponent system. Adsorption capacity of the adsorbent is unaffected by other adsorbate components.
- Antagonistic interaction ($\frac{Q_m}{Q_i} < 1$): The adsorption capacity of the adsorbent for a specific adsorbate is decreased in the presence of a multicomponent system.

Interaction effects can be determined by using experimental techniques as outlined in Section 3.6.1. They emphasize the need for both single and multicomponent data for the project-specific adsorbates used. Consider that, should synergistic or antagonistic interaction be witnessed, the effect on adsorption capacity is expected to be influenced by the initial concentration of the second component relative to that of the competing component. That is, in the case of antagonistic interaction an increase in the second component's initial concentration will result in the decrease of the adsorption capacity of the primary component (Quinlivan, Li and Knappe, 2005).

2.5 Effects of temperature on adsorption

Adsorption is temperature dependent and this influences the adsorbate loading attainable. Temperature effects the strength of the adsorptive forces between the adsorbate molecules and the adsorbent surface (Al-Ghouti and Al-Absi, 2020). Most adsorption processes are known to be exothermic, but some have been found to be endothermic in nature (Al-Ghouti and Al-Absi, 2020). According to Le Chatelier's principle, exothermic operations operated at high temperatures favour desorption more than adsorption. Contrary to this, endothermic processes favour adsorption versus desorption at increased temperatures (Al-Ghouti and Al-Absi, 2020). If the adsorbate loading decreased with increasing temperatures, it is indicative of weaker adsorption forces among the active sites on the adsorbent surface and the adsorbate molecules (Parthasarathy and Narayanan, 2014). If the adsorption process is found to

be endothermic, it is indicative of the adsorbate molecules' need for energy in order to move around and into the pores of the adsorbent (Al-Ghouti and Al-Absi, 2020).

Thus, to increase the adsorbed quantity, system operation should be performed at reduced temperatures. However, in certain industrial processes, the product ought to be purified post-production, which may mean that the product encounters the adsorbent at elevated temperatures. If, at given temperature, the structural integrity of the adsorbent is not compromised, then cooling the liquid to room temperature prior to contact with adsorbent may be uneconomical. Therefore, experiments to determine the performance of adsorbents at slightly elevated temperatures should be conducted. Investigation of adsorption systems at different temperatures improves the accuracy of the system performance and provides insight into the system (Fianu, Gholinezhad and Hassan, 2019).

Bosman (2019) investigated the effect of temperature on primary alcohol adsorption and found that, in the case of single component systems, the equilibrium adsorbate loading increased with increasing temperature. For binary systems, no discernible trend was seen for AA F220, but higher temperatures increased the equilibrium adsorbate loading for SCD and SCDx, which indicate that the adsorption process was endothermic. The endothermic versus exothermic nature of an adsorption process determines the extent of adsorption achieved (Marczewski *et al.*, 2016). If the adsorption process is endothermic in nature, the system should be operated at higher solution temperatures to achieve higher equilibrium adsorbate loadings. On the contrary, if the adsorption process is exothermic in nature the solution temperatures should be lower to promote higher equilibrium adsorbate loadings.

The mechanism and kinetics of adsorption are also temperature dependent. Physisorption and chemisorption is related the bonding mechanisms and subsequent kinetics of adsorption. Chemisorption requires activation energy, which is defined as the minimum energy required to cause a chemical reaction (Ebelegi, Ayawei and Wankasi, 2020). Thus, an increase in system temperature would supply the energy required for the transfer of electrons and, as such, an increased system temperature would promote faster adsorption. In contrast, physisorption increases with a decrease in temperature, because physisorption occurs on account of weak Van der Waals forces. This means that. if the adsorption rate increases with an increase in temperature, the primary mechanism of is chemisorption. In contrast, if the adsorption rate decreased with an increase in temperature physisorption is the primary mechanism of adsorption.

Another possibility to consider is flexibility within the adsorbent framework. Relating to the adsorption of xylene isomers it was found that changes in temperature can affect the adsorbent structure, which effects adsorption (Agrawal *et al.*, 2018). However, this seems unlikely in terms of the present project, as AA is known to be stable at high temperatures.

2.6 Adsorption quantification

The purpose of adsorption has been extensively explained in preceding sections. These demonstrate that the main concern is the amount of adsorbate that can be captured for a certain quantity of adsorbent

used in a given system. Therefore, a mathematical equation to quantify the amount adsorbed is required (Equation 2) (Dada *et al.*, 2012):

$$q_t = \frac{V(C_o - C_e)}{m_{ads}} \quad (2)$$

Where 'q_t' is the amount adsorbed or the adsorbate loading (mg.g⁻¹), 'V' is the volume of the bulk solution (ml), 'm_{ads}' is the mass of adsorbent used (g) and C_o and C_e are the initial and equilibrium concentrations of adsorbate in the bulk solution (mg.ml⁻¹).

It is important to sustain focus on industrial application. In industry, the removal efficiency would be of great interest (Equation 3 below):

$$\%Sorption = \frac{(C_o - C_e)}{C_o} \cdot 100 \quad (3)$$

2.6.1 Equilibrium versus maximum capacity

If the solution/ adsorbate is brought into contact with the solid surface for an extended time, the system approaches equilibrium. This state is defined by an equal distribution of adsorbate between the bulk fluid and adsorbent surface, and can be qualitatively defined (Foo and Hameed, 2010) as the ratio between the adsorbed amount relative to the remaining amount in solution. It is achieved when an adsorbate containing phase has been contacted with an adsorbent surface for an ample period of time (Foo and Hameed, 2010). The adsorbate concentration in the bulk solution is said to approach a dynamic balance with the solid interface concentration. Section 2.7 provides mathematical correlations pertaining to this. The equilibrium behaviour is expressed in terms of the partial pressure (gaseous adsorption) or concentration (liquid adsorption) at a fixed temperature and pressure. Models that predict such equilibrium behaviour are defined as isotherms.

Maximum capacity is defined as the maximum amount of adsorbate that the adsorbent can hold. This ignores the system temperature, operating conditions or bulk concentration involved. Maximum capacity is focused instead on the theoretical adsorption limit towards which all adsorbate-adsorbent systems will tend. The comparison of equilibrium versus maximum capacity is valuable. If the equilibrium capacity is far removed from the maximum capacity, it indicates that the adsorbent-adsorbate system should be re-evaluated. The equilibrium adsorption capacity can be increased by increasing the mass of adsorbent contacted with the adsorbate containing solution. If the solution mass (i.e. mass of adsorbate in the bulk solution) remains the same but the mass of adsorbent present is increased then the equilibrium adsorption capacity may increase on account of increased adsorption sites and a larger surface area (Wang, Wang and Ma, 2010). This modification would not necessarily promote the equilibrium capacity approaching the maximum adsorption capacity. The maximum adsorbent capacity is independent of the mass of adsorbent present in the system whereas the equilibrium capacity is a function of the mass adsorbate present compared to the mass of adsorbent present. Some of the changes that could be implemented to reduce the gap between the equilibrium and maximum capacity are as follows.

- The adsorbate or adsorbent type could be changed:
 - If the adsorbent has a high affinity for polar molecules versus non-polar molecules then it should be ensured that if the adsorbate (1-alcohol) in question is polar or slightly polar it should be in a solution where the majority of the solution consists of non-polar molecules (alkane) to limit the competition for active sites.
- The operating conditions can be modified to promote increased adsorption. Scenarios where this is appropriate includes:
 - Increasing or decreasing the mixing speed to eliminate dead zones or vortices. If the mixing speed was initially too low and dead zones were encountered, then the equilibrium adsorbate loading would be further removed from the maximum adsorbate loading.
 - Increasing the initial adsorbate concentration such that the majority of the active sites are filled and the equilibrium adsorbate loading approaches the maximum adsorbate loading.

2.7 Adsorption kinetic models

The understanding and investigation of the adsorption process for a specific adsorbate(s)-adsorbent system is improved by studying adsorption kinetics. Kinetic models relate the adsorbate uptake rate to the bulk solution concentration (Subha and Namasivayam, 2008). Kinetic studies consider the dynamic element of adsorption taking into account the rate of reaction and, in turn, the reaction mechanism of the process (Marais, 2008). These studies establish the adsorbate uptake rate and are also used to confirm the residence/ contact time required to achieve maximum adsorbate loading on the adsorbent (Qiu *et al.*, 2009). This is useful for determining the scale of the adsorption apparatus required for pilot-plant or industrial applications (Qiu *et al.*, 2009).

Adsorption kinetic models can be classified into two distinct groups: adsorption diffusion and reaction models (Qiu *et al.*, 2009). Although both models describe the adsorption process, the fundamentals are different in each case (Qiu *et al.*, 2009). Adsorption diffusion models account for the following three steps in the adsorption process: diffusion across the liquid film (external/ film diffusion); diffusion in the pores and along the pore walls (internal diffusion); and adsorption between the adsorbate and active sites (Lazaridis and Asouhidou, 2003). Adsorption reaction models, on the other hand, were developed from chemical reaction kinetics and use the rate law to describe the adsorption process (Ho and McKay, 1999; Kurniawan *et al.*, 2011). These models account for the adsorption process without considering the three steps involved in the adsorption diffusion models (Qiu *et al.*, 2009). Evaluation of adsorption-kinetic models in both categories give insight into the rate limiting step as well as surface reaction kinetics.

Bosman (2019) modelled single and binary component systems consisting of 1-decanol, 1-hexanol and/or 1-octanol using both adsorption reaction and diffusion models. It was found that the pseudo-second-order model fitted the data best; however, intra-particle diffusion (IPD) models also provided a good fit. Bosman (2019) proposed that the rate-limiting step was a combination of external mass transfer (EMT), IPD and surface reaction. Therefore, both types of adsorption kinetic models will be investigated in the present study: Lagergren's pseudo-first-order and pseudo-second-order model and Elovich model

(adsorption reaction models); and Weber and Morris model (WMM) (adsorption diffusion model) will be evaluated.

2.7.1 Pseudo-first-order

The Lagergren pseudo-first-order model is an adsorption reaction one that was originally expressed as shown by Equation 4 (Lagergren S.K., 1989). The equation is commonly used in the form of Equation 5 (Trivedi, Patel V.M. and R.D., 1973; Ho and Mckay, 1998). This is a one-parameter model which is computationally simple to use (Ezzati, 2020). It is widely used to describe the adsorption of adsorbate from a liquid phase solution (Chakrapani *et al.*, 2010). For the derivation of the pseudo-first-order model, refer to Ho and McKay (1998).

$$\frac{dq_t}{dt} = k_1(q_e - q_t) \quad (4)$$

$$q_t = q_e(1 - e^{-k_1 t}) \quad (5)$$

Where ' q_e ' is the amount of adsorbate loaded onto the adsorbent at equilibrium (mg.g^{-1}), ' q_t ' is the amount of adsorbate loaded onto the adsorbent (mg.g^{-1}) at time ' t ' (min), while ' k_1 ' is the pseudo-first-order rate constant (min^{-1}).

2.7.2 Pseudo-second order

The pseudo-second-order model is a modification of the first-order model and is presented as Equation 6 (Ho and Mckay, 1998). For the derivation of the pseudo-second-order model, refer to (Ho and Mckay, 1998).

$$q_t = \frac{k_2 q_e^2 t}{1 + k_2 q_e t} \quad (6)$$

Where ' k_2 ' is the pseudo-second order rate constant ($\text{g.}(\text{mg.min})^{-1}$), ' q_e ' is the amount of adsorbate loaded onto the adsorbent at equilibrium (mg.g^{-1}) and ' q_t ' is the amount of adsorbate loaded onto the adsorbent (mg.g^{-1}) at time ' t ' (min).

This model is used widely, and assumes that the target trace organic compounds are the only adsorbates present in the system (Ho and Mckay, 1998). It also assumes that the adsorptives are the compounds that participated in competitive adsorption, while all parameters identified during batch experiments are constant throughout the adsorption process (Ho and Mckay, 1998).

2.7.3 Elovich

The Elovich model (Low, 1960) is known as a reaction model and the shape of the model curve is in most cases representative of the kinetics of chemisorption (Low, 1960; Turner, 1975; Cho, Chu and Kim, 2015). In other words, when adsorption occurs without desorption of the adsorbate, and the rate of reaction decreased with time because of increased surface coverage, the Elovich model describes the system well

(Aharoni and Tompkins, 1970). It has also been found to cover a wide range of low adsorption rates while accounting for heterogeneous surfaces. The Elovich model is represented by Equation 7 (Low, 1960).

The model is based on the following assumptions: sorption occurs at localized sites, interaction occurs between the sorbed molecules and the energy of adsorption increases linearly with surface coverage (Low, 1960). Additionally, the concentration of adsorbates in the bulk fluid are in excess and chemisorption is the primary mechanism of adsorption (Wu, Tseng and Juang, 2009).

$$q_t = \frac{1}{\beta} \ln(\alpha \cdot \beta \cdot t) \quad (7)$$

Where ' α ' is the initial chemisorption rate ($\text{mg.g}^{-1}\text{min}^{-1}$), ' β ' is the extent of surface coverage and activation energy involved in chemisorption (g.mg^{-1}) (Sumalapao *et al.*, 2016), ' q_t ' is the amount of adsorbate loaded onto the adsorbent (mg.g^{-1}) at time t (min). Chien and Clayton (1980) found that as ' β ' decreased and ' α ' increases the reaction rate also increases.

2.7.4 Weber and Morris

The WMM is used to determine whether the rate controlling step is intraparticle diffusion (Chakrapani *et al.*, 2010). The model equation is provided in Equation 8 below (Weber and Morris, 1963). The model does not consider the bulk adsorbate concentration and is based on the assumptions that internal diffusion of the adsorbate is the slowest/ rate-limiting step and that adsorption is instantaneous (negligible external mass transfer) or that external mass transfer takes place rapidly at the start of the process.

$$q_t = k_{ip} t^{0.5} + C \quad (8)$$

Where ' k_{ip} ' is the intraparticle diffusion rate constant ($\text{mg.g}^{-1}\text{min}^{-1/2}$), ' q_t ' is the amount of adsorbate loaded onto the adsorbent at time t (mg.g^{-1}) and ' C ' is the intercept which provides a qualitative indication of the boundary layer thickness (mg.g^{-1}).

When $C = 0$, it indicates that intraparticle diffusion is the rate-limiting step. If $C \neq 0$, it indicates that the effect of the boundary layer on the adsorption process is not negligible. It should be noted that ' C ' does not provide the actual thickness of the boundary layer but rather serves as an indication of whether film diffusion contributes to the rate limiting step or not (Nouri, Haghseresht and Lu, 2002; An, 2020).

The process followed to fit the WMM to experimental data is graphically illustrated in in Figure 4. The experimental determined adsorbate loading (q_t) is plotted versus the square root of time ($t^{0.5}$) generating a curved profile. In such a case, it is not scientifically sound to model the data by using a single straight line. Segmental analysis is required, and the plot can often be divided into 2-3 linearly distinct segments (Fierro *et al.*, 2008). These distinct linear segments are visually identified and Equation 8 is fit to each linear segment using linear regression to determine the intercept (C) and gradient (k_{ip}) of each segment. If there is only one distinct linear segment observed with a y-intercept of 0 ($C=0$) (the experimentally determined profile shown in Figure 4 would then be linear and not curved), the process is said to be solely rate-controlled by intraparticle diffusion. If three distinct line segments are present (Figure 4), the first is

linked the initial rapid surface loading, the second to a combination of EMT and IPD if the y-intercept is non-zero ($C \neq 0$); and the third segment (primarily horizontal) is linked to the equilibrium-reaching stage (Hameed and El-Khaiary, 2008).

The WMM is critiqued by some researchers including Malash and El-Khaiary (2010) because the identification of the linear segments are subjective to the researcher's discretion. Malash and El-Khaiary (2010) developed a statistical method to fit the WMM to experimental data and interpret the results in such a way that minimizes/eliminates the subjectivity of the multi-linear segmental analysis method. This method will not be further outlined nor used in the present study, refer to Malash and El-Khaiary (2010) for more information on this method.

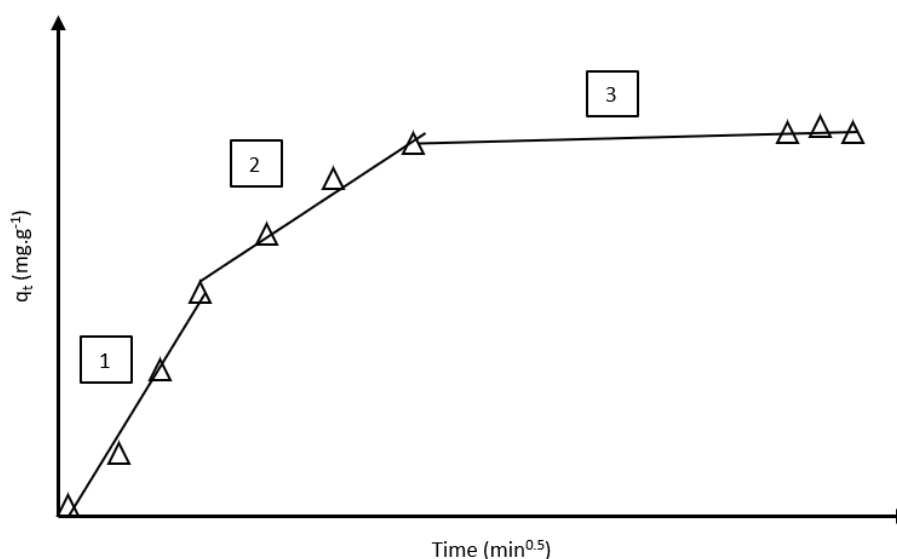


Figure 4 Demonstration of the WMM fit to an arbitrary kinetic profile. Three linear segments are identified with (1) representing film diffusion, (2) intraparticle diffusion and (3) the time taken to reach equilibrium.

2.8 Adsorption equilibrium isotherm models

Adsorption equilibrium isotherms are plots used to describe the relationship at equilibrium between the adsorbate loaded onto the adsorbent versus the bulk concentration of that adsorbate in solution at constant temperature (Webb, 2003; Al-Ghouti and Al-Absi, 2020). The existing adsorption isotherm models were developed based on certain core assumptions regarding the adsorbate-adsorbent system. When the adsorption isotherm models are fitted to experimentally determined data, nonlinear or linear regression is used to determine the model parameters. These parameters describe mechanisms of the adsorption system and, if a model fits data well, it can reasonably be assumed that the core assumptions describe the adsorption mechanism. The three commonly used isotherm models are those of Langmuir, Freundlich and Redlich-Peterson (Subramanyam and Das, 2014). These are to be considered here among others.

Equilibrium isotherm models provide valuable information in terms of the adsorbate, adsorbent, adsorption system and sorption mechanism (Mouelhi *et al.*, 2016). The isotherms developed can follow several different general forms, as illustrated in

Figure 5. The use of isotherms as a method of representing data is a useful tool, and it will be used in this work. Bosman found that all three variations of AA are of Type IV (Bosman, 2019). The latter serves as an indication that the adsorbent has a tendency to be filled in monolayer-multilayer fashion (Thomas and Thommes, 2004). It also indicates that micropores are typically completely filled (Thomas and Thommes, 2004).

Adsorption equilibrium data for a single component can be well-modelled by Langmuir, Freundlich and Redlich-Peterson isotherms (Padilla-Ortega, Leyva-Ramos and Flores-Cano, 2013). Single and binary component systems will be modelled. Single component isotherm models are often the building blocks of most multicomponent system models, so that the two will be discussed in parallel. If the single component models predict the data well it is assumed that the multicomponent models will do the same.

Models with an increased number of parameters may be more accurate than others, but the modelling portion of present project forms part of the secondary aims, so that it was decided to use widely used kinetic and isotherm models that contain only two to three parameters per adsorbate. Models with more than three parameters are typically only applicable to narrow ranges of adsorbate concentration. The models that contain two or three parameters are considered to be more robust and, although accuracy may be sacrificed by using them, they are relevant to industry to a greater degree than models with increased number of parameters. Given this, the focus will mainly be on more robust models here. The derivations of the isotherms are not provided, as these do not form part of the project scope and are not considered to be important for this study.

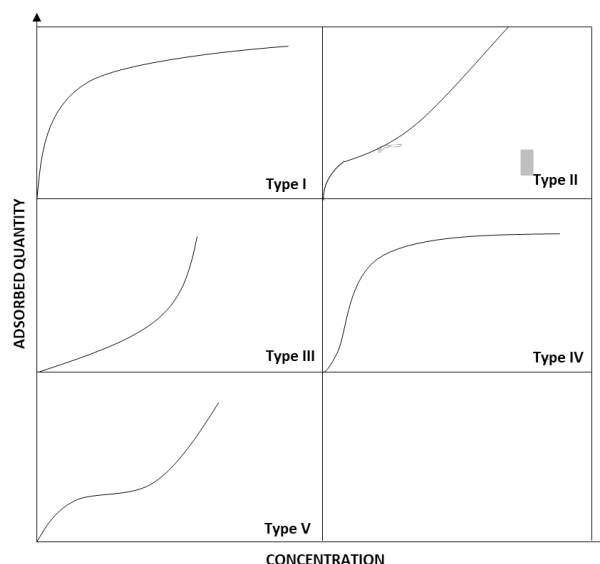


Figure 5 The five different types of adsorption isotherms. Redrawn from (Brunauer, Emmett and Teller, 1938).

2.8.1 Single-component equilibrium isotherm models

The adsorption equilibrium isotherms models outlined in this section are only applicable to single-component, non-competitive adsorption systems. These isotherm models form the basis of multicomponent, competitive adsorption system isotherm models.

2.8.1.1 Langmuir

The Langmuir isotherm is considered to be one of the simplest equilibrium models, while it is known to predict adsorption behaviour well for some systems. This model assumes the following: the surface is homogeneous and flat; all sites are equal in size; an equal distribution of adsorption energy is present; and that rate of desorption equals that of adsorption (Patiha *et al.*, 2016). This isotherm assumes the adsorbate forms a single layer and no interaction occurs between adsorbate molecules, so that the adsorbent bed is said to have a finite capacity.

Adsorption occurs because of interactions between adsorbate molecules and the adsorbent. Five different types of interactions can occur: adsorbent-adsorbate, adsorbate-adsorbate, adsorbate-solvent, adsorbent-solvent and solvent-solvent. A monolayer is formed when the strength of the adsorbate-adsorbent interactions outweighs the strength of the four other types of interactions that may be present. The adsorbed molecule acts as determinants of the position of the next adsorbed molecule. Considering the strong adsorbate-adsorbent bond, the second molecule will adsorb adjacent to the first (maintaining contact with the adsorbent surface) and not above (that is, it is not removed from the adsorbent surface). The Langmuir equation (Equation 9) is given below (Langmuir, 1918).

$$q_e = \frac{q_m K_L C_e}{1 + K_L C_e} \quad (9)$$

Where ' q_e ' is the equilibrium adsorbate loading achieved (mg.g^{-1}), ' C_e ' is this equilibrium concentration (mg.ml^{-1}), ' q_m ' is the maximum adsorbate loading achievable (mg.g^{-1}) and ' K_L ' is a constant related to adsorption/desorption energy (ml.mg^{-1}) (Horsfall and Spiff, 2005).

Although the Langmuir isotherm has its limitations, it is considered to be useful, as it accounts for maximum adsorption capacity of the adsorbent. If the single component isotherm fits the model well, it can be modified to include competitive adsorption and model multi-component systems.

2.8.1.2 Freundlich

The Freundlich isotherm is used to describe heterogeneous surfaces (Equation 10) (Freundlich, 1906). This model is based on an empirical mathematical approximation used originally by Freundlich (1906) and, although it will not be discussed in this dissertation, the derivation can be sourced from the work of Demirbas *et al.* (2004). The Freundlich isotherm model assumes that the adsorbent has a heterogeneous surface and the heat of adsorption is distributed non-uniformly (Freundlich, 1906).

$$q_e = K_f C_e^{\frac{1}{n}} \quad (10)$$

Where ' K_f ' is the Freundlich constant $((\text{mg.g}^{-1}).(\text{ml.mg}^{-1})^{-1/n})$, ' C_e ' is the equilibrium adsorbate concentration in the bulk fluid (mg.ml^{-1}) and ' n ' non-competitive heterogeneity factor. The limitation of this approximation is that the maximum adsorption capacity/ limit is not accounted for (A.O, 2012). ' $1/n_i$ ' serves as an indication of the strength of adsorption. Three possible outcomes of ' $1/n_i$ ' can occur and are interpreted as follows (Freundlich, 1906).

- $\frac{1}{n_i} = 1$, the partition between the two phases is independent from concentration.
- $\frac{1}{n_i} > 1$, cooperative adsorption occurs.
- $\frac{1}{n_i} < 1$, normal adsorption occurs.

2.8.1.3 BET

The BET isotherm is generally applied to gas-solid equilibrium systems and was initially developed to predict multilayer adsorption systems. However, the isotherm was modified to model a liquid-solid interface (Equation 11). This model accounts for monolayer saturation and equilibrium adsorption capacity and has added parameters specific to the BET isotherm (Ayawei, Ebelegi and Wankasi, 2017). The BET model accounts for multilayer adsorption by assuming that interaction between the adsorbent surface and adsorbate molecules is not limited to merely adjacent molecules (Chen *et al.*, 2017).

$$q_e = \frac{q_s C_{\text{BET}} C_e}{(C_s - C_e) \left[1 + (C_{\text{BET}} - 1) \left(\frac{C_e}{C_s} \right) \right]} \quad (11)$$

However, the equation requires three parameters, and thus may be computationally more demanding. If C_{BET} & $C_{\text{BET}} \left(\frac{C_e}{C_s} \right)$ are much larger than 1, the equation can be simplified to Equation 12.

$$q_e = \frac{q_s}{1 - \frac{C_e}{C_s}} \quad (12)$$

The BET model fails to account for surface tension effects and, if these are considered to be noteworthy factors in a given situation, it can be modified, so that the MET isotherm model (Equation 13) should be used instead (Ayawei, Ebelegi and Wankasi, 2017). If c_s/c_e approaches unity, Equation 13 can be simplified to Equation 14.

$$q_e = q_s \left(\frac{k}{\ln \left(\frac{C_s}{C_e} \right)} \right)^{\frac{1}{3}} \quad (13)$$

$$q_e = q_s \left(\frac{k C_e}{C_s - C_e} \right)^{\frac{1}{3}} \quad (14)$$

2.8.1.4 Redlich-Peterson

The Redlich-Peterson model contains fundamental traits of both the Langmuir and Freundlich models. It is an empirical equation with three parameters (Saruchi and Kumar, 2019). On account of the increased number of parameters, it is expected to provide an improved fit when it comes to modelling single

component data. This model can be applied to a wider range of concentrations, and it models hetero- and homogenous systems well. At high concentrations, the model closely resembles the Freundlich isotherm model while, at lower concentrations, it tends towards the Langmuir isotherm model (Singh, Kumari and Balomajumder, 2018). The Redlich-Peterson model is described by Equation 15 below (Redlich and Peterson, 1959).

$$q_e = \frac{k_{RP} C_e}{1 + a_{RP} C_e^g} \quad (15)$$

Where ' k_{RP} ' ($L \cdot g^{-1}$) and ' a_{RP} ' ($ml \cdot mg^{-1}$)^{1/g} are Redlich-Peterson constants, ' g ' is an exponent between 0-1, ' C_e ' is the adsorbate concentration in the bulk solution at equilibrium ($mg \cdot ml^{-1}$) and ' q_e ' is the adsorbate loading onto the adsorbent at equilibrium ($mg \cdot g^{-1}$).

2.8.1.5 Sips

The Sips isotherm (Sips, 1948) is also a combination of the Langmuir and Freundlich isotherm models (Belhachemi and Addoun, 2011). It is calculated by means of Equation 16 (Sips, 1948):

$$q_e = \frac{q_m K_s C_e^m}{1 + K_s C_e^m} \quad (16)$$

Where ' K_s ' is the Sips equilibrium constant ($ml \cdot mg^{-1}$)^m, ' m ' is the Sips constant (where $0 < 1 \cdot m^{-1} \leq 1$), ' C_e ' is the adsorbate concentration in the bulk solution at equilibrium ($mg \cdot ml^{-1}$) and ' q_e ' and ' q_m ' are the equilibrium and maximum adsorbate loadings onto the adsorbent ($mg \cdot g^{-1}$). If m approaches 1, the model approaches the Langmuir isotherm model. As K_s approaches 0, the isotherm reduces to the Freundlich model (Belhachemi and Addoun, 2011).

2.8.2 Binary-component equilibrium-isotherm models

The single-component equilibrium-isotherm models (Langmuir, Freundlich, Redlich-Peterson and Sips) are used to develop binary-component isotherm models, the latter as itemised below.

2.8.2.1 Extended Langmuir

The extended Langmuir model can be applied to multicomponent adsorption systems. It assumes that all active sites and the subsequent adsorption energy are uniform and that adsorbent sites are equally available to all adsorbate species present. Additionally, it presumes that adsorbates do not possess interacting effects (as explained in Section 2.4.3) and all adsorbates adsorb onto identical active sites (Girish, 2017). The model has two parameters, as shown in Equation 17 (Kapoor, Ritter and Yang, 1990):

$$q_{e,i} = \frac{q_{m,binary} K_{L,i(binary)} C_{e,i}}{1 + \sum_{j=1}^N K_{L,j(binary)} C_{e,j}} \quad (17)$$

$$q_{m,binary} = q_{m,i} \theta_i + q_{m,j} \theta_j \quad (18)$$

$$K_{L,i(binary)} = K_{L,i(single)} e^{\frac{\theta_i}{\theta_j}} \quad (19)$$

$$K_{L,j(\text{binary})} = K_{L,j(\text{single})} e^{\frac{\theta_j}{\theta_i}} \quad (20)$$

Where ' $q_{e,i}$ ' is the adsorption loading achieved at equilibrium for component i ($\text{mg}\cdot\text{g}^{-1}$) in the binary component adsorption system, ' $K_{L,i(\text{binary})}$ ' is the Langmuir constant for component i ($\text{L}\cdot\text{mg}^{-1}$), ' $K_{L,j(\text{binary})}$ ' is the Langmuir constant for component j ($\text{L}\cdot\text{mg}^{-1}$), ' $C_{e,j}$ ' is the bulk solution concentration of component j at equilibrium and ' $C_{e,i}$ ' is the bulk solution concentration of component i at equilibrium and ' $q_{m,\text{binary}}$ ' is the combined maximum adsorption capacity of component ' i ' and ' j ' ($\text{mg}\cdot\text{g}^{-1}$). The parameter ' θ ' represents the selectivity of each adsorbate and the fractional adsorbate loading of each component.

It should be noted that the extended model does not adequately account for competitive adsorption and this should be taken into consideration when processing results (Regti *et al.*, 2017). The model is based further on the assumptions that the adsorbent surface is homogeneous (that is, no variability occurs in the surface or energy of adsorption required at each active site) and that no interaction occurs between the adsorbed species with all active sites equally available to all adsorbate species. If this model does not fit the experimental data well, it could suggest that competitive adsorption is prevalent in the binary component adsorption system.

2.8.2.2 Modified competitive Langmuir

As indicated, older multicomponent Langmuir isotherms do not account for interaction effects among various adsorbate components in solution and during adsorption. The modified competitive Langmuir isotherm includes an interaction term (Equation 18) that improves the accurate depiction of the adsorption process by accounting for adsorbate-adsorbate interactions (Wang, Wei and Ma, 2020). The interaction factor accounts for competitive adsorption and shows that the adsorption of one component is dependent on the concentration of the others in solution.

$$q_{e,i} = \frac{q_{m,\text{binary}} K_{L,i} \left(\frac{C_{e,i}}{\eta_{L,i}} \right)}{1 + \sum_{j=1}^N K_{L,j} \left(\frac{C_{e,j}}{\eta_{L,j}} \right)} \quad (18)$$

Where ' $q_{e,i}$ ' is equilibrium adsorption capacity for component i , ' $q_{m,i}$ ' is the monolayer adsorption capacity for component i , ' $K_{L,i}$ ' and ' $K_{L,j}$ ' is the Langmuir constant for component i and j respectively, ' $C_{e,i}$ ' and ' $C_{e,j}$ ' is the bulk solution concentration for component i and j at equilibrium and ' η ' is the interaction parameter which is influenced by the concentration of other components in solution (Girish, 2017).

2.8.2.3 Extended Freundlich

The extended Freundlich model assumes that the adsorbent surface is heterogenous and that interaction takes place between the different adsorbate components in the system (Girish, 2017). The equations are provided below (Equations 19 and 20) (McKay and Al-Duri, 1991).

$$q_{e,1} = \frac{K_{f,1} C_{e,1}^{\left(\frac{1}{n_1}\right)+b_{11}}}{C_{e,1}^{b_{11}} + a_{12} C_{e,2}^{b_{12}}} \quad (19)$$

$$q_{e,2} = \frac{K_{f,2} C_{e,2}^{\left(\frac{1}{n_2}\right)+b_{22}}}{C_{e,2}^{b_{22}} + a_{21} C_{e,1}^{b_{21}}} \quad (20)$$

Where ' $q_{e,1}$ ' and ' $q_{e,2}$ ' is equilibrium adsorption capacity ($\text{mg}\cdot\text{g}^{-1}$) and ' $C_{e,1}$ ' and ' $C_{e,2}$ ' is the bulk concentration in solution ($\text{mg}\cdot\text{ml}^{-1}$) of adsorbate 1 and adsorbate 2. The constants (' b_{11} , b_{12} , a_{12} ' and ' b_{22} , b_{21} , a_{21} ') are the multicomponent (competitive) Freundlich model ones for adsorbate 1 and adsorbate 2 (Srivastava, Mall and Mishra, 2006). ' $K_{f,1}$ ' and ' $K_{f,2}$ ' are the Freundlich constants ($\text{mg}\cdot\text{g}^{-1}$). $(\text{L}\cdot\text{mg}^{-1})^{-1}$ and ' n_1 ' and ' n_2 ' provide the adsorption intensity, all of which is sourced from the single component Freundlich isotherm model.

2.8.2.4 Modified competitive Redlich-Peterson

An interaction parameter is added to the original Redlich-Peterson Isotherm model to show the nature of interaction among the adsorbate components present in the solution (Girish, 2017). The model is represented by Equation 21:

$$q_{e,i} = \frac{k_{RP,i} \left(\frac{C_{e,i}}{\eta_{RP,i}}\right)}{1 + \sum_{j=1}^N a_{RP,j} \left(\frac{C_{e,j}}{\eta_{RP,j}}\right)^{g_j}} \quad (21)$$

Where ' $k_{RP,i}$ ' and ' $a_{RP,j}$ ' are model constants determined when fitting the Redlich-Peterson single component isotherm model to the respective datasets. ' $C_{e,j}$ ' and ' $C_{e,i}$ ' are the equilibrium concentrations of each component in the multicomponent bulk solution and ' g_j ' is an exponent between 0 and 1 that is determined for each component in the multicomponent system by using the single component Redlich-Peterson isotherm model. Finally, ' $\eta_{RP,i}$ ' and ' $\eta_{RP,j}$ ' are the interaction parameters calculated for the various components in the multicomponent system.

2.8.2.5 Extended Sips

The extended Sips isotherm model uses the assumption that the adsorbent surface is homogeneous, as reflected in Equation 22 (Girish, 2017):

$$q_{e,i} = \frac{q_{m,i} K_{s,i} C_{e,i}^m}{1 + \sum_{j=1}^n K_{s,j} C_{e,i}^m} \quad (22)$$

Where ' $q_{e,i}$ ' equilibrium adsorption capacity for component i ($\text{mg}\cdot\text{g}^{-1}$), ' $C_{e,i}$ ' and ' $C_{e,j}$ ' are the equilibrium concentrations of component i and j in the bulk solution ($\text{mg}\cdot\text{ml}^{-1}$), ' $K_{s,i}$ ' and ' $K_{s,j}$ ' are the Sips isotherm equilibrium constants for component i and j, the latter as taken from the single component data ($\text{ml}\cdot\text{mg}^{-1}$), $^{(m)}$ and ' m ' is the Sips model exponent which is dimensionless.

At lower adsorbate concentrations where ' m ' approaches zero, the model approaches the Freundlich one. At higher concentrations, where ' m ' approaches one, the model can be modified to the Langmuir isotherm.

Given that the multicomponent systems of this project contain two components, the respective models for each component are as follows (Equation 23 & 24):

$$q_{e,1} = \frac{q_{m,1} \cdot K_{s,1} \cdot C_{e,1}^m}{1 + K_{s,1} C_{e,1}^m + K_{s,2} C_{e,2}^m} \quad (23)$$

$$q_{e,2} = \frac{q_{m,2} \cdot K_{s,2} \cdot C_{e,2}^m}{1 + K_{s,1} C_{e,1}^m + K_{s,2} C_{e,2}^m} \quad (24)$$

2.9 Model fitting

A decision must be made with regard to using the linear or nonlinear form of the adsorption models. In a study focused on this, it was found that, in the case of a Langmuir isotherm model that was linearised in four different manners, different constants were found on each occasion, as there was a variation in errors (Subramanyam and Das, 2014). Using the linearisation technique provides a simpler method than this that (in some cases) eliminates the need for solver add-in function in Microsoft Excel. However, Subramanyam and Das found that, during linearisation, errors in parameter computation may be responsible for variation in maximum adsorption capacity (2014). So, with the assumption that the transformation of nonlinear to linear alters error functions and error variance, the nonlinearised form of the adsorption models will be used here, except for the WMM, which is used in its linearised form.

Data were collected experimentally for various adsorbate-adsorbent systems. The data collected centred on the concentration of adsorbate remaining in the bulk fluid at specified time intervals. The adsorption capacity could be directly deduced from this information by using a simple mass balance approach, as found in Equation 25. The equation of the isotherm selected was then used and rewritten to ensure that q_e was the dependent variable while C_e was the independent one. The required parameters were then estimated and minimised to the least squares (see Dada *et al.*, 2012).

$$q_{e,i} = \frac{(C_{o,i} - C_{e,i})V}{m} \quad (25)$$

$$\text{Error} = \sum \sum (q_{\text{experimental}} - q_{\text{calculated}})^2 \quad (26)$$

The isotherm equations are presented in Sections 2.7 and 2.8. The adsorption kinetic models and equilibrium isotherm models were fitted by using the Excel Add-In Solver function to perform nonlinear regression analysis by minimising the error between the experimentally determined adsorbate loading and the predicted adsorbate loading. These parameter estimates could then be compared to literature.

The equilibrium model that best fitted the experimental data (where R^2 value is closest to 1) was assumed to describe the adsorbate-adsorbent system most accurately. The assumptions related to the isotherm used were then deemed to be true for the system at hand and, by using this knowledge, scale-ups and future work could be improved upon.

Nonlinear regression was used to estimate parameters and, according to extant literature, it is indeed a valuable tool used for analysing experimental data obtained from adsorption systems. It served as a method for determining the best fitting model and indirectly confirmed the validity of assumptions made.

Various different nonlinear regression methods were available, including sum of squares, hybrid fractional error function, ARE, MPSD, EABS, SNE and the nonlinear chi-square test. The sum of squares method was considered to be the most convenient. However, a major disadvantage was that, at higher concentration ranges of adsorbate, the use of the error function was sound but could nonetheless not be used with confidence at low concentrations. The HYBRID function (Equation 27) improved the discrepancy at low concentrations (Ayawei, Ebelegi and Wankasi, 2017). This function is suitable for lower end liquid phase concentration ranges (Subramanyam and Das, 2014).

$$\text{HYBRID} = \frac{100}{n-p} \sum_{i=1}^n \frac{(q_{e,i,\text{meas}} - q_{e,i,\text{calc}})^2}{q_{e,i,\text{meas}}} \quad (27)$$

Where:

- n – is the number of data points
- p – is the number of parameters

The sum of the squares of the errors (Equation 28) is commonly used for higher-end concentration ranges in the liquid phase and the parameters regressed using this error minimization method will prove more accurate for higher end concentrations (Subramanyam and Das, 2014). The error function will increase as the concentration increases.

$$\text{SSE} = \sum (q_{e,i,\text{calc}} - q_{e,i,\text{meas}})^2 \quad (28)$$

The Marquardt's percent standard error deviation function (MPSD) follows a geometric mean error which accounts for the number of degrees of freedom in the system (Equation 29) (Subramanyam and Das, 2014).

$$\text{MPSD} = \sqrt{\frac{\sum \left(\frac{q_{e,i,\text{meas}} - q_{e,i,\text{calc}}}{q_{e,i,\text{meas}}} \right)^2}{n-p}} \cdot 100 \quad (29)$$

Solver add-in function in Microsoft Excel can be used to minimise Equation 30 to determine the parameters of models mentioned in Sections 2.7 and 2.8. However, this does not provide an indication of the degree of fit of each model. Four parameters can be evaluated to determine the model that best fits experimental data, namely R^2 , R^2_{adj} and SD (Equation 30-32 respectively) (Lima and Adebayo, 2015).

$$R^2 = \frac{\left[\sum_i^n (q_{i,\text{expm}} - \overline{q_{\text{expm}}})^2 - \sum_i^n (q_{i,\text{expm}} - q_{i,\text{calc}})^2 \right]}{\sum_i^n (q_{i,\text{expm}} - \overline{q_{\text{expm}}})^2} \quad (30)$$

$$R^2_{\text{adj}} = 1 - (1 - R^2) \cdot \left(\frac{n-1}{n-p-1} \right) \quad (31)$$

$$SD = \sqrt{\left(\frac{1}{n-p}\right) \cdot \sum_i^n (q_{i,expm} - q_{i,calc})^2} \quad (32)$$

Where n is the number of experiments performed, p the number of parameters of the regressed model, $q_{i,expm}$ the value of q measured experimentally, $q_{i,calc}$ the predicted value of q according to the fitted model and q_{expm} the average of all experimentally determined q 's. The best fit model is the one with the lowest SD or reduced Chi-squared value as well as the model with an R^2_{adj} value closest to unity.

Equations 29-32 are useful, as they provide point to point comparison for kinetic and equilibrium adsorption models. For each experimental point, another point corresponds to a point on the curve. The reduced chi-squared and SD equations can then be used to determine the difference between the experimentally determined value and its corresponding model value. Therefore, the smaller the difference, the better the fit (Lima and Adebayo, 2015). When reviewing the best-fit model, it is necessary to take robustness into consideration. Care must also be taken with respect to R^2 in the event that the range of q values is too large. If this is the case, the average q_{exp} value may result in an R^2 value that is slightly distorted. However, if there is a noticeably even spread of data, the R^2 value would tend towards 1, which may not necessarily be an indication of a truly good fit. The use of reduced chi-squared and SD become important when comparing 2-parameter versus 3-parameter models. The equations with more parameters tend to provide R^2 values that are closer to unity when compared to those with fewer parameters. This could be the case because the model is restricted and accurate to a greater extent. For these reasons, it is recommended that adjusted R^2 be used, as this provides insight into whether the seeming best fit is due to an increased number of parameters or whether the equation truly resembles the system well (Lima and Adebayo, 2015). Both R^2 and adjusted R^2 are of low sensitivity, so it is recommended for use around assessing a combination of R^2 and SD.

2.10 Chapter summary

This chapter provided an in-depth literature review of adsorption and the factors influencing it. An itemised summary of the review is given below.

- Adsorption is a three-step process involving film diffusion, intraparticle diffusion and the final adsorption step.
- The physiochemical properties of adsorbents (surface area, surface chemistry, pore size and shape and PSD) play a significant role in the adsorption process.
- The adsorbate type (organic or inorganic), structure (branched, unbranched and size of functional groups present) and the adsorbate phase all influence adsorption. Therefore, adsorbate properties should correspond to those of the chosen adsorbent.
- Multicomponent adsorption mechanisms typically include pore blockage or direct competition for active sites, but the possibility of displacement and interaction effects should also be considered.

- Various kinetic and equilibrium models are available. Most of these fundamentally similar involving minor adjustments or improvements. The most robust, best-fitting and user-friendly models should be emphasised.
-

Based on this, it was possible to determine parameters, adsorbents and adsorbates to be used, as stipulated in Section 3.2. In accordance with the summary above, the following key decisions were made that will be further explored in subsequent chapters of the present project:

- The adsorbent used in this study will be SCD, and 3,7-DMO will be investigated in a single component adsorption experiment, while two binary systems will be considered (1-octanol&3,7-DMO and 1-decanol&3,7-DMO).
- Multicomponent adsorption mechanisms should be investigated by performing displacement tests and by quantitatively determining the interaction effects.
- The kinetic models that will be considered for the single and binary component adsorption systems are pseudo-first-order, pseudo-second-order, pseudo-nthorder, Elovich and Weber and Morris.
- The equilibrium isotherm models that will be considered for the single component system are the Langmuir, Freundlich, BET, Redlich-Peterson and Sips isotherm models.
- The equilibrium isotherm models that will be considered for the binary component system are the extended Langmuir, modified competitive Langmuir, extended Freundlich, extended Sips and modified competitive Redlich-Peterson isotherms.

Chapter 3 Experimental design and methodology

3.1 Chapter overview

This chapter will focus on the experimental setup and materials to be used in the present project along with the methodology and approach required to perform the experiments needed to address its aims and objectives. The collection of data, data processing methods and uncertainty analysis protocols will also be discussed.

Detailed calculations and methods stipulating data analysis techniques will not be presented in this chapter. However, the methods will be outlined and provided in Appendix A1. The unit of measurement used to track the bulk concentration changes with time was concentration ($\text{mg}\cdot\text{ml}^{-1}$) and mass%. The mass% was favoured where possible, as it was considered to be the most reliable unit of measurement. The concentration ($\text{mg}\cdot\text{ml}^{-1}$) was preferentially used when equilibrium isotherms were generated. Two of the adsorbate types selected were isomers with equal molecular weight (1-decanol and 3,7-DMO), while a third selected adsorbate was of lower molecular weight (1-octanol). A comparison of bulk concentration changes in molar concentrations may be considered suitable when it comes to differences in molecular weights, as the number of molecules adsorbed would then be comparable (as used selectively in Chapter 7). The use of mass concentration is a standard unit of measurement in adsorption. Although the evaluation of bulk concentration changes using molar concentration provides insight into the number of molecules adsorbed, the key interest of this project was to evaluate the removal efficiency of SCD. The removal efficiency was measured in terms of the mass of adsorbate removed per mass of adsorbent and thus the primary unit of measurement was centred on mass.

3.2 Selection of experimental parameter range

Variable parameters were selected according to those identified to be the most critical in the literature review. Temperature and initial adsorbate concentration were identified as the two parameters that will be varied to determine the effect of each on the adsorbate-adsorbent system, each as briefly itemised and discussed below. The mixing speed is an additional parameter but for the scope of the present study it will not be varied. However, it was initially varied to determine the appropriate mixing speed and is discussed below.

3.2.1 Temperature

As discussed, adsorption equilibria and adsorption kinetics are highly temperature dependent. Adsorption generally favours low temperatures due to the exothermic nature of the process. However, Groenewald (2019) and Bosman (2019) found that an increase in system temperature increased the equilibrium adsorbent loading achieved. Groenewald (2019) operated at and measured system temperatures of 25 °C, 30 °C and 35 °C. Bosman (2019) operated at system temperatures of 25 °C and 45 °C. Several other studies showed that some adsorbate-adsorbent systems showed greater adsorption

kinetics and equilibrium adsorbate loading at low temperatures whilst others showed greater adsorption kinetics and equilibrium adsorbate loading at significantly higher temperatures (Mor, Ravindra and Bishnoi, 2007; Vijayakumar, Tamilarasan and Dharmendirakumar, 2012).

In the industry, the alkylation reaction system temperatures generally range from 10-40 °C where the reaction is exothermic (Vora *et al.*, 2003). Therefore, it was decided to maintain operating temperatures within a range of 25-45 °C here. A secondary aim of this study was to fit kinetic and equilibrium isotherm models to single and binary component adsorption systems. Certain binary component isotherm models rely on the single component parameters deduced when fitting isotherm models to single component adsorption data.

The main aim of this study was to define the adsorption of 3,7-DMO in a single and two binary component adsorption system, once more. Thus, the single component adsorption model parameters for 1-octanol and 1-decanol (which are present in the binary component systems) were sourced from literature. Considering that, aside from Bosman (2019) and Groenewald (2019), no other sources were available for the single component adsorption of 1-decanol/ 1-octanol from an n-decane stream using SCD, the operating temperatures that these two authors used were set as the operating temperatures for this study. Bosman (2019) fitted kinetic and equilibrium isotherm models to the single component adsorption data of 1-decanol and 1-octanol onto SCD at 25 °C and 45 °C.

This information, in combination with the need to ensure that the project would be industrially relevant, led to the decision to consider the adsorbate-adsorbent systems at three different solution temperatures for the single component adsorption system (25 °C, 35 °C and 45 °C) and two different solution temperatures for the binary component adsorption systems (25 °C and 45 °C). The solution temperature was maintained constantly for the duration of the experiment, and a ± 0.1 °C fluctuation was observed.

3.2.2 Initial adsorbate concentration

The initial adsorbate (alcohol) concentration range of a typical petrochemical plant is 0.5–3.3 mass% (Vora *et al.*, 2003). Bosman (2019) found that varying the initial adsorbate concentration significantly affected adsorption in the case of single and binary component systems. Therefore, it was decided to perform experiments within the range of 0.5–.3 mass% generating sufficient equilibrium data points to develop the required equilibrium adsorption isotherms.

It was decided to focus on three different initial adsorbate ratios for binary component systems. The initial ratios of adsorbate₁:adsorbate₂ that were used are presented in Table 8.

Table 8 Mixture ratios of binary adsorbate systems.

Mixture ratio (mg:mg)	Note
0.25 : 0.75	Deduce effect of adsorbate ₁ > adsorbate ₂ on kinetics and equilibrium loading
0.5 : 0.5	Deduce effect of adsorbate ₁ = adsorbate ₂ on kinetics and equilibrium loading
0.75 : 0.25	Deduce effect of adsorbate ₁ < adsorbate ₂ on kinetics and equilibrium loading

3.2.3 Mixing speed

The mixing speed was selected by consulting literature and performing some preliminary experiments. Several studies investigating the ideal mixing speed for batch adsorption experiments found that when systems are operated at mixing speeds between 100–400 rpm, the highest percentage of adsorbate removal from the bulk solution was observed at 400 rpm (Javadian *et al.*, 2015; Chatteraj *et al.*, 2016; Darweesh *et al.*, 2022). Bosman (2019) operated at mixing speeds of 350 rpm but based on literature findings it was decided to conduct the present studies at mixing speeds closer to 400 rpm. Preliminary tests were conducted with 10 g of SCD submerged in an n-decane solution containing 2.5 mass% 3,7-DMO at three different temperatures 25 °C, 35 °C and 45 °C. The preliminary tests were conducted at all three temperatures as the solution viscosity decreases with increasing temperature which affects the mixing profile. The water bath was allowed to reach the temperature setpoint, the solution was tested with a thermometer to confirm the setpoint temperature had been reached and the mixing speed was increased in increments of 10 rpm between the range of 380-420 rpm. A mixing speed of 410 rpm was selected because at this mixing speed (at all three temperatures) no vortices formed and at the bottom of the beaker, between the mesh basket and magnetic stirrer bar a good mixing profile was observed, and no dead zones were seen. It was thought that this mixing speed would reduce the boundary layer thickness around the adsorbent particle and allow for equal adsorbate-adsorbent interaction throughout the adsorbent bed.

3.3 Experimental setup

The experimental setup used was designed and constructed by Groenewald (2019). As illustrated in Figure 6, this is a bench-scale setup consisting of beakers that are semi-submerged in a water bath. This method has been used by several researchers to investigate the kinetics and equilibrium data of different adsorbate-adsorbent systems (Özacar, 2003; Quinlivan, Li and Knappe, 2005; Aschermann, Zietzschmann and Jekel, 2018).

The setup consists of 4 main parts (refer to Figure 6): the water bath (items 3 and 6), heater (item 1), magnetic stirrer plate (item 2) and beaker setup (items 4 and 5). The outermost stainless-steel shell

(water bath) houses the heating unit and removable plate (referred to as beaker placeholder plate), which holds the beakers containing the adsorbate-alkane solution in place. A second removable plate (referred to as the outer shell plate) is placed over the beakers covering the entire opening of the water bath with less than 3 mm gaps around the edges. This is put in place to minimize potential evaporation of solution during experiments. For the sake of sampling, ports are present in the outer shell plate and are closed before and after the sampling has been done. Attached to the beaker placeholder plate are hooks which are used to hang the mesh baskets. These mesh baskets house the adsorbents of specific masses and remain submerged in the adsorbate-alkane solution for the duration of the experiment. The magnetic stirrer plate is placed beneath the outer shell of the water bath ensuring that it is near the water bath so as to achieve adequate mixing and ensure the stirrer bars rotation is consistent. The outer shell has a section open to viewing made of plastic and sealed tightly to prevent leaking. This allows the researcher to monitor mixing, water bath and solution levels during experimental runs.

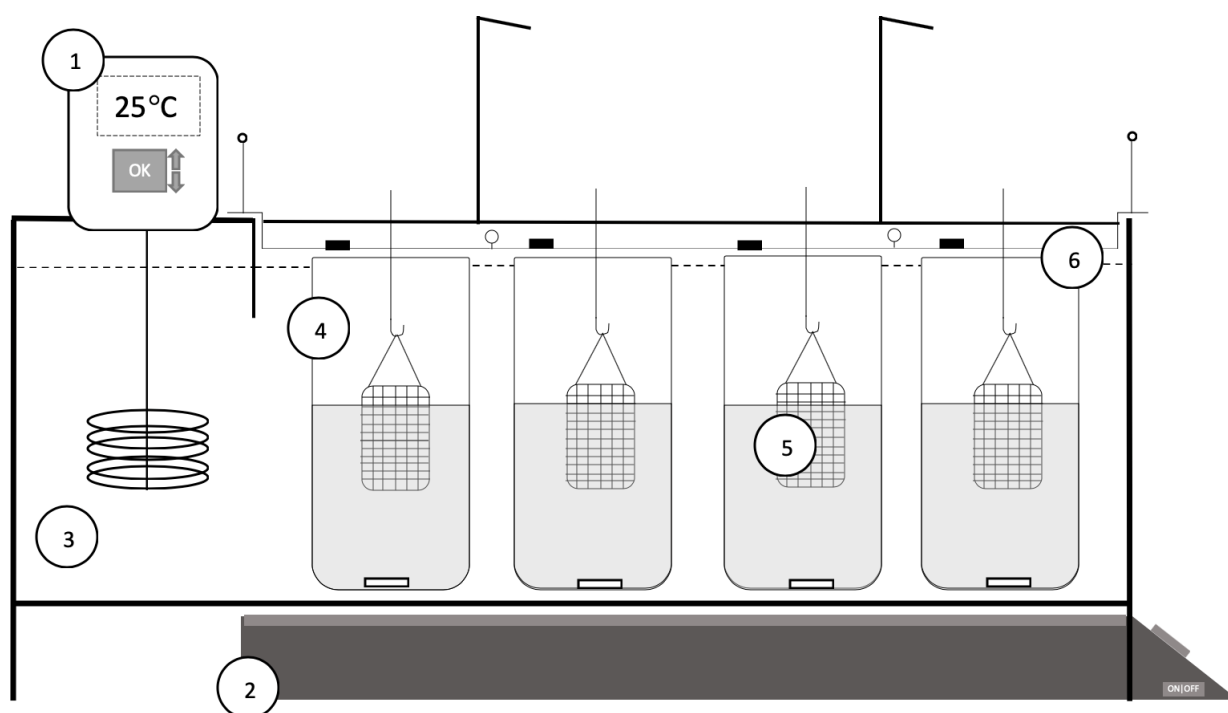


Figure 6 Schematic of experimental setup. Where (1) is the heater with circulation pump, (2) the magnetic stirrer plate (magnetic drive with the magnetic stirrer bars shown placed at the bottom of the beakers), (3) the outer shell of water bath, (4) beakers containing solution and magnetic stirrer bars, (5) mesh baskets containing adsorbent beads and (6) the outer shell plate and beaker placeholder plate that fit on top of one another. Redrawn and adapted from Bosman (2019).

3.4 Experimental plan

The main objectives of the present project were considered around developing the experimental plan. The plan can be broken up into four phases: single component adsorption system experiments, binary component adsorption system experiments, displacement tests as well as data analysis and modelling. Figure 7 schematically illustrates the experimental plan followed.

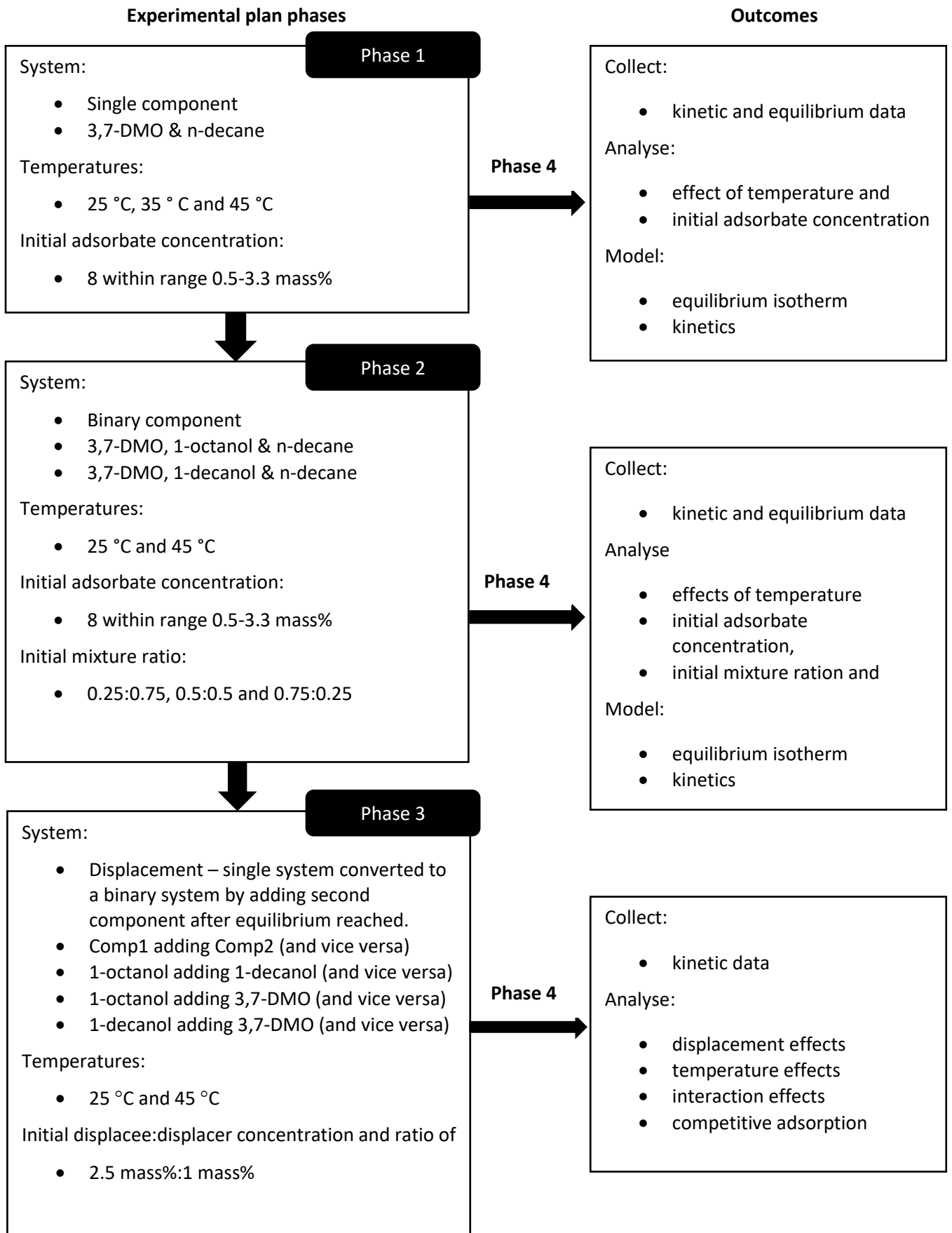


Figure 7 Outline of the experimental plan followed in the present study.

3.5 Materials

The materials required to perform these experiments and collect samples and analyse these are itemised in Table 9. The materials associated with the construction of the experimental setup (Figure 6) will not be reiterated.

Table 9 List of materials required to perform experimental runs and sample preparation for GC analysis.

Materials	Linear formula	Supplier	Product number	Product (mass%) according to supplier	purity according to supplier
<i>Chemicals</i>					
1-octanol	CH ₃ (CH ₂) ₇ OH	Sigma-Aldrich	472328	>99%	
1-decanol	CH ₃ (CH ₂) ₉ OH	Sigma-Aldrich	W236500	>98%	
3,7-DMO	CH ₃ (CH ₂) ₉ OH	Sigma-Aldrich	W239100	≥98%	
n-decane	CH ₃ (CH ₂) ₈ CH ₃	Sigma-Aldrich	30570	>95%	
1-pentanol	CH ₃ (CH ₂) ₄ OH	Sigma-Aldrich	398268	≥99%	
methanol	CH ₃ OH	Sigma-Aldrich	34860	≥99.9%	
<i>Adsorbent</i>					
SCD		UDEC/Sasol			

3.6 Methodology

A broad overview of procedures followed while performing the experiments will subsequently be briefly outlined. The procedures will be discussed according to the four phases reflected in Figure 7 (Section 3.4). Phases 1 and 2 will be discussed together given that the procedure for single component and binary component adsorption systems is the same except for preparation of stock solutions.

The following procedures are discussed in Appendix A.1:

- The preparation of stock solutions
- Start-up and shutdown
- Single component and binary component sampling
- Displacement experiments and sampling
- Sample preparation and GC analysis method

3.6.1 Phases 1 & 2

Phases 1, 2 and 3 all require the same initial steps and will thus not be repeated in Section 3.6.2. The experiments were conducted using the bench-scale water bath (Figure 6). The stock solution (200 ml) for each beaker was made up in accordance with the required initial adsorbate concentration (0.5-3.3 mass%) and, in the case of binary systems, the appropriate mixture. The stock solution was added quantitatively to 500 ml beakers. These were placed in the water bath along with a magnetic stirrer bar

in each. The water bath was set to the desired temperature and the magnetic stirrer plate switched on and set to the 410 rpm mixing speed.

The mesh baskets were prepared by quantitatively adding 10 g of adsorbent to each mesh basket as required. Once the water bath was at temperature, the mesh baskets were hung from the hooks (according to the allocated beaker) and the outer shell plate lowered onto the beaker placeholder plate. Once it had been confirmed that the adsorbent was fully submerged in solution and the stirrer bars were spinning correctly, the outer shell plate was securely fastened with wing nuts.

The experiment was allowed to run for approximately 24 h to ensure that equilibrium was reached. All beakers were used to collect equilibrium data to generate equilibrium adsorption isotherms. Equilibrium was achieved at around 24 hrs and three equilibrium samples taken to ensure an accurate representation of the equilibrium adsorbate loading and bulk solution concentration, and confirm that true equilibrium had in fact been reached. Samples of 400 μ l were withdrawn from each sample port by using a micropipette at 0, 1390, 1420 and 1440 min. The samples were collected in 4 ml vials marked and tightly sealed to be prepared for analysis.

To study the kinetics of the system, more frequent samples were required. Kinetics were only studied for select beakers (lowest, middle and highest initial concentrations) and kinetic samples withdrawn at 0, 15, 30, 160, 240, 360, 480, 1390, 1420 and 1440 min. The samples were collected in 4 ml vials, marked and sealed to be prepared for GC analysis. In between samplings, the ports were closed with plugs to prevent evaporation, and water levels were monitored to ensure that the required water levels were maintained for overnight runs. Often, the kinetic and equilibrium studies were conducted simultaneously. Each water bath had capacity for six solutions and often kinetic samples would be taken for three of the beakers whilst only equilibrium samples were taken for the remaining three beakers. However, the raw data collected from the kinetic samples was also used to contribute to the equilibrium adsorption loading database.

Once equilibrium had been reached, the water bath was switched off and allowed to cool. The mesh baskets containing saturated SCD were removed and the adsorbent properly disposed of. The solutions were decanted into Schott bottles to be re-used later. The purpose of re-using the solutions was to minimise wastage considering how expensive n-decane, 3,7-DMO, 1-octanol and 1-decanol are. It was more economical to analyse the composition of each solution at the end of each experiment and add the required amount of n-decane, 3,7-DMO, 1-octanol or 1-decanol to achieve the required initial solution composition instead of preparing a fresh solution. It was assumed that the maximum 4.4 ml withdrawn was negligible and did not affect the adsorption process as it constituted 2.2 vol% of the original stock solution.

3.6.2 Phase 3

The procedure for phase 3 experiments was similar to those discussed above, except for the fact that the run continued for 48 h rather than 24 h. For the first 24 h, the single component system consisting of the potential 'displacee' and n-decane (initial adsorbate concentration of 2.5 mass%) was allowed to reach

equilibrium with samples taken at 0, 1390, 1420 and 1440 min. Thereafter, an amount of the second component (termed the potential displacer) was added to the system to achieve a 1 mass% initial concentration. This was done after having removed an equal volume from the equilibrated solution to ensure the bulk volume remained constant. The addition and sampling were also done through the sample ports, following the same procedure described in Section 3.6.1. Post addition of the potential displacer, a kinetic study was performed and samples were taken at 0, 15, 30, 160, 240, 360, 480 1390, 1420 and 1440 min. These were collected and labelled as described in Section 3.6.1, and they were subsequently prepared for analysis.

3.6.3 GC sample preparation & analysis

All samples collected were prepared by extracting 400 μl , adding and weighing 20 μl 1-pentanol (internal standard) and diluting the sample twice with HPLC grade methanol in the appropriate GC vials. The prepared samples were then analysed by means of the GC, and the results were used to determine the change in mass percentage, of the adsorbate in the bulk solution, throughout the run.

During the preliminary experimental phase, samples were prepared once, and these were analysed by means of the GC three times to determine the error associated with the analytical analysis technique. Three different samples were also prepared from the same sample withdrawn during the experiment and analysed by means of the GC to determine the error associated with preparation. This was considered in combination with the experimental error.

3.7 Validation of experimental procedures

As mentioned, the experimental procedures followed were similar to those of Bosman (2019) and Groenewald (2019). To validate the results collected and the experimental methodology used in during the current study, it was therefore necessary to reproduce those of previous studies. If the data were reproduced, it would validate the experimental methodology used and in turn results collected in the current study. The following data sets were identified from the work of Bosman (2019) and the required experiments were performed to reproduce the results within the margin of error:

- Single component system: 1-octanol, 1.53 mass%, 45 °C (Figure 8)
- Binary component system: 1-octanol & 1-decanol, 0.5:0.5, 2 mass%, 25 °C (Figure 9)
- Single component system: 1-decanol, 1.63 mass%, 45 °C (Appendix A.1.6)
- Binary component system: 1-octanol & 1-decanol, 0.5:0.5, 2 mass%, 45 °C (Appendix A.1.6)

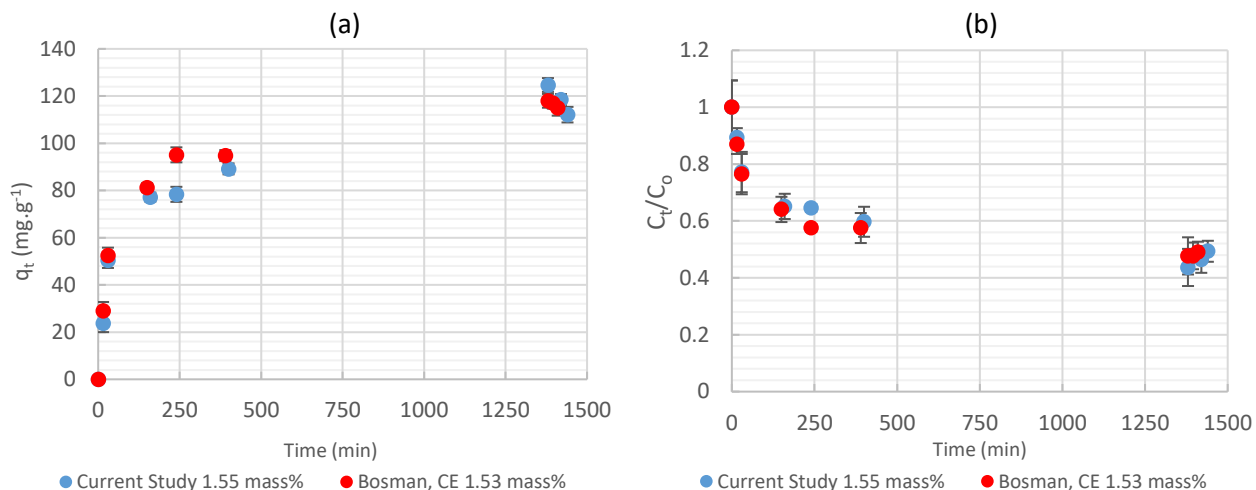


Figure 8 Comparison of validation runs performed to compare the adsorption of 1-octanol from n-decane using SCD at 45 °C with those of Bosman (2019). Figure 8a (left) was used to verify the experimental methodology used and reproduce the concentration profile established by Bosman (2019). Figure 8b (right) was used to verify the experimental and data processing methodology to reproduce the adsorbent loading time profile.

The single and binary component systems were repeated. Figure 8 demonstrates that, in the case of a single component system and within the margin of error, the results achieved in the current study, using the outlined experimental methodology, closely resembled those of Bosman (2019) with a maximum difference of 4 % on the adsorbate loading (Figure 8a) and normalised concentration (Figure 8b). Figure 8 also builds on the verification of the experimental methodology by showing that the data processing methodology used was correct, as the adsorbate loading was found to be a function of the mass fraction. Similar results were noticed when the binary component system results of the work of Bosman (2019) were reproduced. The binary component mass ratios achieved (Figure 9) show that the experimental methodology used gives reproducible results within the margin of error. It is noted that the results were not similar to a degree that was equivalent to those of the single component experiment, but it is assumed that this was due to the compounding effect of small errors.

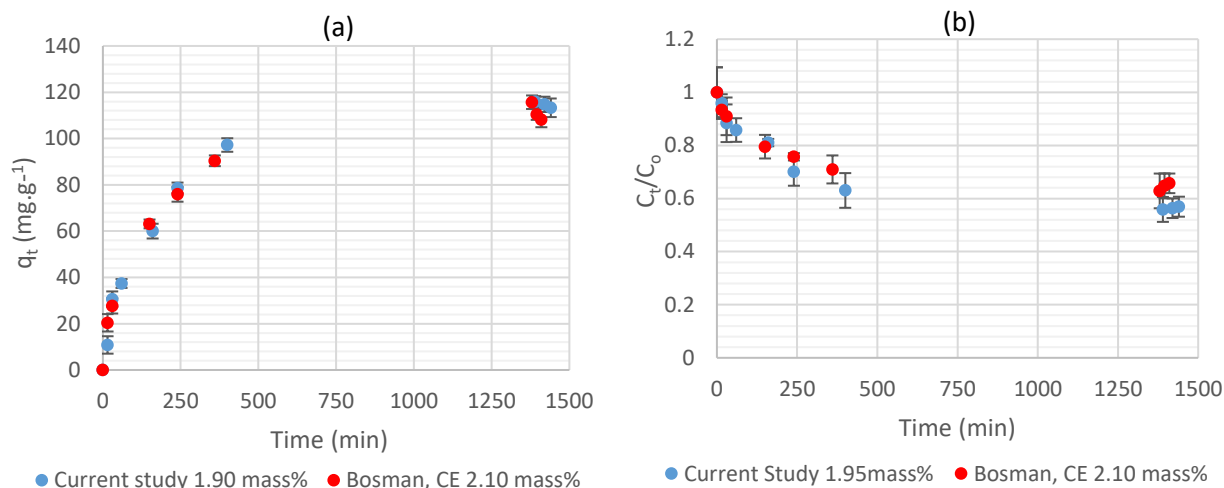


Figure 9 Validating the experimental method used in the current study by comparing results achieved by Bosman (2019). Experiment was performed at 25 °C with a 0.5:0.5 ratio and compared to a data set of similar initial concentration, ratio and solution temperature.

Results of the GC method used in the current study, versus Bosman (2019), are presented in Appendix A.1.5. These were also compared to the method used by Bosman (2019). Prior to verifying this, the GC method used in the current study should be compared to that of the Bosman (2019). As seen in Figure 10, the results achieved were almost identical.

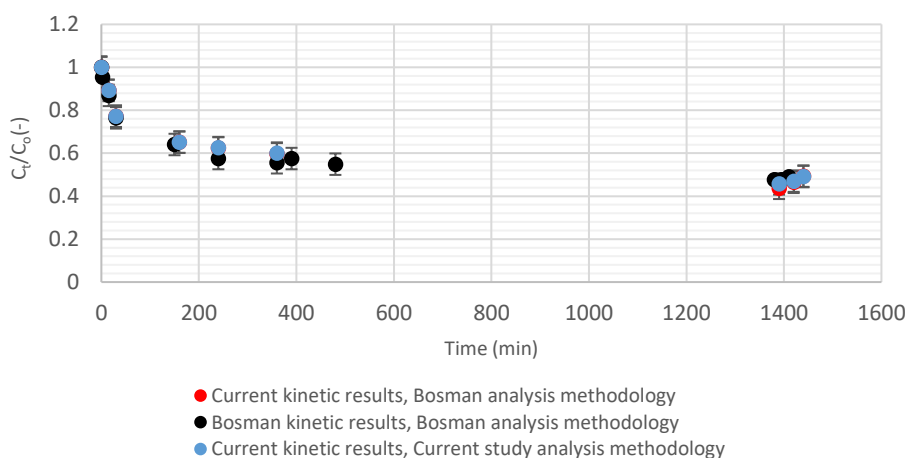


Figure 10 Comparison of two analytical GC methods used in the current study and extant work done by Bosman (2019).

3.8 Secondary batch adsorption experimental setup

As illustrated in Section 3.7, the use of the experimental setup and the corresponding experimental procedure produced results that were similar to those of Bosman (2019) within the margin of error. However, as illustrated in Figure 11, at approximately 24 hr (the identified time required to reach sorption equilibrium), the adsorbate loading was less than that achieved at 7 hr for runs performed at 45 °C. It is noted that this occurred in the single component and binary component systems. This phenomenon was

not observed in extant studies that focused on unbranched alcohols (1-hexanol, 1-octanol, 1-decanol) (Bosman, 2019; Groenewald, 2019). The latter used similar experimental conditions, setups and procedures.

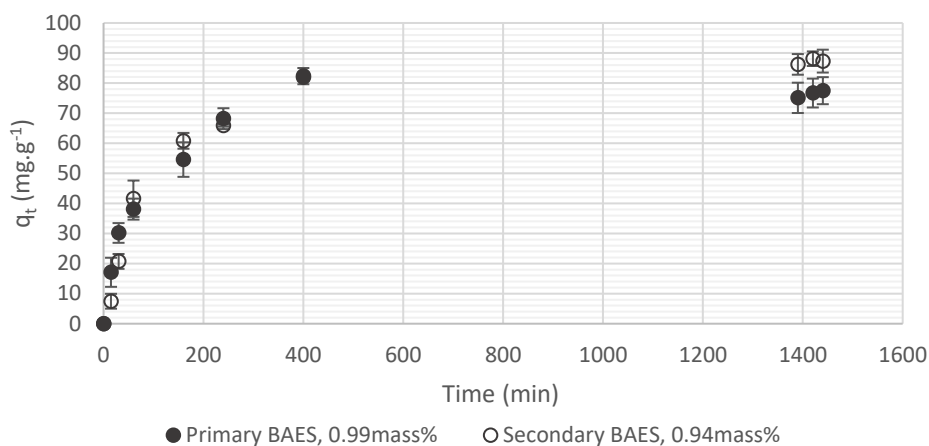


Figure 11 Providing a graphic illustration of the effect of using the two different setups on the sorption equilibrium achieved.

An additional setup, as depicted in Figure 12, while following the same principles but with minor adjustments, was built by a researcher at Stellenbosch University who was performing similar experiments at 65 °C*. The setup used was different to that of this project. The experimental setup shown in Figure 6 will be referred to as the primary batch-adsorption experimental setup (BAES), while the experimental setup shown in Figure 12 will be referred to as the secondary BAES. The experimental procedure followed when operating the secondary BAES is described in Appendix A.2.¹

* Secondary BAES was built well into the current research project, from February-March 2021. The setup was only available for the current project for a limited time and the comparison of these two was thus only done at the end of the research project. Therefore, not all data could be repeated on this system. Note that experimental work was concluded in May 2021.

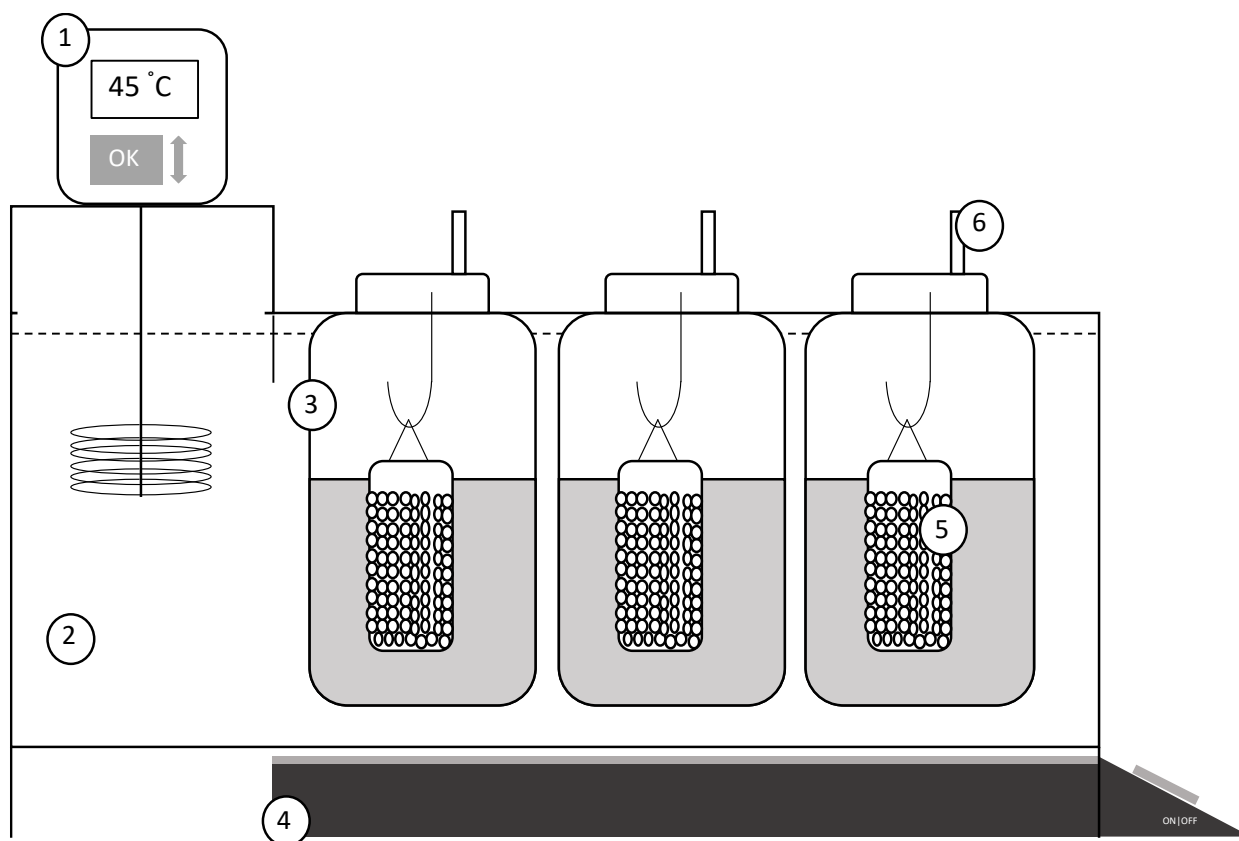


Figure 12 Secondary batch-adsorption experimental setup (BAES) used to identify whether the results achieved by using the primary BAES were comparable. Where (1) is the heater, (2) the water bath, (3) Schott bottles in which the solutions are contained, (4) heating and mixing plate, (5) mesh baskets containing approximately 10 g of adsorbent and (6) the plug for the sample port in the Schott bottle cap.

There are fundamental similarities between the primary and secondary BAES that make these systems comparable. Particularly, both setups are used predominantly for lab-scale batch-adsorption tests. There are some key differences to note, as indicated in Table 10.

Table 10 Comparison of key differences between primary and secondary BAES. Some visual differences were also noted while experiments were conducted and these are also itemised below.

Key Difference	Primary BAES	Secondary BAES
1	Open cylindrical beakers (open to the atmosphere)	Sealed Schott bottles (contents not open to the atmosphere)
2	Cylindrical beakers have larger volume (600 ml) and diameter	Schott bottles have smaller volume (250 ml) and diameter
3	Shorter mesh baskets with wider diameters	Longer mesh baskets with smaller diameters
4	Larger water bath not sealed completely. Notable evaporation observed.	Smaller water bath, most openings are closed. Minimal evaporation observed.
5	In some cases, at 45 °C, water droplets were observed in the solution after 24 h. This did not occur consistently.	In all cases, at 25 °C and 45 °C, no water droplets were observed in the solution.

Given these fundamental similarities, a small selection of experiments were repeated to evaluate the difference in results between the two systems. Due to time constraints, not all experiments were repeated on the secondary BAES, but it was done sufficiently so as to ensure that sound conclusions could be drawn. The outcome of the system comparison brought into question the validity of the sorption equilibrium data collected when using the primary BAES. The outcome of the system comparison will be provided at the end of Chapter 4.

3.8.1 Repeatability

The comparison of the primary versus secondary BAES requires knowledge of the margin of error for both datasets. The repeatability of the secondary BAES was determined by producing triplicates and determining the standard error. In the results presented in Section 4.2 will include the error bars for both systems to deduce the margin of error. This will assist in deducing the range within which the %difference between sorption equilibrium data collected from both setups. The uncertainty analysis procedure is outlined in (Appendix A.3).

3.9 Chapter Outcome

This chapter formed a crucial part in addressing the three objectives provided in Section 1.3. The experimental procedure was outlined for the single component and binary component kinetic and equilibrium tests and the displacement tests. Validation experiments were performed and the certain datasets from Bosman's (2019) work successfully replicated.

In this chapter the following experimental parameters/operating conditions were identified:

- The systems that will be considered are 3,7-DMO as the single adsorption system, 1-octanol & 3,7-DMO and 1-decanol&3,7-DMO as the two binary component adsorption systems
- System operating temperatures to consider for:
 - The single component system: 25 °C, 35 °C and 45 °C
 - The binary component system: 25 °C and 45 °C
 - The displacement tests: 25 °C and 45 °C
- The range of overall initial concentrations will be 0.5 – 3.3 mass%.
- SCD was selected as the only adsorbent to be investigated in this study
- The mixing speed will be 410 rpm
- Three adsorbate ratios will be considered in the binary component adsorption system namely 0.25:0.75, 0.5:0.5 and 0.75:0.25.

The experimental and results processing plan will take place over 4 phases:

- Phase 1 – performing kinetic and equilibrium studies on the adsorption of 3,7-DMO from n-decane using SCD.
- Phase 2 - performing kinetic and equilibrium studies on the adsorption of 1-octanol&3,7-DMO and 1-decanol&3,7-DMO from n-decane using SCD.
- Phase 3 – perform displacement tests on all three 1-alcohols considered
- Phase 4 – the processing and modelling of the kinetic and equilibrium experiment datasets of Phase 1 and 2.

Finally, the secondary BAES was outlined which was only available for a short period of time and used towards the end of the project to determine project shortcomings.

Chapter 4 Evaluation of project shortcomings

4.1 Chapter overview

This section aims to address the discrepancy in data collected at 45 °C by means of a critical review of the experimental setup and data processing methodology used in this study. The experimental setup, experimental and data processing methodologies were verified, as indicated in Section 3.7 and Appendices A.1, A.2 and A.3.

This review of the project shortcomings will be achieved in accordance with the following two steps.

- Comparing the experimental setup used in this study to a secondary BAES that was temporarily available.
- Investigating areas in which the discrepancy in results was notable.

4.2 Comparison of primary BAES and secondary BAES

In this section, the primary and secondary BAES will be compared in terms of the following conditions.

1. Binary component system (1:2 ratio of 1-decanol&3,7-DMO) at 45 °C and 25 °C with a 3 mass% initial concentration.
2. Single component 3,7-DMO system at 45 °C with a 1 mass% initial concentration.
3. Binary component system (0.5:0.5 ratio of 1-decanol&3,7-DMO) at 45 °C with a 2 mass% initial concentration.
4. Binary component system (0.5:0.5 ratio of 1-octanol&3,7-DMO) at 45 °C with a 2 mass% initial concentration.

The objective of this section will be to quantify the discrepancies between the results achieved in terms of operating the two systems with a view to the margin of error. Kinetic studies will be performed, given that the drop in loading was not observable while examining the equilibrium isotherm in isolation. The main outcome of this investigation was to determine which results generated by using the primary BAES should be evaluated in terms of qualitative rather than quantitative aspects.

4.2.1 Binary system comparison at different temperatures

The adsorption kinetics for both systems were compared at 45 °C and 25 °C, as reflected in Figure 13. The main aim was to infer whether differences cropped up in terms of results achieved, and if temperature had an effect in this regard. Figure 13 provides the kinetic plots for a solution of ratio 1:2 (1-octanol&3,7-DMO). The initial composition of the four solutions used were assumed to be comparable, as the maximum difference noted was 0.28 mass% with a standard error of 0.08 mass%. For the first four hours, the loading achieved using the primary and secondary BAES were similar and occurred within the margin of error. A notable difference occurred at 7 h and 24 h. At 7 h, the loading observed indicated that, for both temperatures, greater loading was achieved by using the secondary BAES in contrast with the primary one. At 24 h, the same trend was observed but, due to uncertainties, it was unclear whether the

sorption equilibrium achieved at 25 °C was definitively greater for the secondary than the primary BAES. At 45 °C, a distinct difference in sorption equilibrium was noted where the secondary BAES exceeded that of the primary one. However, the experimental results achieved by using the primary and secondary BAES showed a similar trend where an increased adsorbate loading was achieved at lower temperatures.

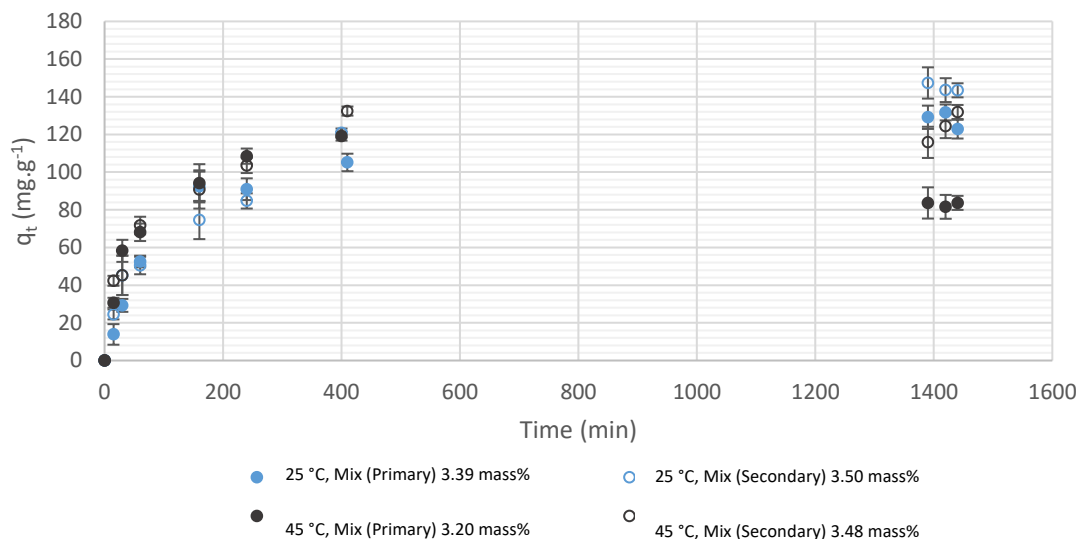


Figure 13 Combined adsorbate loading of a 1:2 ratio of 1-octanol&3,7-DMO at combined initial concentrations ranging from 3.20 – 3.50 mass% by using the primary BAES compared to the secondary BAES.

The overall trend suggests that, at approximately 24 h, the adsorbate loading achieved by using the secondary BAES when compared to the primary BAES was larger at 45 °C and marginally larger at 25 °C. Since the aim was to infer whether adsorbate ratio in a binary system influenced the adsorption of the respective adsorbates, it was necessary to determine whether the overall trend was present for each adsorbate in the 3,7-DMO&1-octanol binary component system (See Figure 14 and 15 for 3,7-DMO and 1-octanol respectively). If both adsorbates displayed the same trend, it is indicative of a shortcoming in the primary BAES that would be accounted for in the secondary BAES.

Upon review of Figure 14, some scatter in the data was noted in the first 2 hours, but it was accounted for by the error bars present. Similarly, to the trends reflected in Figure 13, at approximately 24 h the adsorbate loading achieved at 45 °C was larger for the secondary BAES when compared to the primary one. Unlike the case reflected in Figure 13, the adsorbate loading noted at approximately 24 h was similar for both the primary and secondary BAES at 25 °C. Figure 14 indicates a drop in adsorbate loading in the case of operating the secondary BAES at 45 °C. However, scatter was present in the loadings noted at 24 h: it cannot be concluded that desorption or displacement of 3,7-DMO had taken place.

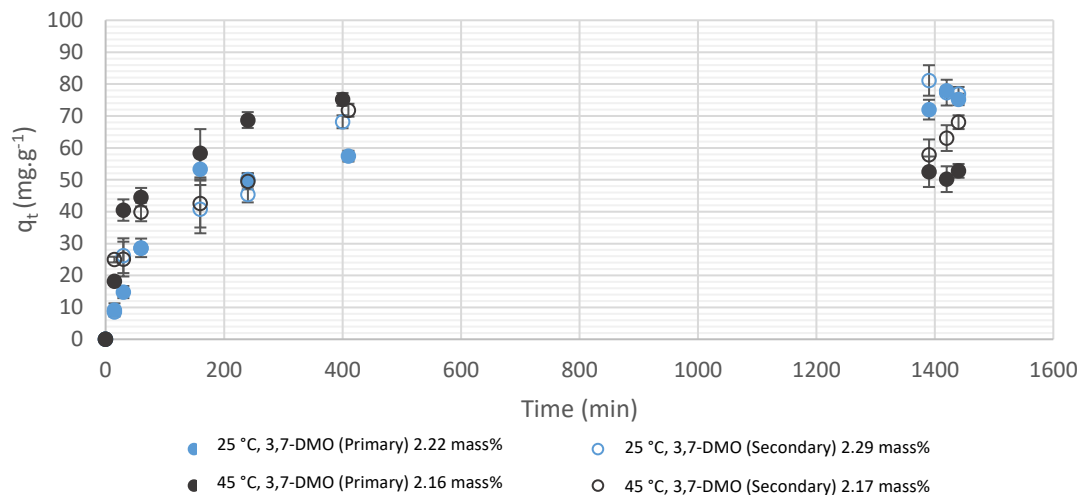


Figure 14 Differences and similarities in results achieved for the sorption of 3,7-DMO in a binary system of ratio 1:2 (1-octanol&3,7-DMO).

Figure 15 depicts a review of the differences in the kinetic experiment results produced when operating the primary and secondary BAES at a system temperature of 25 °C and 45 °C. Similar to the case illustrated by Figure 13, the adsorbate loading achieved was greater at 45 °C and marginally greater at 25 °C when using the secondary BAES, in contrast with the primary one.

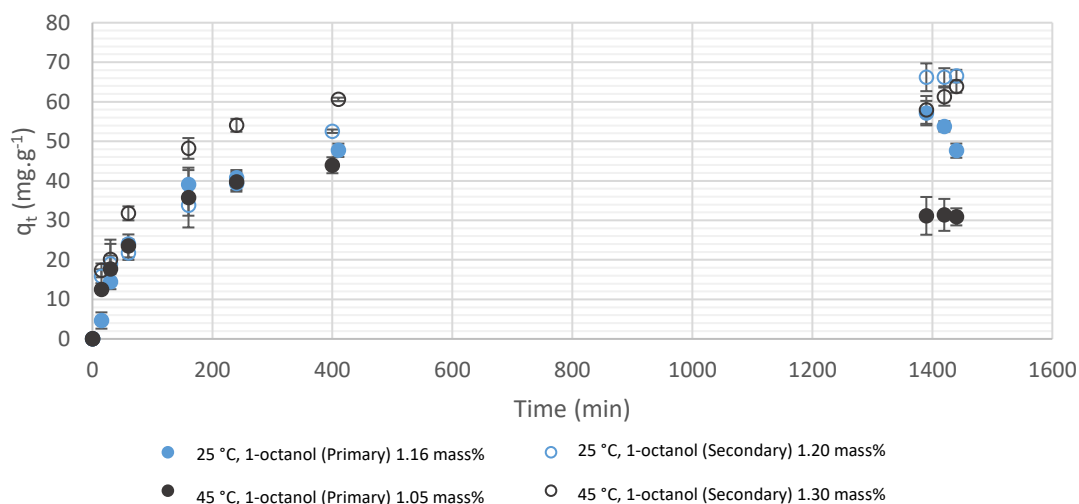


Figure 15 Review of the differences and similarities noted for the adsorption of 1-octanol within a binary system of ratio 1:2 (1-octanol&3,7-DMO) at two different temperatures while using two different experimental setups.

Overall, the key findings reflected in Figure 13, 14 and 15 are two-fold. Firstly, the experimental results produced when using the primary BAES at a system temperature of 25 °C in a binary system of non-equimass adsorbate ratio should be viewed as quantitative in nature. Secondly, when operating the secondary BAES it, appeared that equilibrium was reached around 24 h, as the change in adsorbate loading then was minor.

4.2.2 Comparison of results achieved using Primary versus Secondary BAES 45 °C for single component and binary systems

As shown in Section 4.2.1, it was found that differences among results produced when using the primary versus secondary BAES occurred mainly at 45 °C. Therefore, the primary BAES used in the current study has not been discredited. The present section aims to further investigate the key finding, as discussed in Section 4.2.1, that the first 7 h might be a quantitative representation of the kinetics of the adsorbate-adsorbent interaction that occurred when operating the primary BAES at 45 °C.

4.2.2.1 Single component - 3,7-DMO adsorption system

Figure 16 reflects the single component results for the kinetic study of 3,7-DMO at 45 °C while using the primary and secondary BAES at two different initial concentrations. The results indicated similar trends for the primary and secondary BAES, within the margins of error, for the adsorbate loading at each time segment leading up to 7 h. The main difference in loading was observed at 24 h. Resonating with trends that had been established in Section 4.2.1, the sorption equilibrium was higher than that of the primary BAES when operating the secondary BAES. The percentage difference in equilibrium adsorbate loading was 12 mg.g⁻¹% (Figure 16a) and 15 mg.g⁻¹% (Figure 16b), which was narrowly outside the margin of error. When operating the secondary BAES, the adsorbate loading achieved at 24 h compared to 7 h appeared larger but, since there was an overlap in margin of error, equilibrium may in fact have been reached at 7 h.

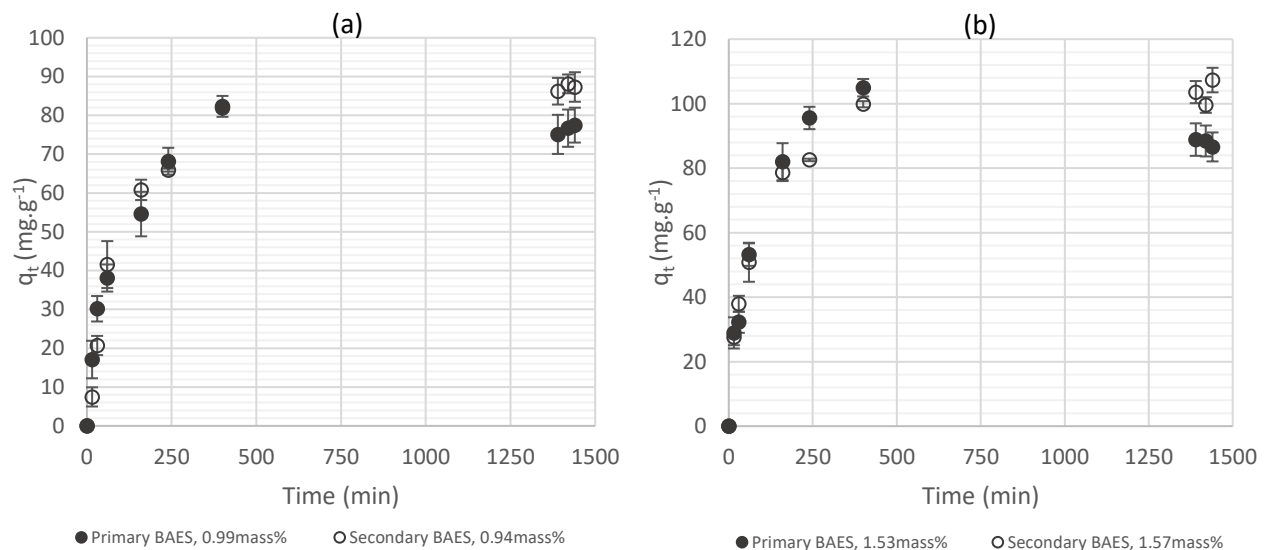


Figure 16 Comparison of kinetic data produced for a single component system of 3,7-DMO at an initial concentration of approximately 0.9 mass% (a) and 1.5 mass% (b) when operating the primary and secondary BAES at 45 °C.

4.2.2.2 Binary component systems

In view of the findings discussed in Section 4.2.2.1, two binary component systems consisting of a different adsorbate ratio and initial mass% concentration each were investigated to confirm the trend observed. Figure 17 and 18 depict a comparison of the kinetic data generated for a 1-decanol&3,7-DMO system and 1-octanol&3,7-DMO system respectively. The results in both figures were found to be similar. The adsorbate loading achieved within the first 7 h was comparable (within the margin of error) for the primary BAES and secondary BAES.

However, at approximately 24 h, a notable difference occurred between the adsorbate loading achieved by using the secondary versus primary BAES. The difference was beyond the range of uncertainty and was 23 $\text{mg}\cdot\text{g}^{-1}$ for 1-decanol&3,7-DMO and 25 $\text{mg}\cdot\text{g}^{-1}$ for 1-octanol&3,7-DMO respectively. This suggested that, from 7 h to 24 h, either the secondary BAES accounted for a shortcoming in the primary BAES, or some of the assumptions made in the data processing methodology were no longer representative of the adsorption system.

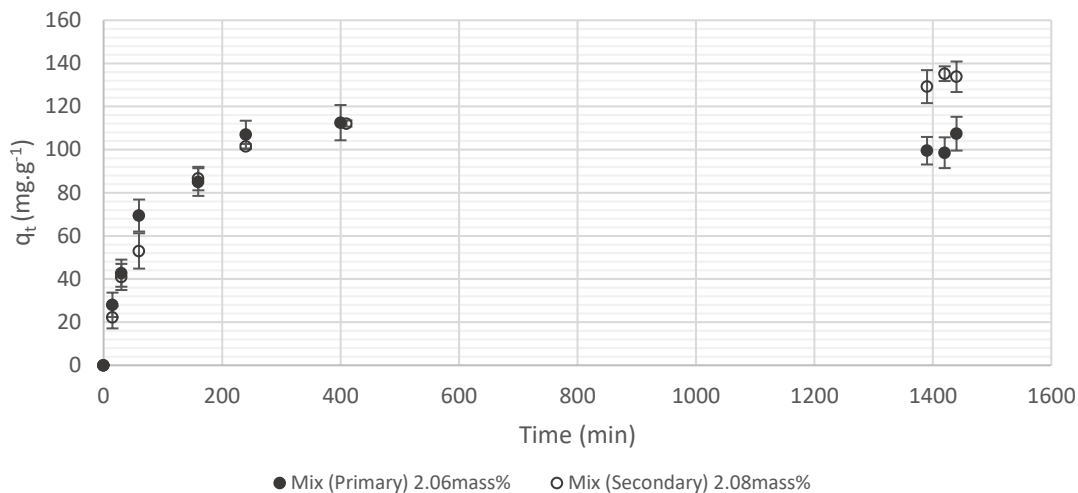


Figure 17 Kinetic data for experiments executed by using the primary and secondary BAES. Both setups were operated at 45 °C at an initial concentration of approximately 2 mass% with a ratio of 0.5:0.5 (1-decanol&3,7-DMO).

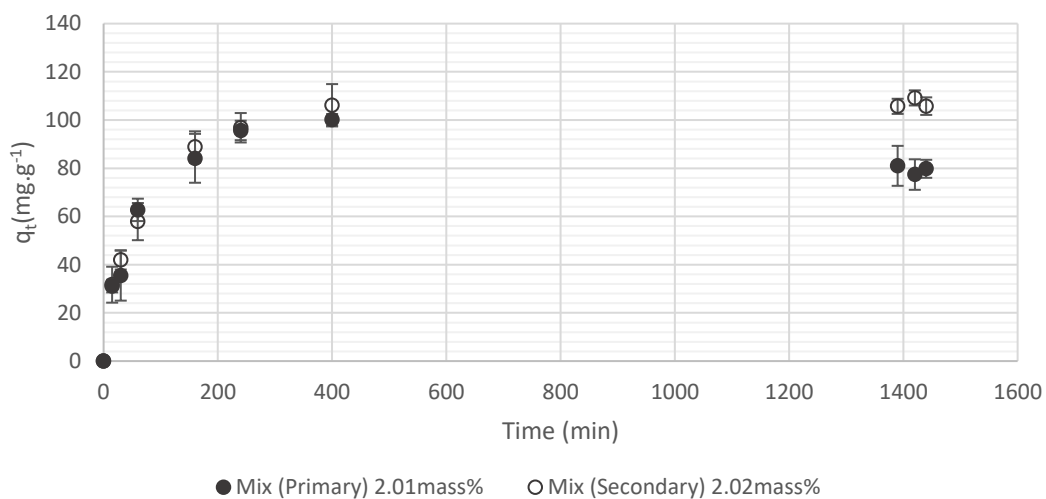


Figure 18 Kinetic data for experiments executed by using the primary and secondary BAES. Both setups were operated at 45 °C at an initial concentration of approximately 2 mass% with a ratio of 0.5:0.5 (1-octanol&3,7-DMO).

4.2.3 Volume Assumption

A key volume assumption was made during the investigation of the drop in loading observed when the primary BAES was used, as opposed to secondary BAES. It was assumed that in both scenarios the solution mass and volume remained constant for the duration of the 24 h experiment. The results noted from both systems for the first 7 h were similar in most cases. With regard to the sorption equilibrium achieved, in the case of the binary components the difference between the loading was found to be outside the margin of error. However, for the single component systems, this difference stayed within the margin of

error. The validation results, as presented in Section 3.7, indicated that, the results produced by Bosman (2019) could be replicated within the margin of error.

A possible cause for the drop in adsorbate loading was due to the presence of water which, after a period of time (7 h7 h), displaced the adsorbed molecules. Literature indicated that the solubility limit of water in n-decane was 0.5 g water/kg n-decane (Bolton *et al.*, 2009). For a solution containing 3.3 mass% adsorbate and 96.7 mass% n-decane the mass of water miscible in n-decane is 0.06 g. This means that although not all adsorbate loaded onto the adsorbent can be displaced by water a portion can (please refer to Appendix A.1.7 for more information). The mass of solution before and after a 24 h experiment was observed. The initial mass of solution, regardless of whether primary or secondary BAES was used, was recorded during the experimental start-up (as explained in Appendix 8.3A.1.1) and came to approximately 144 g of solution. With respect to the primary BAES, on average the solution post-24 hr experiment was 130-135 g (6-7 mass% reduction of initial solution mass) and 115-124 g (13-20 mass% reduction of initial solution mass) for runs operated at 25 °C and 45 °C respectively. It was assumed that the mass loss occurred under the conditions briefly itemised below.

1. During solution preparation (Appendix A.1.), the solution was decanted from a sealed storage Schott bottle into a beaker. Not all solution was decanted, and some remnants remained in the storage bottles. It was assumed that 1-2 ml were lost which totals to 0.5-1 mass% lost.
2. During kinetic studies 10 samples of 400 µl each were withdrawn from the solution. This totals to 4 ml during the experiment (2.5 vol% or 3 mass% of the total solution).
3. The mass of solute adsorbed onto SCD. Which, as provided in sections below, ranges from 0.55-1.40 g of solution (0.4-1 mass%). Some solution also remains trapped within the mesh basket and adsorbents (not adsorbed) and this was assumed to be a further 1 mass% of the initial solution. It is plausible that n-decane was also adsorbed onto SCD which would further reduce the solution volume/mass. However, n-decane is not considered a polar molecule whilst water is highly polar and 1-octanol, 1-decanol and 3,7-DMO is slightly polar. Thus, the adsorbed amount of n-decane is considered marginal in comparison to the 1-alcohols adsorbed.
4. The remaining mass lost was assumed to be related to evaporation. In the case of 25 °C, the remaining average total mass% lost (0-1 mass%) was largely accounted for by the 0.5 mass% uncertainty. However, for experiments performed at 45 °C, a remaining 7-14 mass% was unaccounted for and was assumed have resulted from evaporation.

The total mass percentage of solution lost during the 24 h experiment when operating the secondary BAES was found to be relatively constant ranging from 6-8 mass% regardless of temperature. It was assumed that the mass loss could be accounted for by bullet points 1-3, as explained above. Bullet point 4 was only considered to be applicable for the primary BAES, as the secondary BAES had Schott bottles with caps that minimised evaporation.

As is reflected in the sample calculation section of Appendix A, the mass and volume of solution were assumed to be constant for the 24 h experiment. The 6-8 mass% was considered to be negligible, as this was observed in the primary and secondary BAES. The 7-14 mass% lost due to evaporation when operating the primary BAES at 45 °C brought into question the validity of assuming constant mass and

volume of solution. The possibility of incorporating a variable total volume and mass into the calculations of adsorbate loading had to be considered. The equation to calculate said loading would then be as follows:

$$q_t = \frac{C_o V_o - C_t V_t}{m_{ads}} \quad (34)$$

Where $V_t \leq V_o$

The difficulties engendered by assuming volume and mass changes that occurred in the system are itemised below.

- Quantifying the exact mass that evaporates over time. An overall mass reduction was quantifiable but to measure the mass reduction at each time stamp would have required a disruption of the experimental process and might possibly have incurred a further loss of during the decant.
- Once the mass change had been taken into account, it could also no longer be assumed that the composition of the solution prior- and post-evaporation were identical. Based on vapour pressures (Table 11), it was possible to speculate around the components that were more likely to evaporate, but these could not easily be quantified. This meant that all changes in composition could no longer be assumed, given that the true mass adsorbed was brought into question.
- The total solution mass is expected to decrease on account of sampling, adsorption and potential evaporation but another factor to consider is the potential increase in total solution mass but on account of water bath condensate droplets collecting in the solution.

Table 11 Compilation of predicted vapour pressures of the components as used in the system. Given that n-decane showed the highest vapour pressure, it was the most likely to evaporate at a higher rate while 1-decanol would have evaporated at the slowest rate.

Component	Temperature (K)	Vapour Pressure (Pa)	Reference
n-decane	298.15	123.3	(Carruth and Kobayashi, 1973)
	318.15	300.5	
1-octanol	298.15	10.9	(Geiseler, Fruwert and Hüttig, 1966)
	318.15	64.8	
3,7-DMO	298.15	3.6	(Stull, 1947) Temperatures fall outside of Parameter range
	318.15	23.7	
1-decanol	298.15	1.4	(Pokorný <i>et al.</i> , 2021)
	318.15	9.2	

The water in the water bath is maintained at a contact temperature with a 0.1 °C fluctuation. Initially a large amount of energy is supplied via the heating element to the water to increase the temperature to the required setpoint (for example 45 °C). Once the temperature of the water reaches 45 °C heating element supplies less energy only switching on when the temperature drops and off once the setpoint is

reached. Therefore, it can be assumed that mass loss via evaporation as steam from the surface of the water and solute (largely n-decane) from the surface of the solution would follow a linear trend. As mentioned at the beginning of this section, when comparing total solution mass before and after the adsorption experiments approximately 7-14 mass% of solution remained unaccounted for. Assuming a minor portion of this is because n-decane was adsorbed then an estimated 10 mass% of the overall solution is assumed to evaporate. The effect of assuming constant versus decreasing mass and volume throughout the 24 h for a single component system is presented in Table 12. Note that only mass loss on account of potential evaporation is considered here and the condensation of water droplets that increase the solution mass is not considered.

Table 12 Demonstrating the effect of assuming constant versus variable volume when performing calculations on the adsorbate loading of a single component 3,7-DMO system at 45 °C. The mass and mass percentage of 3,7-DMO in the bulk solution is provided. For illustrative purposes, 10 mass% loss due to evaporation is assumed so occur linearly.

Time	3,7-DMO (mass%)	Constant overall mass		Variable overall mass assumed		
		3,7-DMO mass (g)	Adsorbate loading (mg.g ⁻¹)	Total solution mass (g)	3,7-DMO mass (g)	Adsorbate loading (mg.g ⁻¹)
0	1.53	2.20	0	144.0	2.20	0
15	1.32	1.90	30	143.9	1.90	30
30	1.30	1.87	33	143.7	1.87	34
60	1.15	1.66	55	143.4	1.65	55
160	0.95	1.37	84	142.4	1.35	85
240	0.85	1.22	98	141.6	1.20	100
400	0.78	1.12	108	140.0	1.09	111
1390	0.90	1.30	91	130.1	1.17	103
1420	0.90	1.30	91	129.8	1.17	104
1440	0.91	1.31	89	129.6	1.18	102

It is important to note that binary systems (1-octanol/1-decanol) were repeated from a previous study. and that included the same potential for evaporation, given that the experimental setup used was similar to the primary BAES. This shows that, even if the volume was made variable, multiple factors had to be accounted for and a variable volume might have masked these trends. The adsorbate loading and the sorption equilibrium for experiments performed at 45 °C are not necessarily quantitatively accurate, but the qualitative trends should still be used.

4.2.4 Presence of water

As mentioned, small water droplets were noticed in some of the beakers after a 24 h experiment at 45 °C. A study was done to quantify the water content by withdrawing 2 ml samples and analysing these by

using the Karl Fischer Titration method (Tavar, Turk and Kreft, 2012). Table 13 shows that the water content at the end of the 24 h period was higher at 45 °C than that observed at 25 °C.

It is thought that the evaporation (without equal parts condensation) was due to the structural imperfections of the primary BAES. Such imperfections include the fact that the open glass beakers were placed in a water bath covered with a plate to minimize evaporation of water. This top plate did not seal all openings and therefore, at higher temperatures, a greater degree of evaporation was observed. This was evidenced by the drop in water level during the 24 h period. Although a large portion of water vapour escapes through the gaps and along the sides of the top plate, some of the water vapour remains contained between the top plate and the solution and water bath surfaces. The air below the top plate and above the solution level progressively approaches saturation as the evaporation progresses. Once the air became supersaturated with water vapour, condensate droplets formed on the top plate (which was kept at ambient temperature). As more water vapour condensed on the top plate, the condensate droplets grew larger until the droplets dripped into the solution. This explains why a drop in adsorbate loading was only observed after a few hours as the condensate formation and contamination is not instantaneous.

The atmospheric pressure in Stellenbosch is on average approximately 0.99 atm, and the atmospheric pressure required to condense water vapour at 45 °C is 0.0947 atm. The atmospheric pressure therefore facilitated condensation. As discussed in Section 3.8 key differences exist between the primary and secondary BAES. The water droplets that formed in some beakers when using the primary BAES was noteworthy. At 45 °C, the droplets did not consistently form in the beakers, as depicted in Table 13 and Figure 19. However, beakers were chosen at different locations in the water bath so as to gauge the potential water content of the beakers throughout the 24 h experiment.

Table 13 Comparison of water content at the end of a 24 h experiment at different positions in the water bath.

Temperature (°C)	45	25
Beaker number	Water (mass%)	Water (mass%)
1	0.0420	0.0165
2	0.0211	0.0146
3	0.0244	0.0193
3	0.0332	0.0134

Figure 19 shows that the presence of water at 45 °C may also have contributed to the sorption equilibrium that was lower than that achieved at around 7 h. Figure 19 also indicates the effect of water in the bulk solution when SCD is present versus not present. It was observed that the mass concentration of water in the bulk solution was lower when the adsorbent was present. This indicates that some of the water was adsorbed, which would mean that water was competing with the 1-alcohols in solution for active sites, hence limiting the 1-alcohol adsorbate uptake on SCD. This would also explain why the adsorbate loading of 3,7-DMO, 1-octanol&3,7-DMO and 1-decanol&3,7-DMO was lower at around 24 h.

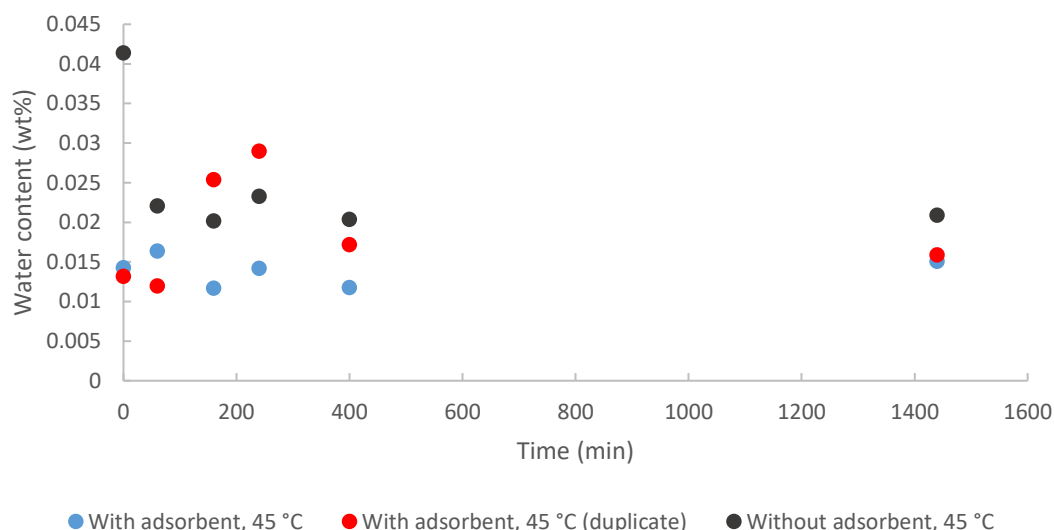


Figure 19 Plot of the water content in the solution as a function of time at 45 °C. The plots are compared for the scenario where the adsorbent was in contact with the solution and when the solution was not brought into contact with the solution.

4.3 Chapter Outcome

The shortcomings of the present project were described in detail in terms of water content analysis, a review of system assumptions and a comparison of kinetic results producible in the primary and secondary BAES. The key contributing factors associated with a drop in adsorbate loading from 7 to 24 h were identified as follows.

- Stock solution evaporation that occurred during the 24 h period.
- Flawed constant volume and mass assumption.
- Water content.
- 3,7-DMO interacting differently in a binary system when compared to 1-octanol and 1-decanol.

A comparison of the kinetic experimental results produced by using the primary and secondary BAES at 25 °C and 45 °C showed that the equilibrium and kinetic data generated at 25 °C by using the primary BAES should be considered quantitative in nature. In contrast, at 45 °C, while the kinetic data generated for the first 7 h is also of a quantitative nature, the adsorbate loading at 24 h and full 24 h kinetic data sets are of a qualitative one.

Chapter 5 Single Component Adsorption

The aim of this chapter is to characterise the single component adsorption of 3,7-DMO from an n-decane stream on SCD by means of kinetic and equilibrium studies. The review of data collected for the single component 3,7-DMO system adsorbed in a non-competitive system is done in an effort to understand and estimate how the component would interact, and how it would be preferentially adsorbed, in a competitive binary system (Çay, Uyanik and Özaşık, 2004).

The present section aims to address a portion of the main aim (Objective 1) and partially address the secondary aim (Objective 4) as presented in Section 1.3. This will be done in terms of the following steps.

- Comparing the kinetics observed at three temperatures (25 °C, 35 °C and 45 °C) while keeping the initial mass% concentration constant. This comparison will be done at multiple initial concentrations to ensure that the trends are observed consistently.
- Comparing the kinetic profiles observed at a range of initial mass% concentrations while maintaining a constant solution temperature.
- Evaluating the equilibrium adsorbate loading achieved at various equilibrium adsorbate bulk solution concentrations as collected at three different temperatures.
- Fitting kinetic and equilibrium isotherm models to the data presented and drawing conclusions based on theoretical model assumptions.

5.1 Effect of Temperature

The present section will evaluate the effect of temperature on the adsorption of 3,7-DMO onto SCD at 25 °C, 35 °C and 45 °C (see Figure 20(a-c)). The effect of temperature was evaluated at three different initial concentrations. Though concentration is not the focus of the present section, it is necessary to mention that comparison of the kinetic profiles at three different initial concentrations enables a qualitative evaluation as to whether the effect of temperature was observed consistently. The discussion will be focused on how temperature affects the adsorption kinetics and the overall 3,7-DMO adsorbate loading on SCD. Additional kinetic studies were performed at other initial mass percentage concentrations (1, 2 and 2.5 mass%) and these are reflected in Appendix B.1. and C.1.

. It should be noted that the kinetic profiles generated at 45 °C were only plotted for the first 7 h while the kinetic profile for the two lower temperatures reflect the full 24 h experimental period.

Figure 20(a-c) shows that, over the first 7 h, an increase in temperature consistently resulted in an increase of q_t for 3,7-DMO on SCD. At the lowest initial 3,7-DMO concentration of approximately 0.5 mass% (Figure 20c) the difference between adsorbate loading achieved at 45 °C versus 35 °C was less distinguishable, but the adsorbate loading achieved at 45 °C remained higher than 25 °C and 35 °C over the first 7 h.

Investigation of the full 24 h period of adsorption and the effect of operating at a solution temperature of 25 °C compared to 35 °C indicated that, at all three initial concentrations, the equilibrium adsorbate

loading achieved at 25 °C was marginally higher than that achieved at 35 °C. However, considering the overlapping of error bars for both data sets around the equilibrium sorption time, it can be concluded that the effect of operating the adsorption system of 3,7-DMO in an n-decane solution at 25 °C as compared to 35 °C produced only minor increased equilibrium of 3,7-DMO loading on SCD. A review of Figure 20(b-c) shows similar trends for the first 7 h of adsorption. These results contradict each other, but the trend seen in Figure 20(a) (where the adsorbate was in excess) showed that the adsorbate loading was considerably higher at 45 °C when compared to the two lower temperatures. Furthermore, an increase in adsorbate loading with increasing temperature aligns with the trends observed for the adsorption of 1-decanol and 1-octanol on SCD, as reported by Bosman (2019). Therefore, the adsorption of 3,7-DMO can be classified as endothermic in nature. This means that the extent of adsorption is increased as the temperature increases. As the temperature increases more energy can be adsorbed which facilitates the adsorption (forward reaction) of the adsorbate and leads to an increased mass of adsorbate uptake which translates to a higher equilibrium adsorbate loading.

In terms of the kinetics of adsorption the increased temperature resulted in an increased kinetic energy, which resulted in greater vibrational and translational movement that bring brought molecules in contact with the active sites on the adsorbent surface. The entropy of the molecules in the bulk fluid phase also increased with increasing temperature. The increased kinetic energy reduced the potential energy of the molecules because the distance between adsorbate and active site was reduced. The increased temperature also provided additional energy for binding to take place and moved the adsorbate molecules from a high energy state to a lower one.

This indicates that binding energy is required to adsorb 3,7-DMO, which is indicative further of chemisorption (see Jiang *et al.*, 2018; Al-Ghouti and Al-Absi, 2020). Chemisorption relies on an addition of energy to create the bond between the active site and the adsorbate molecule. The increase in temperature also increases the kinetic energy of the molecules, which positively affects the diffusion of these through the pore volume.

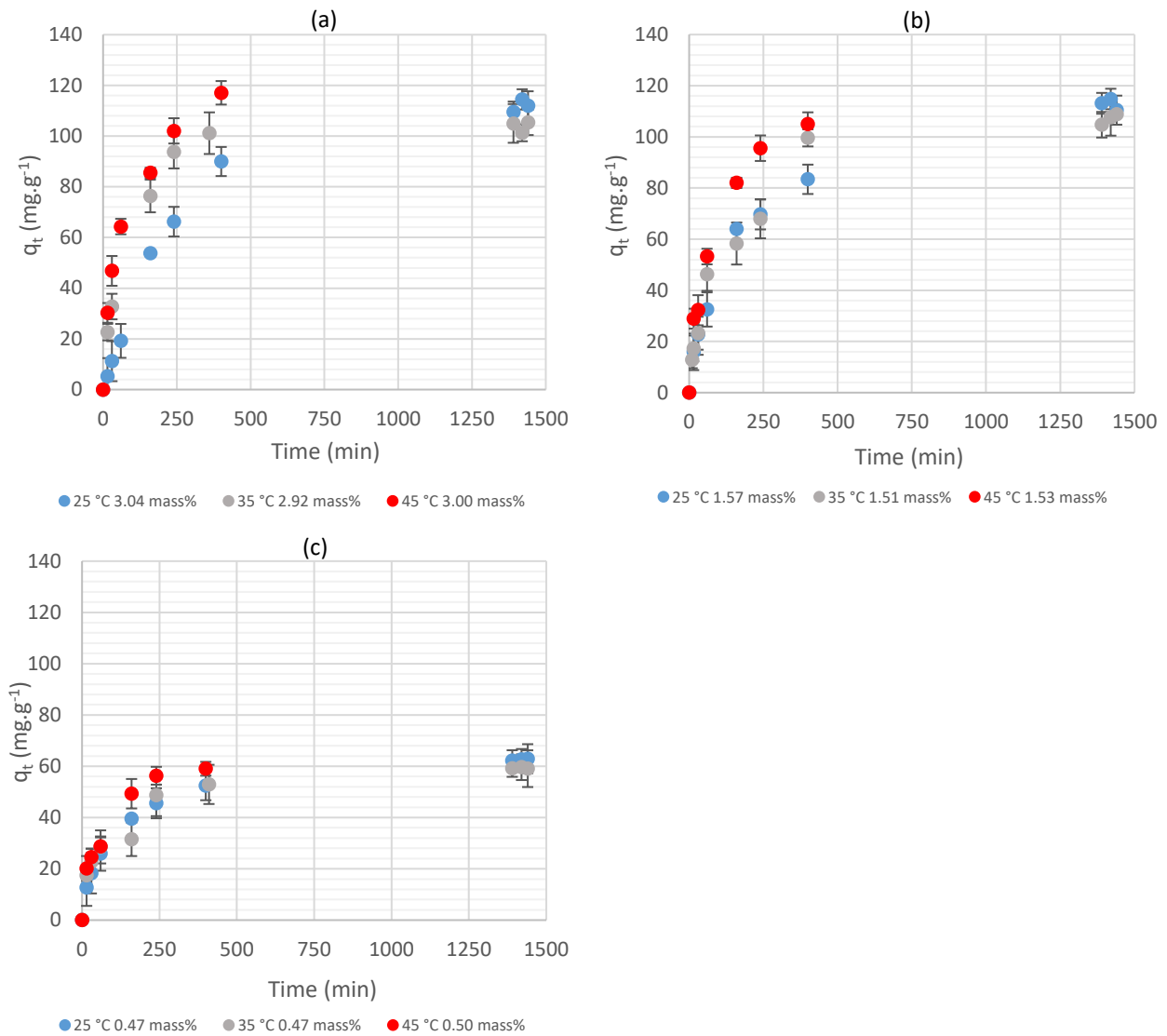


Figure 20 Three plots of the q_t of 3,7-DMO as a function of time at three different temperatures and initial concentrations. Each plot evaluates the kinetic profile of 25 °C, 35 °C and 45 °C at an initial concentration of ± 3 mass%(a), ± 1.5 mass%(b) and ± 0.5 mass%(c).

An increased rate of adsorption can be attributed to a considerable number of factors. Two of these are boundary layer thickness and temperature changes. Two types of boundary layers exist, namely hydrodynamic and thermal ones. The hydrodynamic boundary layer is assumed to have minimal variation at different temperatures, as the mixing speed remained constant for all experiments in which it was involved. The thermal boundary layer is influenced by the hydrodynamic boundary layer. A thermal boundary layer could affect the rate of adsorption, as the molecular diffusivity or rate of adsorbate uptake at the surface could be hindered. However, it is unlikely to see a large change in the thermal boundary layer when increasing the temperature in increments of 10 °C. At lower temperatures, a reduced rate in adsorbate uptake can be the result of decreased kinetic energy and molecular diffusivity in the pores. At both temperatures the rate of adsorption decreased in the second stage (intermediate adsorption stage). The decrease in rate of adsorption is due to a reduction in the number of active sites

available, which increases competition and slows the adsorption process. This decrease is larger at higher temperatures and less severe at lower ones. This situation could be engendered by the fact that, in the case of a thinner boundary layer, a larger number of molecules adsorb onto the surface of the large pores (Xie *et al.*, 2018). After prolonged adsorbent-adsorbate contact, the molecules will preferentially adsorb onto the surfaces of the inner small pores creating a more stable system (Xie *et al.*, 2018), which is less likely to desorb.

The final point of discussion here is the decrease in adsorbate loading noted in most of the results collected at 45 °C. (Rodda, Johnson and Wells, 1996; Builes, Sandler and Xiong, 2013; Senthil Kumar *et al.*, 2014).

It has been demonstrated that the adsorbate loading of 1-decanol, 1-octanol and 1-hexanol increase with increasing temperatures, and this trend remained consistent for the duration of approximately 24 h (Bosman, 2019). 3,7-DMO is a branched version of 1-octanol, but it has the same molecular mass as 1-decanol. The 3,7-DMO molecule is larger and is suspected to encounter more resistance when it moves through the adsorbent to the inner smaller pores.

Water molecules are smaller in size and molecular mass and thus move through the adsorbent to the smaller inner pores with greater ease. It is possible that a large portion of the 3,7-DMO adsorbed occurs on the surface of the larger pores (that are less stable) while fewer are sorbed to the surface of the smaller inner pores (that are more stable). As the water concentration increases, the adsorbed 3,7-DMO are displaced from the active sites on the larger pores by the water molecules, which are preferentially adsorbed.

5.2 Effect of Initial Adsorbate Concentration

Regarding the uncertainty associated with the accuracy of results around 24 h at 45 °C, the present section will primarily focus on the effect of initial concentration at 25 °C and 35 °C. The results observed at 45 °C will be discussed but only in terms of trends observed in the first 7 h. The present section will discuss whether the trend observed at one temperature also occurs at the other two temperatures. If the trend is observed across the board, the results will be considered conclusive.

5.2.1 Effect of initial concentration at 25 °C

The effect of initial concentration on the adsorbate loading at 25 °C is provided in Figure 21 below for three initial mass concentrations (0.47 mass%, 1.47 mass% and 3.12 mass%). The effect of initial concentration is evidenced by the sorption equilibrium achieved. An increase in initial concentration increases the adsorbate loading with a difference of approximately 60 mg.g⁻¹ observed between the intermediate and highest concentration (1.47 and 3.12 mass%) and lowest initial concentration (0.47 mass%).

A During the first 60 min, when the rate of adsorption exceeds the rate of desorption, a clear distinction between the adsorbate loading for the three different compositions cannot be observed. The data points

indicated that an increased composition results in increased loading but, due to error bars, it cannot be said with certainty that this is the case. Within the next 6 h, where the desorption rate gradually tends towards the adsorption rate, the difference in adsorbate loading between the three compositions grows clearer. At 160 min and 240 min, the adsorbate loading achieved for an initial concentration of 1.47 mass% at 25 °C is higher than when the initial concentration is at 3.12 mass% and even higher at 0.47 mass%. Around 400 min, the effect of initial concentration is evidenced by the adsorbate loading being similar for the initial concentration of 3.12 mass% and 1.47 mass% but approximately 40 mg.g⁻¹ lower for the initial concentration of 0.47 mass%.

In the final stages (from 7 h to 24 h) the difference in the rate of adsorption versus desorption approaches zero. A review of the difference between adsorbate loading achieved at 7 h versus 24 h for the initial concentration of 0.47 mass%, 1.47 mass% and 3.12 mass% is an approximate increase of 18 %, 22 % and 33 % respectively. This indicates that, as the initial concentration increases, the adsorbate-adsorbent system takes longer to approach sorption equilibrium. This occurs because there are more molecules to be adsorbed which engenders increased competition for active sites, thus the rate of desorption takes longer to approach the rate of adsorption.

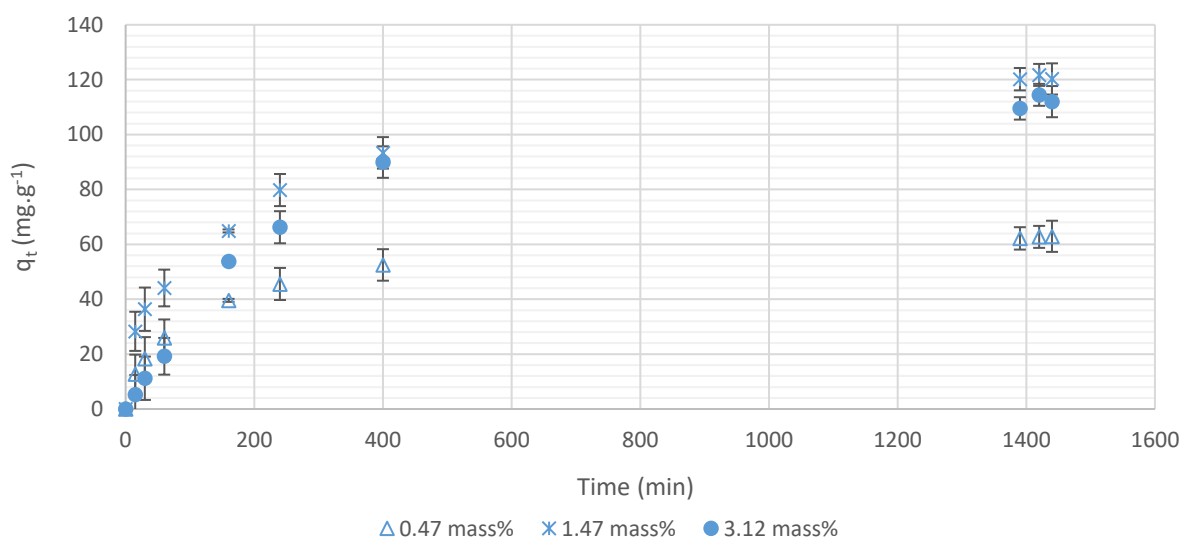


Figure 21 The effect of initial concentration on the adsorbate loading and sorption equilibrium at 25 °C. It is noted that, as the initial concentration increases, so does the adsorbate loading.

The effect of initial concentration of the adsorption of 3,7-DMO as evaluated for a range of 0.5–3 mass%. Figure 22 provides the kinetics observed when the initial concentration is varied between approximately 1.5–3.12 mass% at 25 °C. At around 24 h, the difference in sorption equilibrium is not clearly distinguishable. It appears to range from 110–125 ±5 mg.g⁻¹. It can be said that an increase in initial concentration beyond 1.5 mass% fails to increase the adsorbate loading. The adsorbate loading that is achievable plateaus beyond 1.5 mass% which indicates that SCD has reached its 3,7-DMO loading capacity and its maximum capacity ranges from 110–125mg.g⁻¹.

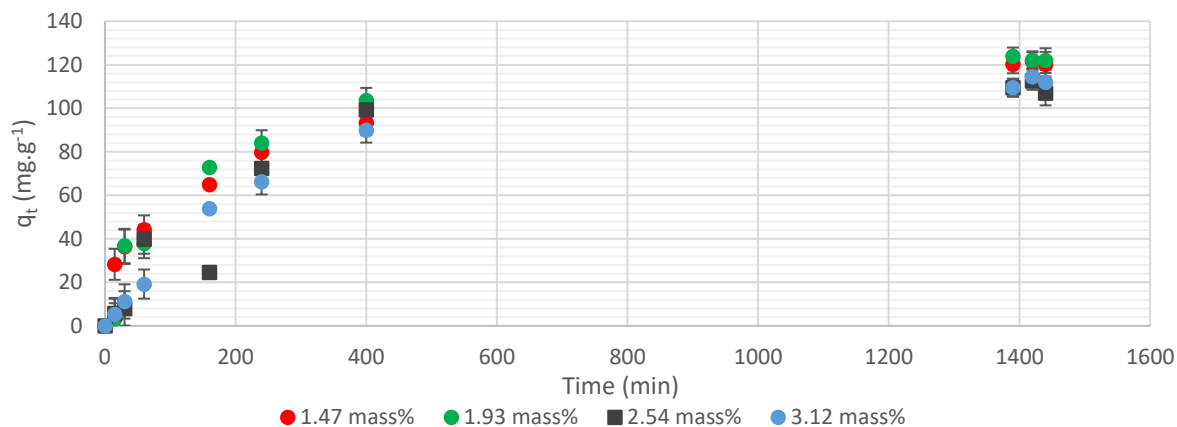


Figure 22 Investigation of the effect of initial concentration when the concentration increases beyond 1.5 mass% at 25 °C.

5.2.2 Effect of initial concentration at 35 °C

In the preceding section, certain trends were observed around varying initial concentrations at 25 °C. The present section aims to identify whether similar trends could be observed for a change in initial concentration regardless of temperature. Figure Figure 23 allows for comparison of the change in adsorbate loading over time for three different initial concentrations (0.47 mass%, 0.98 mass% and 1.51 mass%). The trends observed were similar to those described in Section 5.2.1. During the first 60 min, the effect of an increased initial concentration was not yet clear. From 60 min to 400 min, the adsorbate loading achieved for the highest initial concentration becomes progressively larger than that of the two lower initial concentrations. Around 400 min, a definitive trend was observable, indicating that an increase in initial concentration increased the adsorbate loading.

A review the adsorbate loading difference between 7 h to 24 h revealed similar trends to those observed in Figure 20, where the adsorbent equilibrium loading exceeded that of the loading achieved by 7 h. The adsorbate loading increase from 7 h to 24 h was 20 %, 28 % and 11 % for the initial concentration of 0.47 mass%, 0.98 mass% and 1.51 mass% respectively. The percentage increase in adsorbate loading from 7 h to 24 h is lower than what was observed for the same initial concentration at 25 °C. Upon review of the kinetics observed for the initial concentration of 1.51 mass%, the adsorbate loading achieved around 7 h was perhaps an outlier. A rapid increase of approximately 30 mg.g⁻¹ from 240 min to 7 h was observed, which was larger than the increase consistently observed for the other datasets in Figure 23 and 24.

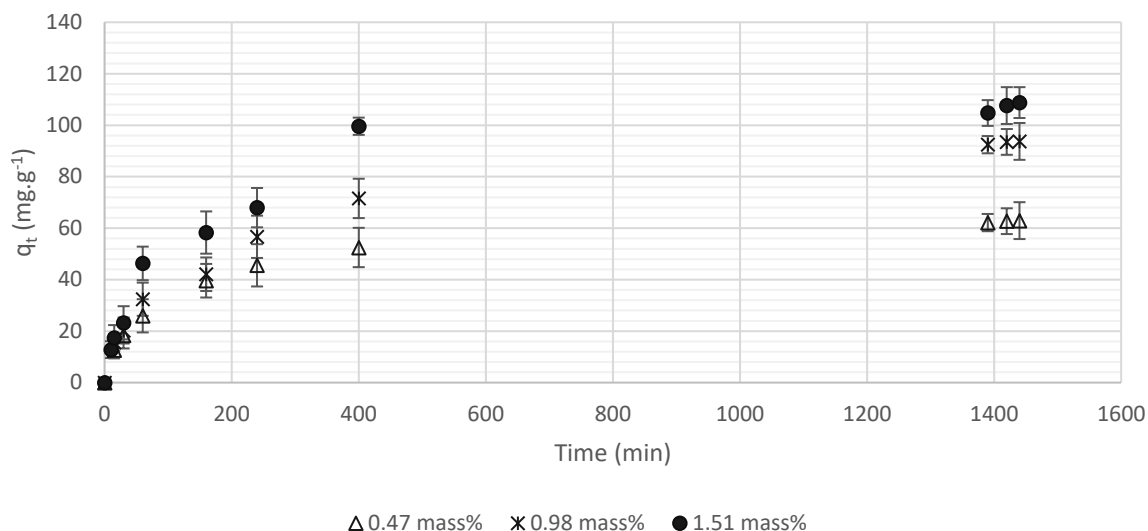


Figure 23 This figure depicts the effect of the initial concentration on the adsorbate loading and sorption equilibrium achieved at 35 °C. The adsorbate loading increased with increasing initial concentration.

Upon further investigation of Figure 24, a similar trend was observed as depicted in Figure 22.. An increase in initial concentration beyond approximately 1.5 mass% failed to increase the equilibrium adsorbate loading notably. Two outliers were observed for the dataset of 2.59 mass%: one at 60 min and the other at approximately 24 h. This variation in 20 % of the data points collected for that set may bring into question whether these results are reliable. Given that 80 % of the dataset appeared as expected and the aim of the comparison in Figure 24 was to draw a qualitative rather than quantitative conclusion, the overall trends will be considered valid Figure 24, similar to Figure 21 and Figure 22 in Section 5.2.1, depict that an increase in initial concentration up to 1.5 mass% increased the adsorbate loading achievable while, beyond this concentration, the adsorbate loading plateaued. This indicates that the maximum adsorbate loading of 3,7-DMO on SCD was approached when the initial concentration of 3,7-DMO was at 1.5 mass% and the maximum adsorption capacity is anticipated to fall within 100 – 118 mg.g⁻¹. This range overlaps with the maximum adsorption capacity range predicted at 25 °C in Section 5.2.1.

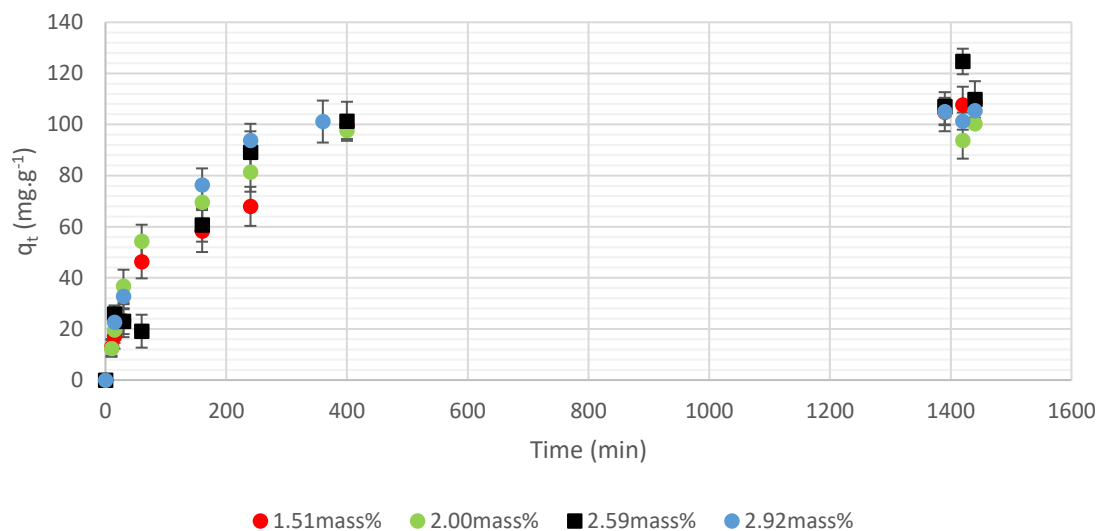


Figure 24 The effect of initial concentration on the adsorption kinetics of 3,7-DMO for an initial concentration ranging from 1.51 – 2.92 mass% at 35 °C.

5.2.3 Effect of initial concentration at 45 °C

The effect of varying the initial concentration of 3,7-DMO on the kinetics and adsorbate loading was consistent at 25 °C and 35 °C. Figure 25 provides the kinetic adsorption data for three different initial concentrations (0.50 mass%, 1.01 mass% and 1.53 mass%) at 45 °C. For reasons mentioned earlier in this chapter, only the first 7 h will be considered. Similar to Figure 21 and Figure 23, an increase in initial concentration increased the adsorbate loading particularly the equilibrium adsorbate loading. Given that the adsorbate loading increased with increasing adsorbate concentration for all three temperatures, the key difference was considered to be the result of the increased temperature rather than varying adsorbate concentration.

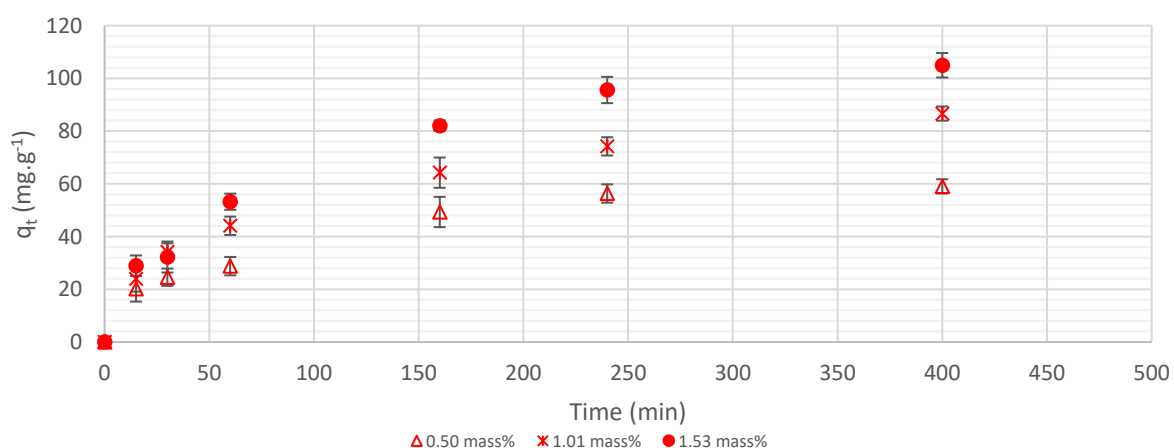


Figure 25 A review of the change in adsorbate loading over time for three initial concentrations at 45 °C, for the first 7 h which resembled the one observed at 25 °C and 35 °C.

Figure 26 was used to determine whether equilibrium adsorbate loading would plateau if the initial adsorbate concentration was increased beyond a 1.5 mass% to 3 mass% as observed in Section 5.2.1 and 5.2.2. The equilibrium adsorbate loading was not considered to be reliable, but the first 7 h showed consistent results with the adsorbate loading not notably exceed that of the 1.53 mass% at 7 h. It was subsequently assumed that, if the shortcomings of the experimental setup and data processing technique were to be improved, an increase in adsorbate concentration beyond 1.5 mass% would have had marginal effects on the equilibrium adsorbate loading.

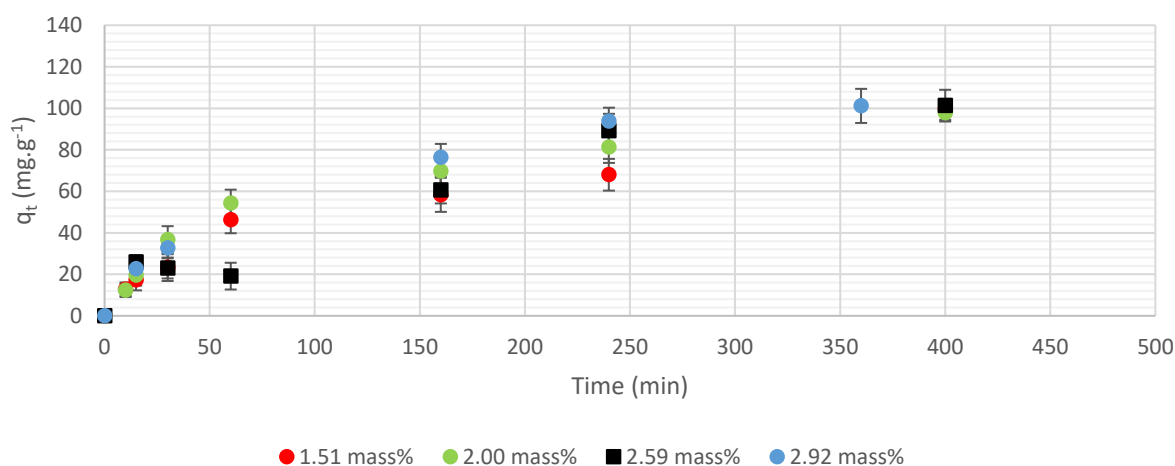


Figure 26 Reviewing the effect of increasing the initial concentration beyond 1.5 mass% at 45 °C. Although the equilibrium adsorbate loading is not accurate, the trend seen in the first 7 h adheres to that observed at 25 °C and 35 °C.

5.2.4 Summary of the effect of initial concentration

The trend regarding the removal of 3,7-DMO amidst varying temperatures was observed consistently at all three temperatures and is conclusive. As discussed in Section 2.8, the adsorption process is quantified through adsorbate loading and adsorption efficiency Figure 27 provides a graphical illustration of the effect of initial adsorbate concentration on the adsorption efficiency (percentage sorbed), for all three temperatures when equilibrium loading is reached. All three temperatures were used so as to qualitatively verify the trend observed. An increase in initial 3,7-DMO concentration was consistently observed to decrease the adsorption efficiency: the quantitative drop in adsorption efficiency was not the key focus). A study focused on the removal of lead using carbon nanofibers found that, when the initial concentration was increased from 5 to 70 mg.l⁻¹ the adsorption efficiency reduced from 90 % to 47 % (Ahmed *et al.*, 2010). This indicates that although the mass of adsorbate in the bulk solution is increasing, the number of active sites available is limited which means the percentage removal declines once the maximum adsorbate loading is achieved. This, in combination with other studies (Padmavathy,

Madhu and Haseena, 2016; Gorzin and Bahri Rasht adi,2018), supports the plausibility of the trend observed in the present project.

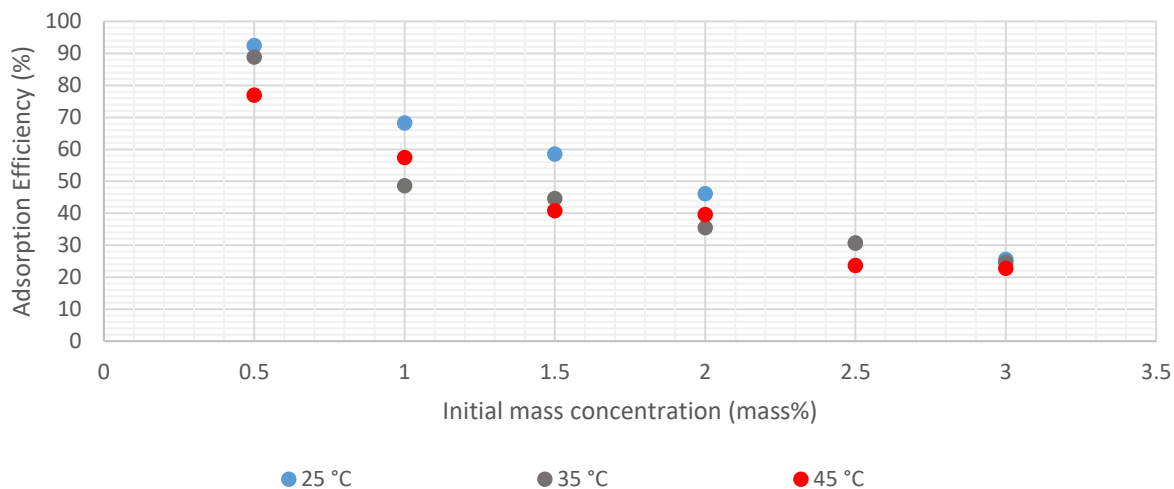


Figure 27 Effect of initial concentration on the adsorption efficiency. As the initial concentration increased, the adsorption efficiency decreased.

This information should be evaluated in conjunction with the equilibrium adsorbate loading achieved so as to identify the initial adsorbate concentration and operating conditions that resulted in the greatest adsorbate loading and adsorption efficiency. This information is important, as adsorption is a separation technology, and two key measures of whether a separation technology is efficient are the quantity of impurity removed but also the percentage mass removal. It is possible to have a high adsorption efficiency (% removal is high) while the actual quantity of adsorbate removed is low ($\text{mg adsorbate.g adsorbent}^{-1}$), and vice versa. This influences whether the desired bulk solution purity is met, whether the adsorbent maximum capacity has been reached, and whether regeneration is required. Furthermore, if purity is met while an excessive amount of adsorbent is required, the choice of separation technology may not be the most efficient.

An increase in adsorbate concentration decreased the adsorption efficiency, but it increased the equilibrium adsorbate loading up to 1.5 mass% (Section 5.2.1-5.2.3). As is illustrated in Figure 27, the adsorption efficiency achieved at solution temperatures of 25 °C, 35 °C and 45 °C at an initial concentration of 1.5 mass% ranged from 45–60 %, while the adsorbate loading ranged from 110–120 mg.g^{-1} . A study investigating the removal of chromium ions by using activated carbon observed similar trends (Gorzin and Bahri Rasht Abadi, 2018). Gorzin and Bahri Rasht Abadi (2018) noted that an increase in initial adsorbate concentration increased the adsorbate loading from 1.82–23.18 mg.g^{-1} while decreasing the adsorption efficiency from 98–77 % (Gorzin and Bahri Rasht Abadi, 2018). These results clearly indicate that the removal of 3,7-DMO is highly concentration dependent (Moyo *et al.*, 2013).

According to Figure 27, the adsorption efficiency decreased, in the case of the present study, from approximately 90–30 %, as the initial concentration increased from 0.5–3.0 mass%. As indicated in Section 5.2.1, the equilibrium adsorbate loading achieved at 0.5 mass% and 1.0 mass% was less than the

maximum equilibrium loading achievable for this adsorbate-adsorbent system at 25 °C. This suggests that, at 0.5 mass% and 1.0 mass% the number of active sites and pore availability exceeded the number of 3,7-DMO molecules present in the system. If more active sites than adsorbate molecules were present in the system, 3,7-DMO would continue to fill the available pores (see Moyo *et al.*, 2013). The adsorption efficiency achieved at 0.5 mass% exceeded that of 1.0 mass%. This indicated that, at 0.5 mass% the active sites were in considerable excess engendering little competition for active sites. At 1.0 mass%, the number of 3,7-DMO molecules had increased and the ratio of adsorbate to active sites had also done so. The adsorbate loading increased, because more adsorbate molecules encountered active sites, while the percentage removal/adsorption efficiency decreased, because the ratio of mass of adsorbate removed from the bulk solution at equilibrium relative to the mass of adsorbate initially present in the bulk solution had decreased. This is because the equilibrium adsorbate loading approached the maximum adsorption capacity of SCD as a higher percentage of the active sites available are filled (Gorzin and Bahri Rasht Abadi, 2018).

Once the initial adsorbate concentration was increased to 1.5 mass% the maximum equilibrium loading achievable for this system was reached. The ratio of 3,7-DMO molecules to active site availability was such that the successful interactions were maximized while minimizing competition so as to achieve the highest equilibrium adsorbate loading. At concentrations exceeding 1.5 mass% the equilibrium adsorbate loading remained constant, but the adsorption efficiency continued to decline. This was to be expected because, if the mass of adsorbate in the system increased while a capped mass of 3,7-DMO was being adsorbed, the mass of excess adsorbate remaining in the bulk solution would have increased.

The observations made in terms of the single component system suggested that the greatest adsorption efficiency and adsorbate loading were achieved at an initial concentration of 1.5 mass% and a temperature of 45 °C. Although this was not experimentally verified, the trends observed for the first 7 h at all three temperatures indicated that higher adsorbate loading was achieved at 45 °C.

5.3 Single-component modelling

The kinetic and equilibrium isotherm models fitted to the single component 3,7-DMO-SCD are discussed in this section.

5.3.1 Single Kinetic Models

The kinetic models were generated for all three temperatures and are shown Figure 28. The models were fitted using nonlinear regression by means of the Excel Solver Add-In function.

Figure 28(a) depicts the manner in which kinetic models fitted to the experiment conducted at 25 °C. The slope of all the models fitted are not as steep, indicating that the rate of adsorption was slower at 25 °C. Upon visual inspection, it appears that the pseudo-1st order model predicts an adsorption rate with the majority of adsorption occurring within the first 600 min. The other models showed a more gradual increase in adsorbate loading. The pseudo-second order and pseudo-nth-order appeared to approach equilibrium closer to 24 h and appeared to fitted the data well. The Elovich model indicates a faster initial

adsorption compared to the other three models on the one hand, and a slow progression in adsorbate loading for the remainder of the overall experimental timeframe on the other.

The models fitted to the kinetic data collected at 35 °C are shown in Figure 28(b). All of these showed a steep slope for the rapid adsorption phase. This suggests that the adsorption rate was faster at 35 °C than at 25 °C. The pseudo-1st order again predicted that equilibrium would be reached prematurely at around four hours. The pseudo-second and pseudo-nth-order (where $n=1.97$ which would round up to $n=2$) models appeared to predict similar behaviour, and this followed the data well. The Elovich model suggests that equilibrium would show a slow adsorption rate beyond the first hour and a higher equilibrium adsorption loading.

Kinetic models were fitted to the kinetic data collected for the first 7 h at 45 °C, as shown in Figure 28(c). A steep slope was observed for the first two hours, which indicates a fast rate of adsorption. Subsequently, it became increased marginally in gradualness for the pseudo-first order and progressively more gradual for pseudo-second order and pseudo-nth-order. The most gradual increase was again achieved in the Elovich model. The latter predicts a higher equilibrium adsorbate loading than the pseudo-nth-order, whereas the pseudo--first-order model predicts a lower equilibrium adsorbate loading.

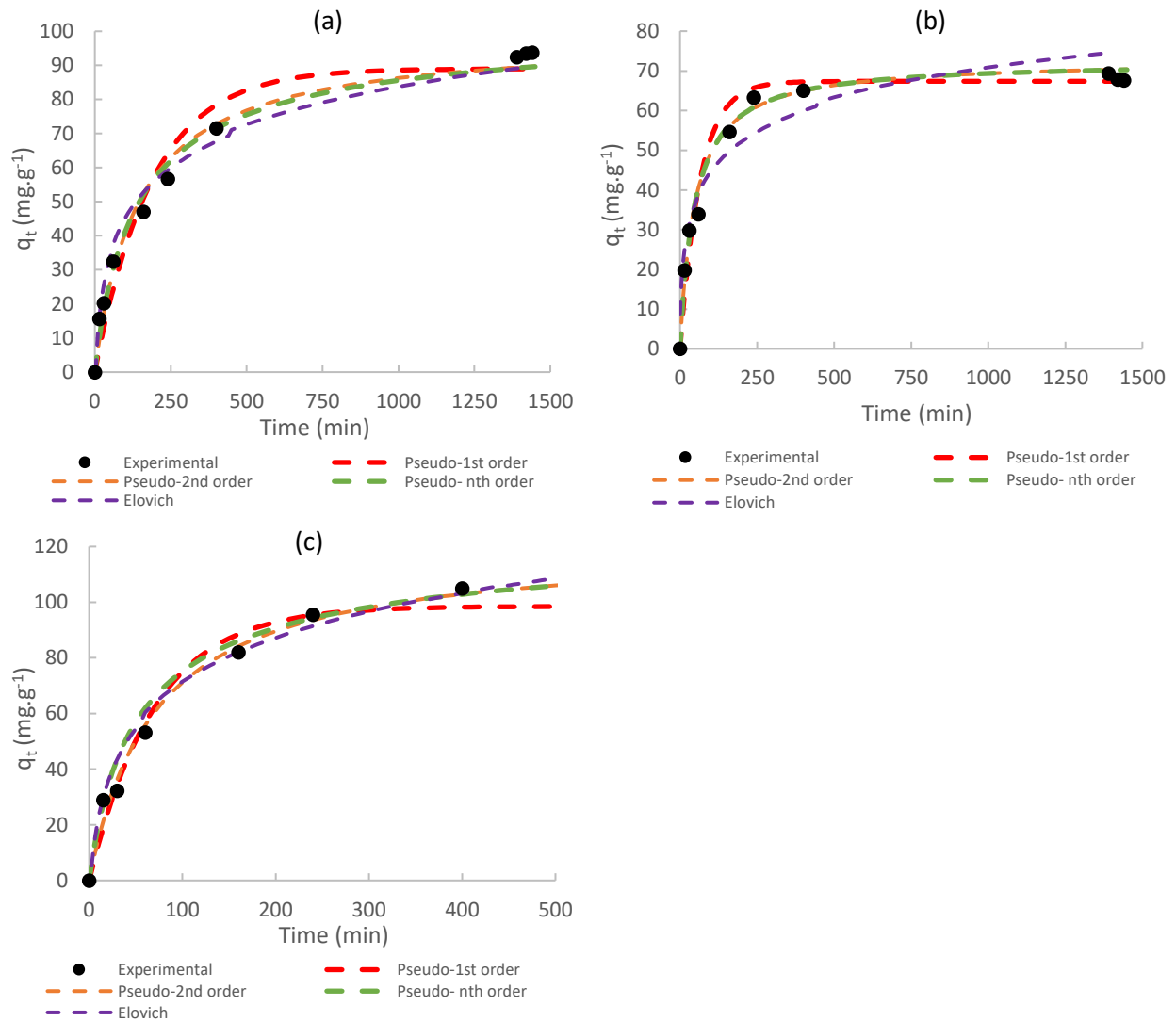


Figure 28 A plot showing q_t of 3,7-DMO as a function of time with kinetic models fitted to the data at 25 °C and 1.03 mass% (a), 35 °C and 1.12 mass% (b) and 45 °C and 1.32 mass% (c).

Figure 29(a-c) provides the WMM fitted to the kinetic profiles at 25 °C, 35 °C and 45 °C. The WMM indicated three distinct phases in the adsorption process at all three temperatures. However, Figure 29(c) indicates a less distinct change in slope between the first and second phase of adsorption. Additionally, 'C', that is, the WMM constant that provides an indication of the boundary layer thickness, was smallest at 45 °C. Figure 29(a-c) shows that film diffusion/ EMT took place from 0-70 min at 25 °C, 0,-80 min at 35 °C and 0-50min at 45 °C. IMT/ intraparticle diffusion took place from 70-420 min at 25 °C, 80-40 min at 35 °C and 50-400 min at 45 °C. At 25 °C, the observation made in the final step indicated that a comparatively large amount of adsorption had taken place towards the end of the 24 h experiment, in contrast with that observed at the elevated temperatures. The WMM shows that the effect of EMT on the rate of adsorption was not negligible, but that it did become progressively less rate-limiting as the solution temperature increased.

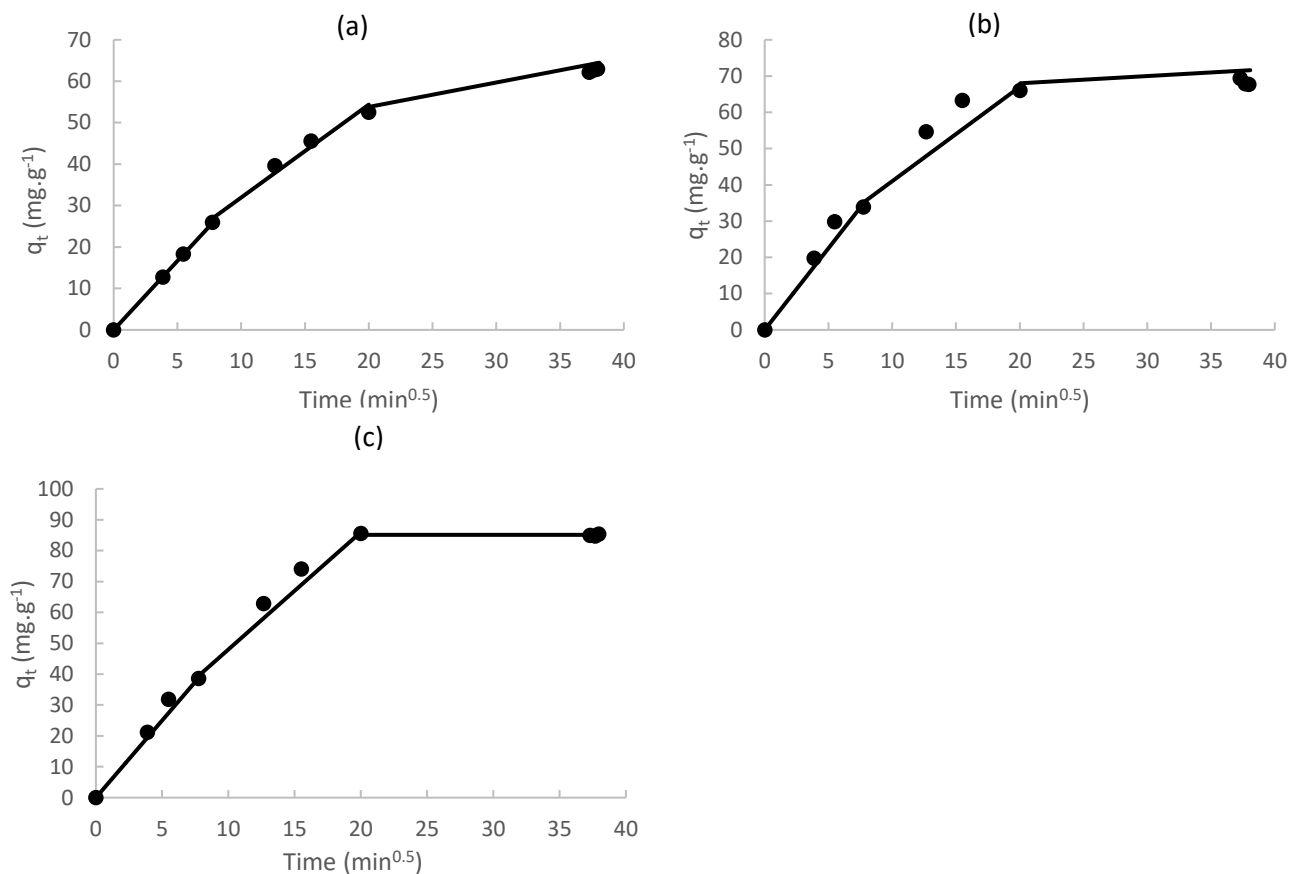


Figure 29 WMM fitted to the single component adsorption data of 3,7-DMO from the n-decane solution using SCD at a temperature and initial concentration of: 25 °C and 0.98 mass% (a), 35 °C and 1.00 mass% (b) and 45 °C and 1.23 mass% (c).

The parameters fitted to the kinetics models shown in Figure 28 and 29 are provided in Table 14 along with the parameters for the single component adsorption of 1-decanol and 2-octanol at 25 °C and 45 °C (Bosman, 2019). The adjusted coefficient of determination suggests that, at 25 °C, pseudo-second order fits the data best (this was verified by the pseudo-nth, which order also gave a good fit with n equal to 2). The next best fits were those related to the Elovich and then Weber & Morris models.

The pseudo-nth-order model suggested that the order of the adsorption was 2.42 at 25 °C, which lay between that of 1-octanol and 1-decanol. The predicted equilibrium adsorbate loading at 25 °C was lower for 3,7-DMO than for 1-octanol and 1-decanol, where 1-octanol had the highest equilibrium adsorbate loading. This confirms the idea that a smaller linear molecule was favoured over a larger one. Furthermore, the higher 1-decanol equilibrium adsorbate loading compared to the equilibrium adsorbate loading of 3,7-DMO also confirms that linear molecules are favoured above branched nonlinear ones. According to the rate constant, the rate of adsorption of 3,7-DMO was five times less than that of 1-decanol, but greater than that of 1-octanol.

At 35 °C, the pseudo-second and pseudo-nth-order fitted the data equally well: n was 1.95, which confirmed the pseudo-second order first the kinetic data. The rate constant was higher than that found

at 25 °C, but lower than that found at 45 °C. This confirms that the rate of adsorption increased with increasing temperature. Interestingly, the adsorbate loading was the lowest for this temperature.

The kinetic parameters at 45 °C will still be discussed here, even though results were not as representative of the system as had been observed at lower temperatures. The equilibrium adsorbate loading achieved was lower than that of 1-decanol and 1-octanol. This was to be expected, since this trend was also observed at 25 °C. However, a portion of the decreased loading can also be attributed to shortcomings in the experimental setup. The rate constant was higher than in the case of 1-decanol, but lower than that of 1-octanol. Overall, the Weber & Morris model (Figure 29) fitted the 35 °C and 45 °C well, which suggests that intra-particle diffusion might have limited the rate of adsorption.

Table 14 The parameters of the models fitted to the kinetic data at 25 °C, 35 °C and 45 °C for an initial concentration of approximately 1 mass%. The kinetic parameters for 1-octanol and 1-decanol at 25 °C and 45 °C were sourced from Bosman (2019) and are italicized.

Temperature (°C)	45 °C			35 °C	25 °C		
Model Parameters	<i>1-octanol</i>	<i>1-decanol</i>	3,7-DMO	3,7-DMO	<i>1-octanol</i>	<i>1-decanol</i>	3,7-DMO
Initial Mass	1.04	0.98	1.23	1.05	1.03	1.13	0.98
$q_{e,exp}$ (mg.g ⁻¹)	113	111	104	67.4	91.7	94.8	93.5
Pseudo-first-order Model							
$q_{e,calc}$ (mg.g ⁻¹)	111	109	98.6	67.4	87.9	92.9	89.0
k_1 (min ⁻¹)	0.03	0.01	0.015	0.016	0.02	0.01	0.005
R^2_{adj}	0.97	0.99	0.97	0.95	0.98	0.96	0.96
MPSD (%)	24.1	24.1	16.5	16.3	9.51	18.9	28.8
Pseudo-second-order model							
$q_{e,calc}$ (mg.g ⁻¹)	117	126	120	72.7	104	112	98.5
k_2 (10 ⁻³ g.(mg.min) ⁻¹)	0.4	0.07	0.12	0.29	0.16	0.1	0.072
R^2_{adj}	0.98	0.99	0.93	0.96	0.99	0.97	0.98
MPSD (%)	18.0	23.5	13.3	10.8	5.23	14.3	19.3
Pseudo-nth-order model							
n (-)	2.45	1.27	2.7	1.95	3.3	2.14	2.42
$q_{e,calc}$ (mg.g ⁻¹)	121	112	131	72.3	132	115	104.4
k_n (10 ⁻⁵ g.(mg.min) ⁻¹)	5.26	219	50	35.3	0.02	5.13	1.00
R^2_{adj}	0.98	1	0.97	0.96	1	0.97	0.98
MPSD(%)	17	23.4	19.5	15.2	4	14	18.9
Elovich Model							
β (g.mg ⁻¹)	0.06	0.06	0.04	0.09	0.05	0.05	0.06
α (mg.(g.min) ⁻¹)	31.7	6.74	4.15	4.98	3.96	3.46	2.20
R^2_{adj}	0.95	0.88	0.96	0.86	1	0.96	0.97
MPSD(%)	10.4	74.2	14.6	13.3	4.42	13.6	15.5
Weber and Morris Model							
C_1 (mg.g ⁻¹)	-	-	0.00	0.00	-	-	0.00
$k_{ip,1}$	-	-	5.00	4.50	-	-	3.98
$R^2_{adj,1}$	-	-	0.96	0.97	-	-	0.95
C_2 (mg.g ⁻¹)	70.9	37.4	21.3	7.81	28.6	15.5	6.07
$k_{ip,2}$	2.34	3.15	4.47	3.51	3.3	4.07	3.18
$R^2_{adj,2}$	0.97	0.83	0.95	0.99	0.92	1.00	0.94
C_3 (mg.g ⁻¹)	-	-	85.1	64.2	-	-	47.0
$k_{ip,3}$	-	-	0.25	0.20	-	-	1.22
$R^2_{adj,3}$	-	-	0.97	0.95	-	-	0.98

5.3.2 Single Isotherm Models

The equilibrium adsorption isotherm models were fitted to the data collected at 25 °C, 35 °C and 45 °C. Figure 30 depicts the adsorption isotherms for data generated at 25 °C. All models fitted suggest that the equilibrium adsorbate loading increased with increasing concentration. The Redlich-Peterson and Langmuir models appeared to fit the data well in terms of the plateau that occurred at higher

concentrations. However, it did suggest that the equilibrium adsorbate loading plateaued at lower concentrations than the experimental data showed. The Sips and Freundlich isotherm models appeared similar and fitted the data at the lower concentrations better, while it overshoot the equilibrium adsorbate loading at higher concentrations. The BET model did not fit the data well at all.

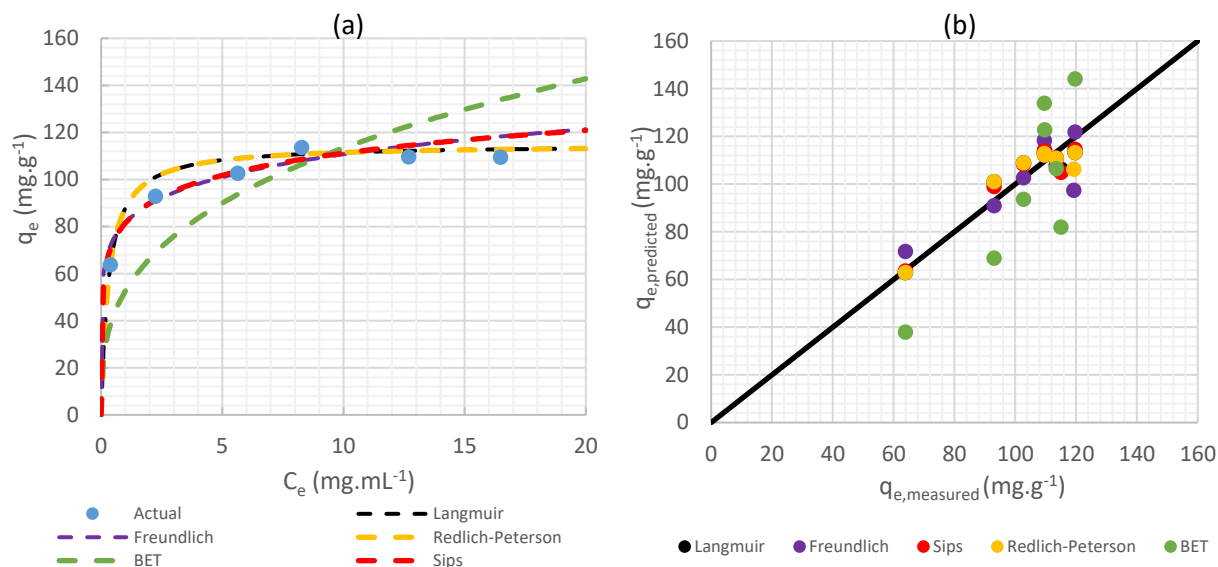


Figure 30 Six different adsorption isotherm models fitted to the equilibrium data generated experimentally at 25 °C, where the equilibrium adsorbate loading is modelled as a function of the equilibrium 3,7-DMO bulk concentration (a). The predicted versus measured/ experimentally determined equilibrium 3,7-DMO loading on SCD is also shown here.

Figure 31 illustrates the isotherm models for the equilibrium adsorbent data generated at 35 °C. Similar to Figure 30, the BET model failed to predict the data well. Figure 31(b) indicates that Sips isotherm fitted the experimental data best. The Redlich Peterson and Freundlich models predicted equilibrium adsorbate loadings similar to, while the Langmuir model varied between predicting higher and lower equilibrium adsorbate loadings compared to those that were achieved by means of experimental work.

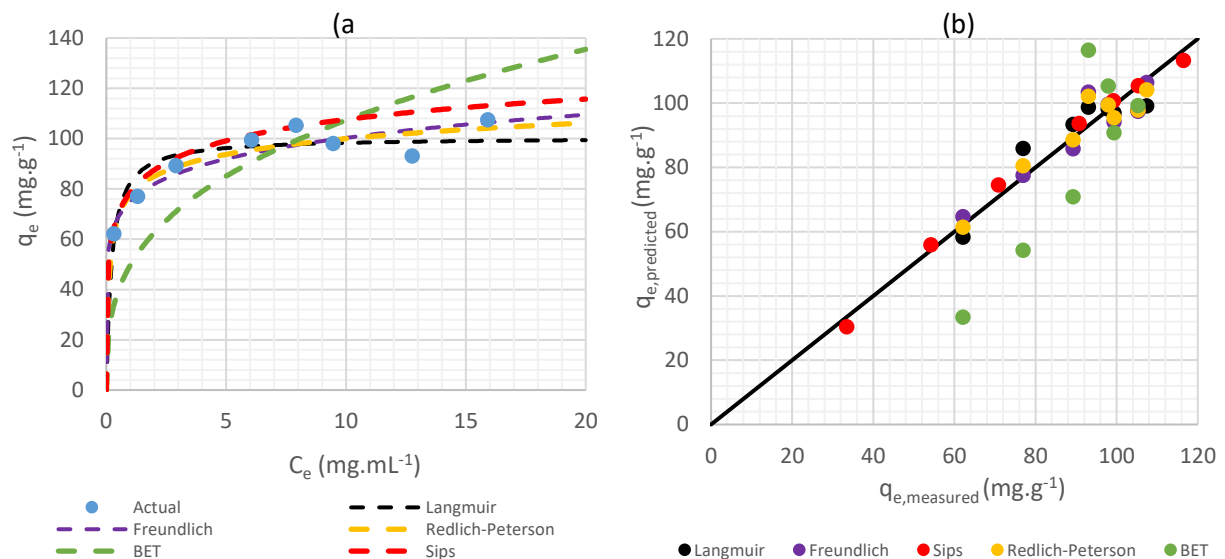


Figure 31 Six different adsorption isotherm models fitted to the equilibrium data generated experimentally at 35 °C, where the equilibrium adsorbate loading is modelled as a function of the equilibrium 3,7-DMO bulk concentration (a). The predicted versus measured/ experimentally determined equilibrium 3,7-DMO loading on SCD is also provided.

Figure 32 further indicates that the BET model failed to model the 45 °C experimental data accurately. Once more, the R-P and Langmuir isotherm models appeared to predict the data well and were similar, suggesting that R-P isotherm model reduced to the Langmuir model. The Sips isotherm model underpredicted the equilibrium adsorbate loading and the Freundlich isotherm underpredicted the lower concentrations and overpredicted higher ones.

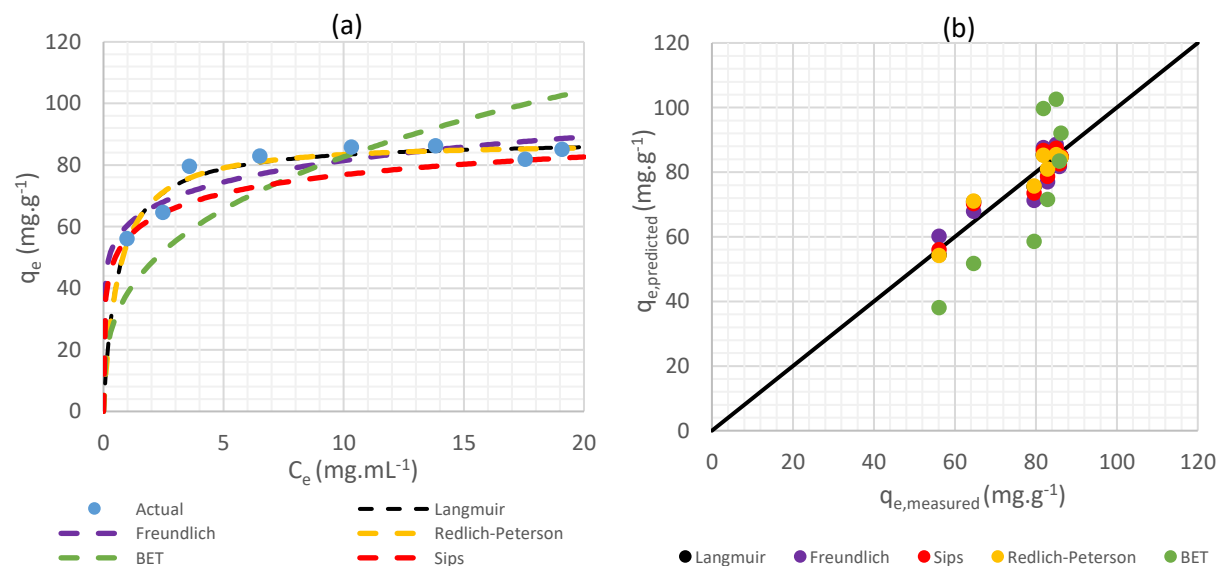


Figure 32 Six different adsorption isotherm models fitted to the equilibrium data generated experimentally at 45 °C, where the equilibrium adsorbate loading is modelled as a function of the equilibrium 3,7-DMO bulk concentration (a). The predicted versus measured/ experimentally determined equilibrium 3,7-DMO loading on SCD is also provided.

Table 15 reflects the adsorption isotherm model parameters. Overall, the MPSD and coefficient of determination (R^2) were the lowest in the R-P isotherm model. The R-P constant (g) was one at 25 °C and 45 °C and 0.92 at 35 °C. This explains why the Langmuir and R-P isotherm models fitted the data well. The latter predicted a maximum adsorption capacity of 115 $\text{mg}\cdot\text{g}^{-1}$, 101 $\text{mg}\cdot\text{g}^{-1}$ and 120 $\text{mg}\cdot\text{g}^{-1}$ at 25 °C, 35 °C and 45 °C respectively.

Table 15 Equilibrium isotherm parameters for the single component adsorption system of 3,7-DMO.

Temperature (°C)	25 °C	35 °C	45 °C
Isotherm Parameters	3,7-DMO	3,7-DMO	3,7-DMO
Langmuir Isotherm			
K_L ($\text{ml}\cdot\text{mg}^{-1}$)	3.23	4.55	1.64
q_{max} ($\text{mg}\cdot\text{g}^{-1}$)	115	101	88.4
R^2_{adj}	0.86	0.83	0.90
MPSD(%)	6.86	7.60	5.25
Freundlich Isotherm			
K_f ($(\text{mg}\cdot\text{g}^{-1})\cdot(\text{ml}\cdot\text{mg}^{-1})^{-1/n}$)	81.7	75.1	60.4
n (-)	7.56	7.94	7.70
R^2_{adj}	0.72	0.87	0.78
MPSD(%)	10.0	6.39	7.46
Redlich-Peterson Isotherm			
K_{rp} ($\text{ml}\cdot\text{mg}^{-1}$)	371	1044	139
a_{rp} ($\text{ml}\cdot\text{mg}^{-1})^{1/g}$	3.23	12.5	1.53
g	1.00	0.92	1.00
R^2_{adj}	0.86	0.98	0.9
MPSD(%)	5.94	6.23	5.8
BET isotherm			
q_s ($\text{mg}\cdot\text{g}^{-1}$)	116	867	1473
k	0.26	0.28	0.13
c_s (10^3)	27.3	1.50	7.16
R^2_{adj}	0.72	0.75	0.70
MPSD(%)	29.9	30.0	32.0
Sips isotherm			
K_s ($\text{ml}\cdot\text{mg}^{-1})^m$	2.63	0.34	0.83
q_{max} ($\text{mg}\cdot\text{g}^{-1}$)	118	200	124
m (-)	1.21	1.88	3.42
R^2_{adj}	0.74	1.00	0.85
MPSD(%)	10.2	1.30	6.64

5.4 Chapter Outcomes

This chapter addressed Objective 2 among the Aims and Objectives of this study (see Section 1.3). It achieved Phase 2 and partially achieved phase 4 of the experimental plan (Section 3.4).

According to the experimental results presented here, an increase in initial concentration increased the adsorbate loading achievable, but plateaued beyond an initial concentration of 1.5 mass%. An increase in initial concentration also increased the time taken to approach equilibrium.

An increase in temperature increased the rate of adsorption and it appeared that the equilibrium adsorbate loading was approached faster along with that increase. An increase in temperature may have decreased the equilibrium adsorbate loading that was achievable.

Kinetic and equilibrium models fitted to the data at all three temperatures. The pseudo-second-order model generally described the kinetic experimental data the best over the range of initial concentrations used. The Langmuir and Redlich-Peterson model fitted the equilibrium data best, at 25 °C and 35 °C.

Chapter 6 Binary Component Adsorption

The aim of this chapter is to characterise two binary component adsorption systems, that is, once more, 1-decanol&3,7-DMO and 1-octanol&3,7-DMO, and their adsorptive uptake from an n-decane solution onto SCD by means of kinetic and equilibrium studies. Chapter 5 reported on the single component adsorption of 3,7-DMO from n-decane by using SCD. The single component data provided an understanding of how 3,7-DMO behaves in a non-competitive system. The behaviour of 1-decanol and 1-octanol in non-competitive systems was gleaned from extant literature (Bosman, 2019) The present section aims to understand the manner in which 3,7-DMO performs with 1-decanol or 1-octanol in a competitive system. The present chapter further serves as a building block for Chapter 7, in which the displacement potential of each adsorbate will come into focus.

This section aims to address a main objective (Objective 2) and the remaining 50% of the secondary objectives as presented in Section 1.3. This will in terms of the items listed below.

- Comparing the kinetics observed at two temperatures (25 °C and 45 °C) while keeping the initial mass% concentration constant. This comparison will be done at multiple initial concentrations to ensure that trends are observed consistently.
- Comparing the kinetics observed at a range of initial mass% concentrations while maintaining a constant temperature.
- Comparing the kinetics observed at different adsorbate₁:adsorbate₂ ratios while maintaining a constant temperature.
- Fitting the kinetic and isotherm models to the binary component adsorption data. The multicomponent adsorption isotherm models are fitted by using the single component isotherm parameters of 3,7-DMO (as reported in Chapter 5) and 1-decanol and 1-octanol (as sourced from Bosman (2019)).

6.1 Effect of temperature

In Section 5.1, the effect of varying temperature on the adsorption of 3,7-DMO onto SCD was investigated. It was found that an increase in temperature increased the adsorbate loading: the system appeared sensitive to temperature changes. The effect of temperature in binary component systems has to do with its effect on selectivity (Huang *et al.*, 2011). This was the reason for investigating a binary system containing equimass components. If the one adsorbate is preferentially adsorbed when only the solution temperature is varied then temperature is said to affect the adsorbent selectivity.

The present section of Chapter 6 will discuss the effect that a change in temperature from 25 °C to 45 °C had on the adsorbate loading over the first 7 h 7 h adsorption period. As indicated, the equilibrium adsorbate loading achieved at 45 °C was not considered to be reliable. Although the results indicated that equilibrium was only reached at around 24 h, the adsorbate loading achieved at 7 h fell within an ambit of 10% of the equilibrium adsorbate loading. Therefore, it was considered reasonable to compare the first 7 h of the various kinetic profiles.

Both systems were examined at an overall concentration of approximately 3.3 mass%. This was the highest mass concentration that was considered in this study. The single component study of 3,7-DMO found that, beyond 1.5 mass% the equilibrium adsorbate loading plateaued. In the cases of 1-octanol and 1-decanol, extant literature indicates that, beyond 1 mass% the equilibrium adsorbate loading plateaus (Bosman, 2019; Groenewald, 2019). It was assumed that, if the mass concentration of the individual adsorbate components exceeded 1.5 mass%, then the adsorbate was present in excess. This would minimize the effect of other variables, and the trends observed could be assumed to have resulted directly from various ranges of temperature.

6.1.1 1-decanol&3,7-DMO

The 1-decanol&3,7-DMO binary system was investigated for an adsorbate ratio of 0.5:0.5 (Figure 33). The loading provided was for the combined adsorption of both adsorbates. The loading achieved for 45 °C was consistently higher than that achieved at 25 °C over the first 7 h 7 h. There was a large difference in loading achieved at 45 °C in the case of the single component system, in contrast with the binary one that contained 3,7-DMO. This information suggests that the single component system was more sensitive to temperature than the binary. The finding might also have been a result of competitive adsorption. As suggested in Section 6.1, when 3,7-DMO was part of a binary system, it interacted strongly with 1-decanol and was more easily displaced by 1-decanol. In the single component system, the kinetic energy was enhanced by increased temperature. In the case of chemisorption, an increased temperature favoured adsorption. The same principle appears to be applicable to the 1-decanol&3,7-DMO binary system.

The effect of temperature on the binary system was smaller than in the case of the single component system, and the reason for this may be two-fold. Firstly, differences in affinity of the adsorbent to the adsorbate present influenced the extent of adsorption. Secondly, the bond strength and interactions between 1-decanol and 3,7-DMO might have been stronger than the interaction of 3,7-DMO with the adsorbent. The combination of these two factors would then result in a more favourable adsorption of 1-decanol and not 3,7-DMO and, despite the availability of active sites, the percentage sorbed of 3,7-DMO would be limited.

The adsorption process was divided into two stages: a rapid one (0-60 min) and an intermediate one (60-400 min). Upon visual inspection, the adsorption rate in the rapid stage appeared faster at 45 °C. This resonated with observations for the single component system (Section 5.1). The increased rate of adsorption might have been due to the increase in energy of the two adsorbates, which would then have enabled faster movement and rapid interaction with active sites to a greater extent. The boundary layer surrounding the adsorbent reduced at higher temperatures, which reduced the resistance experienced in terms of external mass transfer and an increased the rate of adsorption.

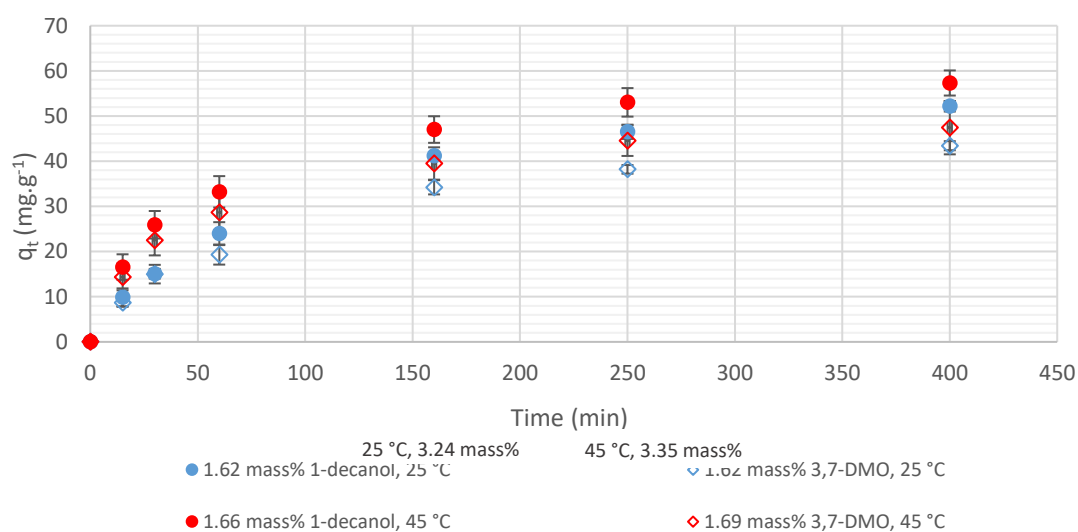


Figure 33 Investigation of effect of temperature on 1-decanol&3,7-DMO system for an overall concentration of 3.3 mass% and an adsorbate ratio of 0.5:0.5. The adsorbate loading is for the total adsorption of both adsorbates.

Due to the shape of 3,7-DMO, it may prefer to adsorb in the mesopores and in micropores to a lesser degree. Since 1-decanol was similar in size compared to 3,7-DMO, the shape would determine which component had the greater extent of pore-filling. The 1-decanol molecules might have diffused into the smaller micropores with greater ease. Given the structural stability of AA, it was unlikely that the adsorbent pores would have expanded (see Agrawal *et al.*, 2018). Therefore, the micropores would have been filled predominantly with 1-decanol and, at an increased temperature, the overall loading would have increased marginally.

6.1.2 1-octanol&3,7-DMO

The second system evaluated was that of the 1-octanol&3,7-DMO binary. According to the results presented in Section 6.1.2, it was expected that the addition of 1-octanol would decrease the adsorbate loading achieved for 3,7-DMO.

Figure 34 indicates that, over the first 7 h, no discernible difference was noted between the adsorbate loading achieved at 25 °C and 45 °C. The difference in initial concentration was of a 0.15 mass% which fell outside the 0.1 mass% confidence interval. Given that both pure components were in excess, it was assumed that this difference in initial concentration would have negligible effects on the system. 3,7,7

In terms of the three stages of adsorption, the rapid and intermediate stages appeared similar for 25 °C and 45 °C. There was no discernible difference among these. Section 5.1 reflects a faster adsorption rate for higher temperatures. Given that the effect of temperature was not discernible in this system, it was assumed that the adsorbate loading achieved would have been similar to that achieved at 25 °C.

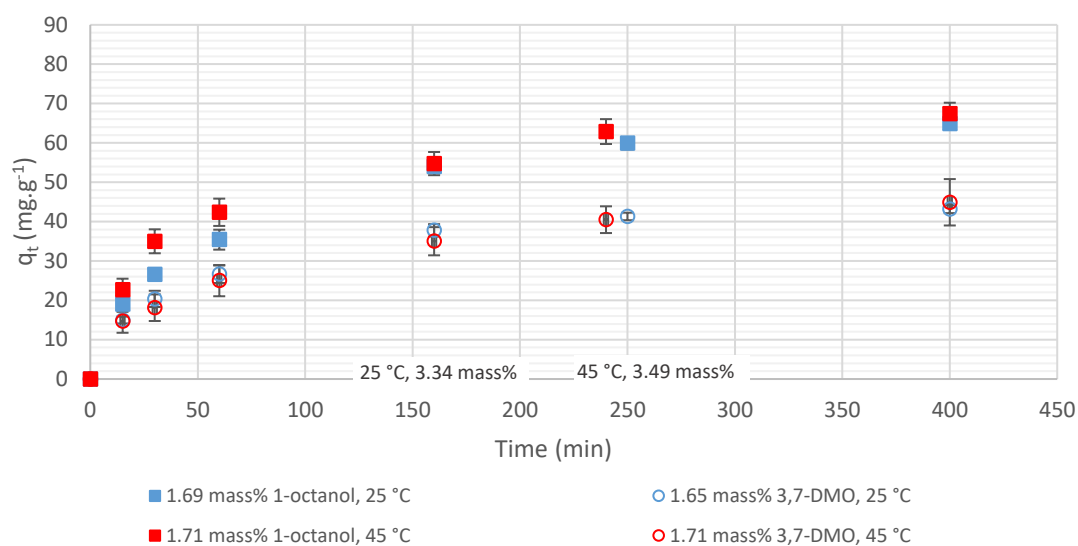


Figure 34 Effect of temperature on the adsorbate loading for an initial concentration of approximately 3.4 mass% for a 0.5:0.5 1-octanol&3,7-DMO system. No discernible difference was noted over the first 7 h.

It is widely accepted that, as the alcohol chain length increases, the solubility of 1-alcohols in water decreases (Alavi *et al.*, 2010). Therefore, 1-octanol would mix more readily with 3,7-DMO, while both are more likely not to mix with water and instead form two distinct phases.

6.2 Effect of composition

The analysis of 3,7-DMO adsorption onto SCD revealed that an increase in adsorbate initial concentration increased the adsorbate loading up until approximately 1.5 mass%. Subsequently, the equilibrium adsorbate loading plateaued. The present section aims to evaluate the effect of initial concentration and adsorbate ratio on the overall and component adsorption for 1-decanol&3,7-DMO and 1-octanol&3,7-DMO.

The results presented below were all recorded at 25 °C due to increased confidence in the process. The results recorded at 45 °C will be provided in Appendices B.2 and B.3. The overall initial concentration evaluated ranged from 1-3.3 mass% and concentrations below 1 mass% were not considered, as a decline in the accuracy of the GC analysis was observed at that stage.

6.2.1 Overall initial concentration

Figure 35 compares the change in adsorbate loading in terms of time accrued for a 0.5:0.5 1-decanol&3,7-DMO system at various initial concentrations. During the rapid adsorption stage (0-60 min), no clear distinction could be made between the adsorbate loading achieved at the three different initial concentrations. This may indicate that the adsorbent was less sensitive to initial concentration in the first

hour of adsorbate₁-adsorbate₂-adsorbent interaction, which contrasts with observations of the single component 3,7-DMO system (Section 5.2.1).

In the intermediate stage (-one to 7 h), a clear difference in adsorbate loading was observed between the lowest and two upper initial concentrations. As the intermediate stage progressed, the difference in adsorbate loading between 1.02 mass% and the two upper concentrations continued to increase and the maximum difference was observed at around 7 h. This suggests that vacant sites were available that were not being filled by the binary component system. Initially, considerable interaction occurred at the active sites but, as greater quantities were adsorbed, the concentration of adsorbate molecules decreased. This decreased the driving force for EMT and reduced the rate and amount of uptake adsorbate. This phenomenon, along with competition for active sites, might have resulted in a slow change in uptake between the upper two concentrations. In this stage, there was no notable difference in adsorbate loading for 2.08 mass% and 3.24 mass%. The first difference was noted at the end of the intermediate stage when 3.24 mass% presented a slightly lower adsorbate loading than 2.08 mass%. According to Bosman (2019), the adsorbate loading of 1-decanol plateaus beyond approximately 1 mass% whereas a plateau is only observed beyond 1.5 mass% for 3,7-DMO. However, given that the adsorbent has a higher affinity for 1-decanol, it would make sense that the plateau would occur earlier.

The slow adsorption stage (7-24 h) showed a large increase in adsorbate loading for the lowest overall concentration, a smaller increase for the intermediate concentration and a minor in for the highest concentration. The increase in adsorbate loading from 7-24 h decreased with increasing initial adsorbate concentration. The rate of adsorption increased with increasing initial concentration. Given the limited number of active sites and pores available, if the number of adsorbate molecules approached and went beyond the maximum adsorbate-to-active-site ratio, the equilibrium adsorbate loading would be achieved faster.

At higher concentrations, the pores would initially fill faster due to attracting forces and, as a result of an increased number of molecules present, was more. This might have been a direct result of a reduction in driving force in terms of external mass transfer (see Wang and Guo, 2020). The difference that was present in adsorbate present in solution as compared to adsorbate on the adsorbent decreased or inverted, and the driving force was reduced. This would slow down the rate of adsorption and EMT with be a prevalent rate-limiting step (Wang and Guo, 2020). This contrasts with that which the present study observed in the 3,7-DMO single component system. The system indicated that an increase in initial concentration resulted in an increase in adsorbate loading from 7-24 h. This might have been caused by the fact that, as soon as the adsorbate molecules were less than the active sites, perhaps 3,7-DMO blocked pores and hindered further adsorption. It could also have been that, in the binary system, a reduced concentration resulted in a distant-dependent potential that affected the pull of the adsorbate towards the adsorbent (Fang and Szeleifer, 2002). There would then have been a greater distance between the adsorbate molecules and the adsorbent and a combination of the 1-decanol-3,7-DMO interactions and the distant-dependent potential would have limited the rate of adsorption.

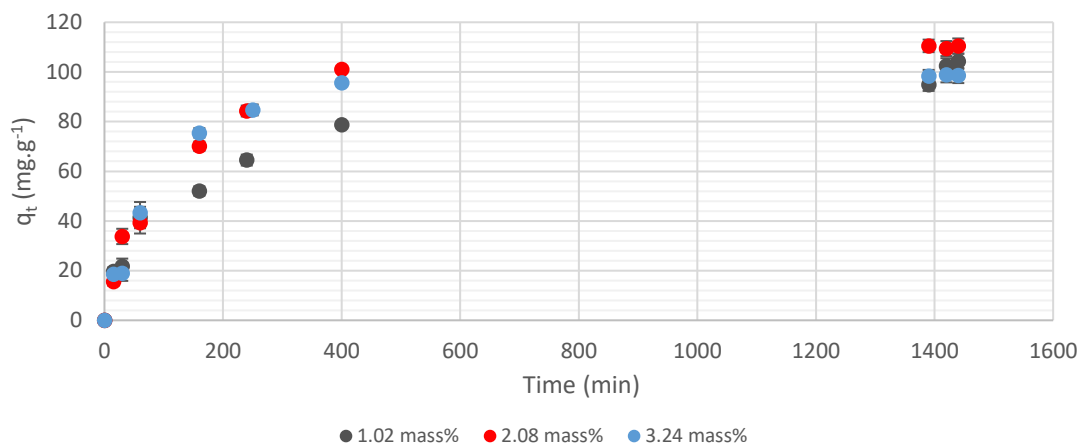


Figure 35 Investigation of effect of combined initial concentration on 0.5:0.5 1-decanol&3,7-DMO binary system at 25 °C.

This trend suggests that a breakdown of the overall adsorbate loading into the loading of 1-decanol and 3,7-DMO was required. The adsorption of 1-decanol and 3,7-DMO within the 0.5:0.5 binary component system was compared at all three initial adsorbate concentrations (Figure 36). In the intermediate adsorption stage, the adsorbate loading achieved for 1-decanol was consistently larger than that of 3,7-DMO. The difference in loading achieved for the lowest adsorbate concentration (1.02 mass%) was consistently smaller than that found in the two upper adsorbate concentrations throughout the intermediate and slow adsorption stages. During the slow adsorption stage, the difference in adsorbate loading of 1-decanol from 7-24 h decreased in tandem with an increase in the overall adsorbate concentration. For 3,7-DMO, the same trend was observed, except that, for the highest initial adsorbate concentration, a drop occurred in adsorbate loading. In terms of the margin of error, the adsorbate loading either dropped or remained the same.

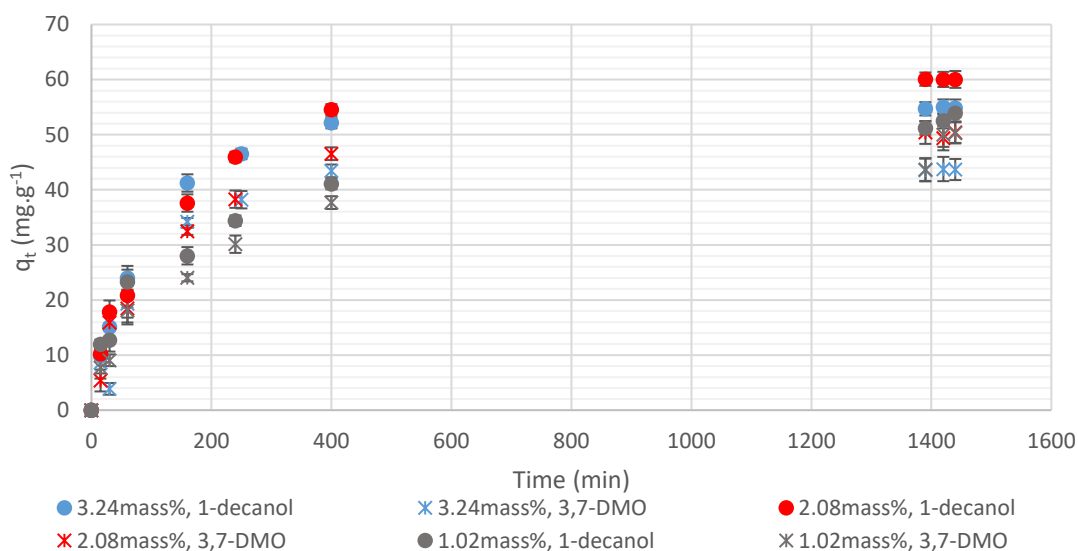


Figure 36 Comparison of the difference in adsorbate loading achieved for 24 h of 1-decanol and 3,7-DMO in a 0.5:0.5 binary system. It was observed that the adsorbate loading achieved for 1-decanol was larger than that of 3,7-DMO.

Figure 37 and Table 16 provide a comparison of the individual adsorbate and overall adsorbate adsorption for a 0.5:0.5 1-decanol&3,7-DMO system at varying overall initial concentrations. As illustrated in Table 16, the lowest overall adsorbate loading achieved occurred at an initial mass concentration of 1.02 mass% while the maximum adsorbate loading was achieved at 2.74 mass%. Minor fluctuations were to be expected for the overall equilibrium adsorbate loading, but the trend observed for the single component adsorption system was not observed here. The range of equilibrium adsorbate loading observed suggests that, contrary to the single component system, a distinct plateau had not been reached. Instead, the equilibrium adsorbate loading appeared to spike and drop back down while remaining in a range of $112\text{--}139 \pm 5 \text{ mg.g}^{-1}$. It may be that this was caused by the interactions with one another and the adsorbent, which then overpowered the effect of the initial concentration. The ideal composition for maximum equilibrium adsorbate loading and adsorption efficiency may occur at a sweet spot in the range of concentrations (2.00 mass%). At this concentration, it was possible that the adsorbate-adsorbent interactions marginally outweighed those of the adsorbate₁-adsorbate₂ interactions, thus favouring adsorption.

Table 16 shows that the percentage sorbed for the overall and individual adsorbate components increased with decreasing initial concentration. This was found to typify an adsorption system where the equilibrium adsorbate loading decreased, but the adsorption efficiency increased with decreasing initial adsorbate concentration. This has to do with the ratio of adsorbate-to-active-site availability and the maximum equilibrium-adsorption capacity. A trend was also observed when the adsorption efficiency of 1-decanol was compared to that of 3,7-DMO. The adsorption efficiency of 1-decanol was consistently higher than that of 3,7-DMO. The molecular weights of 3,7-DMO and 1-decanol are identical: therefore, the percentage sorbed was a true representation of the number of molecules removed. This confirms the idea that 1-decanol was preferentially adsorbed when compared to 3,7-DMO. Figure 36 above also

indicates that, from the beginning, the adsorbate loading of 1-decanol was higher than that of 3,7-DMO, which makes it difficult to determine whether displacement took place in the system.

Table 16 Comparison of percentage sorbed/ adsorption efficiencies at different initial concentrations for a 1-decanol&3,7-DMO 0.5:0.5 binary component system.

Overall Initial mass% (± 0.1 mass%)	Percentage sorbed/adsorption efficiency (\pm)			Overall adsorbate loading ($\text{mg}\cdot\text{g}^{-1}$) ($\pm 5\text{mg}\cdot\text{g}^{-1}$)
	Overall	1-decanol	3,7-DMO	
3.68	24	26	21	122
3.16	25	27	21	112
2.74	35	39	31	139
2.06	41	45	37	117
1.75	46	51	42	130
1.02	72	76	68	104

These results indicate that initial concentration influenced the adsorption efficiency and adsorbate loading, while the effect was difficult to predict. Overall, 1-decanol was always preferentially adsorbed when compared to 3,7-DMO. This confirms the point made in Section 6.1, which suggested that molecular shape influences the 1-decanol&3,7-DMO-SCD system (see Fang and Szleifer, 2002). 1-Decanol has a long carbon chain and has a linear needle-like shape, whereas 3,7-DMO has a shorter carbon chain that takes on an L-like shape with two further protrusions along the core chain. This suggests that the pores structure of SCD varies and that the majority is of pores are shaped in a needle-like manner.

The next system to consider was the 0.5:0.5 1-octanol&3,7-DMO one. Here, the effect of initial concentration on adsorbate loading is provided in Figure 37 below. An overall review suggests that the 1-octanol&3,7-DMO system responds differently from to 1-decanol&3,7-DMO when it comes to an increase in concentration. During the rapid adsorption stage, the difference in adsorbate loading at different initial concentrations increased. Initially, it appeared that an increase in adsorbate concentration increased the adsorbate loading but, given the margin of error, this cannot be conclusively stated. At the end of the rapid adsorption stage, the highest initial concentration (3.34 mass%) produced the largest adsorbate loading, whereas the loadings for the lower two concentrations were not easily distinguishable.

Observation at the intermediate adsorption stage suggests that an increase in initial concentration, that is, where the adsorbate was in excess compared to the active sites, increased the adsorbate loading. An interesting trend was observed for the initial concentration of 2.02 mass%. The adsorbate loading remained similar to that of 1.05 mass% until approximately 160 min. Subsequently, it spiked at around 240 min and achieved an equilibrium adsorbate loading similar to that of 3.34 mass%.

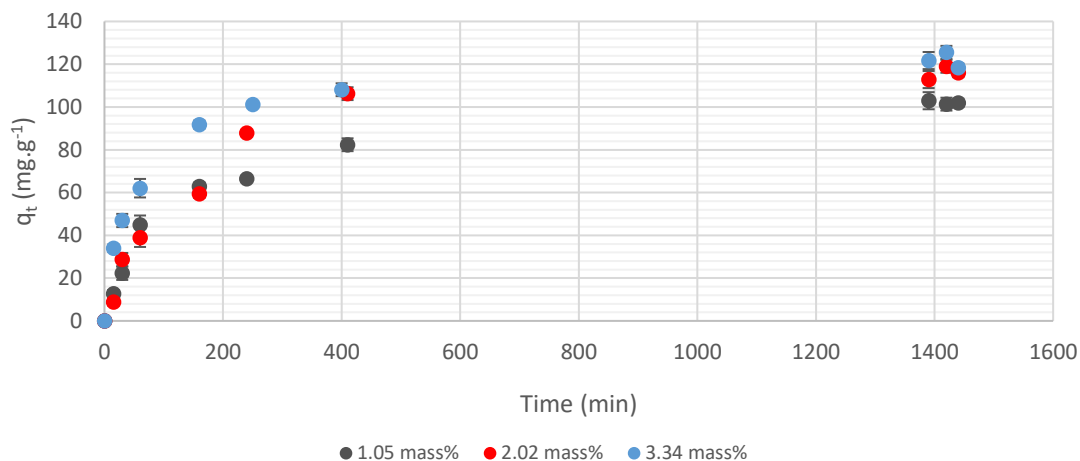


Figure 37 Comparison of various overall adsorbate loading for a 0.5:0.5 1-octanol&3,7-DMO binary system at varying combined initial concentrations.

An increase in overall initial concentration increased the adsorbate loading. Although the trend observed is similar to 1-decanol&3,7-DMO a clear distinction cannot be made between the equilibrium adsorbate loading achieved for 2.02 mass% and 3.34 mass%. Figure 38 illustrates the difference in adsorbate loading between that achieved for 1-octanol and that achieved for 3,7-DMO within the binary component system. It was observed that the adsorbent was loaded with substantially more 1-octanol when compared to 3,7-DMO, except for the initial mass concentration of 1.05 mass% where the difference was smaller but still evident.

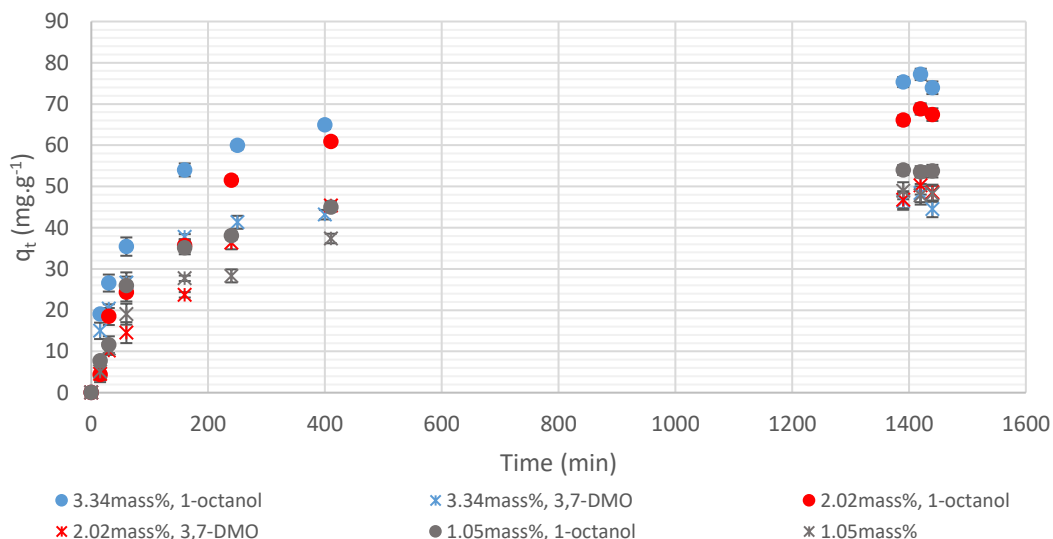


Figure 38 Comparison of various adsorbate loadings achieved for 1-octanol and 3,7-DMO in a binary 0.5:0.5 1-octanol&3,7-DMO system.

As is clearly illustrated in Table 17, the general trend mass% was that an increase in overall initial concentration increased the equilibrium adsorption achieved, despite the fact that a slight dip was observed at 3.31 mass%. The adsorption efficacy was seen to decrease with increasing overall initial

concentration. The same trend was observed with a view to the adsorption efficacy of the individual components in the system. It was found that 1-octanol experienced an adsorption efficacy that was at least 10% higher than that of 3,7-DMO. The displacement studies that were performed indicated that the bond formed between 1-octanol and SCD was stronger than the one that was observed between 3,7-DMO and SCD. It is possible that 1-octanol displaced some of the adsorbed 3,7-DMO or was preferentially adsorbed.

Table 17 Comparison of percentage sorbed/ adsorption efficiency of 1-octanol and 3,7-DMO in a 0.5:0.5 binary component system at different initial mass concentrations.

Overall Initial mass% (±0.1 mass%)	Percentage sorbed (±3%)			Overall adsorbate loading (mg.g ⁻¹) (±5mg.g ⁻¹)
	Overall	1-octanol	3,7-DMO	
3.34	25	31	20	122
3.32	34	39	28	119
3.31	37	43	30	104
2.87	52	59	45	113
2.54	63	67	59	97
1.03	80	84	76	80

According to Girish (2017), a determination of the interaction effect elucidates the way in which each adsorbate is affected by a multicomponent system. As is depicted in Figure 39, the adsorbate loading achieved when 3,7-DMO was contained in a single component system was considerably higher than that achieved in a 1-decanol&3,7-DMO system or a 1-octanol&3,7-DMO system. It was expected that lower loadings for the same component in binary (competitive) systems would be found when compared to single (non-competitive) systems (see Çay, Uyanik and Özaşik, 2004). This can also be verified by determining the interaction parameters. In the present case, these were found to be less than 1 for 3,7-DMO in both binary systems. This suggested antagonistic interaction, which means that the adsorption of 3,7-DMO was damped in the presence of other adsorbate components.

In both binary systems, a lesser amount of 3,7-DMO was adsorbed per gram adsorbent when compared to the single component system. This indicates that some interaction and competition took place between 1-decanol/1-octanol and 3,7-DMO in a binary component system. If the interaction parameters were equal to or greater than one, it would have indicated that the second adsorbate had no effect or promoted the adsorption of 3,7-DMO. An interaction parameter of less than one indicates that both adsorbate types were competing for the available active sites and the second adsorbate was hindering the adsorption of 3,7-DMO.

3,7-DMO interaction parameter in a 1-decanol&3,7-DMO system:

$$\frac{Q_m}{Q_i} = \frac{45}{120} = 0.37$$

3,7-DMO interaction parameter in a 1-octanol&3,7-DMO system:

$$\frac{Q_m}{Q_i} = \frac{50}{120} = 0.42$$

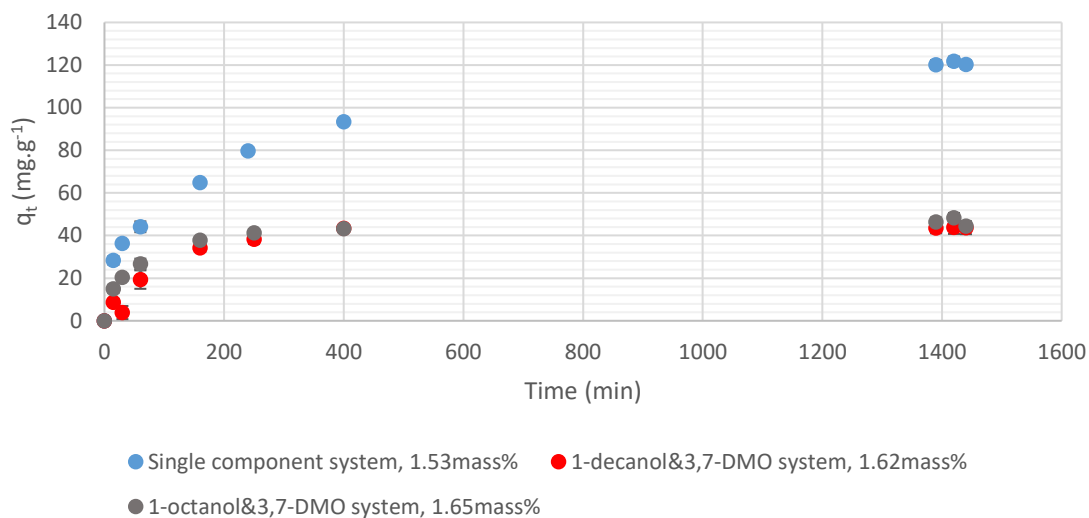


Figure 39 Comparison of 3,7-DMO adsorbed in a single component system as compared to 0.5:0.5 1-decanol&3,7-DMO and 0.5:1 0.5-octanol&3,7-DMO systems.

6.2.2 Adsorbate ratio

The effect of the adsorbate ratio on the overall loading achieved for the two binary component systems is reflected in Figure 40 and Figure 41 below. This initial overall mass% was selected to ensure that both adsorbates were in excess. The results are provided for the overall initial concentration of 3.27 mass% for 1-decanol&3,7-DMO. The effect of adsorbate ratio is also provided for two lower initial concentrations in Appendices B.2 and B.3. The trend observed was inconsistent. It appears that, at lower concentrations, the maximum equilibrium loading was achieved for a 0.5:0.5 adsorbate ratio while, at 3.34 mass% the lowest equilibrium adsorbate loading was achieved for a 0.5:0.5 (1-decanol:3,7-DMO) adsorbate ratio. The highest equilibrium adsorbate loading was achieved for an 0.75:0.25 ratio, while the 0.25:0.75 ratio had an intermediate adsorbate loading. It is suspected that this was caused by the effect of antagonistic interaction. When the amount of the second adsorbate was smaller than, and the system approached a single component system, it appears that the competition for active sites was reduced. This would have resulted in higher adsorbate loadings. Intriguingly, when 3,7-DMO was greater than (0.25:0.75 1-decanol&3,7-DMO), the equilibrium adsorbate loading was lower. This can be ascribed to a decreased adsorbent affinity for 3,7-DMO.

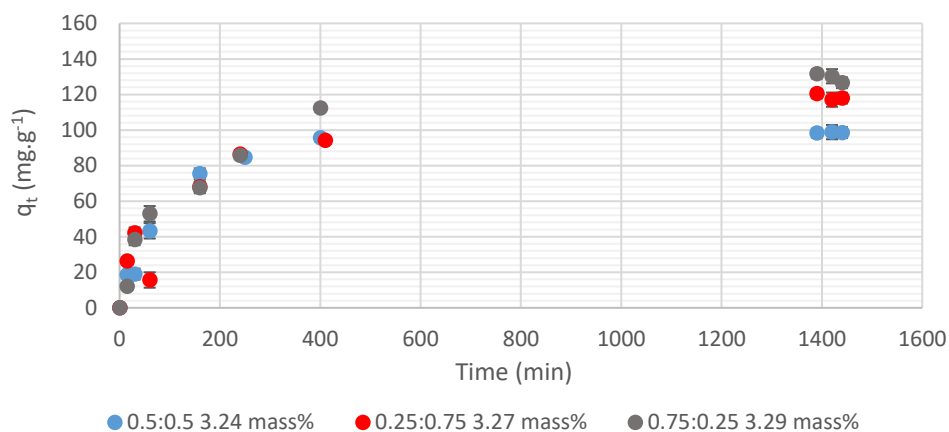


Figure 40 Comparison of the effect of the adsorbate ratio on the kinetics of a 1-decanol&3,7-DMO system at an initial concentration of 3.27 mass%.

Figure 41 shows no distinct difference in equilibrium adsorbate loadings at different initial concentrations. At lower initial concentrations, the maximum equilibrium adsorbate loading was achieved for a 0.5:0.5 ratio. Across the board there, no significant difference was seen in adsorbate loadings achieved for 0.25:0.75 and 0.75:0.25 (1-octanol&3,7-DMO). The reason for this is not clear, as the effect of the interaction of 3,7-DMO in the 1-octanol&3,7-DMO system was antagonistic. It was therefore expected that higher loadings for 1-octanol&3,7-DMO would occur when 3,7-DMO was smaller than.

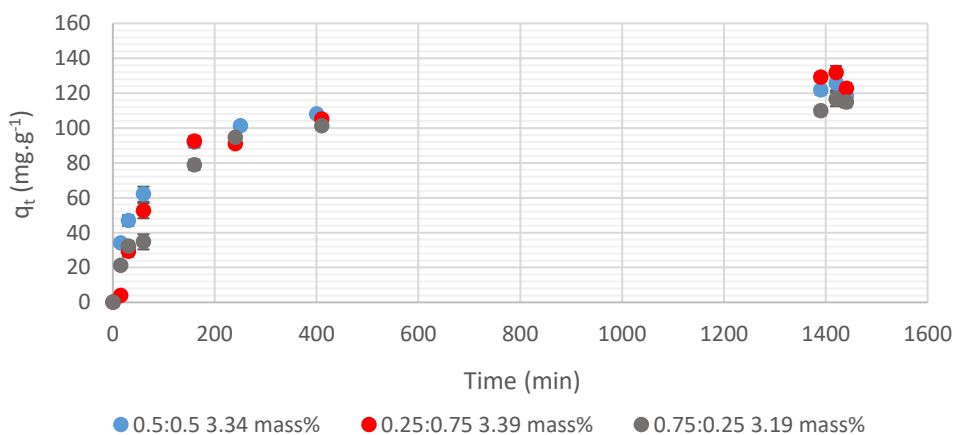


Figure 41 Comparison of the effect of the adsorbate ratio on the kinetics of a 1-octanol&3,7-DMO system at an initial concentration of 3.39 mass% at 25 °C.

6.3 Binary component Modelling

The present section discusses results of the binary component adsorption kinetic and equilibrium isotherm models.

6.3.1 Binary Kinetic Modelling

Kinetic models, that is, pseudo-first, pseudo-second and pseudo- n^{th} -order models and the Elovich one, were fitted to the binary component data of the two systems investigated, namely 1-decanol&3,7-DMO and 1-octanol&3,7-DMO at 25 °C and 45 °C. The kinetic models in the case of 25 °C were fitted for the range of 24 hours' worth of data collected, while the those generated at 45 °C were only fitted over the first 7 h. Both binary component systems investigated were situated at an initial adsorbate ratio of 0.5:0.5. Additional kinetic models fitted to other adsorbate ratios are summarised in Appendix D.1. The results are summarized in Table 18.

Figures 42 and 43 reflect the kinetic model profiles for 1-decanol&3,7-DMO and 1-octanol&3,7-DMO at 25 °C, respectively. The profiles contained in these figures were evaluated in conjunction with the coefficient of determination as well as the MPSD (see Table 18). The binary system of 1-decanol&3,7-DMO was modelled best by means of a combination of the Elovich and pseudo-2nd order model. The Elovich model fitted the data marginally better than the pseudo-second-order order model. This indicates that the adsorption of adsorbates in a 1-decanol&3,7-DMO binary system occurred at localized sites. Some interaction between the adsorbate molecules occurred and the energy of adsorption increased with surface coverage. Additionally, the Elovich model strongly suggests that chemisorption is the primary mechanism of adsorption (Wu, Tseng and Juang, 2009). The fit of the pseudo-second-order order model indicated that the adsorption might also have been somewhat controlled in terms of reaction. This centred on the uptake of adsorptives as governed by a second-order rate reaction where no desorption occurred. These findings indicate that molecules of the same size that have different shapes possess a combination of reaction mechanisms.

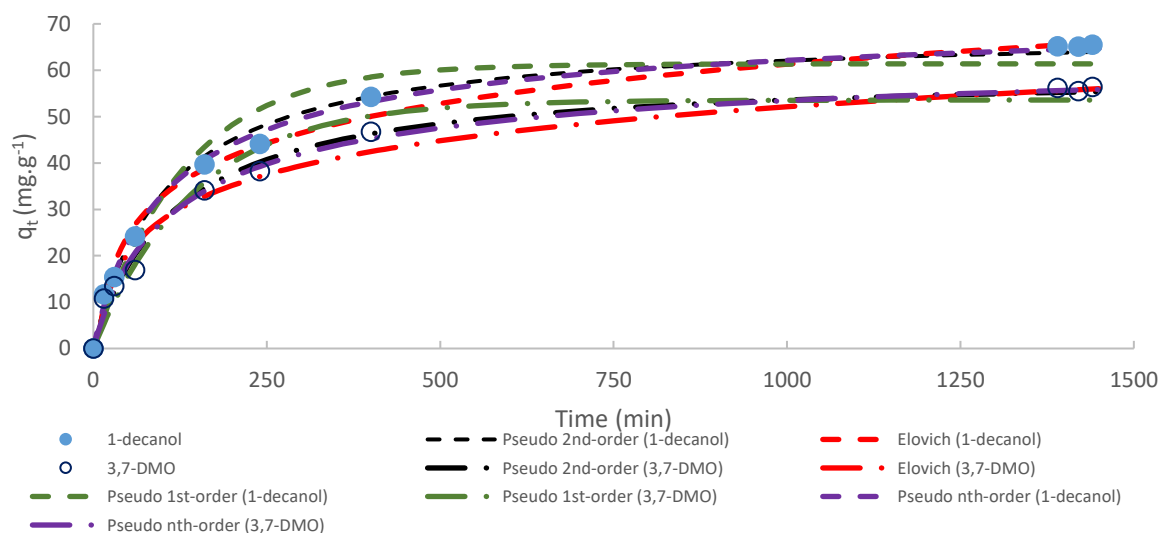


Figure 42 Kinetic models fitted to experimental data generated for a binary system of 1-decanol&3,7-DMO with a 0.5:0.5 ratio at 25 °C.

An evaluation of the MSPD values of the models fitted to the 1-octanol&3,7-DMO binary system at 25 °C indicates that the Elovich model provided the best fit. This suggests that, in a system comprising two adsorbates of different size and shape, interaction occurs between the sorbed ions. Chemisorption was

the primary mechanism of adsorption and adsorption occurred only at localized sites. The adsorption rate, as observed in terms of the Elovich model, was higher for both 1-decanol and 1-octanol than for 3,7-DMO. This was found to be the case in both binary component systems.

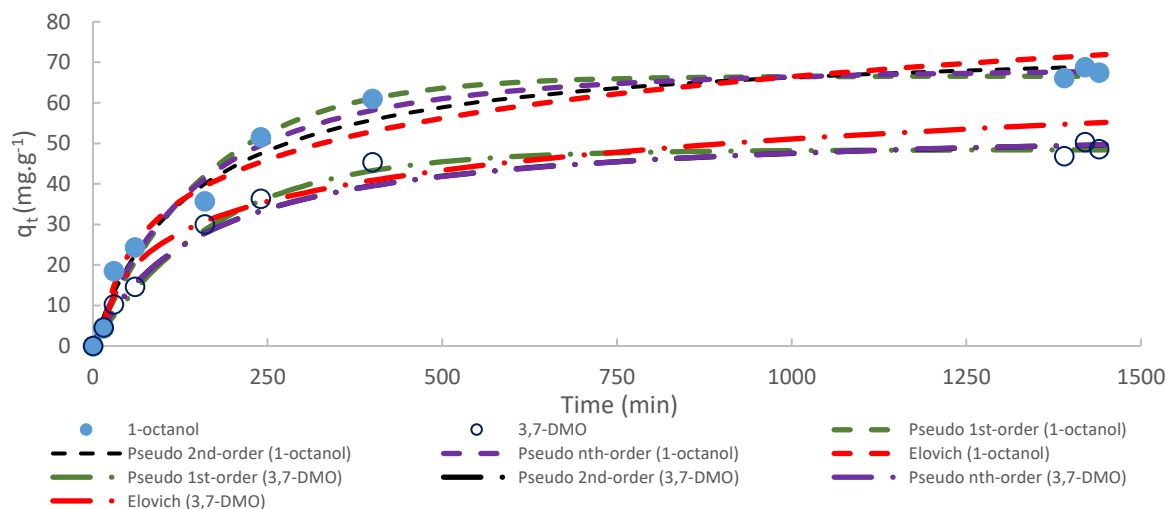


Figure 43 Kinetic models fitted to experimental data generated for the binary system of 1-octanol&3,7-DMO with a 0.5:0.5 ratio at 25 °C.

Figures 44 and Figure 45 reflect the kinetic model profiles for 1-decanol&3,7-DMO and 1-octanol&3,7-DMO at 45 °C. Figure 44 shows two separate graphical plots rather than the combined plots that are presented in Figures 42, 43 and 45. This was done because the kinetic data for both 1-decanol closely matched 3,7-DMO. Separation of the two profiles made it easier to distinguish between the different models for this reason. The MSPD values and goodness of fit were better than those observed at 25 °C. The reason is that fitting the models was done for the first 7 h of kinetic data only. According to Table 18, the Elovich model provided the best fit for both binary systems. In both cases, this model fitted 1-decanol or 1-octanol better than 3,7-DMO. The Elovich model parameter ' α ' was indicative of the rate of adsorption, which was marginally higher for the 1-decanol&3,7-DMO binary system was marginally higher for 1-decanol compared to 3,7-DMO. A similar phenomenon was observed at 25 °C, except that the rate of adsorption of 1-decanol was 1.3 times greater than that of 3,7-DMO. As shown in Table 18, the Elovich model ' α ' indicated that the rate of adsorption of 1-octanol was 1.5 times greater than that of 3,7-DMO.

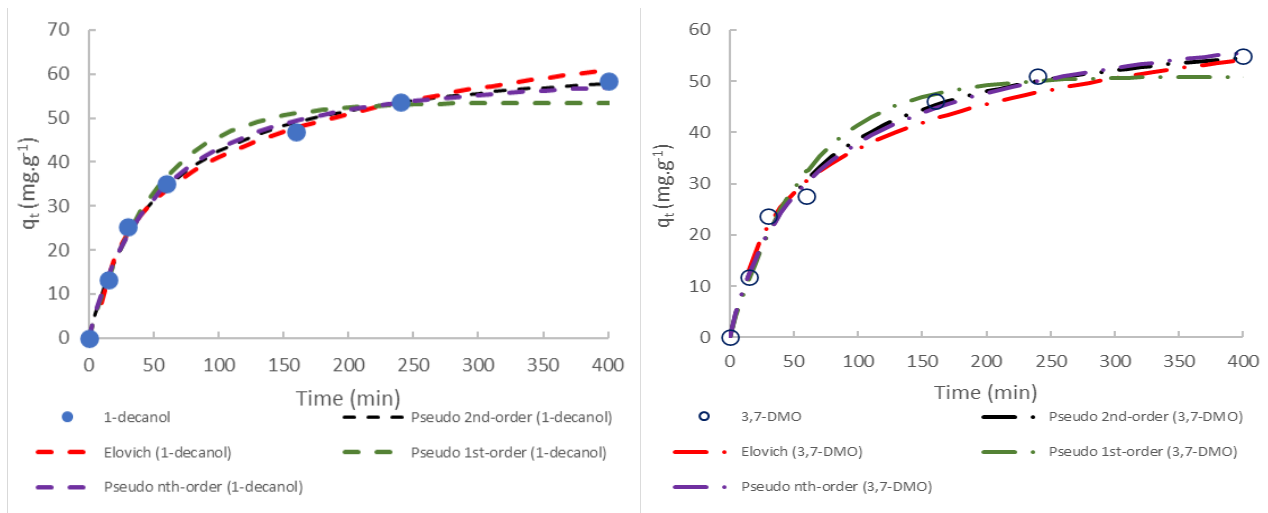


Figure 44 Kinetic models fitted to experimental data generated for the binary system of 1-decanol&3,7-DMO with a 0.5:0.5 ratio at 45 °C. Given that the adsorbent loading adsorbate loading at time t was similar for both components, the fit of the models to the data is shown here.

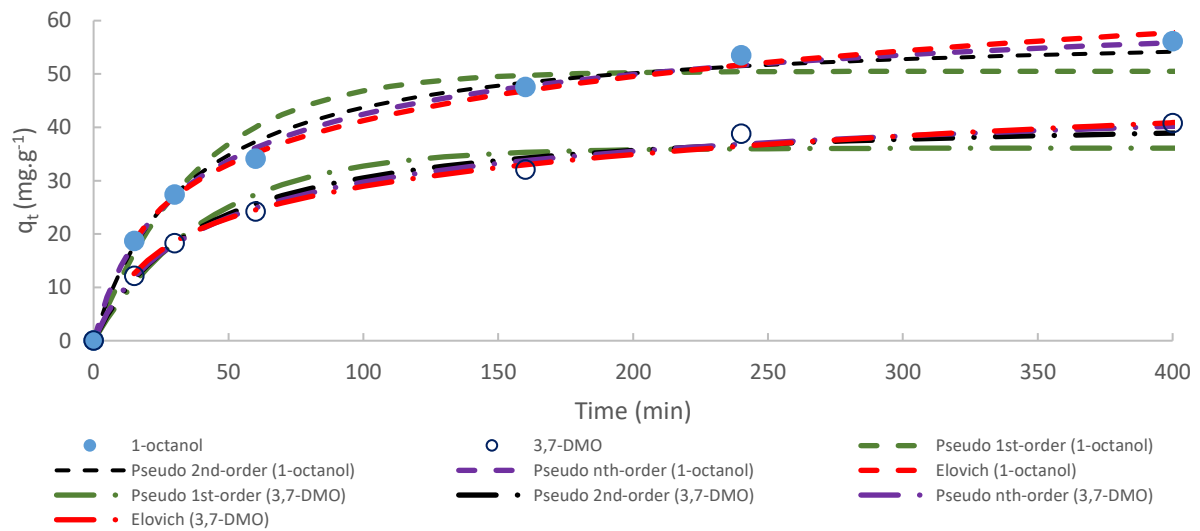


Figure 45 Kinetic models fitted to experimental data generated for the binary system of 1-octanol&3,7-DMO with a 0.5:0.5 ratio at 45 °C.

Table 18 Binary component kinetic model parameter estimation for a 1-D&3,7-DMO and 1-O&3,7-DMO with a ratio of 0.5:0.5 at 25 °C and 45 °C.

Temperature (°C) model parameters	25 °C (24 hr period)				45 °C (7 hr period)			
	1-D&3,7-DMO		1-O&3,7-DMO		1-D&3,7-DMO		1-O&3,7-DMO	
	1-decanol	3,7-DMO	1-octanol	3,7-DMO	1-decanol	3,7-DMO	1-octanol	3,7-DMO
Initial mass concentration (mass%)	1.04	1.06	1.01	1.01	1.0	1.07	0.96	0.94
$q_{e,exp}$ (mg.g ⁻¹)	65	56	67	49	58	55	56	41
pseudo-first-order model								
$q_{e,calc}$ (mg.g ⁻¹)	61	54	67	48	54	51	51	36
k_1 (min ⁻¹)	0.008	0.007	0.006	0.006	0.02	0.02	0.03	0.02
R^2_{adj}	0.97	0.98	0.98	0.97	0.98	0.97	0.95	0.94
MPSD (%)	20	23	22	12	5.6	11	11	11
Pseudo-second-order model								
$q_{e,calc}$ (mg.g ⁻¹)	69	60	76	55	66	63	59	43
k_2 (10 ⁻³ g.(mg.min) ⁻¹)	0.14	0.14	0.09	0.12	0.17	0.25	0.5	0.6
R^2_{adj}	0.99	0.99	0.89	0.93	0.99	0.99	0.98	0.98
MPSD (%)	11	17	28	30	5.1	8.5	5.3	5.4
Pseudo-nth-order model								
n (-)	2.6	2.6	1.3	2.0	1.7	2.8	3.3	3.3
$q_{e,calc}$ (mg.g ⁻¹)	75	66	69	55	61	74	74	55
k_n (10 ⁻⁵ g.(mg.min) ⁻¹)	1.00	1.00	126	10.8	122	0.70	0.1	0.2
R^2_{adj}	0.99	0.99	0.93	0.96	0.99	0.98	0.99	0.98
MPSD(%)	9.4	16	27	12	5.5	9.2	3.6	4.1
Elovich Model								
β (g.mg ⁻¹)	0.08	0.91	0.07	0.09	0.07	0.08	0.08	0.12
α (mg.(g.min) ⁻¹)	1.9	1.5	1.3	1.1	2.5	2.4	3.8	2.47
R^2_{adj}	0.97	0.97	0.96	0.96	1	0.98	0.99	0.99
MPSD(%)	11	15	12	18	3.6	8.9	2.6	3.5

6.3.2 Binary Isotherm Modelling

The adsorption isotherm models were fitted to the two binary systems at 25 °C and 45 °C. The isotherm models fitted to the data generated at 45 °C were not fully representative of the equilibrium adsorbate loadings, as the loadings achieved at approximately 7 h were used to fit the models. The adsorption data collected at 25 °C indicated that the adsorbate loading achieved at 7 h was within 10% of the equilibrium adsorbate loading. The results obtained in terms of the model fitting was therefore considered to be representative of the adsorbate-adsorbent system. The estimated parameters are provided in Table 18 above.

Figures 46 and 47 show an evaluation of five different multicomponent isotherm models fitted to the 0.5:0.5 1-decanol&3,7-DMO adsorption system at 25 °C and 45 °C respectively. Figures 46(a), 47(a) and 47(b) show that the extended Langmuir, modified Langmuir and extended Freundlich models predicted adsorbate loadings on levels that align with the experimentally determined adsorbate loadings. Figure 46(a) shows that, although the measured equilibrium adsorbate loading ranged from 40-70 $\text{mg}\cdot\text{g}^{-1}$, the predicted adsorbate loading was lower.

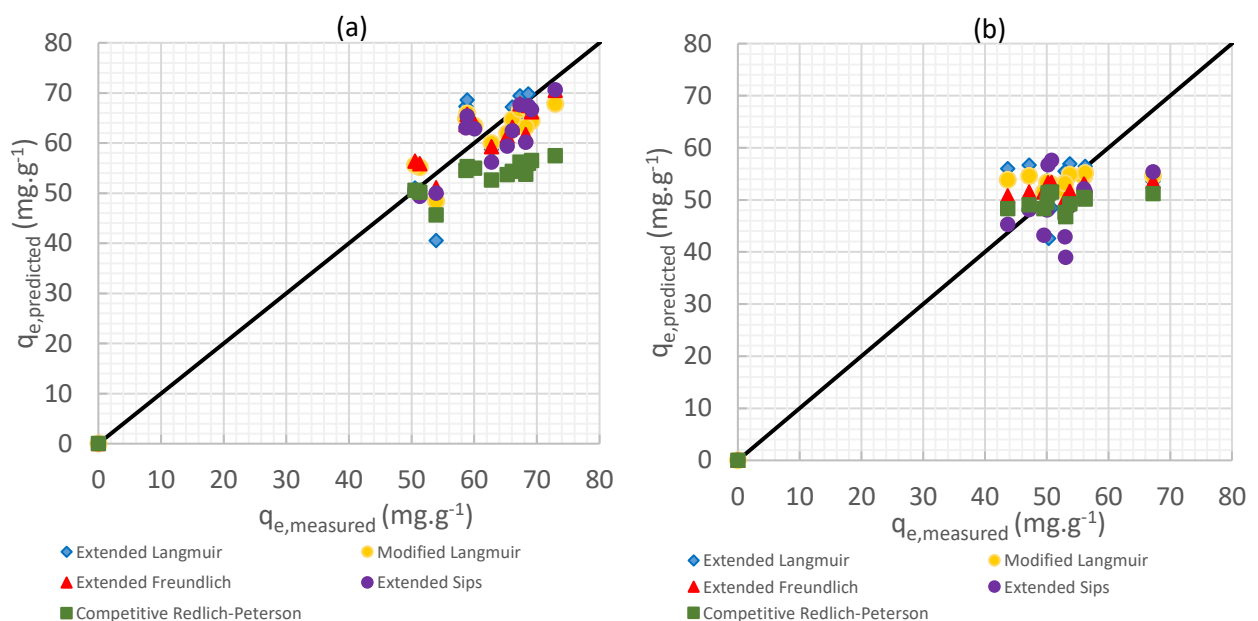


Figure 46 Predicted versus measured equilibrium adsorbent loading of 1-decanol (a) and 3,7-DMO (b) in the 0.5:0.5 1-decanol&3,7-DMO adsorption system at 25 °C.

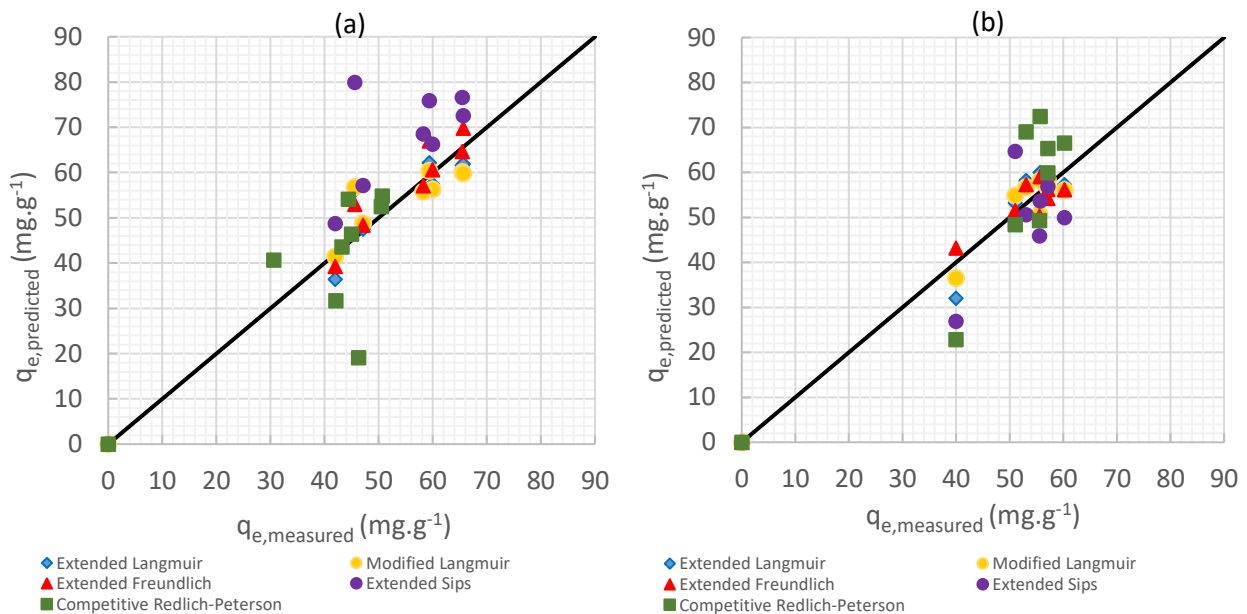


Figure 47 Predicted versus measured adsorbent loading at 7 hrs of 1-decanol (a) and 3,7-DMO (b) in the 0.5:0.5 1-decanol&3,7-DMO adsorption system at 45 °C.

A review of the adjusted R^2 -value and the MPSD in all fitted isotherm models confirms that the extended Sips isotherm and modified competitive Redlich-Peterson isotherm models did not fit the 1-decanol&3,7-DMO binary system well at either 25 °C or 45 °C. The extended Freundlich isotherm model provided the best fitted for the data with the modified competitive Langmuir isotherm providing the second best fitted. These two models indicated that interaction occurred between 1-decanol and 3,7-DMO in a binary component system when they were interacting with SCD. The modified competitive Langmuir model predicted a maximum 1-decanol&3,7-DMO adsorbate loading of 122-123 mg.g^{-1} .

Figures 48 and 49 show the predicted versus measured adsorbate loading in terms of five different adsorption isotherm models fitted to the 0.5:0.5 1-decanol&3,7-DMO adsorption system at 25 °C and 45 °C. Figure 48(a) shows that the modified competitive Redlich-Peterson and extended Sips models predicted lower equilibrium adsorbate loadings for 1-octanol than that which was measured. These did not, therefore, provide a good fit. Figure 48(b) shows that, at 25 °C, the extended Langmuir and modified competitive Redlich-Peterson models predicted lower 3,7-DMO loadings those that were actually measured and provided a poor fit. Figures 48(a) and 48(b) show that the isotherm models fitted the 1-octanol&3,7-DMO system better at higher temperatures. A difference between the predicted 1-octanol loading and the 3,7-DMO loading was that, at adsorbate loadings measured at higher levels, lower 3,7-DMO loadings were predicted.

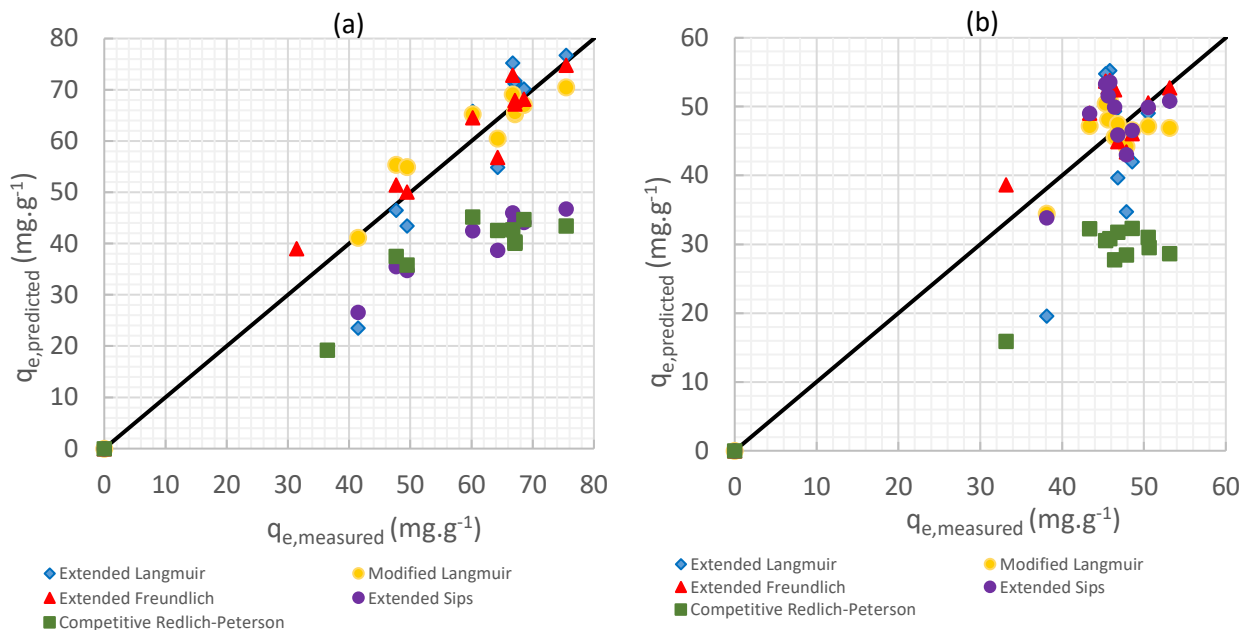


Figure 48 Predicted versus measured adsorbent loading after 7 h of 1-octanol (a) and 3,7-DMO (b) in the 0.5:0.5 1-octanol&3,7-DMO adsorption system at 25 °C.

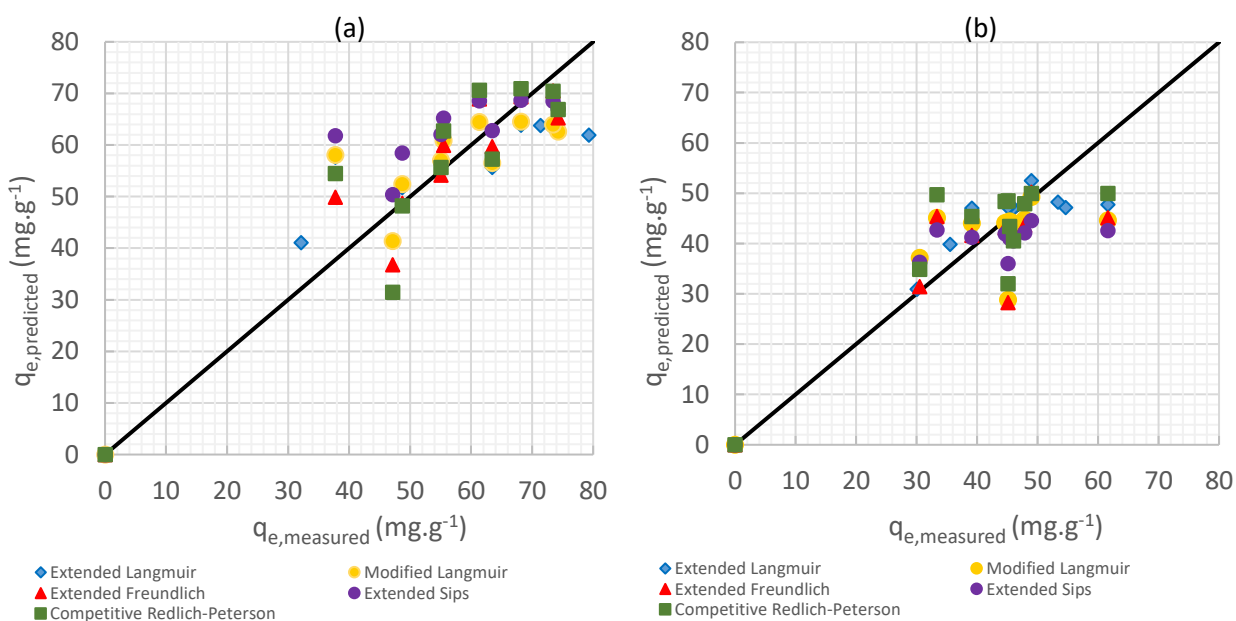


Figure 49 Predicted versus measured adsorbent loading after 7 h of 1-octanol (a) and 3,7-DMO (b) in the 0.5:0.5 1-octanol&3,7-DMO adsorption system at 45 °C.

Table 19 depicts models that provided the best fit. A comparison of the MPSD and R^2_{adj} values indicated that the multicomponent isotherm models fitted the 1-decanol&3,7-DMO system better than the 1-octanol&3,7-DMO one at both temperatures. The modified competitive Langmuir model provides the best fitted for the adsorption of 1-octanol&3,7-DMO onto SCD at 25 °C and predicts a maximum adsorbate loading of 120 mg.g^{-1} . At 45 °C, the extended Freundlich and modified competitive Langmuir models provide the best fit, but neither amounted to a good one.

Overall, the extended Freundlich and modified competitive Langmuir isotherm models fitted the measured equilibrium adsorbate loadings best for both binary systems and temperatures. According to the model assumptions of the extended Freundlich model, can be inferred that the interaction between 1-decanol&3,7-DMO or 1-octanol&3,7-DMO binary systems with SCD formed a heterogeneous adsorption system. Furthermore, it can be said that interaction did occur between 1-decanol and 3,7-DMO in a binary system at both temperatures for the reason that both the modified competitive Langmuir and extended Freundlich models were designed to fit such systems. In the case of the 1-octanol&3,7-DMO binary system, at 25 °C the success of the fit of the modified competitive Langmuir and extended Freundlich model also indicated that interaction had occurred between 1-octanol and 3,7-DMO.

Table 18 Summary of the multicomponent adsorption isotherm models for two binary component systems (1-decanol&3,7-DMO and 1-octanol&3,7-DMO) at 25 °C and 45 °C.

Temperature (°C)	25 (°C)		45 (°C)	
	1-D&3,7-DMO	1-O&3,7-DMO	1-D&3,7-DMO	1-O&3,7-DMO
Extended Langmuir isotherm				
θ_1	0.69	0.95	0.56	0.47
θ_2	0.81	0.57	0.43	0.67
$K_{L1,binary} (ml \cdot mg^{-1})$	0.91	0.54	1.00	1.29
$K_{L2,binary} (ml \cdot mg^{-1})$	0.70	0.31	0.90	0.82
$q_{max,binary} (mg \cdot g^{-1})$	133	143	128	118
$R^2_{1,adj}$	0.57	0.67	0.65	0.37
$R^2_{2,adj}$	0.53	0.59	0.75	0.54
MPSD ₁ (%)	11	17	12	24
MPSD ₂ (%)	13	23	11	13
Modified Competitive Langmuir isotherm				
$q_{max,binary} (mg \cdot g^{-1})$	123	120	122	114
η_{L1}	1.3	0.46	1.4	4.2
η_{L2}	0.93	1.3	2.3	2.1
$R^2_{1,adj}$	0.55	0.78	0.60	0.75
$R^2_{2,adj}$	0.53	0.65	0.72	0.75
MPSD ₁ (%)	8.3	10	13	23
MPSD ₂ (%)	11	9.4	8.0	22
Extended Freundlich isotherm				
b_{11}	3.1	1.6	0.050	0.22
b_{22}	0.63	0.11	0.34	2.1
a_{12}	0.08	0.031	1.2	1.3
a_{21}	0.22	0.51	0.78	1.5
b_{12}	3.8	2.4	0.085	0.12
B_{21}	1.1	0.15	0.41	2.0
$R^2_{1,adj}$	0.62	0.86	0.83	0.68
$R^2_{2,adj}$	0.64	0.23	0.60	0.59
MPSD ₁ (%)	8.0	12	10	16
MPSD ₂ (%)	10	14	8.1	21
Extended Sips isotherm				
m	3.2	0.67	2.9	0.61
R_1^2	0.55	0.76	0.21	0.47
R_2^2	0.54	0.29	0.36	0.52
MPSD ₁ (%)	13	36	34	23
MPSD ₂ (%)	13	11	19	19
Modified Competitive Redlich-Peterson isotherm				
n_1	2.0	26	4.7	8.8
n_2	0.42	4.5	6.4	2.9
R^2_1	0.59	0.17	0.43	0.78
R^2_2	0.32	0.17	0.68	0.75
MPSD ₁ (%)	16	41	31	21
MPSD ₂ (%)	11	43	26	26

6.4 Chapter Outcomes

This Chapter aimed at addressing Objective 2 (described in Section 1.3) and Phase 2 and partially Phase 4 of the experimental plan (see Section 3.4).

The effect of temperature on the 1-decanol&3,7-DMO binary system was greater than on the 1-octanol&3,7-DMO binary system. It was found that, in the case of the 1-octanol&3,7-DMO binary system, an increase in overall adsorbate concentration increased the adsorbate loading with a maximum loading measured at 122 mg.g^{-1} ($\sim 5 \text{ mg.g}^{-1}$). It was found further that 1-octanol was preferentially adsorbed. In the case of an increase in overall initial adsorbate concentration in the 1-decanol&3,7-DMO system, 1-decanol was marginally more preferentially adsorbed. An increase in initial concentration showed the highest equilibrium adsorbate loading of 139 mg.g^{-1} ($\sim 5 \text{ mg.g}^{-1}$) in terms of an overall initial concentration of 2.00 mass%. Subsequently, the equilibrium adsorbate loading decreased. The effect of varying the adsorbate ratio on the adsorption of 1-octanol&3,7-DMO was that highest equilibrium adsorbate loading was achieved at 0.75:0.25, while it was intermediate at 0.5:0.5 and lowest at 0.25:0.75. The effect of varying the adsorbate ratio on the adsorption of 1-decanol&3,7-DMO was greater sensitivity towards and dependence on the initial concentration. The highest adsorbate loading was achieved at 0.75:0.25, while it was intermediate at 0.25:0.75 and lowest at 0.5:0.5.

The kinetic and equilibrium isotherm models were fitted to both binary component systems at both temperatures. The Elovich model provided the best fitted for both binary component systems. It also modelled the adsorption of 1-decanol and 1-octanol with greater accuracy than 3,7-DMO at both temperatures. This indicates that chemisorption was a predominant mechanism of adsorption. Furthermore, the extended Freundlich and modified competitive Langmuir model fitted both binary component systems best and indicated heterogenous adsorption systems centred on interaction between the adsorbates.

Chapter 7 Evaluation of displacement potential

Evaluation of competitive adsorption focuses on the adsorbate-adsorbent interactions, while investigation of the displacement potential focuses on the adsorbate₁-adsorbate₂ interactions (Li *et al.*, 2002). The inclusion of displacement potential studies incorporates the idea that the extent of adsorption achieved is affected by the strength of the three-way interaction between adsorbate₁, adsorbate₂ and the adsorbent. The present chapter aims to identify the displacement potential of each alcohol in the respective binary component systems. The displacement potential was defined as the ability to displace another component in a binary system. The main objective was to identify and compare the displacement potential of the 1-alcohols used, determine the causes for the results obtained and determine whether these were system or molecule dependent. As such, the present discussion will elucidate the way in which the components interact with one another.

A single component system containing a high concentration of the 'displacee' was allowed to reach equilibrium (pre-loading the adsorbent). Subsequently, a lower concentration of the 'displacer' was added and the effect on adsorbate loading monitored. Three binary component systems were investigated by means of two different displacement tests performed for each system at 25 °C and 45 °C. However, only the results of the displacement tests at 25 °C will be presented here. The mass of displacer used was selected to ensure that it was less than the mass of displacee present in the solution pre- and post-adsorbent loading. This was done to ensure that the concentration of displacee molecules sufficiently outnumbered those of the displacer in the bulk solution. This approach ensured that any changes observed in percentage adsorbed or displaced was predominantly caused by displacement.

In the first displacement test, component 1 was used as the displacee (referred to here as displacement test A) and, in the second, test component 1 was used as the displacer (referred to here as displacement test B). The three systems investigated are as follows:

1. 1-octanol & 1-decanol
2. 1-octanol&3,7-DMO
3. 1-decanol&3,7-DMO

Table 20 summarises the percentage adsorbed and displaced in terms of the displacer and displacee respectively. Because the initial concentration of the displacee and displacer differed, the percentage adsorbed and displaced should be considered in parallel with the moles adsorbed and displaced.

Comparison of all six tests performed (Table 19) shows that the highest percentage displaced was achieved for the 1-decanol&3,7-DMO binary system, where 1-decanol was the displacer. The lowest percentage displaced was achieved for the 1-octanol&3,7-DMO system, where 3,7-DMO was the displacer. The common denominator observed at opposite ends of the displaced spectrum was 3,7-DMO. At the higher end of the spectrum, 3,7-DMO was the displacee.

At the lower end of the spectrum; 3,7-DMO was the displacer, the percentage adsorbed was the lowest and the displacement ratio was the highest when compared to the other five tests. This suggests that the interaction and bond formed between 3,7-DMO and SCD was the weakest, in contrast with the other two

1-alcohols. It may also suggest that 3,7-DMO favoured adsorbate-adsorbate interactions above adsorbate-adsorbent interactions. It is possible that, due to the size and shape of the molecule, a large portion of the pre-loaded 3,7-DMO was found in the larger mesopores where a less stable complex had been formed (see Li *et al.*, 2002). This would also have increased the likelihood of being displaced by smaller and linear molecules.

Review of the binary 1-octanol & 1-decanol systems indicates that the difference in displacement ratio between Test A and Test B was the smallest, in contrast with the two other binary systems. This implies that the interaction between adsorbate and adsorbent surface was relatively equal in strength for 1-octanol and 1-decanol. However, the bond strength of 1-octanol-SCD appeared marginally stronger. This could have been caused by the fact that the adsorbent had a higher affinity for the short chain 1-alcohols. Its linear shape and smaller size meant a greater extent of adsorption in the micropores also possibly resulted in more stable adsorption complexes. This would have made it more difficult for 1-decanol or 3,7-DMO to displace 1-octanol.

Table 19 Evaluation of the percentage adsorbed and displaced for three binary systems at 25 °C. The experiment was performed twice to ensure that both components in the binary system were used as the displacer.

Displacement (Displacer&Displacee)	Test	Percentage adsorbed (±2%)	Percentage displaced (±2%)	moles adsorbed (10 ⁻³ mol)	moles displaced (10 ⁻³ mol)	Displacement Ratio
Test B (1-octanol&1-decanol)		27	23	2.77	3.42	1.2
Test A (1-decanol&1-octanol)		22	17	2.08	2.93	1.4
Test B (1-octanol&3,7-DMO)		26	20	3.03	3.13	1.0
Test A (3,7-DMO&1-octanol)		12	14	1.09	2.78	2.6
Test B (1-decanol&3,7-DMO)		25	25	2.29	2.81	1.2
Test A (3,7-DMO&1-decanol)		17	21	1.52	2.98	0.5

7.1 1-octanol&1-decanol

This section examines the possibility that only size affects the displacement potential. The displacement potential of the two components in the 1-octanol & 1-decanol system were investigated as follows:

- Displacement test A: 1-octanol (displacee) and 1-decanol (displacer)
- Displacement test B: 1-decanol (displacee) and 1-octanol (displacer)

The change in adsorbent loading of both components over time is represented in Figure 50. The concentration of displacee and displacer was similar, although 0.1 mass% higher overall for Test A than Test B. For Test A, 1-decanol was added and, within the first 15 min, the effect was notable indicating that the system was sensitive to 1-decanol. The adsorbent loading of 1-octanol decreased and continued to be displaced until equilibrium was reached at around 24 h. The removal of 1-decanol increased as more pores became available. The same trend was observed in Test B indicating that the system was also

sensitive to 1-octanol. The percentages that were displaced and adsorbed were quantified and are represented in Section 6.1.4. Overall, 1-octanol had a higher displacement potential than 1-decanol.

The main point that Figure 50 illustrates is that both 1-octanol and 1-decanol appear to have the capacity to displace each other in a binary system. A structural comparison of both components indicates that both were linear, 1-decanol was heavier ($158.28 \text{ g}\cdot\text{mol}^{-1}$) and longer than 1-octanol ($130.23 \text{ g}\cdot\text{mol}^{-1}$). It was anticipated that 1-octanol would have had a higher displacement potential than 1-decanol, as 1-octanol would have moved through the pores with greater ease. The moles of 1-octanol displaced ($2.93 \cdot 10^{-3} \text{ mol}$) were lower than those of 1-decanol ($3.42 \cdot 10^{-3} \text{ mol}$). The difference was larger than the overall 0.1 mass% difference observed between the initial concentrations, as described. Therefore, the increased displacement of 1-decanol compared to 1-octanol indicates that the bond formed between 1-decanol and SCD was weaker than that formed between 1-octanol and SCD (Billinge, Docherty and Bevan, 1984). Because 1-octanol was smaller in size and not as wide it would probably have moved into the pores with greater ease, displacing an increased number of 1-decanol molecules.

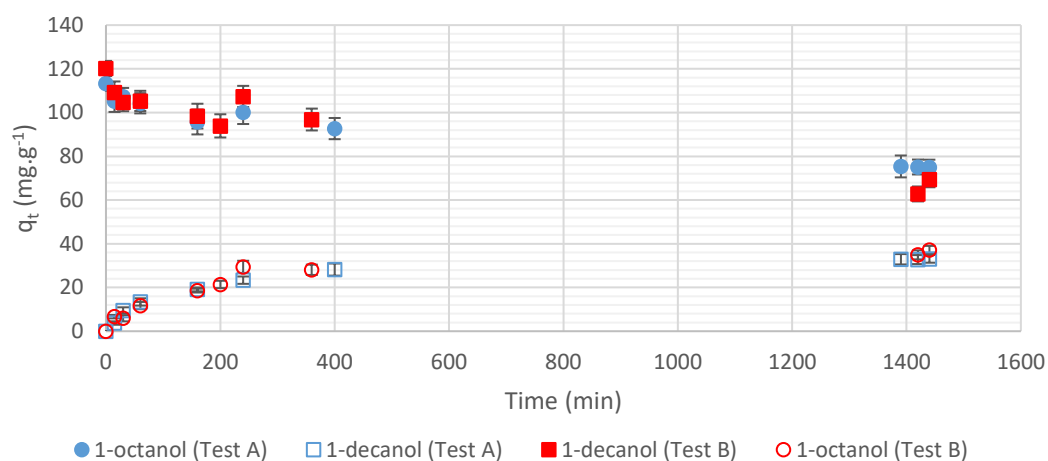


Figure 50 Comparison of displacement potential of 1-octanol and 1-decanol when used in a 1-decanol & 1-octanol binary system. The initial concentration for Test A was 2.50 mass% 1-octanol and 1.10 mass% 1-decanol. The initial concentration for Test B was 2.40 mass% 1-decanol and 1.05 mass% 1-octanol.

This possibly explains the difference in displacement ratios, that is, ratio of moles displaced to moles adsorbed, as illustrated in Table 13. The displacement ratio was higher in Test A (1.4) than in Test B (1.2). The moles displaced did not equal the ones adsorbed, which means that not all displaced molecules were replaced by the adsorption of the added displacer. It can be said that the 1-octanol-SCD bond was stronger than that of 1-decanol-SCD. However, given that the displacement ratios were not vastly different, it can be said that the adsorbate₁-adsorbate₂ interactions were weaker than the adsorbate-adsorbent interactions in this system.

7.2 1-octanol&3,7-DMO

The present section evaluates whether a combination of size and shape differences affected adsorption potential. The displacement potential of the two components in the 1-octanol&3,7-DMO system were investigated as follows:

- Displacement test A: 1-octanol (displacee) and 3,7-DMO (displacer)
- Displacement test B: 3,7-DMO (displacee) and 1-octanol (displacer)

The initial concentration of the displacee at the pre-loading stage, the displacer at the post-loading stage and the ratio of displacee to displacer was similar in Test A and B in the 1-octanol&3,7-DMO system. Any changes observed are thus considered solely due to adsorbate-adsorbate or adsorbate-adsorbent interactions.

According to Figure 51, the equilibrium adsorbent loading achieved by means of pre-loading was similar for Tests A and B. Upon visual inspection, the drop in displacee adsorbent loading that occurred beyond 60 min was greater in Test B, where 3,7-DMO was the displacee. The increase in displacer adsorbent loading was also greater in Test B when 1-octanol was the displacer. Structural comparison indicates that 1-octanol was linear while 3,7-DMO was branched, while 1-octanol has a molecular mass of $130.23 \text{ g}\cdot\text{mol}^{-1}$ and 3,7-DMO $158.28 \text{ g}\cdot\text{mol}^{-1}$.

According to the results, as presented in Section 6.1.1, it was expected that 1-octanol would be favoured and have a higher displacement potential, because it was a smaller molecule. Figure 51 shows a greater displacement potential of 1-octanol compared to 3,7-DMO in a 1-octanol&3,7-DMO system. Figure 51 confirms the information obtained thus, as the moles of 3,7-DMO displaced was larger than the moles of 1-octanol displaced. This seems to indicate that a smaller, linear-shaped molecule was favoured by SCD and that these formed stronger bonds. It is possible that a branched molecule moved through the micropores with greater difficulty and were thus adsorbed in the larger pores. They would then have formed less stable adsorption complexes. Thus, 3,7-DMO may be displaced more readily due to the weaker bonds between 3,7-DMO and SCD.

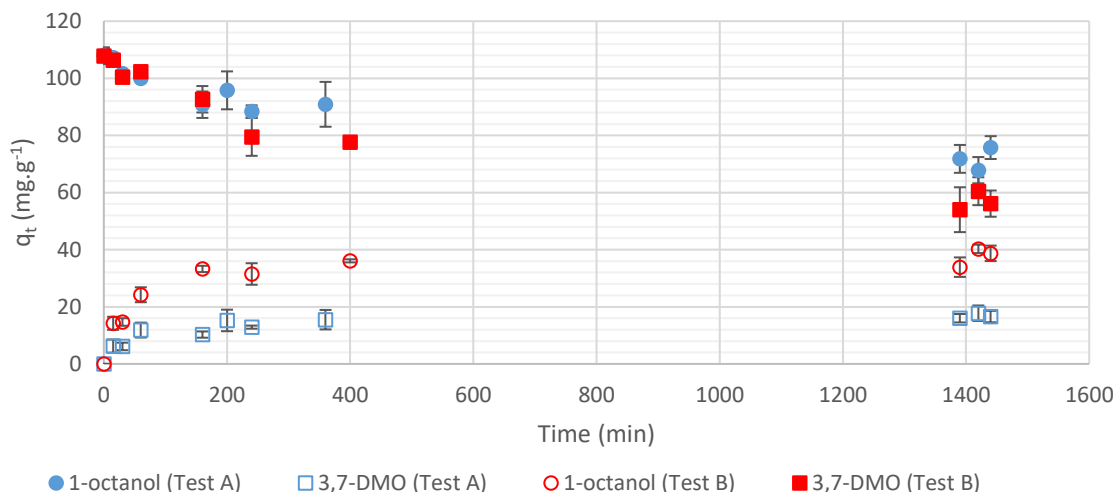


Figure 51 Comparison of displacement potential of 1-octanol and 3,7-DMO when used in a 1-octanol&3,7-DMO binary system. The initial concentration for Test A was 2.43 mass% 1-octanol and 1.00 mass% 3,7-DMO. The initial concentration for Test B was 2.52 mass% 3,7-DMO and 1.00 mass% 1-octanol. The displacement ratio for Test A (2.6) was more than double that of Test B (1.0). The unity observed for Test B indicated that, for every mole of 3,7-DMO displaced, a mole of 1-octanol was adsorbed and that the latter filled the available sites. The larger displacement ratio observed in Test A indicated that less 3,7-DMO was adsorbed. This suggests weaker interaction between 3,7-DMO and the adsorbent and may suggest stronger adsorbate₁-adsorbate₂ than adsorbate-adsorbent interactions. Both 1-octanol and 3,7-DMO exhibited displacement potential but, in a binary component system, 1-octanol was more likely to displace it.

7.3 1-decanol&3,7-DMO

Finally, the present section discusses whether a variation in shape would affect the displacement potential on its own, and more so than a variation in size. The displacement potential of the two components in the 1-decanol&3,7-DMO system were investigated as follows:

- Displacement test A: 1-decanol (displacee) and 3,7-DMO (displacer)
- Displacement test B: 3,7-DMO (displacee) and 1-decanol (displacer)

A structural comparison indicates that both 1-decanol and 3,7-DMO had a molecular weight of 15.28 g.mol⁻¹ (equal in size), while 1-decanol was linear and 3,7-DMO branched. The compositions of displacee and displacer in both tests were found to be similar, and it was assumed that the marginal differences that did occur in these terms did not affect the results observed. Figure 52 indicates a similar drop in displacee loading in Test A and Test B, but a larger increase in displacer adsorbent loading in Test B than Test A. This may indicate that both components had a similar displacement potential, whereas the 1-decanol-SCD interactions were stronger than those of 3,7-DMO - SCD. Reviewing Figure 52 shows that a marginally less 3,7-DMO moles ($2.81 \cdot 10^{-3}$ mol) were displaced than 1-decanol ones ($2.98 \cdot 10^{-3}$ mol). This

suggests that a branched molecule exhibited marginally greater displacement potential than a linear one of equal size.

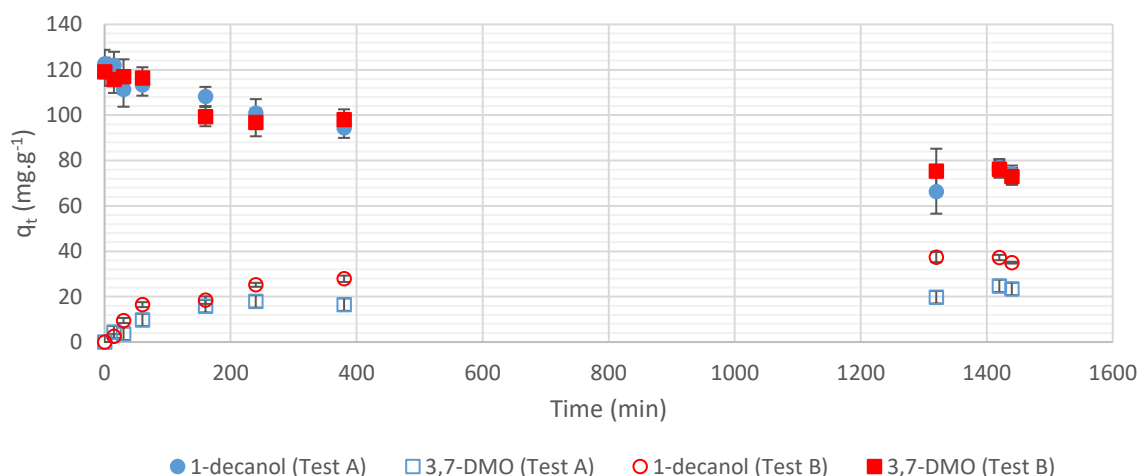


Figure 52 Comparison of displacement potential of 1-decanol and 3,7-DMO when used in a 1-decanol&3,7-DMO binary system. The initial concentration for Test A was 2.62 mass% 1-decanol and 0.98 mass% 3,7-DMO. The initial concentration for Test B was 2.56 mass% 3,7-DMO and 1.16 mass% 1-decanol.

However, according to the percentage displaced in the two situations, 1-decanol appeared to have displaced a larger portion of the pre-loaded 3,7-DMO. In terms of fraction displaced, 3,7-DMO displaced a smaller fraction of 1-decanol. This indicated that 1-decanol had a marginally higher displacement potential than 3,7-DMO.

7.4 Chapter Outcomes

This chapter aimed to address Objective 3 (as found in Section 1.3) as well as Phases 3 and 4 of the experimental plan. Displacement tests were performed on each of the three 1-alcohols studied in this study (1-octanol, 1-decanol and 3,7-DMO) in three binary systems (1-decanol & 1-octanol, 1-octanol&3,7-DMO and 1-decanol&3,7-DMO). It was found that, overall, the displacement potential was ranked from lowest to highest in the following order: 3,7-DMO, 1-decanol and 1-octanol. It is concluded that, in SCD, that smaller or linear molecules were preferentially adsorbed. The difference in displacement potential between 3,7-DMO and 1-decanol appeared larger than the one between 1-octanol and 1-decanol. This indicates that both size and shape affected adsorption and that smaller linear molecules were favoured by SCD. The interaction of the three adsorbates with SCD shows that the branched larger molecules were more readily displaced than the smaller or linear molecules.

Chapter 8 Conclusion and Recommendations

Prior to presenting the major conclusions for this study and the recommendations for further research, the shortcomings of the project should be re-iterated. The experimental setup showed shortcomings that contributed to the discrepancy in data observed at 45 °C. The flaws in the experimental setup facilitated large amounts of evaporation of the water in the water bath and it was noted toward the end of the study that some of the solution was also evaporating. Additionally, water vapours were condensing on the top plate of the setup and these were dripping into the solution contained in the open beakers. This influenced the composition and adsorbate loading that were achievable at 45 °C. It is recommended that a bench-scale setup similar to the secondary BAES is used to minimise evaporation and water contamination in further research. The datasets collected at 45 °C can be repeated on these systems to improve the accuracy of the results presented in the present study.

8.1 3,7-DMO adsorption from n-decane solution on SCD

The investigation of 3,7-DMO adsorption at different initial concentrations and solution temperatures proved that the adsorption process was dependent on temperature and initial concentration. The results obtained during the first 7 h were used to draw the conclusion that, as temperature increased, so did the adsorbate loading. The rate of adsorption was dependent on the temperature of the system as the rate of diffusion of molecules through the adsorbent pores increases with increasing temperature.

It was found that increasing the initial 3,7-DMO concentration in the bulk solution resulted in distinct increased adsorbate loading after 60 min up to and including at 24 h. The increased initial adsorbate concentration increases the probability of more adsorbent active sites being filled by an adsorbate molecule. However, the adsorbate loading achieved did not increase beyond an initial concentration of 1.5 mass%, at all three system temperatures, and served as a first indicator that the maximum adsorption capacity of SCD for 3,7-DMO ranged between 110-118 mg.g⁻¹.

The equilibrium isotherm model that fitted the single component data best was the Redlich-Peterson model. The maximum adsorption capacity of 3,7-DMO in SCD was found to be 115, 101 and 120 mg.g⁻¹ for 25 °C, 35 °C and 45 °C. The increased solution temperature increased the entropy and kinetic energy of the molecules and resulted in more adsorbate molecules coming into contact with active sites more frequently. The kinetic models that fitted the kinetic data best were the pseudo-second order and Elovich models. This indicates that the adsorption of 3,7-DMO in a single component system followed a the second-order rate law and that chemisorption was a predominant mechanism of adsorption.

8.2 1-Octanol&3,7-DMO and 1-decanol&3,7-DMO adsorption from n-decane solution on SCD

Temperature, overall initial concentration and adsorbate ratio each proved to influence the adsorption of both binary systems. Temperature had at least some effect, and mostly affected the 1-decanol&3,7-DMO binary system. The highest adsorbent loading was achieved at an initial concentration of 3.3 mass%

in the case of 1-octanol&3,7-DMO and 2.2 mass% in that of 1-decanol&3,7-DMO. Varying the adsorbate ratio showed that the highest equilibrium adsorbent loading was achieved when the linear molecules (1-decanol and 1-octanol) were in excess when compared to the branched molecule (3,7-DMO) in both binary systems.

The 1-octanol&3,7-DMO, 1-decanol&3,7-DMO and 1-decanol&1-octanol systems were examined to determine the ways in which 1-octanol, 1-decanol and 3,7-DMO behaved within the competitive adsorption systems studied here. This was done by performing displacement tests on all three adsorption systems. All three adsorbates (1-octanol, 1-decanol and 3,7-DMO) in the three binary component systems were used as displacers to determine the displacement potential of each.

In the 1-octanol&1-decanol system, 1-octanol and 1-decanol displayed similar displacement potential. It was established that 1-octanol had a slightly higher displacement potential than 1-decanol. It is hypothesised that this was a consequence of molecular size with 1-octanol being smaller than 1-decanol. Additionally, the bond strength between 1-octanol and SCD is stronger than the bond strength between 1-decanol and SCD. In the case of 1-octanol&3,7-DMO, 1-octanol had a higher displacement potential than 3,7-DMO and a larger percentage of this material was adsorbed after it had displaced 3,7-DMO. This suggests that a small linear molecule is more easily adsorbed and readily displaces a larger nonlinear one. In the 1-decanol&3,7-DMO system, 1-decanol had a slightly higher displacement potential than 3,7-DMO and was more readily adsorbed. This suggests that molecular shape plays a role in adsorption and that linear-shaped molecules are favoured above nonlinear ones. Additionally, adsorbate polarity and bond strength play a key role in adsorbent affinity. Extant literature says that smaller molecules displace larger ones more easily. It is more challenging to draw distinct conclusions regarding the displacement potential of equi-sized molecules and different shapes. However, it appears that linear molecules display greater displacement potential. The study of the effects of interaction between molecules indicated that both 1-octanol and 1-decanol hindered the adsorption of 3,7-DMO when these were present in a binary component system.

The binary component kinetic and isotherm models were fitted to both binary systems at 25 °C and 45 °C. It was found that for 1-decanol&3,7-DMO, the pseudo-second order and Elovich models fitted the data best. In the case of 1-octanol&3,7-DMO, the Elovich model fitted the data best. The coefficient of determination and MPSD of the binary component isotherm models indicated a poor fit for most models.

The equilibrium isotherm model that fitted the two binary component systems best were the extended Freundlich one. The modified competitive Langmuir model providing the second best fit in this respect. The maximum adsorption capacities for 1-decanol&3,7-DMO and 1-octanol&3,7-DMO were 122 mg.g⁻¹ and 117mg.g⁻¹. This indicates that, in a binary system, 1-decanol, 1-octanol and 3,7-DMO interact with one another.

In conclusion, the project proved that SCD was capable of removing 3,7-DMO from an n-decane stream in a single and binary component system. In contrast with extant widely accepted ideas, though, the present study showed that the adsorbent removes larger quantities of linear alcohols (1-octanol and 1-decanol) per gram of adsorbent than non-linear molecules such as 3,7-DMO.

8.3 Recommendations

Some of the outcomes did not meet the expected standards. Further work will be required to ensure the results are truly representative of the adsorption system. Although this was not the desired outcome, the causes for discrepancies at 45 °C did add an interesting element to the study and required further investigation in and of itself. It is recommended that changes be made to the analysis method and experimental setup for a study such as the present one. Furthermore, an in-depth study of the thermodynamic properties of the adsorption system may elucidate the lack of sensitivity to temperature in binary systems (see Senthil Kumar *et al.*, 2014). The thermodynamic study proposed would entail experiments designed for the sole purpose of evaluating the Gibbs free energy of adsorption and in turn the adsorption entropy. A semi-continuous flow experimental setup should be used in further studies (Li *et al.*, 2003). This would involve contacting the adsorbent with a recycled fluid to achieve a falling film and improve the contact time of each adsorbent bead with solution (Li *et al.*, 2003).

In future, the heat of adsorption can be studied by pre-heating the solution to a temperature that is two °C higher than desired temperature while placing the solution, with an agitator, in a tightly sealed and insulated container. During the entire process of transfer into the container, the temperature of the solution would decrease to the desired temperature. At this time the adsorbent should be introduced to the system and the system tightly sealed while maintaining sufficient and constant agitation. The temperature should then be monitored and an increase or decrease in temperature would provide an indication as to whether the heat of adsorption was involved in the process. The system can subsequently be defined as exothermic or endothermic in nature.

References

- Abdullahi, A.S. and Galadima, W. (2014) 'Petrochemicals and Economic Development: Issues and Challenges', *Academic Journal of Interdisciplinary Studies*, 3(5), pp. 47–54. doi:10.5901/ajis.2014.v3n5p47.
- Abrams, D.S. *et al.* (1984) 'Physical and Thermodynamic Properties of Aliphatic Alcohols', *Physical Properties of Chemical Substances*, 29(3), p. 47. Available at: <https://pubs.acs.org/sharingguidelines> (Accessed: 22 May 2020).
- Agrawal, M. *et al.* (2018) 'Liquid-Phase Multicomponent Adsorption and Separation of Xylene Mixtures by Flexible MIL-53 Adsorbents', *Journal of Physical Chemistry C*, 122(1), pp. 386–397. doi:10.1021/acs.jpcc.7b09105.
- Aharoni, C. and Tompkins, F.C. (1970) 'Kinetics of Adsorption and Desorption and the Elovich Equation', *Advances in Catalysis*, 21(C), pp. 1–49. doi:10.1016/S0360-0564(08)60563-5.
- Ahmed, Y.M. *et al.* (2010) 'Effect of Adsorbate Initial Concentration on the Removal of Pb from Aqueous Solutions by Carbon Nanofibers', *24th Symposium of Malaysian Chemical Engineers (SOMChE 2010) and 1st International Conference on Process Engineering and Advanced Materials 2010 (ICPEAM2010)*, (July), pp. 15–17.
- Al-Ghouti, M.A. and Al-Absi, R.S. (2020) 'Mechanistic understanding of the adsorption and thermodynamic aspects of cationic methylene blue dye onto cellulosic olive stones biomass from wastewater', *Scientific Reports*, 10(1), pp. 1–18. doi:10.1038/s41598-020-72996-3.
- Alavi, S. *et al.* (2010) 'Hydrogen-bonding alcohol-water interactions in binary ethanol, 1-propanol, and 2-propanol+methane structure II clathrate hydrates', *Journal of Chemical Physics*, 133(7), pp. 1–8. doi:10.1063/1.3469776.
- Alturki, A.A. and Simonetti, D.A. (2017) *A Single Component Adsorption of Alcohols in Zeolites*, *Professional Geographer*. University of California, Los Angeles. doi:10.1111/j.0033-0124.1957.93_28.x.
- An, B. (2020) 'Cu(II) and As(V) adsorption kinetic characteristic of the multifunctional amino groups in chitosan', *Processes Journal*, 8(1194). doi:10.3390/PR8091194.
- Aschermann, G., Zietzschmann, F. and Jekel, M. (2018) 'Influence of dissolved organic matter and activated carbon pore characteristics on organic micropollutant desorption', *Water Research*, 133, pp. 123–131. doi:10.1016/j.watres.2018.01.015.
- Ayawei, N., Ebelegi, A.N. and Wankasi, D. (2017) 'Modelling and Interpretation of Adsorption Isotherms', *Journal of Chemistry*, 2017. doi:10.1155/2017/3039817.
- BASF (2009) 'Product Data Sheet: F-200 Activated Alumina For Liquid and Gas Drying', (BF-9201 Rev. 12/09). Available at: <https://www.interraglobal.com/portals/0/pdf/specsheets/basf-f200-activated-alumina.pdf>.
- BASF (2014) 'Smooth , spherical adsorbent for the removal', (BF-8571 Rev. 10/16), pp. 4–5. Available at: https://catalysts.basf.com/files/pdf/BF-8571_US_Selexsorb-CD_Datasheet.pdf.
- Bayuo, J. *et al.* (2020) 'Desorption of chromium (VI) and lead (II) ions and regeneration of the exhausted adsorbent', *Applied Water Science*, 10(7), pp. 1–6. doi:10.1007/s13201-020-01250-y.
- Belhachemi, M. and Addoun, F. (2011) 'Comparative adsorption isotherms and modeling of methylene blue onto activated carbons', *Applied Water Science*, 1(3–4), pp. 111–117. doi:10.1007/s13201-011-0014-1.
- Bhatta, L.K.G. *et al.* (2015) 'Progress in hydrotalcite like compounds and metal-based oxides for CO₂ capture: A review', *Journal of Cleaner Production*, 103(December), pp. 171–196.

doi:10.1016/j.jclepro.2014.12.059.

Binnie, C., Kimber, M. and Thomas, H. (2017) 'Activated carbon adsorption', in *Basic Water Treatment*. ICE Publishing, pp. 147–155. doi:10.1680/bwtse.63341.147.

Bolton, K. *et al.* (2009) 'Simulation of water clusters in vapour, alkanes and polyethylenes', *Molecular Simulation*, 35(10–11), pp. 888–896. doi:10.1080/08927020902787804.

Bondarenko, T. *et al.* (2020) 'Investments to the petrochemical sector: The value of the competitiveness of petrochemical companies', *Entrepreneurship and Sustainability Issues*, 7(3), pp. 2510–2525. doi:10.9770/jesi.2020.7.3(70).

Bosman, C.E. (2019) *Single and binary component adsorption of 1-alcohols from an alkane using various activated alumina adsorbents* by. Stellenbosch University. Available at: <https://scholar.sun.ac.za/handle/10019.1/107204>.

Bosman, C.E. and Schwarz, C.E. (2019) *Single and binary component adsorption of 1-alcohols from an alkane using various activated alumina adsorbents*, *AIChE Annual Meeting, Conference Proceedings*. Stellenbosch University.

Brunauer, S., Emmett, P.H. and Teller, E. (1938) 'Adsorption of Gases in Multimolecular Layers', *Journal of the American Chemical Society*, 60(2), pp. 309–319. doi:10.1021/ja01269a023.

Budi, A., Stipp, S.L.S. and Andersson, M.P. (2018) 'Calculation of Entropy of Adsorption for Small Molecules on Mineral Surfaces', *Journal of Physical Chemistry Chemistry*, 122(15), pp. 8236–8243. doi:10.1021/acs.jpcc.7b11860.

Builes, S., Sandler, S.I. and Xiong, R. (2013) 'Isosteric heats of gas and liquid adsorption', *Langmuir*, 29(33), pp. 10416–10422. doi:10.1021/la401035p.

Çay, S., Uyanik, A. and Özaşık, A. (2004) 'Single and binary component adsorption of copper(II) and cadmium(II) from aqueous solutions using tea-industry waste', *Separation and Purification Technology*, 38(3), pp. 273–280. doi:10.1016/j.seppur.2003.12.003.

Chakrapani, C. *et al.* (2010) 'Adsorption kinetics for the removal of fluoride from aqueous solution by activated carbon adsorbents derived from the peels of selected citrus fruits', *E-Journal of Chemistry*, 7. doi:10.1155/2010/582150.

Chattoraj, S. *et al.* (2016) 'Optimization of Adsorption Parameters for Removal of Carbaryl Insecticide Using Neem Bark Dust by Response Surface Methodology', *Water Conservation Science and Engineering*, 1(2), pp. 127–141. doi:10.1007/s41101-016-0008-9.

Chen, A.S.C. *et al.* (2015) 'Journal (American Water Works Association)', 81(1), pp. 53–60. doi:10.142.66.3.42.

Chiang, W.S. *et al.* (2018) 'A non-invasive method to directly quantify surface heterogeneity of porous materials', *Nature Communications*, 9(1), pp. 1–7. doi:10.1038/s41467-018-03151-w.

Chien, S.H. and Clayton, W.R. (1980) 'Application of Elovich Equation to the Kinetics of Phosphate Release and Sorption in Soils', *Soil Science Society of America Journal*, 44(2), pp. 265–268. doi:10.2136/sssaj1980.03615995004400020013x.

Chiou, C.T. (2003) 'Fundamentals of the Adsorption Theory', *Partition and Adsorption of Organic Contaminants in Environmental Systems*, (October), pp. 39–52. doi:10.1002/0471264326.ch4.

Cho, D.H., Chu, K.H. and Kim, E.Y. (2015) 'A critical assessment of the use of a surface reaction rate equation to correlate biosorption kinetics', *International Journal of Environmental Science and Technology*, 12(6), pp. 2025–2034. doi:10.1007/s13762-014-0590-3.

Choma, J. and Jaroniec, M. (2001) 'Determination of the specific surface areas of non-porous and macroporous carbons', *Adsorption Science and Technology*, 19(9), pp. 765–776.

doi:10.1260/0263617011494565.

Choon Ng, K. *et al.* (2017) 'A Universal Isotherm Model to Capture Adsorption Uptake and Energy Distribution of Porous Heterogeneous Surface', *Scientific Reports*, 7(1), pp. 1–11. doi:10.1038/s41598-017-11156-6.

Dąbrowski, A. (2001) 'Adsorption - From theory to practice', *Advances in Colloid and Interface Science*, 93(1–3), pp. 135–224. doi:10.1016/S0001-8686(00)00082-8.

Dada, A.O. *et al.* (2012) 'Langmuir, Freundlich, Temkin and Dubinin–Radushkevich Isotherms Studies of Equilibrium Sorption of Zn²⁺ Unto Phosphoric Acid Modified Rice Husk', *IOSR Journal of Applied Chemistry*, 3(1), pp. 38–45. doi:10.9790/5736-0313845.

Darweesh, M.A. *et al.* (2022) 'Adsorption isotherm, kinetic, and optimization studies for copper (II) removal from aqueous solutions by banana leaves and derived activated carbon', *South African Journal of Chemical Engineering*, 40(January), pp. 10–20. doi:10.1016/j.sajce.2022.01.002.

DeCanio, E.C., Nero, V.P. and Bruno, J.W. (1992) 'Identification of alcohol adsorption sites on γ -alumina', *Journal of Catalysis*, 135(2), pp. 444–457. doi:10.1016/0021-9517(92)90046-K.

Demirbas, E. *et al.* (2004) 'Adsorption kinetics for the removal of chromium (VI) from aqueous solutions on the activated carbons prepared from agricultural wastes', *Water SA*, 30(4), pp. 533–539. doi:10.4314/wsa.v30i4.5106.

Díaz, E. *et al.* (2004) 'Adsorption characterisation of different volatile organic compounds over alumina, zeolites and activated carbon using inverse gas chromatography', *Journal of Chromatography A*, 1049(1–2), pp. 139–146. doi:10.1016/j.chroma.2004.07.061.

Dubinin, M.M. (1974) 'On physical feasibility of Brunauer's micropore analysis method', *Journal of Colloid And Interface Science*, 46(3), pp. 351–356. doi:10.1016/0021-9797(74)90044-7.

Ebelegi, A.N., Ayawei, N. and Wankasi, D. (2020) 'Interpretation of Adsorption Thermodynamics and Kinetics', *Journal of Physical Chemistry*, 10(3). doi:10.4236/ojpc.2020.103010.

Ezzati, R. (2020) 'Derivation of Pseudo-First-Order, Pseudo-Second-Order and Modified Pseudo-First-Order rate equations from Langmuir and Freundlich isotherms for adsorption', *Chemical Engineering Journal*, 392, p. 123705. doi:10.1016/J.CEJ.2019.123705.

Fang, F. and Szleifer, I. (2002) 'Effect of molecular structure on the adsorption of protein on surfaces with grafted polymers', *Langmuir*, 18(14), pp. 5497–5510. doi:10.1021/la020027r.

Fianu, J., Gholinezhad, J. and Hassan, M. (2019) 'Comparison of Single, Binary and Temperature-Dependent Adsorption Models Based on Error Function Analysis', *Journal of Oil, Gas and Petrochemical Sciences*, 2(2), pp. 77–91. doi:10.30881/jogps.00027.

Foo, K.Y. and Hameed, B.H. (2010) 'Insights into the modeling of adsorption isotherm systems', *Chemical Engineering Journal*, 156(1), pp. 2–10. doi:10.1016/j.cej.2009.09.013.

Freundlich, H.M.. (1906) 'Over the Adsorption in Solution', *The Journal of Physical Chemistry*, 57, pp. 385–471.

Gautam, R.K. *et al.* (2014) 'Biomass-derived biosorbents for metal ions sequestration: Adsorbent modification and activation methods and adsorbent regeneration', *Journal of Environmental Chemical Engineering*, 2(1), pp. 239–259. doi:10.1016/j.jece.2013.12.019.

Girish, C.R. (2017) 'Various isotherm models for multicomponent adsorption: A review', *International Journal of Civil Engineering and Technology*, 8(10), pp. 80–86. Available at: <http://www.iaeme.com/IJCIET/issues.asp?JType=IJCIET&VType=8&IType=10>.

Gorzin, F. and Bahri Rasht Abadi, M.M. (2018) 'Adsorption of Cr(VI) from aqueous solution by adsorbent prepared from paper mill sludge: Kinetics and thermodynamics studies', *Adsorption Science and*

Technology, 36(1–2), pp. 149–169. doi:10.1177/0263617416686976.

Groenewald, J. (2019) *Evaluation and Comparison of three industrially relevant adsorbents of their ability to remove alcohol contaminants from an alkane solvent*. Stellenbosch University.

Hameed, B.H. and El-Khaiary, M.I. (2008) 'Malachite green adsorption by rattan sawdust: Isotherm, kinetic and mechanism modeling', *Journal of Hazardous Materials*, 159(2–3), pp. 574–579. doi:10.1016/j.jhazmat.2008.02.054.

Harrison, A. *et al.* (2014) 'Branched versus linear alkane adsorption in carbonaceous slit pores', *Adsorption*, 20(2–3), pp. 427–437. doi:10.1007/s10450-013-9589-1.

Ho, Y.S. and McKay, G. (1998) 'a Comparison of Chemisorption Kinetic Models Applied To Pollutant Removal on Various Sorbents', 76. doi:10.1205/095758298529696.

Ho, Y.S. and McKay, G. (1999) 'Pseudo-second order model for sorption processes', *Process Biochemistry* [Preprint]. doi:10.1016/S0032-9592(98)00112-5.

Horsfall, M. and Spiff, A.I. (2005) 'Effects of temperature on the sorption of Pb²⁺ and Cd²⁺ from aqueous solution by Caladium bicolor (Wild Cocoyam) biomass', *Electronic Journal of Biotechnology*, 8(2), pp. 162–169. doi:10.2225/vol8-issue2-fulltext-4.

Hu, F. *et al.* (2015) 'Graphene-Catalyzed Direct Friedel-Crafts Alkylation Reactions: Mechanism, Selectivity, and Synthetic Utility', *Journal of the American Chemical Society*, 137(45), pp. 14473–14480. doi:10.1021/jacs.5b09636.

Huang, H. *et al.* (2011) 'Effect of temperature on gas adsorption and separation in ZIF-8: A combined experimental and molecular simulation study', *Chemical Engineering Science*, 66(23), pp. 6297–6305. doi:10.1016/j.ces.2011.09.009.

International Union of Pure and Applied Chemistry (1994) 'Recommendations for the characterization of porous solids', *Pure Applied Chemistry*, 66(8), pp. 1739–1758. doi:doi.org/10.1351/pac199466081739.

Javadian, H. *et al.* (2015) 'Study of the adsorption of Cd (II) from aqueous solution using zeolite-based geopolymer, synthesized from coal fly ash; kinetic, isotherm and thermodynamic studies', *Arabian Journal of Chemistry*, 8(6), pp. 837–849. doi:10.1016/j.arabjc.2013.02.018.

Jiang, L.L. *et al.* (2018) 'The effect of temperatures on the synergistic effect between a magnetic field and functionalized graphene oxide-carbon nanotube composite for Pb²⁺ and phenol adsorption', *Journal of Nanomaterials*, 2018. doi:10.1155/2018/9167938.

Kapoor, A., Ritter, J.A. and Yang, R. (1990) 'An Extended Langmuir Model for Adsorption of Gas Mixtures on Heterogeneous Surfaces', pp. 660–664. doi:doi:10.1021/1a00093a022.

Knözinger, H. and Stübner, B. (1978) 'Adsorption of alcohols on alumina. 1. Gravimetric and infrared spectroscopic investigation', *Journal of Physical Chemistry*, 82(13), pp. 1526–1532. doi:10.1021/j100502a013.

Kose, H. (2010) 'The Effects of Physical Factors on the Adsorption of Synthetic Organic Compounds By Activated Carbons and Activated Carbon Fibers', pp. 1–101. doi:10.1111/j.1600-0714.2011.01008.x.

Krishna, R. *et al.* (2016) 'Effect of Alkali Carbonate/Bicarbonate on Citral Hydrogenation over Pd/Carbon Molecular Sieves Catalysts in Aqueous Media', *Modern Research in Catalysis*, 05(01), pp. 1–10. doi:10.4236/mrc.2016.51001.

Kulkarni, S.J. (2016) 'Role of Adsorption in Petroleum Industries and Refineries', *International Journal of Petroleum and Petrochemical Engineering*, 2(1), pp. 16–19. doi:10.20431/2454-7980.0201004.

Kumar, K.V. *et al.* (2019) 'Characterization of the adsorption site energies and heterogeneous surfaces of porous materials', *Journal of Materials Chemistry A*, 7(17), pp. 10104–10137. doi:10.1039/c9ta00287a.

- Kurniawan, A. *et al.* (2011) 'Evaluation of cassava peel waste as lowcost biosorbent for Ni-sorption: Equilibrium, kinetics, thermodynamics and mechanism', *Chemical Engineering Journal*, 172(1), pp. 158–166. doi:10.1016/j.cej.2011.05.083.
- Lagergren S.K. (1989) 'About the Theory of So-called Adsorption of Soluble Substances', *Kungliga Svenska Vetenskapsakademiens Handlingar*, 24(4), pp. 1–39.
- Langmuir, I. (1918) 'The adsorption of gases on plane surfaces of glass, mica and platinum', *Journal of the American Chemical Society*, 40(9), pp. 1361–1403. doi:10.1021/JA02242A004.
- Lapczynski, A. *et al.* (2008) 'Fragrance material review on 3,7-dimethyl-1-octanol', *Food and Chemical Toxicology*, 46(11 SUPPL.), pp. 139–141. doi:10.1016/j.fct.2008.06.023.
- Lazaridis, N.K. and Asouhidou, D.D. (2003) 'Kinetics of sorptive removal of chromium(VI) from aqueous solutions by calcined Mg-Al-CO₃ hydrotalcite', *Water Research*, 37(12), pp. 2875–2882. doi:10.1016/S0043-1354(03)00119-2.
- Li, D. *et al.* (2002) 'Preparation of nanometer dispersed polypropylene / polystyrene interpenetrating network using supercritical CO₂ as a swelling agent', 43, pp. 5363–5367. doi:10.1016/S0032-3861(02)00374-9.
- Li, Q. *et al.* (2003) 'Three-component competitive adsorption model for flow-through PAC systems. 1. Model development and verification with a PAC/membrane system', *Environmental Science and Technology*, 37(13), pp. 2997–3004. doi:10.1021/es020989k.
- Li, S. *et al.* (2014) 'Separation of primary alcohols and saturated alkanes from fisher-tropsch synthesis products', *Chinese Journal of Chemical Engineering*, 22(9), pp. 980–983. doi:10.1016/j.cjche.2014.06.025.
- Lim, K., Kim, J. and Lee, J. (2019) 'Comparative study on adsorbent characteristics for adsorption thermal energy storage system', *International Journal of Energy Research*, 43(9), pp. 4281–4294. doi:10.1002/er.4553.
- Lima, É.C. and Adebayo, M.A. (2015) *Carbon Nanomaterials as Adsorbents for Environmental and Biological Applications*. doi:10.1007/978-3-319-18875-1.
- Lin, D.R. *et al.* (2015) 'Mechanisms of competitive adsorption organic pollutants on hexylene-bridged polysilsesquioxane', *Materials*, 8(9), pp. 5806–5817. doi:10.3390/ma8095275.
- Lorenzen, L. *et al.* (2009) 'Activated alumina-based adsorption and recovery of excess fluoride ions subsequent to calcium and magnesium removal in base metal leach circuits', *Journal of the Southern African Institute of Mining and Metallurgy*, 109(8), pp. 447–453. doi:109(8):447-453.
- Low, M.J.D. (1960) 'Kinetics of chemisorption of gases on solids', *Chemical Reviews*, 60(3), pp. 267–312. doi:10.1021/CR60205A003.
- Maccallum, J.L. and Tieleman, D.P. (2002) 'Structures of Neat and Hydrated 1-Octanol from Computer Simulations', (23), pp. 15085–15093.
- Maghsoudi, H., Abdi, H. and Aidani, A. (2020) 'Temperature- And Pressure-Dependent Adsorption Equilibria and Diffusivities of Propylene and Propane in Pure-Silica Si-CHA Zeolite', *Industrial and Engineering Chemistry Research*, 59(4), pp. 1682–1692. doi:10.1021/acs.iecr.9b05451.
- Malash, G.F. and El-Khaiary, M.I. (2010) 'Piecewise linear regression: A statistical method for the analysis of experimental adsorption data by the intraparticle-diffusion models', *Chemical Engineering Journal*, 163(3), pp. 256–263. doi:10.1016/j.cej.2010.07.059.
- Marais, C.G. (2008) *Thermodynamics and kinetics of sorption*. Edited by L.J. Barbour, C. Esterhuysen, and Stellenbosch University. Faculty of Science. Dept. of Chemistry and Polymer Science. Doctoral Dissertation. Stellenbosch University.
- Marczewski, A.W. *et al.* (2016) 'Adsorption equilibrium and kinetics of selected phenoxyacid pesticides

on activated carbon: effect of temperature', *Adsorption*, 22(4–6), pp. 777–790. doi:10.1007/s10450-016-9774-0.

McKay, G. and Al-Duri, B. (1991) 'Extended empirical Freundlich isotherm for binary systems: a modified procedure to obtain the correlative constants', *Chemical Engineering and Processing*, 29(3), pp. 133–138. doi:10.1016/0255-2701(91)85012-D.

Meshcheryakov, E.P. *et al.* (2021) 'Efficient adsorbent-desiccant based on aluminium oxide', *Applied Sciences (Switzerland)*, 11(6). doi:10.3390/app11062457.

Milestone, N.B. and Bibby, D.M. (1981) 'Concentration of Alcohols by Adsorption on Silicalite', *Journal of Chemical Technology and Biotechnology*, (April), pp. 732–736. Available at: <https://doi.org/10.1002/jctb.503310198>.

Mor, S., Ravindra, K. and Bishnoi, N.R. (2007) 'Adsorption of chromium from aqueous solution by activated alumina and activated charcoal', *Bioresource Technology*, 98(4), pp. 954–957. doi:10.1016/j.biortech.2006.03.018.

Mouelhi, M. *et al.* (2016) 'Competitive adsorption of fluoride and natural organic matter onto activated alumina', *Environmental Technology (United Kingdom)*, 37(18), pp. 2326–2336. doi:10.1080/09593330.2016.1149521.

Moyo, M. *et al.* (2013) 'Adsorption batch studies on the removal of Pb(II) using maize tassel based activated carbon', *Journal of Chemistry*, 2013. doi:10.1155/2013/508934.

Nguyen, C.M., Reyniers, M.F. and Marin, G.B. (2010) 'Theoretical study of the adsorption of C1-C4 primary alcohols in H-ZSM-5', *Physical Chemistry Chemical Physics*, 12(32), pp. 9481–9493. doi:10.1039/c000503g.

Nouri, S., Haghseresht, F. and Lu, M. (2002) 'Adsorption of aromatic compounds by activated carbon: Effects of functional groups and molecular size', *Adsorption Science and Technology*, 20(1), pp. 1–16. doi:10.1260/026361702760120890.

Okhrimenko, D. V. *et al.* (2013) 'Energies of the adsorption of functional groups to calcium carbonate polymorphs: The importance of -OH and -COOH groups', *Langmuir*, 29(35), pp. 11062–11073. doi:10.1021/la402305x.

Özacar, M. (2003) 'Equilibrium and kinetic modelling of adsorption of phosphorus on calcined alunite', *Adsorption*, 9(2), pp. 125–132. doi:10.1023/A:1024289209583.

Padilla-Ortega, E., Leyva-Ramos, R. and Flores-Cano, J. V. (2013) 'Binary adsorption of heavy metals from aqueous solution onto natural clays', *Chemical Engineering Journal*, 225, pp. 535–546. doi:10.1016/j.cej.2013.04.011.

Padmavathy, K.S., Madhu, G. and Haseena, P.V. (2016) 'A study on Effects of pH, Adsorbent Dosage, Time, Initial Concentration and Adsorption Isotherm Study for the Removal of Hexavalent Chromium (Cr (VI)) from Wastewater by Magnetite Nanoparticles', *Procedia Technology*, 24, pp. 585–594. doi:10.1016/j.protcy.2016.05.127.

Panja, C., Saliba, N. and Koel, B.E. (1998) 'Adsorption of methanol, ethanol and water on well-characterized Pt-Sn surface alloys', *Surface Science*, 395(2–3), pp. 248–259. doi:10.1016/S0039-6028(97)00629-8.

Parhi, P. *et al.* (2009) 'Volumetric Interpretation of Protein Adsorption: Capacity Scaling with Adsorbate Molecular Weight and Adsorbent Surface Energy', *Biomaterials*, 36(1), pp. 14–24. doi:10.1016/j.biomaterials.2009.09.005.Volumetric.

Parthasarathy, P. and Narayanan, S.K. (2014) 'Effect of Hydrothermal Carbonization Reaction Parameters on', *Environmental Progress & Sustainable Energy*, 33(3), pp. 676–680. doi:10.1002/ep.

- Patel, H. (2019) 'Fixed-bed column adsorption study: a comprehensive review', *Applied Water Science*, 9(3), pp. 1–17. doi:10.1007/s13201-019-0927-7.
- Patiha *et al.* (2016) 'The langmuir isotherm adsorption equation: The monolayer approach', *IOP Conference Series: Materials Science and Engineering*, 107(1). doi:10.1088/1757-899X/107/1/012067.
- Pfnür, H., Feulner, P. and Menzel, D. (1983) 'The influence of adsorbate interactions on kinetics and equilibrium for CO on Ru(001). II. Desorption kinetics and equilibrium', *The Journal of Chemical Physics*, 79(9), pp. 4613–4623. doi:10.1063/1.446378.
- Qiu, H. *et al.* (2009) 'Critical review in adsorption kinetic models', *Journal of Zhejiang University: Science A*, 10(5), pp. 716–724. doi:10.1631/jzus.A0820524.
- Quinlivan, P.A., Li, L. and Knappe, D.R.U. (2005) 'Effects of activated carbon characteristics on the simultaneous adsorption of aqueous organic micropollutants and natural organic matter', *Water Research*, 39(8), pp. 1663–1673. doi:10.1016/j.watres.2005.01.029.
- Rabia, A.R., Ibrahim, A.H. and Zulkepli, N.N. (2018) 'Activated alumina preparation and characterization: The review on recent advancement', *E3S Web of Conferences*, 34, pp. 1–8. doi:10.1051/e3sconf/20183402049.
- Rao, M.B. and Sircar, S. (1993) 'Liquid-phase adsorption of bulk ethanol-water mixtures by alumina', *Adsorption Science and Technology*, 10(1–4), pp. 93–104. doi:10.1177/0263617499010001-409.
- Redlich, O. and Peterson, D.L. (1959) 'A useful adsorption isotherm', *Journal of Physical Chemistry*, 63(6), p. 1024. doi:10.1021/J150576A611.
- Regti, A. *et al.* (2017) 'Competitive adsorption and optimization of binary mixture of textile dyes: A factorial design analysis', *Journal of the Association of Arab Universities for Basic and Applied Sciences*, 24, pp. 1–9. doi:10.1016/j.jaubas.2016.07.005.
- Rodda, D.P., Johnson, B.B. and Wells, J.D. (1996) 'Modeling the effect of temperature on adsorption of lead(II) and zinc(II) onto goethite at constant pH', *Journal of Colloid and Interface Science*, 184(2), pp. 365–377. doi:10.1006/jcis.1996.0631.
- Ruthven, D.M. (1984) *Principles of adsorption and adsorption processes*. New York, N.Y.: John Wiley & Sons.
- Saridede, M.N., Çizmecioğlu, Z. and Değerli, S. (2005) 'The production of activated alumina from aluminum hydroxide based waste', *Canadian Metallurgical Quarterly*, 44(1), pp. 131–136. doi:10.1179/cmq.2005.44.1.131.
- Saruchi and Kumar, V. (2019) 'Adsorption kinetics and isotherms for the removal of rhodamine B dye and Pb +2 ions from aqueous solutions by a hybrid ion-exchanger', *Arabian Journal of Chemistry*, 12(3), pp. 316–329. doi:10.1016/j.arabjc.2016.11.009.
- Senthil Kumar, P. *et al.* (2014) 'Effect of Temperature on the Adsorption of Methylene Blue Dye Onto Sulfuric Acid-Treated Orange Peel', *Chemical Engineering Communications*, 201(11), pp. 1526–1547. doi:10.1080/00986445.2013.819352.
- Singh, N., Kumari, A. and Balomajumder, C. (2018) 'Modeling studies on mono and binary component biosorption of phenol and cyanide from aqueous solution onto activated carbon derived from saw dust', *Saudi Journal of Biological Sciences*, 25(7), pp. 1454–1467. doi:10.1016/j.sjbs.2016.01.007.
- Sips, R. (1948) 'On the structure of a catalyst surface', *The Journal of Chemical Physics*, 16(5), pp. 490–495. doi:10.1063/1.1746922.
- Srivastava, V.C., Mall, I.D. and Mishra, I.M. (2006) 'Equilibrium modelling of single and binary adsorption of cadmium and nickel onto bagasse fly ash', *Chemical Engineering Journal*, 117(1), pp. 79–91. doi:10.1016/j.cej.2005.11.021.

- Subha, R. and Namasivayam, C. (2008) 'Modeling of adsorption isotherm and kinetics of 2,4,6-Trichlorophenol onto microporous ZnCl₂ activated coir pith carbon', *J. Environ. Eng. Manage*, 18(4), pp. 275–280. Available at: <https://pdfs.semanticscholar.org/e399/1d7171d901d5b17c601f83abe44dfe6d8386.pdf>.
- Subramanyam, B. and Das, A. (2014) 'Linearised and non-linearised isotherm models optimization analysis by error functions and statistical means', *Journal of Environmental Health Science and Engineering*, 12(1), pp. 1–6. doi:10.1186/2052-336X-12-92.
- Sudiyarmanto *et al.* (2017) 'Preparation and characterization of Ni based on natural zeolite catalyst for citronellol conversion to 3,7-Dimethyl-1-Octanol', *AIP Conference Proceedings*, 1904(December). doi:10.1063/1.5011919.
- Sumalapao, D.E.P. *et al.* (2016) 'Biosorption kinetic models on the removal of congo red onto unripe calamansi (*Citrus microcarpa*) peels', *Oriental Journal of Chemistry*, 32(6), pp. 2889–2900. doi:10.13005/ojc/320607.
- Thomas, M.A. and Thommes, M. (2004) *Characterization of Porous Solids and Powders: Surface Area, Pore Size and Density, Handbook of Porous Solids*. John Wiley & Sons. doi:10.5860/choice.42-5288.
- Trivedi, H.C., Patel V.M. and R.D., P. (1973) 'Adsorption of cellulose and triacetate on calcium silicate', *European Polymer Journal*, 9(6), pp. 525–531. doi:10.1016/0014-3057(73)90036-0.
- Turner, N.H. (1975) 'Kinetics of chemisorption: An examination of the Elovich equation', *Journal of Catalysis*, 36(3), pp. 262–265. doi:10.1016/0021-9517(75)90035-4.
- Unger, K. (1972) 'Structure of Porous Adsorbents', *Angewandte Chemie International Edition in English*, 11(4), pp. 267–278. doi:10.1002/anie.197202671.
- USDA (2016) 'Fatty Alcohols (Octanol and Decanol).', *Technical evaluation report. Agricultural Analytics Division for the USDA National Organic Program*, pp. 1–16. Available at: <https://www.ams.usda.gov/sites/default/files/media/FattyAlcohols020217.pdf>.
- Vijayakumar, G., Tamilarasan, R. and Dharmendirakumar, M. (2012) 'Adsorption , Kinetic , Equilibrium and Thermodynamic studies on the removal of basic dye Rhodamine-B from aqueous solution by the use of natural adsorbent perlite', *Journal of Materials and Environmental Science*, 3(June), pp. 157–170.
- Vlugt, T.J.H., Krishna, R. and Smit, B. (1999) 'Molecular Simulations of Adsorption Isotherms for Linear and Branched Alkanes and Their Mixtures in Silicalite', pp. 1102–1118. doi:10.1021/jp982736c.
- Vora, B. V *et al.* (2003) 'Alkylation', in *Kirk-Othmer Encyclopedia of Chemical Technology*. John Wiley & Sons, Inc., pp. 169–198. doi:10.1002/0471238961.0112112508011313.a01.pub2.
- Wang, F.Y., Wang, H. and Ma, J.W. (2010) 'Adsorption of cadmium (II) ions from aqueous solution by a new low-cost adsorbent-Bamboo charcoal', *Journal of Hazardous Materials*, 177(1–3), pp. 300–306. doi:10.1016/j.jhazmat.2009.12.032.
- Wang, J. and Guo, X. (2020) 'Adsorption kinetic models: Physical meanings, applications, and solving methods', *Journal of Hazardous Materials*, 390(January), p. 122156. doi:10.1016/j.jhazmat.2020.122156.
- Wang, J., Wei, Y. and Ma, Z. (2020) 'Modified dual-site langmuir adsorption equilibrium models from a GCMC molecular simulation', *Applied Sciences (Switzerland)*, 10(4), pp. 1–15. doi:10.3390/app10041311.
- Wang, T.Q. and Yang, Z.G. (2004) 'Scattering of plane wave from moving body underwater with finite impedance surface', *Journal of Sound and Vibration*, 273(4–5), pp. 969–987. doi:10.1016/S0022-460X(03)00515-7.
- Wang, Y. and LeVan, M.D. (2010) 'Adsorption Equilibrium of Binary Mixtures of Carbon Dioxide and Water Vapor on Zeolites 5A and 13X', *Journal of Chemical & Engineering Data*, 55(9), pp. 3189–3195. doi:10.1021/jc100053g.

- Webb, P. a (2003) 'Introduction to Chemical Adsorption Analytical Techniques and their Applications to Catalysis', *MIC Technical Publications*, 13(January), pp. 1–4. doi:21572702.
- Weber, W.J. and Morris, J.C. (1963) 'Kinetics of Adsorption on Carbon from Solution', *Journal of the Sanitary Engineering Division*, 89(2), pp. 31–59. doi:10.1061/JSEDAI.0000430.
- Wick, C.D., Martin, M.G. and Siepmann, J.I. (2000) 'Transferable Potentials for Phase Equilibria. 4. United-Atom description of linear and branched alkenes and alkylbenzenes', *Journal of Physical Chemistry B*, 104(33), pp. 8008–8016. doi:10.1021/jp001044x.
- Worch, E. (2012) '2 Adsorbents and adsorbent characterization', *Adsorption Technology in Water Treatment* [Preprint]. doi:10.1515/9783110240238.11.
- Wu, F.C., Tseng, R.L. and Juang, R.S. (2009) 'Characteristics of Elovich equation used for the analysis of adsorption kinetics in dye-chitosan systems', *Chemical Engineering Journal*, 150(2–3), pp. 366–373. doi:10.1016/j.cej.2009.01.014.
- Xavier, M.G. and Banda, S.F. (2016) 'Specific surface area and porosity measurements of aluminosilicate adsorbents', *Oriental Journal of Chemistry*, 32(5), pp. 2401–2406. doi:10.13005/ojc/320511.
- Yamaguchi, T. *et al.* (2002) 'Pore Properties of Activated Alumina Prepared from Polyhydroxoaluminium - Tetraalkylammonium Ion Composite Gels', *Journal of the Ceramic Society of Japan*, 958, pp. 954–958. doi:110-10-954-958.
- Yi, H. *et al.* (2015) 'Effect of the adsorbent pore structure on the separation of carbon dioxide and methane gas mixtures', *Journal of Chemical and Engineering Data*, 60(5), pp. 1388–1395. doi:10.1021/je501109q.
- Zhou, K. *et al.* (2020) 'Applied Surface Science Effect of surface energy on protein adsorption behaviours of treated CoCrMo alloy surfaces', *Applied Surface Science*, 520(30), p. 146354. doi:10.1016/j.apsusc.2020.146354.
- Zotov, R. *et al.* (2018) 'Influence of the composition, structure, and physical and chemical properties of aluminium-oxide-based sorbents on water adsorption ability', *Materials*, 11(1). doi:10.3390/ma11010132.

Appendix A Methodology

A.1 Preliminary Experiments to determine equilibrium sorption time

Preliminary experiments were performed at 25 °C, and equilibrium was reached faster at higher temperatures, so that equilibrium sorption time was assumed to be shorter at higher temperatures. However, the same time duration was used at all temperatures.

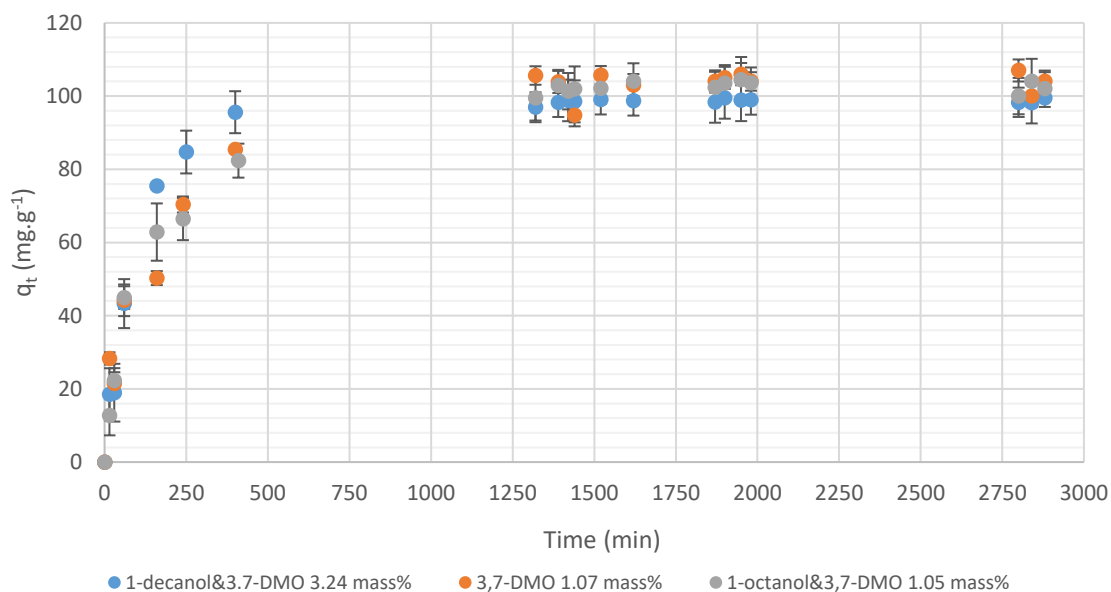


Figure 53 Determination of equilibrium time by using the single and binary component systems in the present study. At 25 °C, the equilibrium time was found to be approximately 24 h.

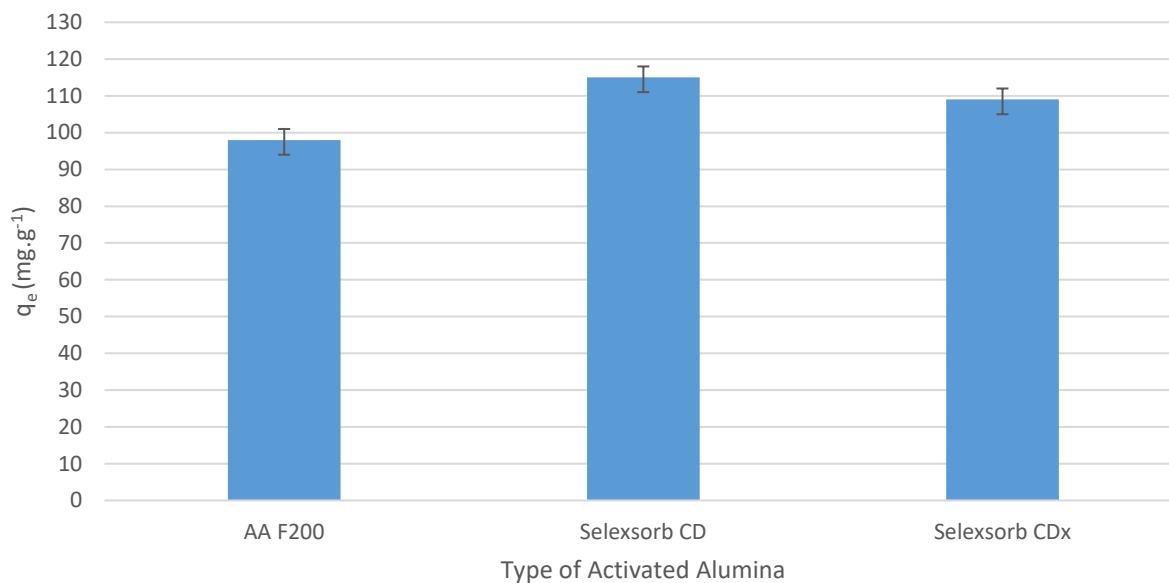


Figure 54 Plot showing the equilibrium 3,7-DMO loading achieved at approximately 24 h for three different types of AA. The initial concentration was 3.5 mass% 3,7-DMO and the solution temperature was set to 25 °C. The adsorbents compared well, but SCD marginally outperformed AA F200 and SCDx. Thus, SCD will be the adsorbent used in the study.

A.1.1 Sample preparation and start-up

- Wash all required glassware, pipette tips and measuring beakers with sunlight liquid and rinse with acetone.
- Wash GC vials with sunlight liquid and rinse with acetone.
- Label each GC vial according to experiment number and sample number and cross-check with Excel spreadsheet.
- Weigh the required amount of adsorbate and solvent and decant into water bath beakers.
- Place agitator in each beaker.
- Place beaker in water bath.
- Set water bath temperature.
- Switch on mixing plate.
- Weigh adsorbent required and place in mesh baskets.
- Allow water bath to reach required temperature.
- Lower mesh baskets into beakers.
- Check that stirrer bars are spinning without interference.
- Note the time. Take first sample by using a 200 μ l pipette and decant into correctly labelled GC vial. Seal tightly.

Sample calculation for solution make up:

Note:

- All solutions are prepared on mass basis.
- The method followed must be the same, regardless of whether a fresh solution is made or an old solution is used; it has to be topped up to the required new concentration.

Fresh solution:

In a binary system, 1-octanol&3,7-DMO with a 0.5:0.5 ratio and an initial concentration of approximately 3 mass%. The required mass percentage of 1-octanol and 3,7-DMO is 1.5 mass% for both.

Step 1: Determine average density.

$$\rho_{sol} = x_{octanol}(\rho_{octanol}) + x_{3,7DMO}(\rho_{3,7DMO}) + x_{decane}(\rho_{decane})$$

$$\rho_{sol} = 0.015(826.2) + 0.015(820) + (1 - 0.03)(726.53)$$

$$\rho_{sol} = 729 \text{ g} \cdot \text{L}^{-1}$$

Step 2: Determine the mass of solution required to achieve a volume of 200ml.

$$m_{sol} = \rho_{sol} \cdot V_{sol}$$

$$m_{sol} = 729 \cdot 0.2$$

$$m_{sol} = 145.88 \text{ g}$$

Step 3: Determine the required amount of each component.

$$m_{octanol} = m_{total} \cdot x_{octanol}$$

$$m_{octanol} = 145.9 \cdot 0.015$$

$$m_{octanol} = 2.19 \text{ g}$$

$$m_{3,7DMO} = m_{total} \cdot x_{3,7DMO}$$

$$m_{3,7DMO} = 145.9 \cdot 0.015$$

$$m_{3,7DMO} = 2.19 \text{ g}$$

$$m_{decane} = m_{sol} - m_{octanol} - m_{3,7DMO}$$

$$m_{decane} = 145.9 - 2.19 - 2.19$$

$$m_{decane} = 141.5 \text{ g}$$

In the event that a solution from a previous experiment is reused and topped up, steps 1-2 are to be repeated, while step 3 is adjusted:

Step 3 (adjusted): Determine the top-up amount of component to be added.

Use the GC results to determine the composition of the previously used solution:

$$m_{sol,old} = 130 \text{ g}$$

$$x_{octanol,GC} = 0.009$$

$$x_{3,7DMO,GC} = 0.012$$

$$x_{decane,GC} = 0.979$$

Now, determine the top-up amount required for each component.

$$m_{octanol,topup} = m_{sol} \cdot x_{octanol} - m_{sol,old} \cdot x_{octanol,GC}$$

$$m_{octanol,topup} = 145.9 \cdot 0.015 - 130 \cdot 0.009$$

$$m_{octanol,topup} = 1.02 \text{ g}$$

$$m_{37DMO,topup} = m_{sol} \cdot x_{37DMO} - m_{sol,old} \cdot x_{37DMO,GC}$$

$$m_{37DMO,topup} = 145.9 \cdot 0.015 - 130 \cdot 0.012$$

$$m_{37DMO,topup} = 0.63 \text{ g}$$

$$m_{decane,topup} = m_{sol} - m_{sol,old} - m_{octanol,topup} - m_{37DMO,topup}$$

$$m_{decane,topup} = 145.9 - 130 - 1.02 - 0.63$$

$$m_{decane,topup} = 14.2 \text{ g}$$

A.1.2 Sampling procedure

The experimental runs follow the same procedure in each setup, although shutdown procedures will be different. The procedure to be followed is itemised below.

- Label all GC vials to be used according to beaker number and water bath number.
- Place vial in front of the water baths and place each vial in line with the corresponding beaker.
- At the designated time of sampling, place pipette tip on pipette.
- Remove top plate cap above the beaker that is being sampled from.
- Withdraw sample.
- Decant sample into GC vial.
- Tightly seal cap of GC vial.
- Place top plate cap back to minimise evaporation.
- Place vial in the fridge for storage.
- Repeat steps 3-9 until all samples have been taken, as indicated in steps 11-12.
- In the case of kinetic studies, take samples at 0, 15, 30, 60, 160, 240, 400, 1390, 1420 and 1440 min. Withdraw a 400 μ L sample on each of these occasions.
- In the case of equilibrium studies, take samples at 0, 1390, 1420 and 1440 min. Again, withdraw a 400 μ L sample on each of these occasions.

A.1.3 Displacement experiments

The procedure for displacement experiments is set out below.

- Allow the single component system (2.5 mass% of adsorbate₁) to approach equilibrium. The total time expired will be approximately 24h.
- Take samples at 0, 1390, 1420 and 1440 min.
- Withdraw a 2ml sample from each beaker and decant into a prepared GC by means of (preparation explain in previous section).
- Inject 200 μ l sample of the second alcohol: that is, the required amount to achieve a predicted mass percentage of approximately 1-1.5 mass% for adsorbate₂.
- Allow system to approach equilibrium by running for a further 24h.
- Take samples as per kinetic studies (where t=0min is t=1441 min and so forth) at 0, 15, 30, 60, 160, 240, 400, 1390, 1420 and 1440 min.

Calculation is performed as follows:

Again, first determine the qt at t=1440 min.

Then assume qt(1440 min)= qt(0 min (second day))

From there onwards, work in a change in MASS and do not change concentration, so that the formula will be $q_t - (m_{i+1} - m_i) / m(\text{adsorbent})$.

A.1.4 Shutdown procedures

The shutdown procedure for the water bath setup is as follows.

- Prepare and label storage beakers according to the number of these that are to be used in the experiment.
- Take last sample at 1440 min.
- Switch off water bath.
- Switch off magnetic stirrer plate.
- Allow system to cool for 5-10 min.
- Lift top plate, allow solution to drip from mesh baskets into the beakers and hang it carefully on hooks.
- Open waste container for used adsorbent and decant the adsorbent from the mesh baskets into the container.
- Decant the solution used in the experiment from the beakers into the designated storage bottles.
- Ensure that bottles are tightly sealed and labelled.
- Prepare boiling water and soap and wash all beakers, pipette tips, vials and any other laboratory glassware.
- Place glassware on drying rack to dry.
- Rinse glassware with acetone and pack away the equipment.
- Check that the water bath is clean and shows no signs of deposits forming.
- Clean all used surfaces and pack away any equipment, tools or waste containers used.

A.1.5 GC sample preparation and operation

The GC sample preparation method is a crucial part of the project, as it determines the accuracy of sample composition measured. The project relies on analysis of the samples to determine the composition and ultimately adsorbent loading for the experiments performed.

Care must be taken to calibrate the GC in such a way as to ensure that all samples prepared fall within the calibrated range. This increases the likelihood of accurate results.

The sample preparation and GC operation methodology is as follows.

1. Take labelled GC vials out of the fridge and allow these to cool down to room temperature.
2. Clean and prepare scale.
3. Decant 1-pentanol and methanol into separate beakers.
4. Place all pipettes, pipette tips and required vials on the work bench.
5. Place an empty, clean and sealed intermediate 4ml vial on the scale.

6. Tare the scale.
7. Withdraw the required amount of sample according to the ratios required so as to fall within calibration range and decant into intermediate vial
8. Tare the scale.
9. Add $22\mu\text{L}$ of 1-pentanol to the intermediate vial.
10. Seal vial with cap and place on scale.
11. Allow scale to stabilise and record internal standard mass.
12. Remove intermediate vial cap.
13. Dilute the sample-internal standard mixture with 1.2ml of methanol.
14. Place intermediate vial cap on vial and seal tightly.
15. Shake intermediate vial for approximately 1 min.
16. Withdraw a $200\mu\text{L}$ sample from the intermediate vial.
17. Decant diluted sample into 2ml GC vial.
18. Dilute further by adding 1.2ml of methanol to the GC vial
19. Place cap on vial and seal tightly.
20. Repeat steps 5-19 until all samples have been prepared.
21. Take internal standard recordings and samples to the GC.
22. Start up GC.
23. Load GC method specific to this study and calibrated in the manner prescribed above.
24. Enter internal standard mass for each sample.
25. Click run.
26. Observe system for first sample analysis to ensure that no issues occur.
27. Collect results once the analysis is complete.

Sample calculations to determine adsorbent loading:

Step 1: Assume constant volume and mass of solution to determine the concentration of the bulk solution at every time interval.

$$C_{0,\text{octanol}} = x_{0,\text{octanol}} \cdot \frac{m_{\text{sol}}}{Vol_{\text{sol}}}$$

$$C_{0,\text{octanol}} = 0.01 \cdot \frac{145}{0.2}$$

$$C_{0,\text{octanol}} = 7250 \text{ mg} \cdot \text{L}^{-1}$$

$$C_{t,\text{octanol}} = x_{t,\text{octanol}} \cdot \frac{m_{\text{sol}}}{Vol_{\text{sol}}}$$

$$C_{t,\text{octanol}} = 0.006 \cdot \frac{145}{0.2}$$

$$C_{t,octanol} = 4350 \text{ mg} \cdot \text{L}^{-1}$$

Where $t=1440$ min and $x_{octanol}$ is the mass fraction of octanol in the bulk fluid at a specific time.

Step 2: Use calculated

$$q_t = \frac{C_o - C_t}{m_{ads}} \cdot V_{sol}$$

$$q_t = \frac{7250 - 4350}{10} \cdot 0.2$$

$$q_t = 58 \text{ mg} \cdot \text{g}^{-1}$$

Where q_t is the adsorbent loading achieved at a specific time.

A.1.6 Validation

The validation experiment is performed by comparing the method used by Bosman (Bosman, 2019) to that of the current study with the aim of reproducing the results.

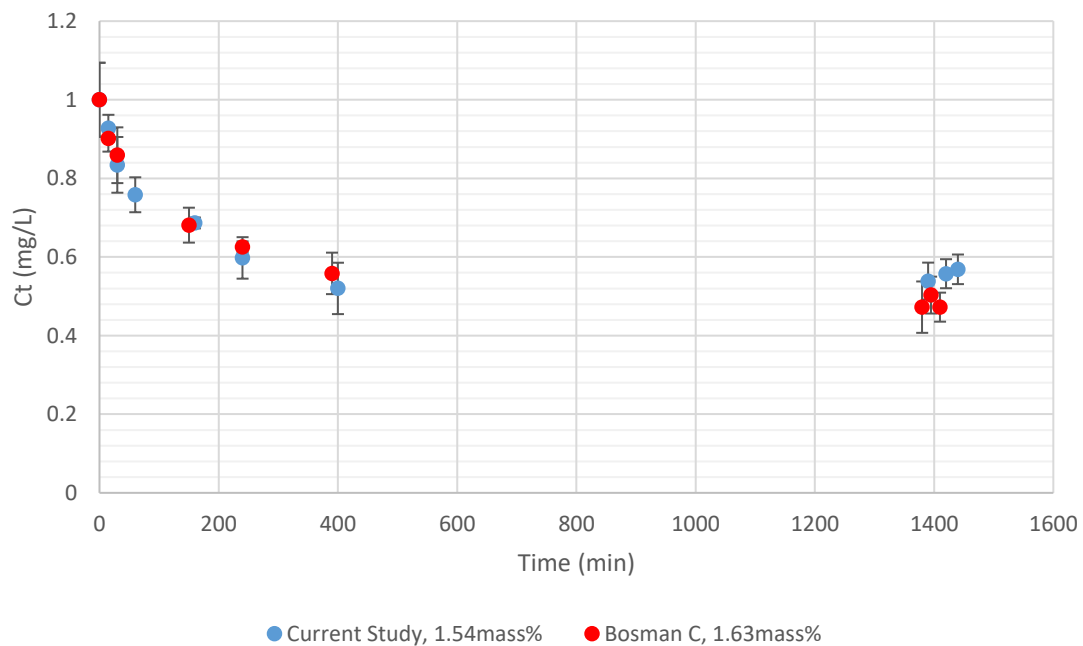


Figure 55 Validation experiment performed for the single component system of 1-octanol at 25 °C.

A.1.7 Solubility limit of water in n-decane

The calculations and thought process regarding the plausibility of water displacing one of the primary alcohols considered in this study is outlined below. Note that this is an approximation used to demonstrate that water can displace the primary 1-alcohols adsorbed.

Bolton *et al.* (2009) found that the solubility limit of water in n-decane is 0.5 g water/kg n-decane.

For illustrative purposes the worst case scenario is considered based on the following assumptions:

- The feed stock solution contains 96.7 mass% n-decane which for a total feedstock of 144 g equates to 139.2 g n-decane.
- Minimal adsorption of n-decane onto SCD has occurred.
- The feedstock only contains one adsorbate type: 3,7-DMO which is present at 3.3 mass%. As per Figure 27 the adsorption efficiency is 20% which means approximately 1 g of 3,7-DMO would be adsorbed onto SCD.

The maximum mass of water that is miscible in a 139 g n-decane solution is:

$$\frac{0.5 \text{ g water}}{\text{kg n-decane}} \cdot 139 \text{ g n-decane} = 0.0696 \text{ g water}$$

According to the analysis performed as outlined in Section 4.2.4 the mass% water present can vary but 0.05 mass% water content is assumed for this example.

$$\text{mass of water in solution} = 0.05\% \cdot 144 \text{ g}$$

$$\text{mass of water in solution} = 0.072 \text{ g water}$$

This means that approximately 97 mass% of the water in solution is miscible with n-decane. Considering the high affinity of SCD to highly polar molecules such as water, it is assumed that at least 80% of the miscible water is adsorbed by SCD.

This would mean that 0.056 g water is adsorbed onto SCD. If these water molecules displace the 3,7-DMO molecules adsorbed the following scenario is possible:

$$\text{moles water} = \frac{\text{mass water}}{M_{r_{\text{water}}}}$$

$$\text{moles water} = \frac{0.056}{18.015}$$

$$\text{moles water} = 0.0031 \text{ mol}$$

Then the number of molecules of water is:

$$\text{Number of molecules} = \text{moles water} \cdot \text{Avogadro's number}$$

$$\text{Number of molecules} = 0.0031 \cdot 6.02(10^{23})$$

$$\text{Number of molecules} = 1.86(10^{21})$$

Following the same principle for 1 g of 3,7-DMO adsorbed onto SCD:

$$\text{moles 3,7 - DMO} = 0.0063 \text{ mols}$$

$$\text{Number of molecules} = 3.8(10^{21})$$

This means that water is able to displace:

$$\% \text{molecules 3,7 - DMO that can be displaced by water} = \left(\frac{1.86}{3.8} \cdot (10^{21}) \right) \cdot 100$$

%molecules 3,7 – DMO that can be displaced by water = 48.9 %

The mass of 3,7-DMO (worst case scenario) displaced:

$$\text{mass 3,7 – DMO displaced} = \frac{\text{number of molecules}}{\text{Avogadro's number}} \cdot M_{r_{3,7-DMO}}$$

$$\text{mass 3,7 – DMO displaced} = \frac{1.94(10^{21})}{6.02(10^{23})} \cdot 158.28$$

$$\text{mass 3,7 – DMO displaced} = 0.5 \text{ g}$$

A.2 Secondary BAES Experimental Procedure

A.2.1 Solution & Adsorbent Preparation

Upon the first experiment performed for a specific solution composition, fresh solutions comprising unused n-decane, 1-decanol, 1-octanol or 3,7-DMO were prepared. Thereafter, due to cost of chemicals and in order to limit chemical waste, solutions used in preceding experiments were recycled and the necessary components were added in the correct dosages to achieve the required composition and volume. In the present section, the sample preparation will be discussed on the basis that the solutions used were recycled.

Adsorbent preparation procedure:

- 24h prior to the start-up of the secondary BAES, the required mass of adsorbent (+/- 10g per Schott bottle) must be weighed and placed in an oven tray.
- Multiple oven trays are to be used to ensure that an approximate height of 5 mm is reached. This ensures that most adsorbent beads receive equal heating.
- Place the oven trays on the top level of the oven.
- Seal the oven door tightly, close the vent fully and open the vacuum entirely.
- Once the vacuum gauge indicates that the oven is operating under vacuum conditions, switch the oven on and set the temperature to 120 °C.
- The adsorbent used in the experiment is required to be at room temperature before placing said adsorbent into the solutions and commencing the experiment.
- Therefore, switch off the oven prior to sample, release the vacuum and open the vent completely.
- The required number of mesh baskets (that is, one for each Schott bottle used) must be identified and placed near the mass balance.
- Remove the oven trays while hot by using the appropriate gloves.
- Place a weighing boat on the mass balance.
- Tare the mass balance.
- Decant the adsorbent onto the weighing boat until +/- 10g is noted.
- Decant the adsorbent from the weighing boat into the mesh baskets.

- Place the filled mesh baskets in a sealed desiccator with copper sulphate crystals. The adsorbent must be allowed to cool while contact with the air must be limited along with the water vapour captured by the adsorbent.

Solution preparation procedure:

- Wash all beakers and Schott bottles, rinse with acetone and dry properly.
- Ensure that the appropriate number of cleaned or unused pipette tips are available.
- Label all beakers and Schott bottles.
- Note the composition of solution present in each Schott bottle and the chemicals required for top-up.
- Decant the required volume of chemicals into individual beakers.
- Place each clean, dry Schott bottle on the mass balance with the appropriate stirrer bar.
- Tare the mass balance.
- Add the recycled solution to the Schott bottle and note the mass of solution.
- Use the mass noted and the appropriate methodology to determine the approximate volume of each chemical (n-decane, 1-decanol, 1-octanol, 3,7-DMO) required to top up the recycled solution.
- The method used for top-up in the case of larger mass required (> 2-3g) involves decanting the solution from the beaker into the Schott bottle by using a funnel. When smaller quantities are required (< 2-3 g), the appropriate pipette and pipette tips are to be used in order to enhance the accuracy of the procedure.
- Note the actual mass of each component and determine the approximate mass of solution. This must be compared to the results obtained when the HPLC was used in order to confirm the correct composition.
- Remove the Schott bottle from the mass balance and seal it with a cap until the experimental setup start-up is made.
- Repeat this procedure for the number of Schott bottles/ solutions required.

A.2.2 Secondary BAES start-up

Upon completion of the solution and adsorbent preparation procedure, the start-up procedure commences.

Start-up procedure:

- Place Schott bottles with the prepared solution in the placeholders of the water bath and loosely fit the caps that contain the hook to hang the mesh basket from and the appropriate sample port onto the bottle. Ensure that the top plate of the water bath is located between the Schott bottle and the loosely fitted cap.

- Place the sample port plugs in the sample port holes to minimise evaporation of Schott bottle contents.
- Top up the water in the bath to just below the maximum level allowed with respect to the number of Schott bottles in it.
- Switch on the heater and mixing plate.
- Set the mixing plate speed to 410 rpm.
- Perform checks to ensure that all stirrer bars are rotating as required, without any obstructions. At this stage, if any issues with mixing are noted, the necessary adjustments are to be made to ensure smooth mixing.
- Set the heater to the desired temperature.
- Allow the water bath to reach its temperature. After this, a 5-10 min period must be allowed to ensure that the temperature inside the Schott bottles reaches the desired temperature.
- Once this has been reached, take the first sample of 700 μ l from each Schott bottle. Set the pipette to 700 μ l, attach a new/ clean pipette tip and remove the sample port plug. Draw the sample and consider it to be the t=0 min sample. Place the adsorbent in the beaker. Decant the sample into a labelled GC vial and seal it with a cap. Place the plug in the sample port hole.
- Remove the mesh baskets from the desiccator, lift the caps from each Schott bottle, hang the mesh basket on the hook and attach the cap while slowly lowering the basket into the Schott bottle.
- Repeat this step for each Schott bottle present and make adjustments, where necessary, to ensure that the adsorbents are fully submerged in the solution.
- Start the timer.
- The experiments performed in this system are largely aimed at cross-referencing the kinetics and adsorbent loading achieved when the same initial concentration is used in a secondary versus primary BAES. Therefore, samples are to be taken for each component at 0, 15, 30, 60, 160, 240, 400, 1390, 1420 and 1440 min.

A.2.3 Sampling procedure

- Clean sample vials were labelled prior to sample taking.
- Remove the sample port plug.
- Attach a new/clean pipette tip to the pipette. Withdraw each 400 μ l sample from each Schott bottle at the designated time, that is, at 0, 15, 30, 60, 160, 240, 400, 1390, 1420 and 1440 min.
- Decant the sample from the pipette tip into the appropriate GC vial and seal the latter with a cap.
- Dispose of pipette or wash it.
- Return the sample port plug to the hole.
- Repeat this procedure until one sample has been withdrawn from each Schott bottle.

A.2.4 Sample preparation procedure

The sample preparation procedure is performed in the same way as described in Section and will not be repeated here.

A.3 Repeatability

The repeatability of the experiments is determined for the following, each in terms of triplicates or quadruplicates:

1. Single component system (3,7-DMO) at 25°C, 35°C and 45°C.
2. Binary component system (1-octanol&3,7-DMO and 1-decanol & 3,7-DMO) at 25°C and 45°C
3. Primary BAES:
 - a. Single component 3,7-DMO system at 25 °C and 45 °C
 - b. Binary component system 1-decanol, 3,7-DMO (0.5:0.5) at 25 °C and 45 °C
 - c. Binary component system 1-octanol/3,7-DMO (0.5:0.5) at 25 °C and 45 °C
4. Secondary BAES:
 - a. Single component 3,7-DMO system at 25 °C and 45 °C
 - b. Binary component system 1-decanol, 3,7-DMO (0.5:0.5) at 25 °C and 45 °C
 - c. Binary component system 1-octanol/3,7-DMO (0.5:0.5) at 25 °C and 45 °C

The sample calculations shown below are centred on the repeatability that has been determined in the manner indicated above. The standard error is calculated and used to provide error bars (margins of error). These are calculated by using Microsoft Excel®.

A.3.1 Error and uncertainty analysis

The following approach is used to determine the standard error associated with all data generated. Sample calculations will however only be shown for one instance. The demonstration will be based on the experimental kinetic data generated for the adsorption of 3,7-DMO onto SCD at 25°C and an initial adsorbate concentration of approximately 1.5 mass%.

The average 3,7-DMO alcohol concentration at t=60 min is determined by using the following equation.

$$C_{avg} = \frac{C_{run,1} + C_{run,2} + C_{run,3}}{n}$$

Which, when inputting the data specifically related to t=60 min leads to:

$$C_{avg} = \frac{1.00 + 1.33 + 1.15}{3}$$

$$C_{avg} = 1.15 \text{ mass\%}$$

The standard deviation is then calculated by using the following equation:

$$S = \sqrt{\frac{\sum(C_{run,i} - C_{avg})^2}{n - 1}}$$

Therefore, inputting the data related to t=60 min produces the following standard deviation:

$$S = \sqrt{\frac{(1 - 1.15)^2 + (1.33 - 1.15)^2 + (1.15 - 1.15)^2}{3 - 1}}$$

$$S = 0.18 \text{ mass\%}$$

Given the calculated standard deviation, it is possible to determine the standard error by using the following equation:

$$S_n = \frac{S}{\sqrt{n}}$$

Using the standard deviation calculated above, the standard error can be calculated:

$$S_n = \frac{0.18}{\sqrt{3}}$$

$$S_n = 0.1 \text{ mass\%}$$

A significance level of 0.05 is used and the students' t-statistic is considered to be appropriate to determine the uncertainty associated with the experimental measurements taken. The uncertainty is determined by using the statistic functions included in Microsoft Excel®.

$$\Delta_{C,measured} = \bar{t}(\alpha, n - 1)S_n = \bar{t}(0.05, (3 - 1))(0.1)$$

$$\Delta_{C,measured} = 0.05 \text{ mass\%}$$

A.3.2 3,7-DMO single component repeatability data**Table 21** Repeatability experiments performed for single component experiments at approximately 1.5 mass% and 25 °C.

Time (min)	Run 1		Run 2		Run 3		Run 4	
	3,7-DMO mass percentage (%)	Adsorbent loading (mg/g)	3,7-DMO mass percentage (%)	Adsorbent loading (mg/g)	3,7-DMO mass percentage (%)	Adsorbent loading (mg/g)	3,7-DMO mass percentage (%)	Adsorbent loading (mg/g)
0	1.63	0	1.36	0	1.57	0	1.47	0
15	1.49	20	1.08	41	1.45	16	1.26	28
30	1.45	26	1.01	50	1.40	23	1.21	36
60	1.36	36	0.97	56	1.33	33	1.15	44
160	1.22	59	0.90	66	1.11	64	1.00	65
240	1.13	71	0.73	90	1.07	70	0.90	80
400	1.14	70	0.64	103	0.97	83	0.80	93
1390	1.06	81	0.47	127	0.76	113	0.61	120
1420	1.07	80	0.46	129	0.74	115	0.60	122
1440	1.06	82	0.45	130	0.77	110	0.61	120

Table 22 Repeatability experiments performed for 3,7-DMO system at approximately 1.5 mass percentage and 35 °C.

Time (min)	Run 1		Run 2		Run 3	
	3,7-DMO mass percentage (%)	Adsorbent loading (mg/g)	3,7-DMO mass percentage (%)	Adsorbent loading (mg/g)	3,7-DMO mass percentage (%)	Adsorbent loading (mg/g)
0	1.54	0	1.45	0	1.51	0
15	1.38	24	1.31	20	1.40	17
30	1.31	34	1.24	31	1.36	23
60	1.21	45	1.19	36	1.22	46
160	1.07	68	1.02	62	1.14	58
240	0.94	86	0.91	77	1.08	68
400	0.89	94	0.85	86	0.88	100
1390	0.84	102	0.82	91	0.85	105
1420	0.83	102	0.84	89	0.83	108
1440	0.87	97	0.87	83	0.82	109

Table 23 Repeatability experiments performed for 3,7-DMO at an initial adsorbate concentration of approximately 1 mass percentage and 45 °C.

Time (min)	Run 1		Run 2		Run 3	
	3,7-DMO mass percentage (%)	Adsorbent loading (mg/g)	3,7-DMO mass percentage (%)	Adsorbent loading (mg/g)	3,7-DMO mass percentage (%)	Adsorbent loading (mg/g)
0	0.99	0	1.03	0	1.12	0
15	0.87	17	0.82	31	1.01	15
30	0.78	30	0.77	38	0.93	27
60	0.72	38	0.69	50	0.80	46
160	0.60	55	0.54	74	0.70	60
240	0.51	68	0.49	80	0.60	74
400	0.41	82	0.42	91	0.53	83
1390	0.46	75	0.42	92	0.50	88
1420	0.45	77	0.41	93	0.53	84
1440	0.44	77	0.41	93	0.52	85

A.3.3 Binary component repeatability data

Table 24 Repeatability data for the 0.5:0.5 binary component system of 1-decanol&3,7-DMO at 25 °C and an overall mass concentration of approximately two mass percentage.

Time (min)	Run 1		Run 2		Run 3		Run 4	
	1-decanol mass percentage (%)	3,7-DMO mass percentage (%)	1-decanol mass percentage (%)	3,7-DMO mass percentage (%)	1-decanol mass percentage (%)	3,7-DMO mass percentage (%)	1-decanol mass percentage (%)	3,7-DMO mass percentage (%)
0	1.04	1.03	1.04	1.06	1.05	1.04	0.99	1.04
15	0.97	0.99	0.96	0.98	0.99	0.94	0.90	0.99
30	0.92	0.92	0.93	0.96	0.89	0.91	0.90	0.94
60	0.90	0.90	0.87	0.93	0.83	0.85	0.82	0.86
160	0.78	0.80	0.75	0.81	0.74	0.78	0.74	0.80
240	0.72	0.76	0.72	0.78	0.70	0.75	0.65	0.73
400	0.66	0.70	0.65	0.72	0.66	0.72	0.63	0.70
1390	0.62	0.67	0.57	0.65	0.59	0.66	0.55	0.63
1420	0.62	0.68	0.57	0.66	0.58	0.64	0.54	0.63
1440	0.62	0.67	0.57	0.65	0.57	0.63	0.54	0.63

Table 25 Repeatability data for the 0.5:0.5 binary component system of 1-decanol&3,7-DMO at 45 °C and an overall mass concentration of approximately two mass percentage.

Time (min)	Run 1		Run 2		Run 3		Run 4	
	1-decanol mass percentage (%)	3,7-DMO mass percentage (%)	1-decanol mass percentage (%)	3,7-DMO mass percentage (%)	1-decanol mass percentage (%)	3,7-DMO mass percentage (%)	1-decanol mass percentage (%)	3,7-DMO mass percentage (%)
0	1.07	1.15	0.95	0.95	1.01	0.98	1.01	1.01
15	0.94	1.04	0.89	0.89	0.89	0.96	0.98	0.98
30	0.91	1.03	0.83	0.85	0.85	0.88	0.88	0.94
60	0.87	1.01	0.78	0.81	0.81	0.86	0.83	0.91
160	0.70	0.85	0.66	0.72	0.74	0.82	0.75	0.84
240	0.71	0.87	0.66	0.73	0.69	0.76	0.64	0.75
400	0.63	0.83	0.58	0.67	0.66	0.74	0.57	0.69
1390	0.53	0.72	0.48	0.58	0.70	0.77	0.53	0.68
1420	0.57	0.77	0.50	0.61	0.72	0.79	0.52	0.65
1440	0.51	0.77	0.48	0.58	0.71	0.78	0.48	0.59

Table 26 Repeatability data for the 0.5:0.5 binary component system of 1-octanol&3,7-DMO at 25 °C and an overall mass concentration of approximately two mass percentage.

Time (min)	Run 1		Run 2		Run 3		Run 4	
	1-octanol mass percentage (%)	3,7-DMO mass percentage (%)	1-octanol mass percentage (%)	3,7-DMO mass percentage (%)	1-octanol mass percentage (%)	3,7-DMO mass percentage (%)	1-octanol mass percentage (%)	3,7-DMO mass percentage (%)
0	1.08	1.09	0.96	0.96	1.04	1.02	1.07	1.05
15	0.90	0.90	0.89	0.88	0.94	0.92	0.95	0.96
30	0.84	0.84	0.86	0.86	0.88	0.88	0.89	0.91
60	0.80	0.82	0.81	0.85	0.77	0.79	0.86	0.86
160	0.72	0.75	0.66	0.75	0.71	0.74	0.75	0.79
240	0.65	0.67	0.64	0.68	0.63	0.66	0.67	0.72
400	0.60	0.64	0.58	0.60	0.61	0.64	0.61	0.66
1390	0.67	0.69	0.68	0.70	0.67	0.68	0.71	0.75
1420	0.66	0.69	0.69	0.69	0.66	0.70	0.69	0.73
1440	0.70	0.72	0.71	0.72	0.63	0.66	0.68	0.72

Table 27 Repeatability data for the 0.5:0.5 binary component system of 1-octanol&3,7-DMO at 45 °C and an overall mass concentration of approximately two mass percentage.

Time (min)	Run 1		Run 2		Run 3	
	1-octanol mass percentage (%)	3,7-DMO mass percentage (%)	1-octanol mass percentage (%)	3,7-DMO mass percentage (%)	1-octanol mass percentage (%)	3,7-DMO mass percentage (%)
0	1.01	1.03	1.00	0.99	1.00	1.00
15	0.85	0.94	0.88	0.92	0.86	0.92
30	0.79	0.87	0.89	0.97	0.84	0.92
60	0.73	0.81	0.76	0.83	0.75	0.83
160	0.61	0.71	0.65	0.85	0.65	0.78
240	0.61	0.72	0.63	0.74	0.60	0.71
400	0.60	0.70	0.59	0.71	0.60	0.71
1390	0.63	0.73	0.67	0.76	0.71	0.82
1420	0.66	0.75	0.70	0.81	0.69	0.79
1440	0.66	0.78	0.66	0.76	0.69	0.80

A.3.4 Secondary BAES repeatability data**Table 28** Repeatability data using secondary BAES for 3,7-DMO system at an overall concentration of approximately three mass percentage and 45 °C.

Time (min)	Run 1		Run 2		Run 3	
	3,7-DMO mass percentage (%)	Adsorbent loading (mg/g)	3,7-DMO mass percentage (%)	Adsorbent loading (mg/g)	3,7-DMO mass percentage (%)	Adsorbent loading (mg/g)
0	3.12	0	3.00	0	3.06	0
15	3.20	11	2.85	21	3.02	5
30	3.04	11	3.02	3	3.03	4
60	2.98	19	2.65	49	2.82	34
160	2.73	54	2.45	78	2.59	66
240	2.65	66	2.39	85	2.52	76
410	2.48	90	2.33	94	2.40	92
1390	2.34	110	2.08	129	2.21	119
1420	2.30	114	2.36	90	2.33	102
1440	2.44	94	2.07	131	2.26	112

Table 29 Repeatability data using secondary BAES for 3,7-DMO system at an overall concentration of approximately one mass percentage and 45 °C.

Time (min)	Run 1		Run 2		Run 3	
	3,7-DMO mass percentage (%)	Adsorbent loading (mg/g)	3,7-DMO mass percentage (%)	Adsorbent loading (mg/g)	3,7-DMO mass percentage (%)	Adsorbent loading (mg/g)
0	0.94	0	0.98	0	0.96	0
15	0.89	7	0.86	16	0.87	12
30	0.79	21	0.77	30	0.78	25
60	0.65	42	0.67	43	0.66	42
160	0.51	61	0.52	64	0.52	62
240	0.48	66	0.46	72	0.47	69
410	0.37	82	0.38	83	0.38	83
1390	0.34	86	0.25	102	0.29	94
1420	0.32	88	0.25	101	0.29	95
1440	0.33	87	0.25	102	0.29	95

Table 23 Repeatability data using secondary BAES for 0.25:0.75 1-decanol&3,7-DMO system at an overall concentration of approximately 3.3 mass percentage and 25 °C.

Time	Run 1		Run 2		Run 3	
	1-decanol mass percentage (%)	3,7-DMO mass percentage (%)	1-decanol mass percentage (%)	3,7-DMO mass percentage (%)	1-decanol mass percentage (%)	3,7-DMO mass percentage (%)
0	1.12	2.15	1.11	2.16	1.11	2.16
15	1.04	2.03	1.06	2.09	1.05	2.06
30	1.00	1.96	1.04	2.03	1.02	2.00
60	1.06	2.09	1.02	2.00	1.04	2.05
160	0.98	1.78	0.93	1.90	0.96	1.84
240	0.87	1.76	0.89	1.77	0.88	1.77
400	0.86	1.72	0.84	1.70	0.85	1.71
1390	0.77	1.61	0.73	1.53	0.75	1.57
1420	0.78	1.63	0.74	1.54	0.76	1.59
1440	0.78	1.62	0.74	1.55	0.76	1.58

Table 31 Repeatability data using secondary BAES for 0.25:0.75 1-octanol&3,7-DMO system at an overall concentration of approximately 3.3 mass percentage and 25 °C.

Time	Run 1		Run 2		Run 3	
	1-octanol mass percentage (%)	3,7-DMO mass percentage (%)	1-octanol mass percentage (%)	3,7-DMO mass percentage (%)	1-octanol mass percentage (%)	3,7-DMO mass percentage (%)
0	1.16	2.22	1.21	2.29	1.19	2.26
15	1.13	2.23	1.10	2.23	1.11	2.23
30	1.06	2.11	1.08	2.11	1.07	2.11
60	0.99	2.01	1.06	2.09	1.02	2.05
160	0.88	1.83	0.98	2.01	0.93	1.92
240	0.87	1.85	0.94	1.97	0.90	1.91
400	0.81	1.80	0.85	1.81	0.83	1.81
1390	0.75	1.69	0.75	1.72	0.75	1.71
1420	0.77	1.65	0.75	1.75	0.76	1.70
1440	0.82	1.67	0.75	1.75	0.78	1.71

Table 32 Repeatability data using secondary BAES for 0.5:0.5 1-decanol&3,7-DMO system at an overall concentration of approximately two mass percentage and 45 °C.

Time (min)	Run 1		Run 2		Run 3	
	1-decanol mass percentage (%)	3,7-DMO mass percentage (%)	1-decanol mass percentage (%)	3,7-DMO mass percentage (%)	1-decanol mass percentage (%)	3,7-DMO mass percentage (%)
0	1.05	1.03	1.00	0.94	0.96	0.99
15	0.96	0.98	0.88	0.83	0.90	0.94
30	0.85	0.89	0.82	0.78	0.85	0.89
60	0.80	0.83	0.81	0.87	0.74	0.79
160	0.67	0.71	0.66	0.67	0.66	0.73
240	0.65	0.70	0.59	0.60	0.59	0.65
410	0.60	0.64	0.55	0.58	0.56	0.61
1390	0.50	0.54	0.50	0.52	0.54	0.80
1420	0.51	0.55	0.49	0.51	0.46	0.52
1440	0.48	0.54	0.53	0.54	0.47	0.52

Table 33 Repeatability data using secondary BAES for 0.5:0.5 1-octanol&3,7-DMO system at an overall concentration of approximately two mass percentage and 45 °C.

Time (min)	Run 1		Run 2		Run 3	
	1-octanol mass percentage (%)	3,7-DMO mass percentage (%)	1-octanol mass percentage (%)	3,7-DMO mass percentage (%)	1-octanol mass percentage (%)	3,7-DMO mass percentage (%)
0	1.03	1.04	0.97	0.99	1.01	1.02
15	0.84	0.89	0.86	0.94	0.90	0.95
30	0.83	0.91	0.78	0.86	0.86	0.93
60	0.73	0.82	0.76	0.85	0.79	0.89
160	0.61	0.72	0.61	0.75	0.67	0.79
240	0.58	0.70	0.58	0.75	0.62	0.75
410	0.54	0.67	0.53	0.66	0.62	0.77
1390	0.58	0.71	0.48	0.71	0.59	0.73
1420	0.56	0.71	0.48	0.68	0.58	0.71
1440	0.57	0.70	0.52	0.67	0.59	0.74

Appendix B Processed and Raw data

B.1 Single component system

Table 34 Evaluation of kinetic data at three different temperatures for the same initial mass concentration of approximately 3 mass percentage.

Time (min)	Temperature 25 °C		Temperature 35 °C		Temperature 45 °C	
	Mass concentration (mass percentage)	Adsorbent Loading (mg/g)	Mass concentration (mass percentage)	Adsorbent Loading (mg/g)	Mass concentration (mass percentage)	Adsorbent Loading (mg/g)
0	3.12	0	2.92	0	2.98	0
15	3.20	5	2.76	23	2.76	30
30	3.04	11	2.69	33	2.64	47
60	2.98	19	-	-	2.51	64
160	2.73	54	2.39	76	2.36	86
240	2.65	66	2.27	94	2.24	102
400	2.48	90	2.22	101	2.13	117
1390	2.34	110	2.19	105	2.29	95
1420	2.30	114	2.22	101	2.29	95
1440	2.32	112	2.19	105	2.32	91

Table 35 Evaluation of kinetic data at three different temperatures for the same initial mass concentration of approximately 2.5 mass percentage.

Time (min)	Temperature 25 °C		Temperature 35 °C		Temperature 45 °C	
	Mass concentration (mass percentage)	Adsorbent Loading (mg/g)	Mass concentration (mass percentage)	Adsorbent Loading (mg/g)	Mass concentration (mass percentage)	Adsorbent Loading (mg/g)
0	2.54	0	2.59	0	2.52	0
15	2.50	6	2.41	26	2.36	23
30	2.49	8	2.43	23	2.25	38
60	2.26	40	2.46	19	2.14	55
160	2.37	25	2.17	61	1.97	79
240	2.03	72	1.97	89	1.87	93
400	1.84	99	1.88	101	1.80	103
1390	1.76	109	1.84	107	1.92	86
1420	1.74	113	1.72	125	1.92	86
1440	1.78	107	1.82	110	1.92	86

Table 36 Evaluation of kinetic data at three different temperatures for the same initial mass concentration of approximately 2 mass percentage.

Time (min)	Temperature 25 °C		Temperature 35 °C		Temperature 45 °C	
	Mass concentration (mass percentage)	Adsorbent Loading (mg/g)	Mass concentration (mass percentage)	Adsorbent Loading (mg/g)	Mass concentration (mass percentage)	Adsorbent Loading (mg/g)
0	1.93	0	2.00	0	2.00	0
15	1.91	3	1.91	12	1.88	16
30	1.67	37	1.86	20	1.85	20
60	1.66	38	1.74	37	1.58	58
160	1.41	73	1.62	54	1.48	72
240	1.32	84	1.51	70	1.32	95
400	1.18	104	1.42	81	1.23	106
1390	1.03	124	1.31	98	1.19	113
1420	1.05	122	1.25	105	1.21	110
1440	1.05	122	1.33	94	1.22	108

Table 37 Evaluation of kinetic data at three different temperatures for the same initial mass concentration of approximately 1.5 mass percentage.

Time (min)	Temperature 25 °C		Temperature 35 °C		Temperature 45 °C	
	Mass concentration (mass percentage)	Adsorbent Loading (mg/g)	Mass concentration (mass percentage)	Adsorbent Loading (mg/g)	Mass concentration (mass percentage)	Adsorbent Loading (mg/g)
0	1.47	0	1.51	0	1.53	0
15	1.26	28	1.43	13	1.32	29
30	1.21	36	1.40	17	1.30	32
60	1.15	44	1.36	23	1.15	53
160	1.00	65	1.22	46	0.95	82
240	0.90	80	1.14	58	0.85	96
400	0.80	93	1.08	68	0.78	105
1390	0.61	120	0.88	100	0.90	89
1420	0.60	122	0.85	105	0.90	88
1440	0.61	120	0.83	108	0.91	87

Table 38 Evaluation of kinetic data at three different temperatures for the same initial mass concentration of approximately 1 mass percentage.

Time (min)	Temperature 25 °C		Temperature 35 °C		Temperature 45 °C	
	Mass concentration (mass percentage)	Adsorbent Loading (mg/g)	Mass concentration (mass percentage)	Adsorbent Loading (mg/g)	Mass concentration (mass percentage)	Adsorbent Loading (mg/g)
0	0.98	0	1.00	0	1.01	0
15	0.87	16	0.86	20	0.85	24
30	0.83	20	0.79	30	0.77	34
60	0.75	32	0.76	34	0.70	44
160	0.68	42	0.61	55	0.57	64
240	0.57	57	0.55	63	0.50	74
400	0.46	72	0.46	76	0.41	87
1390	0.32	92	0.51	69	0.44	83
1420	0.31	94	0.52	68	0.43	85
1440	0.31	94	0.52	68	0.42	85

Table 39 Evaluation of kinetic data at three different temperatures for the same initial mass concentration of approximately 0.5 mass percentage.

Time (min)	Temperature 25 °C		Temperature 35 °C		Temperature 45 °C	
	Mass concentration (mass percentage)	Adsorbent Loading (mg/g)	Mass concentration (mass percentage)	Adsorbent Loading (mg/g)	Mass concentration (mass percentage)	Adsorbent Loading (mg/g)
0	0.47	0	0.47	0	0.50	0
15	0.38	13	0.35	17	0.36	20
30	0.35	18	0.31	23	0.33	25
60	0.29	26	0.27	29	0.30	29
160	0.20	40	0.25	32	0.15	49
240	0.16	46	0.13	49	0.11	56
400	0.11	52	0.10	53	0.09	59
1390	0.04	62	0.05	59	0.11	56
1420	0.04	63	0.05	60	0.11	55
1440	0.03	63	0.05	59	0.12	54

B.2 1-decanol&3,7-DMO system

B.2.1 0.5:0.5 ratio

Table 40 Kinetic data for the adsorption of a 0.5:0.5 1-decanol&3,7-DMO binary system at 25 °C for an overall initial concentration of 3.24 mass percentage.

Time (min)	1-decanol mass percentage (%)	1-decanol adsorbent loading (mg/g)	3,7-DMO mass percentage (%)	3,7-DMO adsorbent loading (mg/g)	Overall mass percentage (%)	Overall adsorbent loading (mg/g)
0	1.62	0	1.62	0	3.24	0
15	1.55	10	1.56	9	3.11	19
30	1.52	15	1.59	4	3.11	19
60	1.46	24	1.49	19	2.95	43
160	1.34	41	1.39	34	2.73	75
250	1.31	47	1.37	38	2.67	85
400	1.27	52	1.33	43	2.60	96
1390	1.25	55	1.33	44	2.58	98
1420	1.25	55	1.33	44	2.58	99
1440	1.25	55	1.33	44	2.58	99

Table 41 Kinetic data for the adsorption of a 0.5:0.5 1-decanol&3,7-DMO binary system at 25 °C for an overall initial concentration of 3.24 mass percentage.

Time (min)	1-decanol mass percentage (%)	1-decanol adsorbent loading (mg/g)	3,7-DMO mass percentage (%)	3,7-DMO adsorbent loading (mg/g)	Overall mass percentage (%)	Overall adsorbent loading (mg/g)
0	1.04	0	1.03	0	2.08	0
15	0.97	10	0.99	5	1.97	16
30	0.92	18	0.92	16	1.84	34
60	0.90	21	0.90	18	1.80	39
160	0.78	38	0.80	32	1.58	70
250	0.72	46	0.76	38	1.48	84
400	0.66	55	0.00	47	0.66	101
1390	0.62	60	0.00	50	0.62	110
1420	0.62	60	0.68	49	1.30	109
1440	0.62	60	0.67	50	1.29	110

Table 42 Kinetic data for the adsorption of a 0.5:0.5 1-decanol&3,7-DMO binary system at 25 °C for an overall initial concentration of 2.09 mass percentage.

Time (min)	1-decanol mass percentage (%)	1-decanol adsorbent loading (mg/g)	3,7-DMO mass percentage (%)	3,7-DMO adsorbent loading (mg/g)	Overall mass percentage (%)	Overall adsorbent loading (mg/g)
0	1.04	0	1.06	0	2.09	0
15	0.96	12	0.98	11	1.93	22
30	0.93	15	0.96	13	1.89	29
60	0.87	24	0.93	17	1.80	41
160	0.75	40	0.81	34	1.57	74
250	0.72	44	0.78	38	1.50	82
400	0.65	54	0.72	47	1.37	101
1390	0.57	65	0.65	56	1.22	121
1420	0.57	65	0.66	55	1.23	121
1440	0.57	65	0.65	56	1.22	122

Table 43 Kinetic data for the adsorption of a 0.5:0.5 1-decanol&3,7-DMO binary system at 25 °C for an overall initial concentration of 3.24 mass percentage.

Time (min)	1-decanol mass percentage (%)	1-decanol adsorbent loading (mg/g)	3,7-DMO mass percentage (%)	3,7-DMO adsorbent loading (mg/g)	Overall mass percentage (%)	Overall adsorbent loading (mg/g)
0	0.50	0	0.52	0	1.02	0
15	0.42	12	0.47	8	0.88	20
30	0.41	13	0.46	9	0.87	22
60	0.34	23	0.39	18	0.73	41
160	0.30	28	0.35	24	0.65	52
250	0.26	34	0.31	30	0.57	65
400	0.21	41	0.26	38	0.47	79
1390	0.14	51	0.21	44	0.35	95
1420	0.13	53	0.17	50	0.30	103
1440	0.12	54	0.17	50	0.29	104

Table 44 Kinetic data for the adsorption of a 0.5:0.5 1-decanol&3,7-DMO binary system at 45 °C for an overall initial concentration of 3.35 mass percentage.

Time (min)	1-decanol mass percentage (%)	1-decanol adsorbent loading (mg/g)	3,7-DMO mass percentage (%)	3,7-DMO adsorbent loading (mg/g)	Overall mass percentage (%)	Overall adsorbent loading (mg/g)
0	1.66	0	1.69	0	3.35	0
15	1.54	17	1.58	14	3.13	31
30	1.47	26	1.52	23	3.00	48
60	1.42	33	1.48	29	2.90	62
160	1.32	47	1.40	39	2.72	87
240	1.28	53	1.36	45	2.64	98
400	1.25	57	1.34	47	2.59	105
1390	1.31	49	1.41	39	2.71	87
1420	1.29	52	1.40	40	2.69	92
1440	1.29	53	1.39	41	2.68	94

Table 45 Kinetic data for the adsorption of a 0.5:0.5 1-decanol&3,7-DMO binary system at 45 °C for an overall initial concentration of 2.06 mass percentage.

Time (min)	1-decanol mass percentage (%)	1-decanol adsorbent loading (mg/g)	3,7-DMO mass percentage (%)	3,7-DMO adsorbent loading (mg/g)	Overall mass percentage (%)	Overall adsorbent loading (mg/g)
0	0.99	0	1.07	0	2.06	0
15	0.90	13	0.99	12	1.89	25
30	0.81	25	0.90	24	1.72	49
60	0.79	29	0.88	27	1.66	57
160	0.80	27	0.87	29	1.67	75
240	0.61	54	0.71	51	1.32	105
400	0.58	58	0.68	55	1.26	113
1390	0.66	47	0.76	44	1.42	91
1420	0.68	45	0.78	41	1.46	86
1440	0.68	44	0.78	41	1.47	85

Table 46 Kinetic data for the adsorption of a 0.5:0.5 1-decanol&3,7-DMO binary system at 45 °C for an overall initial concentration of 1.19 mass percentage.

Time (min)	1-decanol mass percentage (%)	1-decanol adsorbent loading (mg/g)	3,7-DMO mass percentage (%)	3,7-DMO adsorbent loading (mg/g)	Overall mass percentage (%)	Overall adsorbent loading (mg/g)
0	0.56	0	0.63	0	1.19	0
15	0.47	13	0.46	24	0.93	37
30	0.38	25	0.40	32	0.79	57
60	0.32	34	0.33	42	0.65	75
160	0.26	42	0.26	51	0.52	94
240	0.21	49	0.23	56	0.44	106
400	0.19	52	0.20	60	0.40	111
1390	0.34	31	0.34	41	0.68	71
1420	0.34	31	0.34	41	0.68	71
1440	0.34	32	0.33	41	0.67	73

B.2.2 0.25:0.75 ratio**Table 47** Kinetic data for the adsorption of a 0.25:0.75 1-decanol&3,7-DMO binary system at 25 °C for an overall initial concentration of 3.27 mass percentage.

Time (min)	1-decanol mass percentage (%)	1-decanol adsorbent loading (mg/g)	3,7-DMO mass percentage (%)	3,7-DMO adsorbent loading (mg/g)	Overall mass percentage (%)	Overall adsorbent loading (mg/g)
0	1.12	0	2.15	0	3.27	0
15	1.04	10	2.03	16	3.08	26
30	1.00	16	1.96	26	2.96	42
60	1.06	7	2.09	8	3.15	16
160	0.98	18	1.78	50	2.77	68
240	0.87	34	1.76	53	2.63	86
410	0.86	35	1.72	59	2.58	94
1390	0.77	47	1.61	73	2.38	120
1420	0.78	46	1.63	71	2.41	117
1440	0.78	46	1.62	72	2.40	118

Table 48 Kinetic data for the adsorption of a 0.25:0.75 1-decanol&3,7-DMO binary system at 25 °C for an overall initial concentration of 2.08 mass percentage.

Time (min)	1-decanol mass percentage (%)	1-decanol adsorbent loading (mg/g)	3,7-DMO mass percentage (%)	3,7-DMO adsorbent loading (mg/g)	Overall mass percentage (%)	Overall adsorbent loading (mg/g)
0	0.75	0	1.32	0	2.08	0
15	0.65	15	1.27	7	1.92	22
30	0.73	3	1.22	14	1.95	17
60	0.55	28	1.11	30	1.66	58
160	0.50	35	1.02	43	1.52	77
240	0.48	38	0.99	46	1.47	84
410	0.43	45	0.90	59	1.33	104
1390	0.41	48	0.86	64	1.27	112
1420	0.40	49	0.86	65	1.26	114
1440	0.40	49	0.85	66	1.25	116

Table 49 Kinetic data for the adsorption of a 0.25:0.75 1-decanol&3,7-DMO binary system at 25 °C for an overall initial concentration of 1.06 mass percentage.

Time (min)	1-decanol mass percentage (%)	1-decanol adsorbent loading (mg/g)	3,7-DMO mass percentage (%)	3,7-DMO adsorbent loading (mg/g)	Overall mass percentage (%)	Overall adsorbent loading (mg/g)
0	0.37	0	0.69	0	1.06	0
15	0.31	9	0.59	14	0.90	22
30	0.29	12	0.55	19	0.84	31
60	0.31	8	0.54	21	0.85	29
160	0.20	24	0.40	40	0.59	64
240	0.20	24	0.38	42	0.58	66
410	0.15	31	0.31	51	0.46	82
1390	0.15	30	0.25	60	0.40	91
1420	0.11	36	0.24	61	0.35	97
1440	0.11	36	0.23	62	0.34	99

Table 50 Kinetic data for the adsorption of a 0.25:0.75 1-decanol&3,7-DMO binary system at 45 °C for an overall initial concentration of 3.26 mass percentage.

Time (min)	1-decanol mass percentage (%)	1-decanol adsorbent loading (mg/g)	3,7-DMO mass percentage (%)	3,7-DMO adsorbent loading (mg/g)	Overall mass percentage (%)	Overall adsorbent loading (mg/g)
0	1.15	0	2.11	0	3.26	0
15	1.02	19	1.99	16	3.01	36
30	1.01	20	1.99	18	3.00	37
60	0.95	28	1.88	32	2.83	61
160	0.98	25	1.77	49	2.74	73
240	0.88	39	1.76	49	2.64	88
400	0.82	47	1.68	61	2.50	107
1390	0.92	32	1.84	38	2.77	70
1420	0.91	35	1.82	41	2.73	75
1440	0.93	31	1.85	37	2.78	68

Table 51 Kinetic data for the adsorption of a 0.25:0.75 1-decanol&3,7-DMO binary system at 45 °C for an overall initial concentration of 2.37 mass percentage.

Time (min)	1-decanol mass percentage (%)	1-decanol adsorbent loading (mg/g)	3,7-DMO mass percentage (%)	3,7-DMO adsorbent loading (mg/g)	Overall mass percentage (%)	Overall adsorbent loading (mg/g)
0	0.77	0	1.61	0	2.37	0
15	0.68	12	1.43	24	2.12	36
30	0.62	21	1.27	47	1.90	67
60	0.62	21	1.58	4	2.20	25
160	0.52	35	1.11	70	1.63	105
240	0.48	40	1.03	80	1.52	120
400	0.45	45	0.98	89	1.42	133
1390	0.56	29	1.17	62	1.72	91
1420	0.55	30	1.15	64	1.70	94
1440	0.58	27	1.20	57	1.78	84

Table 52 Kinetic data for the adsorption of a 0.25:0.75 1-decanol&3,7-DMO binary system at 45 °C for an overall initial concentration of 0.89 mass percentage.

Time (min)	1-decanol mass percentage (%)	1-decanol adsorbent loading (mg/g)	3,7-DMO mass percentage (%)	3,7-DMO adsorbent loading (mg/g)	Overall mass percentage (%)	Overall adsorbent loading (mg/g)
0	0.27	0	0.62	0	0.89	0
15	0.21	9	0.49	18	0.70	28
30	0.19	11	0.46	23	0.66	34
60	0.17	14	0.41	30	0.58	44
160	0.12	21	0.32	44	0.44	64
240	0.11	23	0.28	49	0.39	72
400	0.10	24	0.27	50	0.37	74
1390	0.20	10	0.48	20	0.69	30
1420	0.20	10	0.48	20	0.68	30
1440	0.21	9	0.49	19	0.70	27

B.2.3 0.75:0.25 ratio**Table 53** Kinetic data for the adsorption of a 0.75:0.25 1-decanol&3,7-DMO binary system at 25 °C for an overall initial concentration of 2.01 mass percentage.

Time (min)	1-decanol mass percentage (%)	1-decanol adsorbent loading (mg/g)	3,7-DMO mass percentage (%)	3,7-DMO adsorbent loading (mg/g)	Overall mass percentage (%)	Overall adsorbent loading (mg/g)
0	1.31	0	0.70	0	2.01	0
15	1.22	13	0.65	6	1.88	19
30	1.16	22	0.62	11	1.78	33
60	1.06	37	0.58	17	1.63	54
160	1.22	45	0.72	20	1.94	65
240	0.90	60	0.51	27	1.41	87
400	0.81	73	0.46	34	1.27	107
1390	0.76	80	0.42	41	1.17	121
1420	0.67	92	0.40	43	1.07	135
1440	0.72	86	0.43	39	1.14	126

Table 54 Kinetic data for the adsorption of a 0.75:0.25 1-decanol&3,7-DMO binary system at 25 °C for an overall initial concentration of 3.29 mass percentage.

Time (min)	1-decanol mass percentage (%)	1-decanol adsorbent loading (mg/g)	3,7-DMO mass percentage (%)	3,7-DMO adsorbent loading (mg/g)	Overall mass percentage (%)	Overall adsorbent loading (mg/g)
0	2.14	0	1.15	0	3.29	0
15	2.15	3	1.14	1	3.29	12
30	1.98	22	1.04	16	3.02	38
60	1.92	32	1.01	21	2.92	53
160	1.83	44	0.99	23	2.82	67
240	1.75	56	0.94	30	2.70	86
400	1.63	74	0.88	38	2.51	112
1390	1.53	89	0.85	43	2.38	132
1420	1.54	87	0.85	43	2.39	130
1440	1.55	85	0.86	42	2.41	127

Table 55 Kinetic data for the adsorption of a 0.75:0.25 1-decanol&3,7-DMO binary system at 25 °C for an overall initial concentration of 1.21 mass percentage.

Time (min)	1-decanol mass percentage (%)	1-decanol adsorbent loading (mg/g)	3,7-DMO mass percentage (%)	3,7-DMO adsorbent loading (mg/g)	Overall mass percentage (%)	Overall adsorbent loading (mg/g)
0	0.88	0	0.34	0	1.21	0
15	0.64	34	0.29	7	0.92	41
30	0.50	53	0.26	11	0.77	64
60	0.47	58	0.25	13	0.72	71
160	0.37	72	0.20	19	0.57	91
250	0.33	78	0.18	22	0.51	100
400	0.30	83	0.16	25	0.46	108
1390	0.19	98	0.11	32	0.30	130
1420	0.20	98	0.11	32	0.31	130
1440	0.22	94	0.12	31	0.34	126

Table 56 Kinetic data for the adsorption of a 0.75:0.25 1-decanol&3,7-DMO binary system at 45 °C for an overall initial concentration of 3.32 mass percentage.

Time (min)	1-decanol mass percentage (%)	1-decanol adsorbent loading (mg/g)	3,7-DMO mass percentage (%)	3,7-DMO adsorbent loading (mg/g)	Overall mass percentage (%)	Overall adsorbent loading (mg/g)
0	2.20	0	1.12	0	3.32	0
15	2.07	19	1.06	8	3.13	27
30	2.01	27	1.03	12	3.04	39
60	1.93	39	1.00	17	2.92	56
160	1.76	61	0.93	26	2.70	87
240	1.69	72	0.90	31	2.58	103
400	1.67	75	0.89	32	2.56	106
1390	1.73	66	0.93	26	2.67	92
1420	1.72	67	0.92	28	2.64	95
1440	1.76	62	0.93	26	2.69	88

Table 57 Kinetic data for the adsorption of a 0.75:0.25 1-decanol&3,7-DMO binary system at 45 °C for an overall initial concentration of 2.04 mass percentage.

Time (min)	1-decanol mass percentage (%)	1-decanol adsorbent loading (mg/g)	3,7-DMO mass percentage (%)	3,7-DMO adsorbent loading (mg/g)	Overall mass percentage (%)	Overall adsorbent loading (mg/g)
0	1.33	0	0.70	0	2.04	0
15	1.22	16	0.65	8	1.86	24
30	1.10	32	0.59	16	1.69	48
60	1.02	44	0.55	21	1.56	66
160	0.91	59	0.50	28	1.41	87
240	0.87	65	0.48	30	1.35	95
400	0.84	69	0.47	32	1.31	101
1390	0.89	61	0.49	29	1.39	90
1420	0.94	55	0.51	26	1.45	81
1440	0.94	55	0.52	26	1.46	81

Table 58 Kinetic data for the adsorption of a 0.75:0.25 1-decanol&3,7-DMO binary system at 45 °C for an overall initial concentration of 0.97 mass percentage.

Time (min)	1-decanol mass percentage (%)	1-decanol adsorbent loading (mg/g)	3,7-DMO mass percentage (%)	3,7-DMO adsorbent loading (mg/g)	Overall mass percentage (%)	Overall adsorbent loading (mg/g)
0	0.64	0	0.33	0	0.97	0
15	0.51	18	0.27	8	0.78	27
30	0.48	22	0.26	10	0.74	32
60	0.42	31	0.23	14	0.64	45
160	0.32	45	0.17	21	0.49	66
240	0.27	51	0.15	25	0.42	76
400	0.24	56	0.13	27	0.37	83
1390	0.33	43	0.17	21	0.50	64
1420	0.34	42	0.18	21	0.51	63
1440	0.33	43	0.18	21	0.51	64

B.3 1-octanol&3,7-DMO system

B.3.1 0.5:0.5 ratio

Table 59 Kinetic data for the adsorption of a 0.5:0.5 1-octanol&3,7-DMO binary system at 25 °C for an overall initial concentration of 2.02 mass%.

Time (min)	1-octanol mass percentage (%)	1-octanol adsorbent loading (mg/g)	3,7-DMO mass percentage (%)	3,7-DMO adsorbent loading (mg/g)	Overall mass percentage (%)	Overall adsorbent loading (mg/g)
0	1.01	0	1.01	0	2.02	0
15	0.98	4	0.98	5	1.96	9
30	0.88	18	0.94	10	1.82	29
60	0.83	24	0.91	15	1.74	39
160	0.75	36	0.84	24	1.60	59
240	0.64	52	0.75	36	1.39	88
400	0.57	61	0.69	45	1.26	106
1390	0.53	66	0.68	47	1.21	113
1420	0.52	69	0.65	50	1.17	119
1440	0.52	67	0.67	49	1.19	116

Table 60 Kinetic data for the adsorption of a 0.5:0.5 1-octanol&3,7-DMO binary system at 25 °C for an overall initial concentration of 1.99 mass percentage.

Time (min)	1-octanol mass percentage (%)	1-octanol adsorbent loading (mg/g)	3,7-DMO mass percentage (%)	3,7-DMO adsorbent loading (mg/g)	Overall mass percentage (%)	Overall adsorbent loading (mg/g)
0	1.01	0	0.98	0	1.99	0
15	0.89	17	0.96	3	1.86	19
30	0.85	23	0.88	15	1.73	37
60	0.81	28	0.86	18	1.67	46
160	0.74	38	0.82	24	1.56	61
240	0.69	45	0.76	31	1.45	77
410	0.66	50	0.74	34	1.40	84
1390	0.70	44	0.77	30	1.47	74
1420	0.72	41	0.79	27	1.51	68
1440	0.71	43	0.78	29	1.48	72

Table 61 Kinetic data for the adsorption of a 0.5:0.5 1-octanol&3,7-DMO binary system at 25 °C for an overall initial concentration of 1.05 mass percentage.

Time (min)	1-octanol mass percentage (%)	1-octanol adsorbent loading (mg/g)	3,7-DMO mass percentage (%)	3,7-DMO adsorbent loading (mg/g)	Overall mass percentage (%)	Overall adsorbent loading (mg/g)
0	0.53	0	0.53	0	1.05	0
15	0.47	8	0.49	5	0.96	13
30	0.44	12	0.45	11	0.89	22
60	0.34	26	0.39	19	0.73	45
160	0.27	35	0.33	28	0.60	63
240	0.25	38	0.32	28	0.58	66
410	0.20	45	0.26	37	0.46	82
1390	0.14	54	0.18	49	0.32	103
1420	0.14	54	0.18	48	0.33	101
1440	0.14	54	0.18	48	0.32	102

Table 62 Kinetic data for the adsorption of a 0.5:0.5 1-octanol&3,7-DMO binary system at 25 °C for an overall initial concentration of 1.99 mass percentage.

Time (min)	1-octanol mass percentage (%)	1-octanol adsorbent loading (mg/g)	3,7-DMO mass percentage (%)	3,7-DMO adsorbent loading (mg/g)	Overall mass percentage (%)	Overall adsorbent loading (mg/g)
0	0.99	0	1.00	0	1.99	0
15	0.89	15	0.93	10	1.82	24
30	0.93	9	0.99	1	1.92	10
60	0.79	29	0.87	19	1.66	47
160	0.67	47	0.79	30	1.46	77
240	0.65	49	0.75	35	1.41	84
410	0.61	54	0.73	39	1.34	93
1390	0.59	58	0.71	41	1.30	99
1420	0.60	56	0.72	40	1.32	96
1440	0.61	55	0.72	40	1.33	95

Table 63 Kinetic data for the adsorption of a 0.5:0.5 1-octanol&3,7-DMO binary system at 25 °C for an overall initial concentration of 3.34 mass percentage.

Time (min)	1-octanol mass percentage (%)	1-octanol adsorbent loading (mg/g)	3,7-DMO mass percentage (%)	3,7-DMO adsorbent loading (mg/g)	Overall mass percentage (%)	Overall adsorbent loading (mg/g)
0	1.69	0	1.65	0	3.34	0
15	1.56	19	1.55	15	3.10	34
30	1.50	27	1.51	20	3.01	47
60	1.44	35	1.46	27	2.91	62
160	1.32	54	1.39	38	2.70	92
240	1.28	60	1.36	41	2.64	101
410	1.24	65	1.35	43	2.59	108
1390	1.17	75	1.32	46	2.49	122
1420	1.16	77	1.31	48	2.47	126
1440	1.18	74	1.34	44	2.52	118

Table 64 Kinetic data for the adsorption of a 0.5:0.5 1-octanol&3,7-DMO binary system at 45 °C for an overall initial concentration of 3.49 mass percentage.

Time (min)	1-octanol mass percentage (%)	1-octanol adsorbent loading (mg/g)	3,7-DMO mass percentage (%)	3,7-DMO adsorbent loading (mg/g)	Overall mass percentage (%)	Overall adsorbent loading (mg/g)
0	1.74	0	1.75	0	3.49	0
15	1.58	23	1.64	15	3.23	37
30	1.56	25	1.61	18	3.18	44
60	1.46	40	1.67	11	3.13	51
160	1.36	55	1.50	35	2.86	90
240	1.30	63	1.46	40	2.76	103
400	1.27	67	1.43	45	2.70	112
1390	1.38	52	1.58	24	2.95	76
1420	1.40	49	1.60	21	3.00	70
1440	1.41	47	1.59	21	3.00	68

Table 65 Kinetic data for the adsorption of a 0.5:0.5 1-octanol&3,7-DMO binary system at 45 °C for an overall initial concentration of 1.90 mass percentage.

Time (min)	1-octanol mass percentage (%)	1-octanol adsorbent loading (mg/g)	3,7-DMO mass percentage (%)	3,7-DMO adsorbent loading (mg/g)	Overall mass percentage (%)	Overall adsorbent loading (mg/g)
0	0.96	0	0.94	0	1.90	0
15	0.83	19	0.86	12	1.68	31
30	0.76	27	0.81	18	1.58	46
60	0.72	34	0.77	24	1.49	58
160	0.62	48	0.71	32	1.33	80
240	0.58	53	0.67	39	1.24	92
400	0.56	56	0.65	41	1.21	97
1390	0.61	49	0.70	34	1.31	83
1420	0.63	45	0.72	31	1.36	76
1440	0.61	49	0.71	33	1.32	82

Table 66 Kinetic data for the adsorption of a 0.5:0.5 1-octanol&3,7-DMO binary system at 45 °C for an overall initial concentration of 0.95 mass percentage.

Time (min)	1-octanol mass percentage (%)	1-octanol adsorbent loading (mg/g)	3,7-DMO mass percentage (%)	3,7-DMO adsorbent loading (mg/g)	Overall mass percentage (%)	Overall adsorbent loading (mg/g)
0	0.49	0	0.46	0	0.95	0
15	0.39	15	0.44	4	0.82	19
30	0.34	21	0.36	14	0.71	35
60	0.30	28	0.32	20	0.62	48
160	0.23	37	0.26	28	0.50	65
240	0.21	40	0.24	32	0.45	72
400	0.22	38	0.25	31	0.47	69
1390	0.30	27	0.33	19	0.63	47
1420	0.29	29	0.31	22	0.60	50
1440	0.30	28	0.32	21	0.62	48

B.3.2 0.25:0.75 ratio**Table 67** Kinetic data for the adsorption of a 0.25:0.75 1-octanol&3,7-DMO binary system at 25 °C for an overall initial concentration of 3.39 mass percentage.

Time (min)	1-octanol mass percentage (%)	1-octanol adsorbent loading (mg/g)	3,7-DMO mass percentage (%)	3,7-DMO adsorbent loading (mg/g)	Overall mass percentage (%)	Overall adsorbent loading (mg/g)
0	1.16	0	2.22	0	3.39	0
15	1.13	5	2.23	-1	3.36	4
30	1.06	14	2.11	15	3.17	29
60	0.99	24	2.01	29	3.00	53
160	0.88	39	1.83	53	2.71	92
240	0.87	41	1.85	50	2.72	91
410	0.81	48	1.80	57	2.61	105
1390	0.75	57	1.69	72	2.44	129
1420	0.77	54	1.65	78	2.42	132
1440	0.82	48	1.67	75	2.49	123

Table 68 Kinetic data for the adsorption of a 0.25:0.75 1-octanol&3,7-DMO binary system at 25 °C for an overall initial concentration of 1.95 mass percentage.

Time (min)	1-octanol mass percentage (%)	1-octanol adsorbent loading (mg/g)	3,7-DMO mass percentage (%)	3,7-DMO adsorbent loading (mg/g)	Overall mass percentage (%)	Overall adsorbent loading (mg/g)
0	0.67	0	1.28	0	1.95	0
15	0.62	6	1.23	5	1.85	11
30	0.60	10	1.19	13	1.79	22
60	0.53	20	1.11	25	1.63	45
160	0.50	24	1.07	30	1.57	54
240	0.43	34	0.95	47	1.38	81
410	0.49	26	1.15	44	1.64	70
1390	0.44	33	0.96	45	1.40	78
1420	0.46	30	0.99	41	1.45	71
1440	0.45	32	0.98	42	1.43	74

Table 69 Kinetic data for the adsorption of a 0.25:0.75 1-octanol&3,7-DMO binary system at 25 °C for an overall initial concentration of 1.02 mass percentage.

Time (min)	1-octanol mass percentage (%)	1-octanol adsorbent loading (mg/g)	3,7-DMO mass percentage (%)	3,7-DMO adsorbent loading (mg/g)	Overall mass percentage (%)	Overall adsorbent loading (mg/g)
0	0.36	0	0.65	0	1.02	0
15	0.29	10	0.57	13	0.86	23
30	0.27	14	0.53	18	0.80	31
60	0.23	19	0.70	22	0.93	41
160	0.20	23	0.43	33	0.63	56
240	0.17	28	0.37	40	0.54	68
410	0.16	30	0.34	44	0.50	74
1390	0.14	32	0.30	51	0.44	83
1420	0.13	33	0.30	51	0.43	84
1440	0.16	29	0.34	44	0.50	74

Table 70 Kinetic data for the adsorption of a 0.25:0.75 1-octanol&3,7-DMO binary system at 45 °C for an overall initial concentration of 3.20 mass percentage.

Time (min)	1-octanol mass percentage (%)	1-octanol adsorbent loading (mg/g)	3,7-DMO mass percentage (%)	3,7-DMO adsorbent loading (mg/g)	Overall mass percentage (%)	Overall adsorbent loading (mg/g)
0	1.05	0	2.16	0	3.20	0
15	0.95	12	2.02	18	2.98	31
30	0.92	18	1.86	41	2.78	58
60	0.87	24	1.83	45	2.71	68
160	0.79	36	1.73	58	2.52	94
240	0.76	40	1.66	69	2.41	108
400	0.73	44	1.61	75	2.34	119
1390	0.82	31	1.77	53	2.59	84
1420	0.82	31	1.79	50	2.61	82
1440	0.82	31	1.77	53	2.59	84

Table 71 Kinetic data for the adsorption of a 0.25:0.75 1-octanol&3,7-DMO binary system at 45 °C for an overall initial concentration of 2.00 mass percentage.

Time (min)	1-octanol mass percentage (%)	1-octanol adsorbent loading (mg/g)	3,7-DMO mass percentage (%)	3,7-DMO adsorbent loading (mg/g)	Overall mass percentage (%)	Overall adsorbent loading (mg/g)
0	0.68	0	1.31	0	2.00	0
15	0.58	15	1.30	3	1.88	17
30	0.54	21	1.13	27	1.67	48
60	0.50	27	1.07	35	1.56	62
160	0.43	37	0.97	50	1.39	87
240	0.39	42	0.90	60	1.29	102
400	0.35	49	0.82	71	1.17	120
1390	0.40	41	0.94	53	1.35	94
1420	0.40	41	1.11	29	1.51	70
1440	0.39	43	0.91	57	1.30	100

Table 71 Kinetic data for the adsorption of a 0.25:0.75 1-octanol&3,7-DMO binary system at 45 °C for an overall initial concentration of 1.01 mass percentage.

Time (min)	1-octanol mass percentage (%)	1-octanol adsorbent loading (mg/g)	3,7-DMO mass percentage (%)	3,7-DMO adsorbent loading (mg/g)	Overall mass percentage (%)	Overall adsorbent loading (mg/g)
0	0.35	0	0.66	0	1.01	0
15	0.27	12	0.54	17	0.81	28
30	0.24	15	0.50	22	0.74	37
60	0.21	20	0.44	30	0.65	50
160	0.15	27	0.34	43	0.50	71
240	0.14	29	0.32	47	0.46	76
400	0.12	32	0.27	53	0.39	85
1390	0.16	27	0.34	43	0.50	70
1420	0.16	27	0.34	44	0.49	71
1440	0.16	27	0.34	44	0.50	71

B.3.3 0.75:0.25 ratio**Table 73** Kinetic data for the adsorption of a 0.75:0.25 1-octanol&3,7-DMO binary system at 25 °C for an overall initial concentration of 0.84 mass percentage.

Time (min)	1-octanol mass percentage (%)	1-octanol adsorbent loading (mg/g)	3,7-DMO mass percentage (%)	3,7-DMO adsorbent loading (mg/g)	Overall mass percentage (%)	Overall adsorbent loading (mg/g)
0	0.54	0	0.30	0	0.84	0
15	0.53	1	0.36	-8	0.89	9
30	0.60	-10	0.30	0	0.90	15
60	0.51	5	0.26	6	0.76	32
160	0.34	28	0.21	12	0.55	41
240	0.30	35	0.19	15	0.49	50
410	0.26	39	0.17	18	0.43	58
1390	0.16	54	0.10	28	0.26	81
1420	0.16	55	0.10	28	0.26	82
1440	0.17	52	0.11	27	0.28	79

Table 74 Kinetic data for the adsorption of a 0.75:0.25 1-octanol&3,7-DMO binary system at 25 °C for an overall initial concentration of 1.96 mass percentage.

Time (min)	1-octanol mass percentage (%)	1-octanol adsorbent loading (mg/g)	3,7-DMO mass percentage (%)	3,7-DMO adsorbent loading (mg/g)	Overall mass percentage (%)	Overall adsorbent loading (mg/g)
0	1.28	0	0.68	0	1.96	0
15	1.15	19	0.62	8	1.77	27
30	1.09	28	0.61	10	1.69	38
60	1.05	34	0.59	12	1.64	46
160	0.90	54	0.53	21	1.43	75
240	0.82	65	0.59	13	1.41	78
410	0.77	72	0.48	28	1.25	100
1390	0.78	72	0.49	27	1.27	98
1420	0.79	70	0.50	26	1.28	96
1440	0.79	70	0.50	25	1.29	95

Table 75 Kinetic data for the adsorption of a 0.75:0.25 1-octanol&3,7-DMO binary system at 25 °C for an overall initial concentration of 3.19 mass percentage.

Time (min)	1-octanol mass percentage (%)	1-octanol adsorbent loading (mg/g)	3,7-DMO mass percentage (%)	3,7-DMO adsorbent loading (mg/g)	Overall mass percentage (%)	Overall adsorbent loading (mg/g)
0	2.09	0	1.10	0	3.19	0
15	1.97	17	1.07	4	3.04	21
30	1.91	26	1.06	6	2.97	32
60	1.89	29	1.05	6	2.95	35
160	1.68	60	0.96	19	2.64	79
240	1.60	71	0.93	24	2.53	95
410	1.56	77	0.93	25	2.49	101
1390	1.50	85	0.92	25	2.43	110
1420	1.48	89	0.90	28	2.38	116
1440	1.48	88	0.91	27	2.39	115

Table 76 Kinetic data for the adsorption of a 0.75:0.25 1-octanol&3,7-DMO binary system at 45 °C for an overall initial concentration of 3.25 mass percentage.

Time (min)	1-octanol mass percentage (%)	1-octanol adsorbent loading (mg/g)	3,7-DMO mass percentage (%)	3,7-DMO adsorbent loading (mg/g)	Overall mass percentage (%)	Overall adsorbent loading (mg/g)
0	2.15	0	1.11	0	3.25	0
15	1.93	30	1.03	10	2.97	41
30	1.88	38	1.01	13	2.89	51
60	1.80	50	0.99	17	2.78	67
160	1.78	52	0.94	24	2.72	76
240	1.61	77	0.92	27	2.53	103
400	1.57	82	0.91	28	2.48	110
1390	1.72	61	0.98	18	2.70	80
1420	1.70	64	0.97	20	2.67	83
1440	1.70	63	0.97	19	2.67	83

Table 77 Kinetic data for the adsorption of a 0.75:0.25 1-octanol&3,7-DMO binary system at 45 °C for an overall initial concentration of 1.91 mass percentage.

Time (min)	1-octanol mass percentage (%)	1-octanol adsorbent loading (mg/g)	3,7-DMO mass percentage (%)	3,7-DMO adsorbent loading (mg/g)	Overall mass percentage (%)	Overall adsorbent loading (mg/g)
0	1.26	0	0.65	0	1.91	0
15	1.10	23	0.60	7	1.69	31
30	1.04	30	0.58	10	1.62	41
60	1.04	31	0.57	12	1.60	43
160	0.84	59	0.50	22	1.34	81
240	0.78	68	0.47	25	1.25	93
400	0.85	58	0.48	24	1.33	82
1390	0.82	62	0.50	21	1.32	83
1420	0.83	61	0.51	20	1.33	81
1440	0.82	61	0.51	20	1.33	81

Table 78 Kinetic data for the adsorption of a 0.75:0.25 1-octanol&3,7-DMO binary system at 45 °C for an overall initial concentration of 1.01 mass percentage.

Time (min)	1-octanol mass percentage (%)	1-octanol adsorbent loading (mg/g)	3,7-DMO mass percentage (%)	3,7-DMO adsorbent loading (mg/g)	Overall mass percentage (%)	Overall adsorbent loading (mg/g)
0	0.66	0	0.36	0	1.01	0
15	0.53	19	0.31	6	0.84	25
30	0.49	25	0.29	10	0.78	35
60	0.42	34	0.26	15	0.68	49
160	0.39	40	0.22	20	0.60	60
240	0.30	52	0.20	24	0.49	76
400	0.24	61	0.16	29	0.40	90
1390	0.29	54	0.18	26	0.47	80
1420	0.30	52	0.18	25	0.48	78
1440	0.30	52	0.18	25	0.48	78

B.4 Primary versus Secondary BAES

B.4.1 3,7-DMO at 25 °C and 45 °C

Table 79 Comparison of mass concentration and adsorbent loading achieved when operating the primary versus secondary BAES for an initial concentration of approximately 1 mass percentage at 45 °C.

Time (min)	Mass concentration (mass percentage)		Adsorbent loading (mg/g)	
	Primary BAES	Secondary BAES	Primary BAES	Secondary BAES
0	3.12	3.06	0	0
15	3.20	3.02	5	5
30	3.04	3.03	11	4
60	2.98	2.82	19	34
160	2.73	2.59	54	66
240	2.65	2.52	66	76
410	2.48	2.40	90	92
1390	2.34	2.21	110	119
1420	2.30	2.33	114	102
1440	2.32	2.26	112	112

Table 80 Comparison of mass concentration and adsorbent loading achieved when operating the primary versus secondary BAES for an initial concentration of approximately 1 mass percentage at 45 °C.

Time (min)	Mass concentration (mass percentage)		Adsorbent loading (mg/g)	
	Primary BAES	Secondary BAES	Primary BAES	Secondary BAES
0	0.99	0.96	0	0
15	0.87	0.87	17	12
30	0.78	0.78	30	25
60	0.72	0.66	38	42
160	0.60	0.52	55	62
240	0.51	0.47	68	69
410	0.41	0.38	82	83
1390	0.46	0.29	75	94
1420	0.45	0.29	77	95
1440	0.44	0.29	77	95

B.4.2 1-decanol&3,7-DMO at 25 °C and 45 °C

Table 81 Comparison of change in bulk solution composition and overall adsorbent loading when using the primary versus secondary BAES for 0.25:0.75 1-decanol&3,7-DMO system with an overall initial composition of 3.3 mass percentage at 25 °C.

Time	Primary BAES		Secondary BAES		Overall adsorbent loading (mg/g)	
	1-decanol mass percentage (%)	3,7-DMO mass percentage (%)	1-decanol mass percentage (%)	3,7-DMO mass percentage (%)	Primary BAES	Secondary BAES
0	1.12	2.15	1.11	2.16	0	0
15	1.04	2.03	1.06	2.09	26	18
30	1.00	1.96	1.04	2.03	42	29
60	1.06	2.09	1.02	2.00	16	36
160	0.98	1.78	0.93	1.90	68	64
240	0.87	1.76	0.89	1.77	86	88
400	0.86	1.72	0.84	1.70	94	107
1390	0.77	1.61	0.73	1.53	120	145
1420	0.78	1.63	0.74	1.54	117	143
1440	0.78	1.62	0.74	1.55	118	143

Table 82 Comparison of change in bulk solution composition and overall adsorbent loading when using the primary versus secondary BAES for 0.25:0.75 1-decanol&3,7-DMO system with an overall initial composition of 3.3 mass percentage at 45 °C.

Time	Primary BAES		Secondary BAES		Overall adsorbent loading (mg/g)	
	1-decanol mass percentage (%)	3,7-DMO mass percentage (%)	1-decanol mass percentage (%)	3,7-DMO mass percentage (%)	Primary BAES	Secondary BAES
0	1.15	2.11	1.15	2.17	0	0
15	1.02	1.99	1.04	2.11	36	23
30	1.01	1.99	0.99	1.91	37	59
60	0.95	1.88	0.96	1.84	61	74
160	0.98	1.77	0.94	2.11	73	38
240	0.88	1.76	0.87	1.70	88	106
400	0.82	1.68	0.81	1.59	107	132
1390	0.92	1.84	0.77	1.53	70	145
1420	0.91	1.82	0.76	1.52	76	148
1440	0.93	1.86	0.75	1.50	67	153

B.4.3 1-octanol&3,7-DMO at 25 °C and 45 °C

Table 83 Comparison of change in bulk solution composition and overall adsorbent loading when using the primary versus secondary BAES for 0.25:0.75 1-octanol&3,7-DMO system with an overall initial composition of 3.3 mass percentage at 25 °C.

Time	Primary BAES		Secondary BAES		Overall adsorbent loading (mg/g)	
	1-octanol mass percentage (%)	3,7-DMO mass percentage (%)	1-octanol mass percentage (%)	3,7-DMO mass percentage (%)	Primary BAES	Secondary BAES
0	1.16	2.22	1.21	2.29	0	0
15	1.13	2.23	1.10	2.23	14	24
30	1.06	2.11	1.08	2.11	29	45
60	0.99	2.01	1.06	2.09	53	50
160	0.88	1.83	0.98	2.01	92	75
240	0.87	1.85	0.94	1.97	91	85
400	0.81	1.80	0.85	1.81	105	121
1390	0.75	1.69	0.75	1.72	129	147
1420	0.77	1.65	0.75	1.75	132	144
1440	0.82	1.67	0.75	1.75	123	143

Table 84 Comparison of change in bulk solution composition and overall adsorbent loading when using the primary versus secondary BAES for 0.25:0.75 1-octanol&3,7-DMO system with an overall initial composition of 3.3 mass percentage at 45 °C.

Time	Primary BAES		Secondary BAES		Overall adsorbent loading (mg/g)	
	1-octanol mass percentage (%)	3,7-DMO mass percentage (%)	1-octanol mass percentage (%)	3,7-DMO mass percentage (%)	Primary BAES	Secondary BAES
0	1.05	2.11	1.15	2.17	0	0
15	0.95	1.99	1.04	2.11	31	23
30	0.92	1.99	0.99	1.91	58	59
60	0.87	1.88	0.96	1.84	68	74
160	0.79	1.77	0.94	2.11	94	38
240	0.76	1.76	0.87	1.70	108	106
400	0.73	1.68	0.81	1.59	119	132
1390	0.82	1.84	0.77	1.53	84	145
1420	0.82	1.82	0.76	1.52	82	148
1440	0.82	1.86	0.75	1.50	84	153

Appendix C Additional Graphical Experimental results

C.1 Single component adsorption

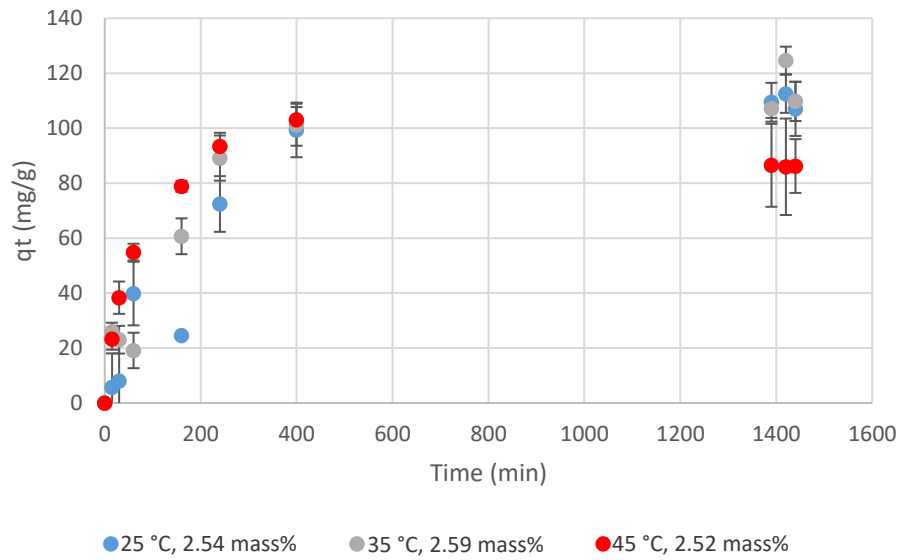


Figure 56 Demonstrating the effect of temperature at an initial concentration of +/-2.5mass percentage. For 25 °C an outlier is visible at 160min. The adsorbent loading for 25 and 35 °C is higher than 45 °C.

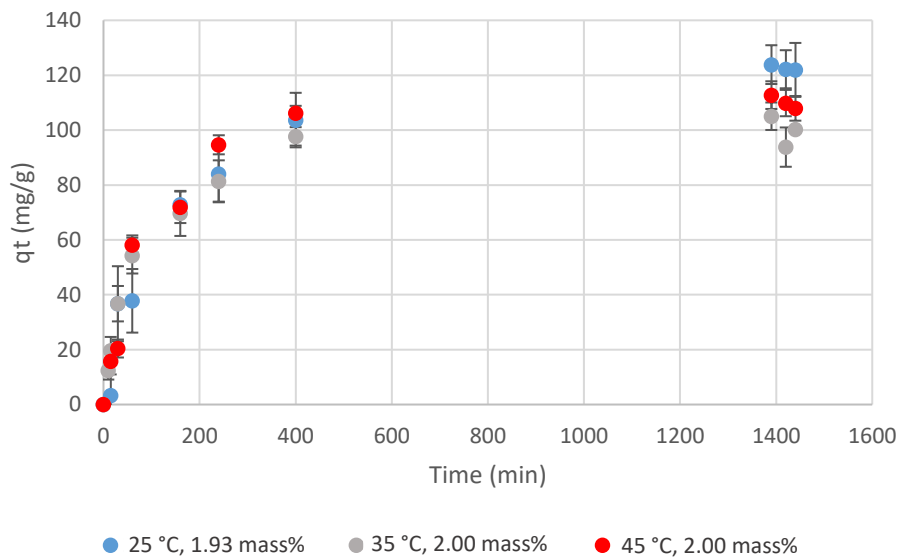


Figure 57 At an initial concentration of +/-2.00 mass percentage seems to have less of a distinguishable trend with regard to temperature effects. The adsorbent loading also shows less of the trend that is seen with the rest.

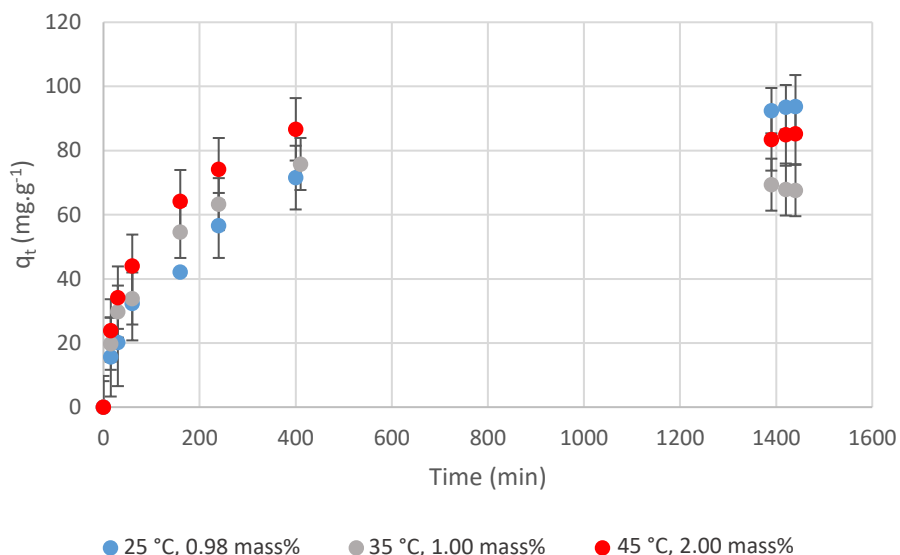


Figure 58 The trend of rate of adsorption is in line with the temperature effects visible in earlier sections. The adsorbent loading shows that the loading is higher at 25 °C but 35 °C is the lowest while 35 °C is in the middle.

C.2 Comparison of Primary and Secondary BAES (Batch-adsorption Experimental Setup)

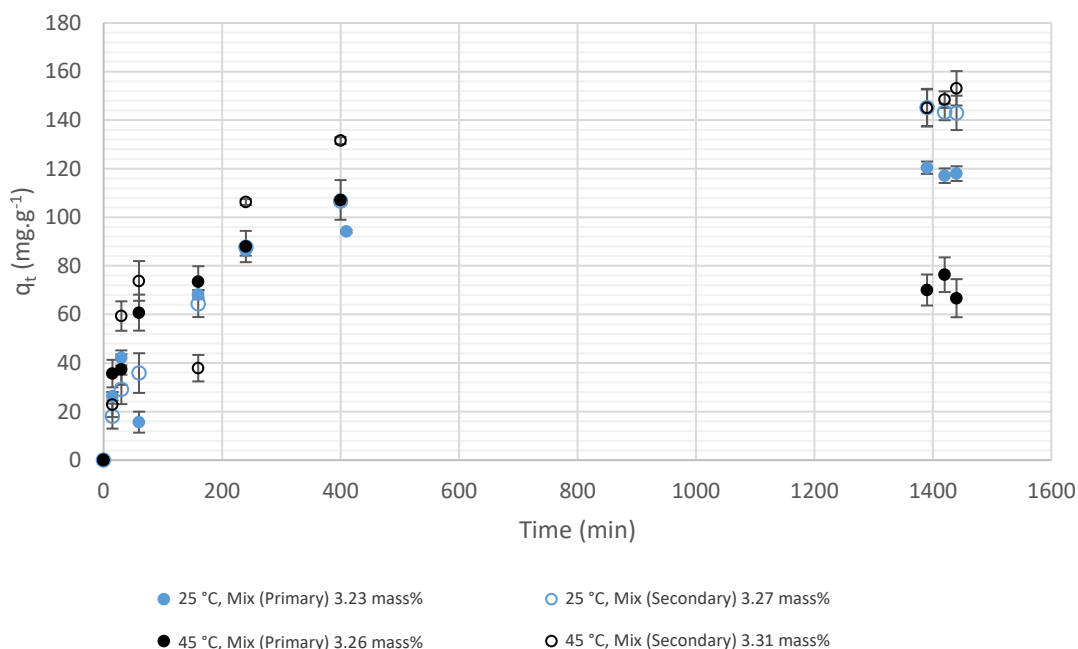


Figure 59 Demonstrating the difference in results achieved at 25 °C and 45 °C using the primary and secondary systems for solutions of similar composition. The composition is a 1:2 ratio of 1-decanol/3,7-DMO.

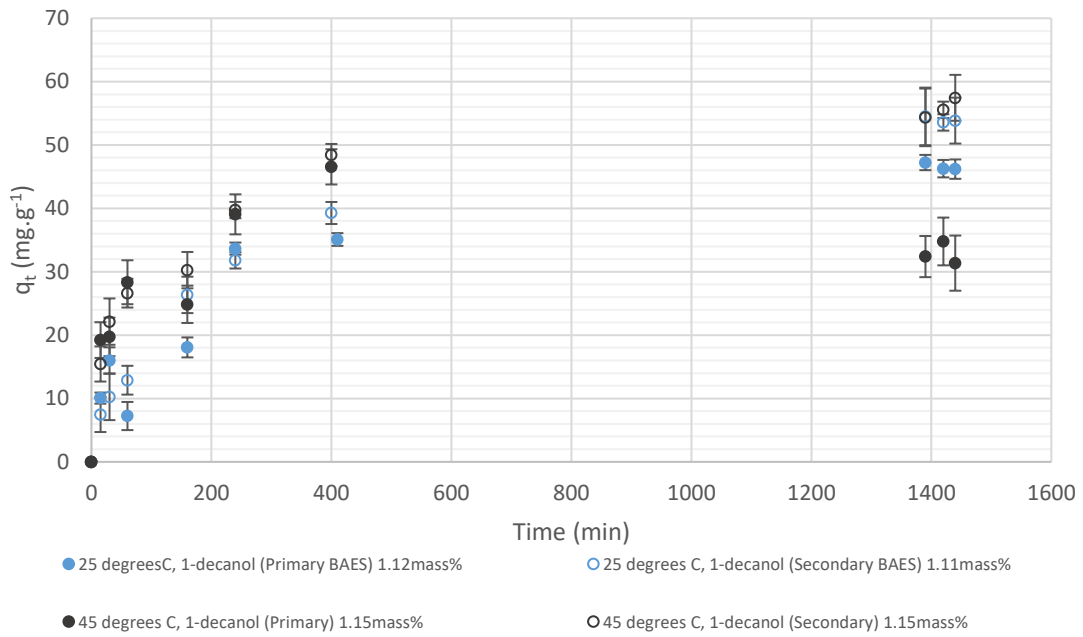


Figure 60 Demonstrating the results achieved at different temperatures using the primary and secondary systems.

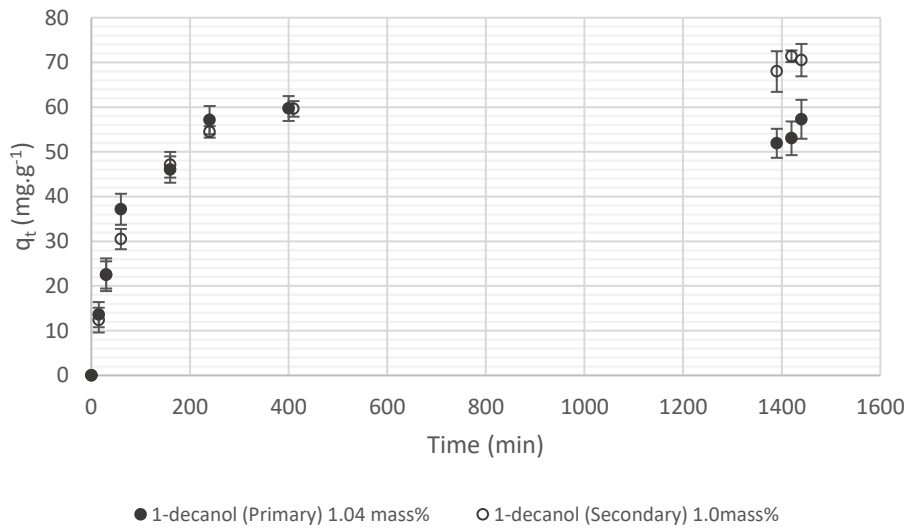


Figure 61 Demonstrating the effect of operating a 1-decanol/3,7-DMO at a 0.5:0.5 ratio at 45 °C for 24h on the 1-decanol sorption. The kinetics seem similar, within the margin of error, for the first 7 hours. Thereafter, the sorption loading is different.

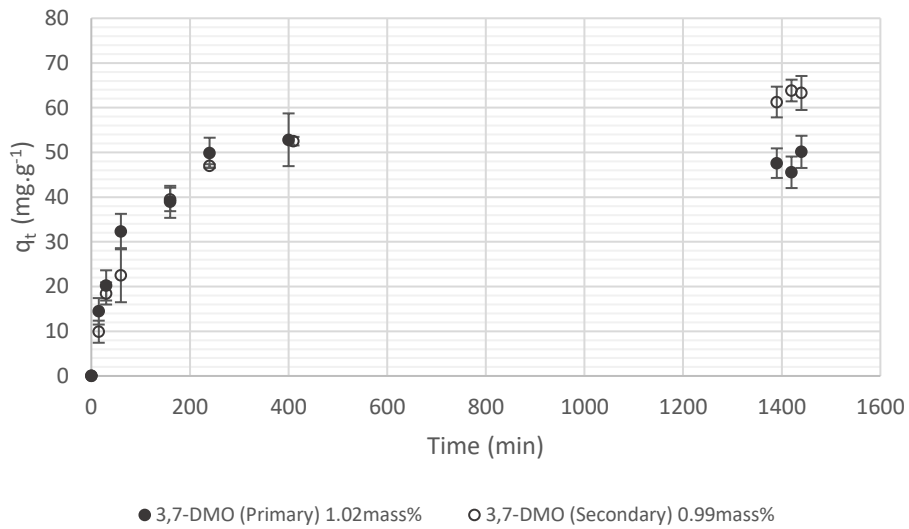


Figure 62 Effect of operating a 1-decanol/3,7-DMO using the primary and secondary BAES on the 3,7-DMO sorption. Each mixture consisting of a 0.5:0.5 ratio at 45 °C. The kinetics are similar for the first 7 h but the sorption equilibrium achieved is different.

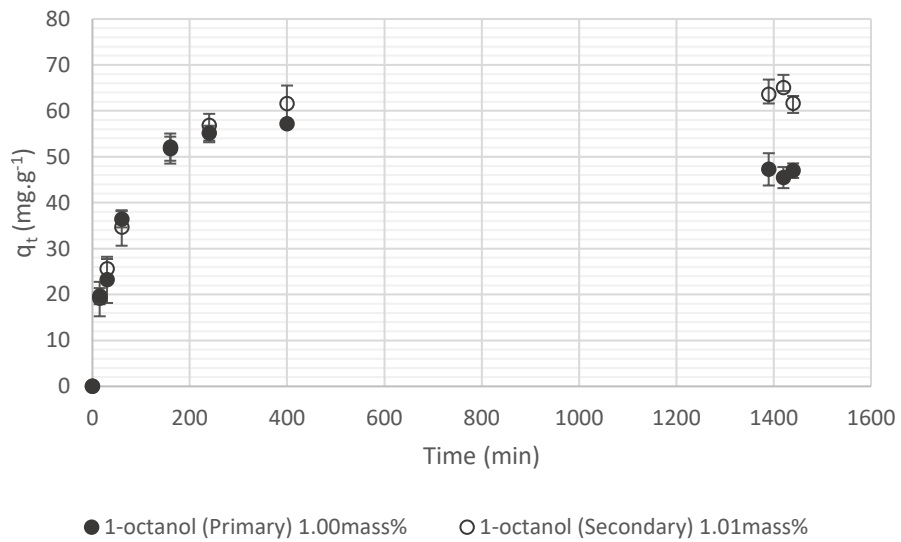


Figure 63 Demonstrating the effect of operating the two different systems at 45 °C for a 0.5:0.5ratio of 1-octanol/3,7-DMO on the sorption equilibrium and kinetics. The major difference occurs around 24hrs.

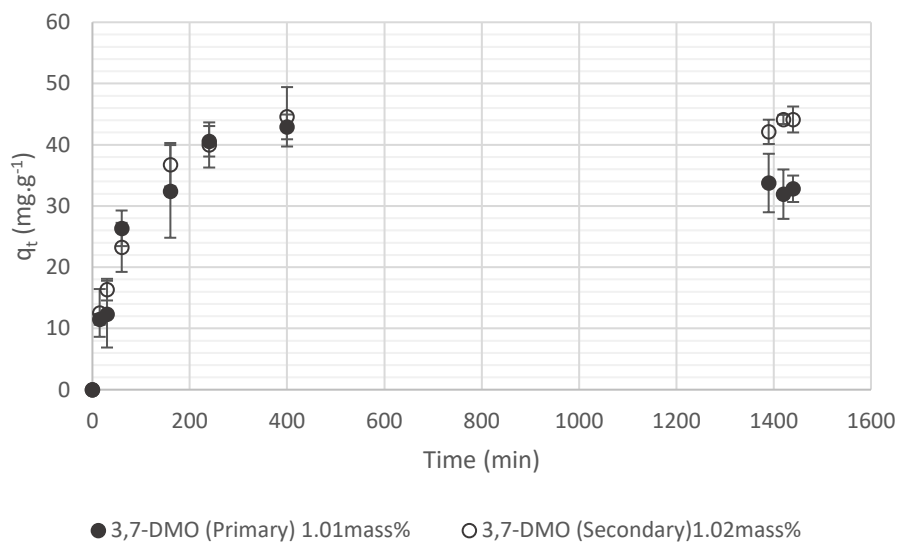


Figure 64 Demonstrating the effect on 3,7-DMO sorption when solutions of similar composition 0.5:0.5 ratio of 1-octanol/3,7-DMO are operated on two different systems at 45 °C for 24hrs. For a large portion the kinetics are similar but the sorption loading is different with the secondary BAES producing the expected results.

C.3 Binary component experiments

C.3.1 Effect of overall initial concentration at 45 °C

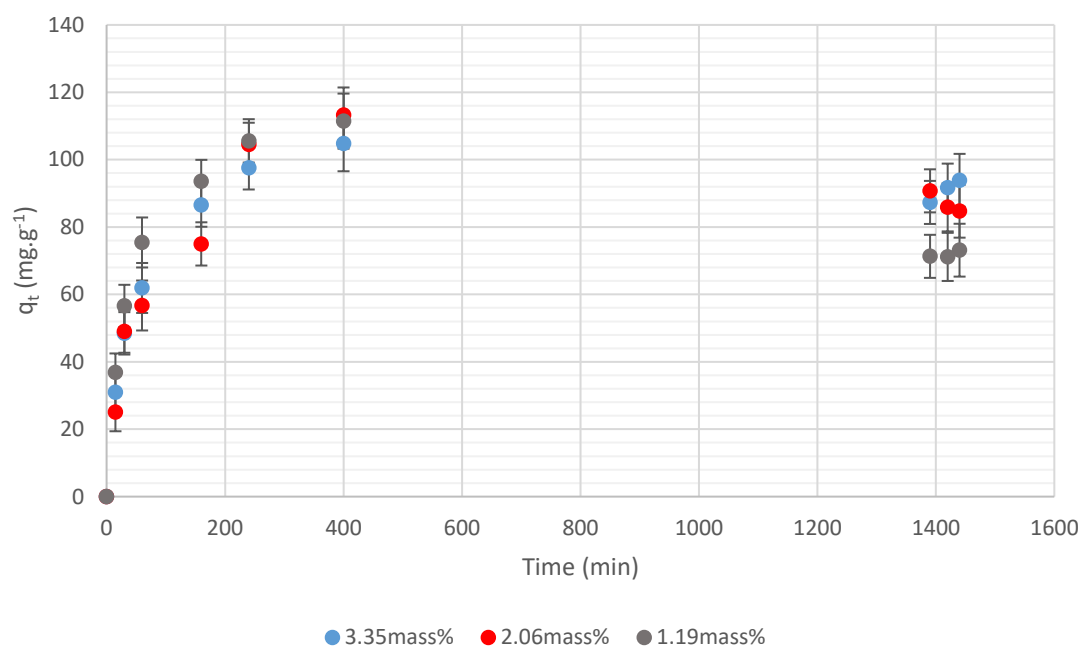


Figure 65 Effect of overall initial concentration of 0.5:0.5 1-decanol&3,7-DMO on the adsorbent loading with time at 45 °C. No clear distinction can be made but it appears that an increase in initial concentration increased the equilibrium adsorbent loading.

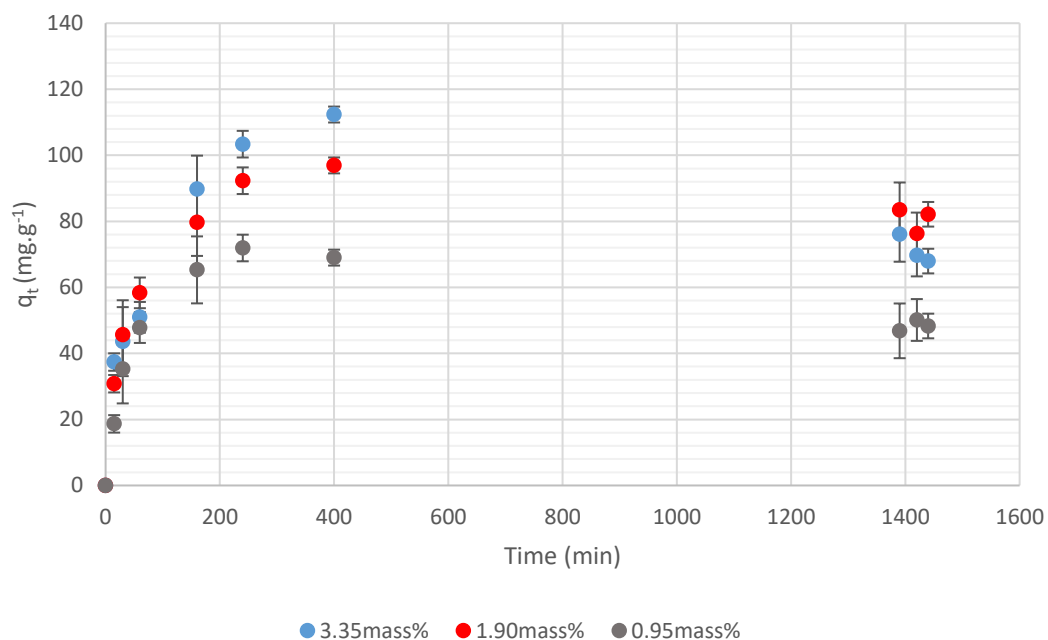


Figure 66 Effect of overall initial concentration on 0.5:0.5 1-octanol&3,7-DMO adsorption at 45 °C. The effect of initial concentration is more evident compared to that of the 1-decanol&3,7-DMO.

adsorbent loading increased with increasing initial adsorbate concentration and does not approach as a plateau as seen in single component systems.

C.3.2 Effect of adsorbate ratios at 25°C

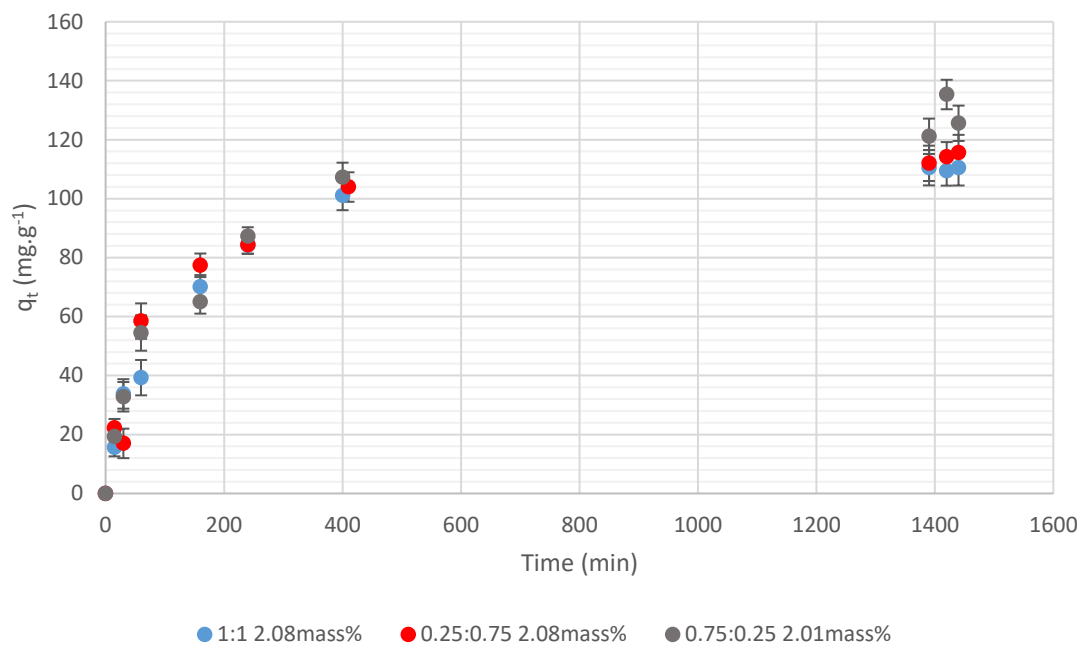


Figure 67 Effect of adsorbate ratio on the adsorption of 1-decanol&3,7-DMO binary system at 25 °C and an initial mass concentration of approximately 2mass percentage.

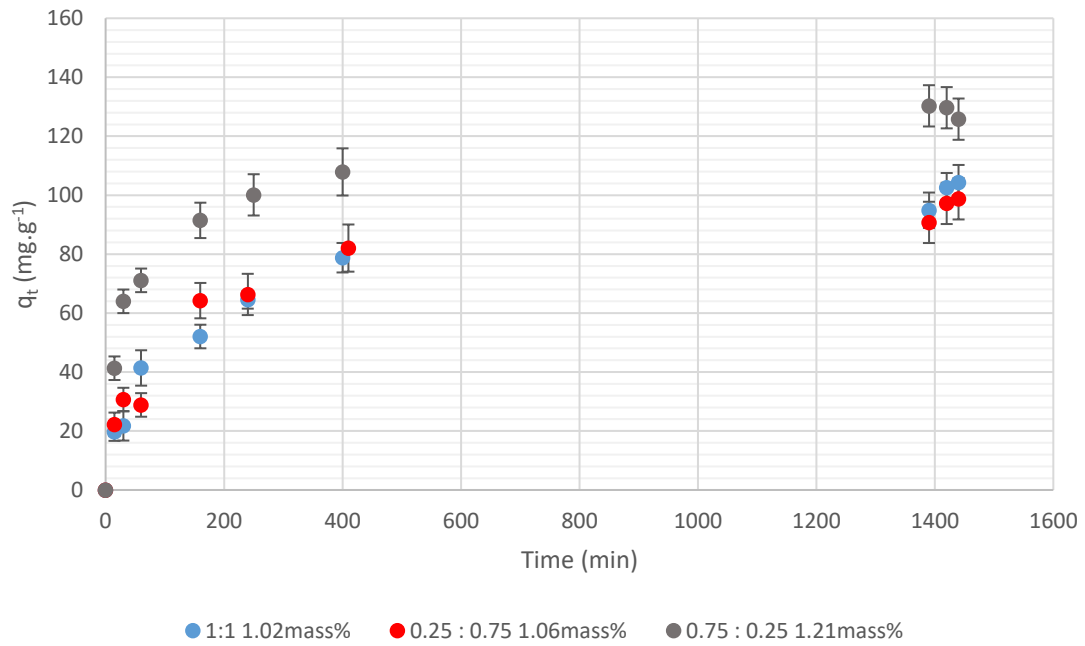


Figure 68 Effect of adsorbate ratio on the adsorption of 1-decanol&3,7-DMO binary system at 45 °C and an initial mass concentration of approximately 1mass percentage.

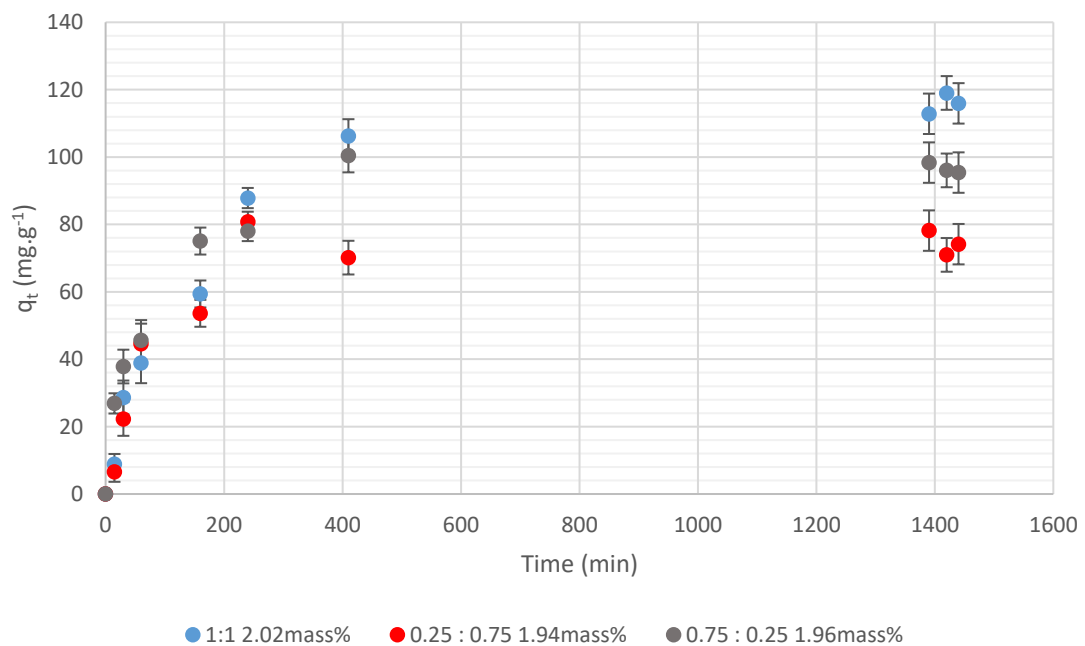


Figure 69 Effect of adsorbate ratio on the adsorption of 1-octanol&3,7-DMO binary system at 25 °C and an initial mass concentration of approximately 2mass percentage.

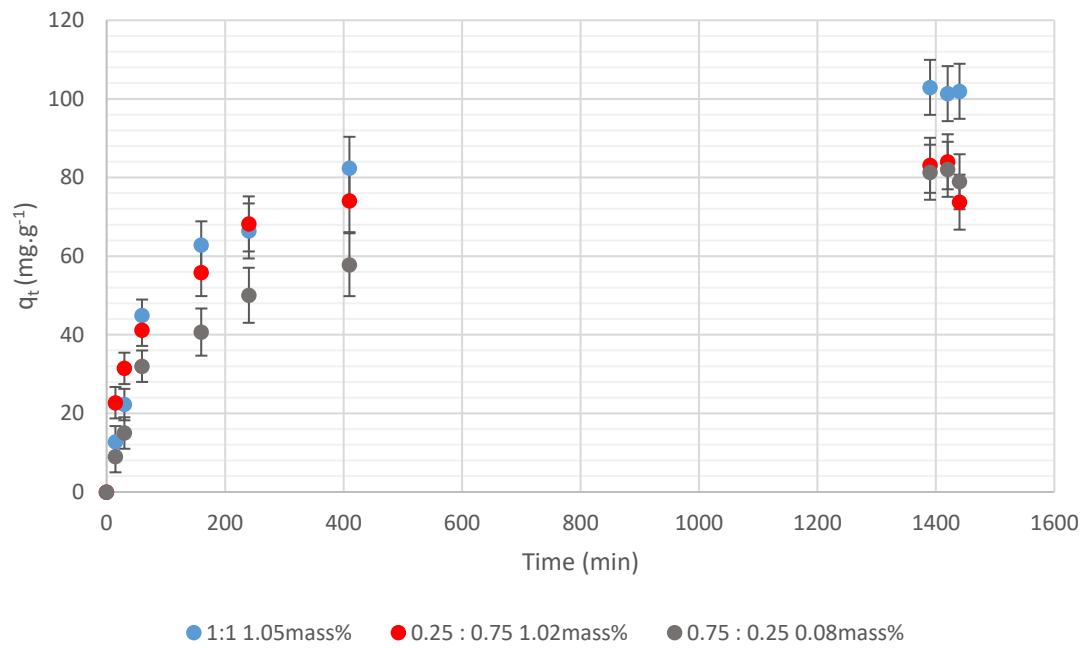


Figure 70 Effect of adsorbate ratio on the adsorption of 1-octanol&3,7-DMO binary system at 25 °C and an initial mass concentration of approximately 1mass percentage.

C.3.3 Effect of adsorbate ratio at 45°C

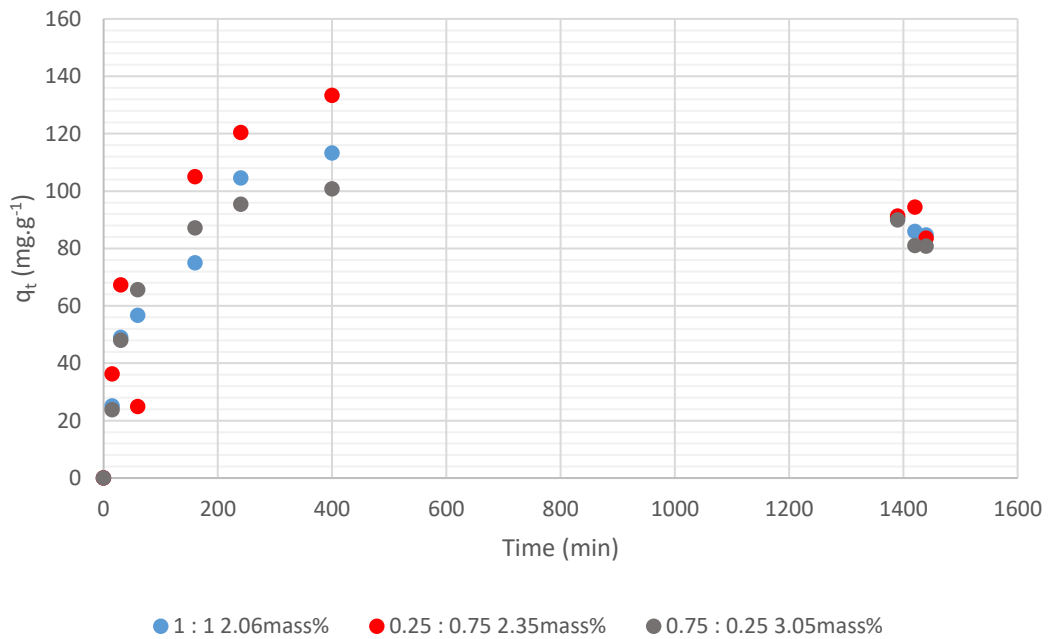


Figure 71 Effect of adsorbate ratio on the adsorption of 1-decanol&3,7-DMO binary system at 45 °C and an initial mass concentration of approximately 3mass percentage.

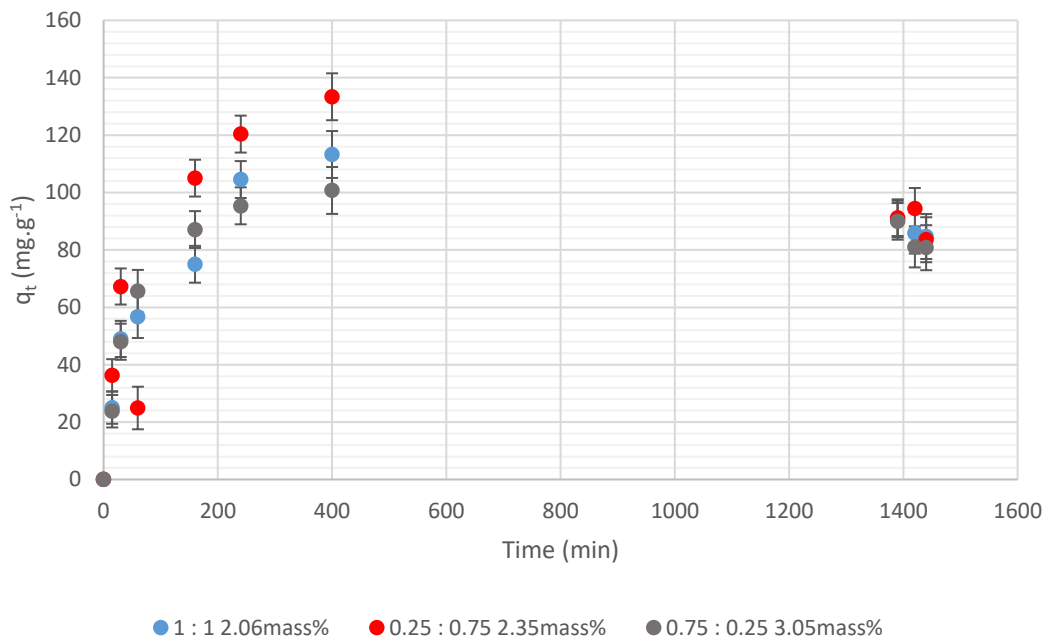


Figure 72 Effect of adsorbate ratio on the adsorption of 1-decanol&3,7-DMO binary system at 45 °C and an initial mass concentration of approximately 2 mass percentage.

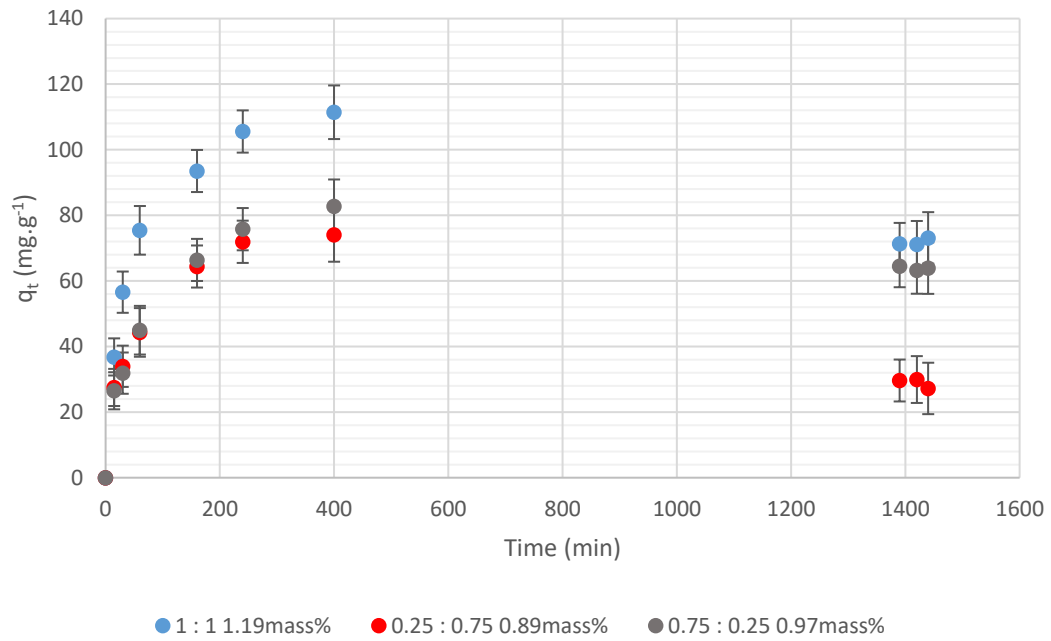


Figure 73 Effect of adsorbate ratio on the adsorption of 1-octanol&3,7-DMO binary system at 45 °C and an initial mass concentration of approximately 1 mass percentage.

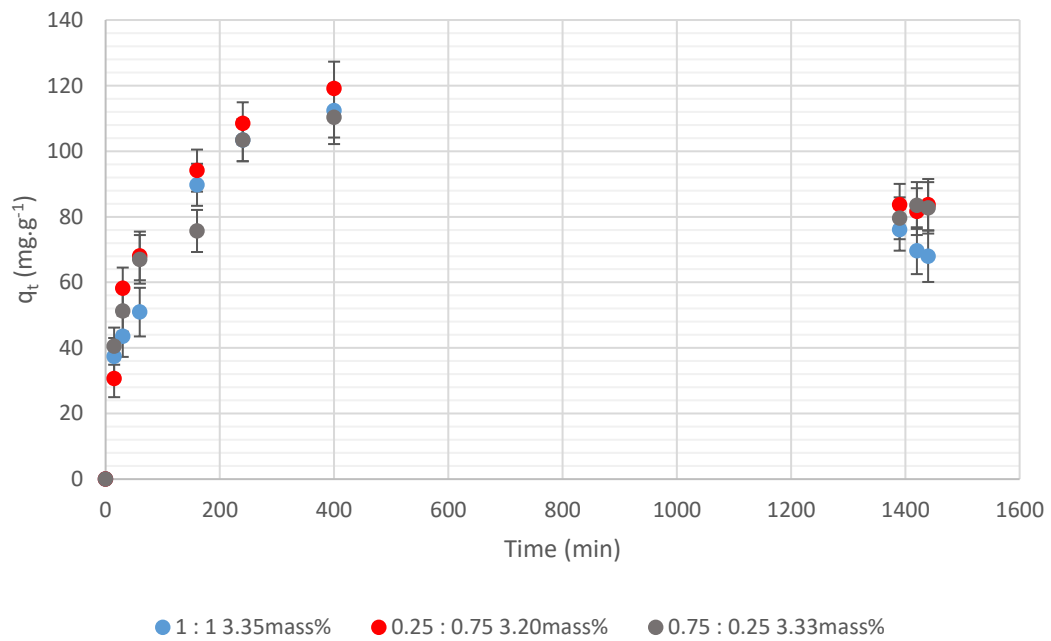


Figure 74 Effect of adsorbate ratio on the adsorption of 1-octanol&3,7-DMO binary system at 45 °C and an initial mass concentration of approximately 3.3 mass percentage.

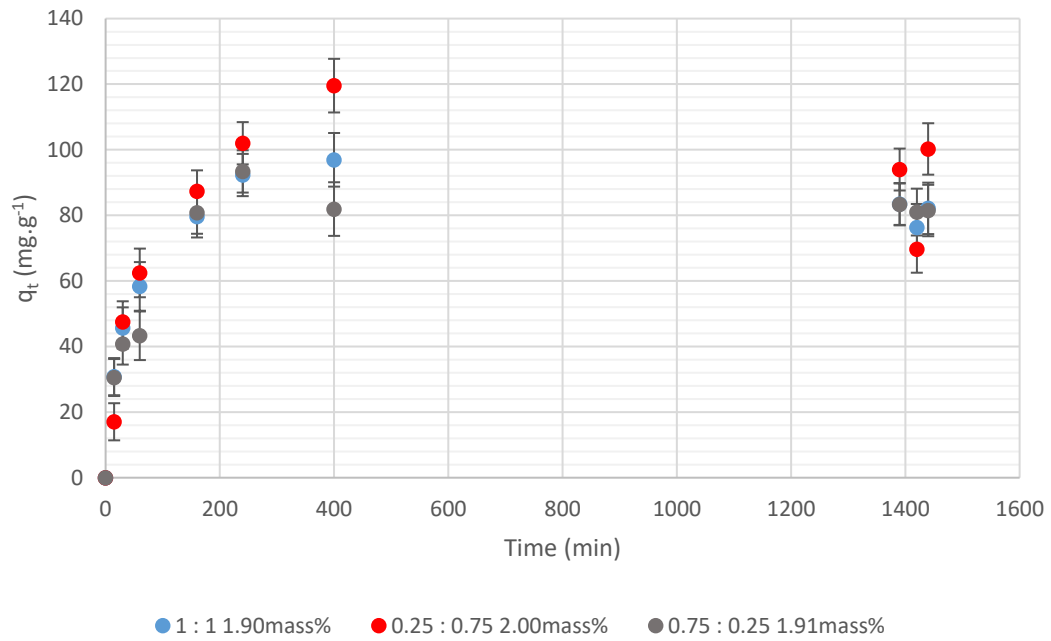


Figure 75 Effect of adsorbate ratio on the adsorption of 1-octanol&3,7-DMO binary system at 45 °C and an initial mass concentration of approximately 2 mass percentage.

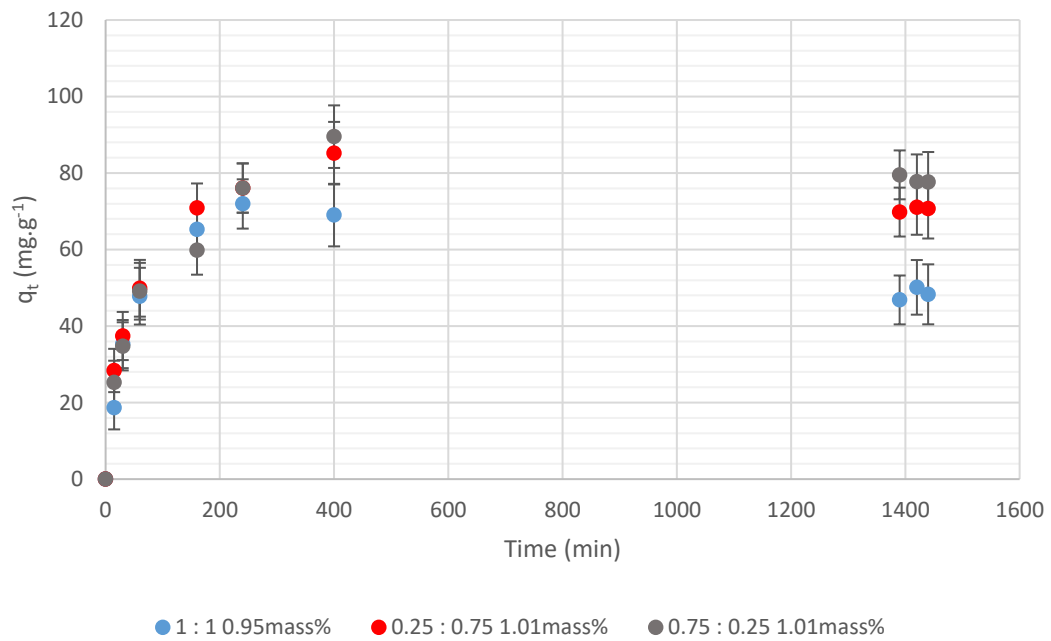


Figure 76 Effect of adsorbate ratio on the adsorption of 1-octanol&3,7-DMO binary system at 45 °C and an initial mass concentration of approximately 1 mass percentage.

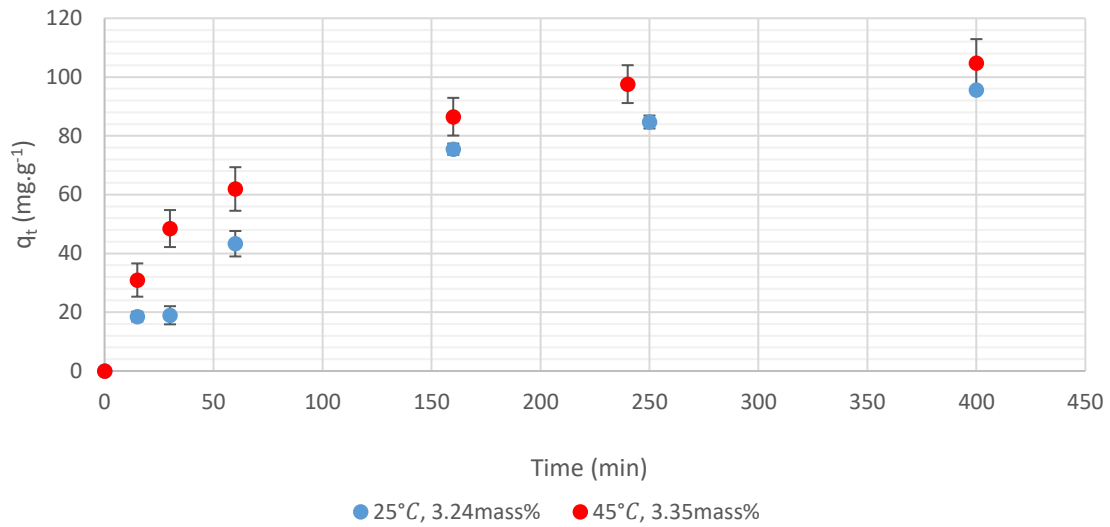


Figure 77 Investigation of effect of temperature on 1-decanol&3,7-DMO system for an overall concentration of 3.3 mass% and an adsorbate ratio of 0.5:0.5. The adsorbate loading provided is for the total adsorption of both adsorbates.

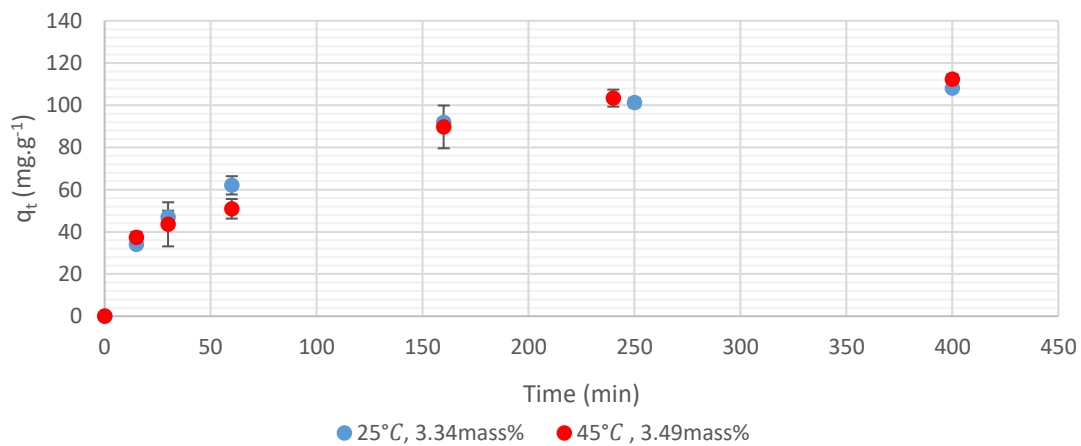


Figure 78 Effect of temperature on the adsorbate loading for an initial concentration of approximately 3.4 mass% for a 1-octanol&3,7-DMO system. There is no discernible difference noted for the first 7hrs.

Appendix D Additional kinetic modelling results

D.1 Single Component system

D.1.1 Temperature of 25°C

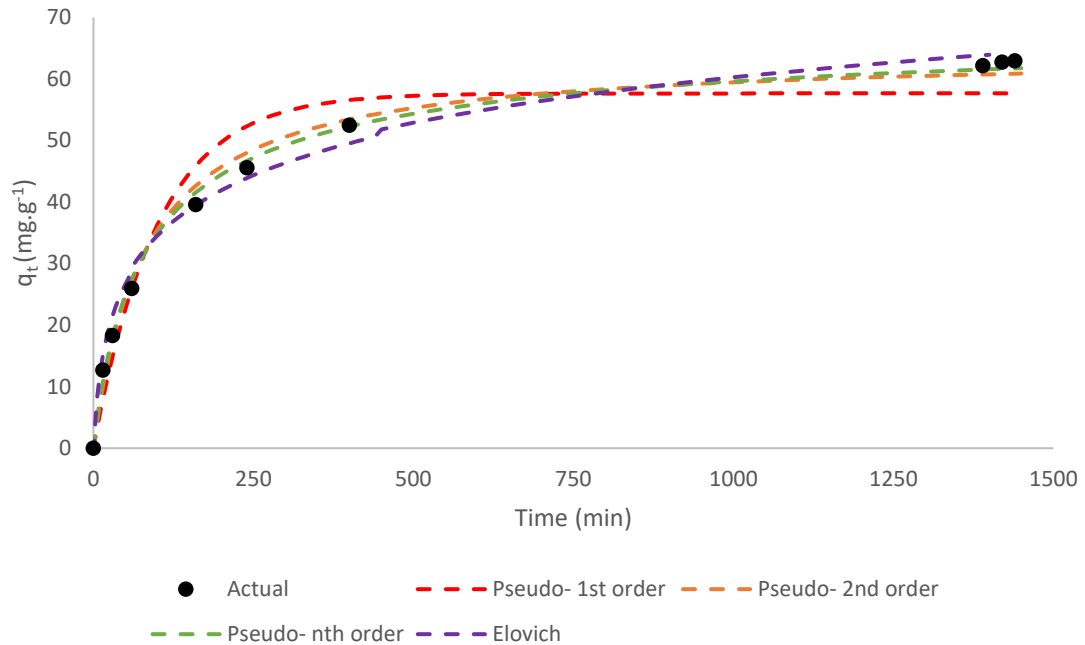


Figure 79 Kinetic model results for adsorption experiment performed on 3,7-DMO single component system at 25 °C and an initial concentration of 0.5 mass percentage.

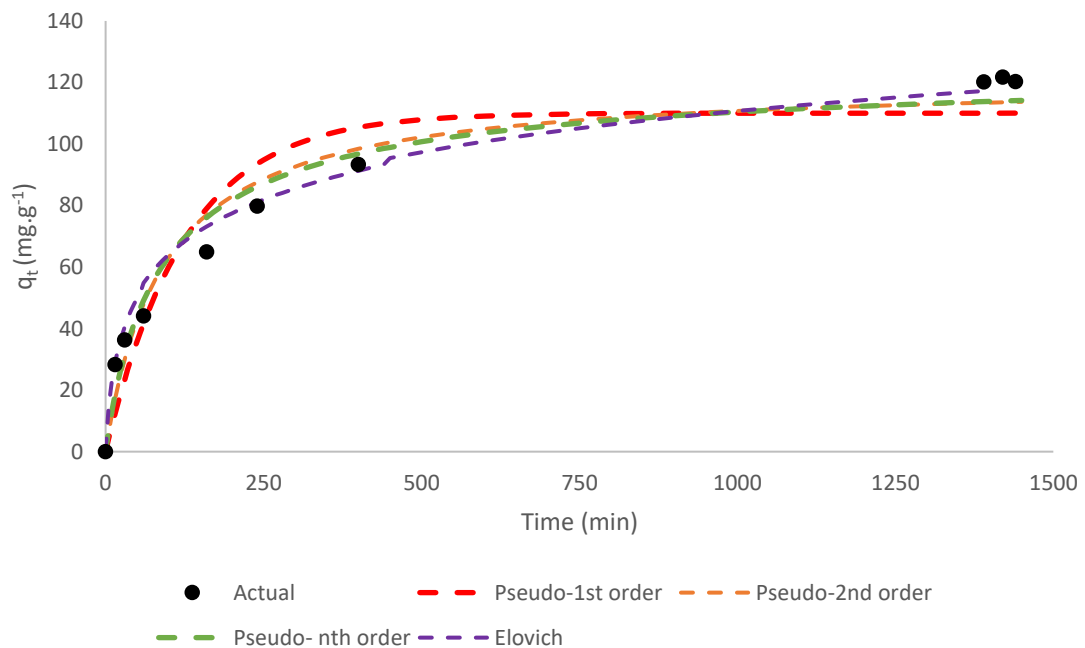


Figure 80 Kinetic model results for adsorption experiment performed on 3,7-DMO single component system at 25 °C and an initial concentration of 1.5 mass percentage.

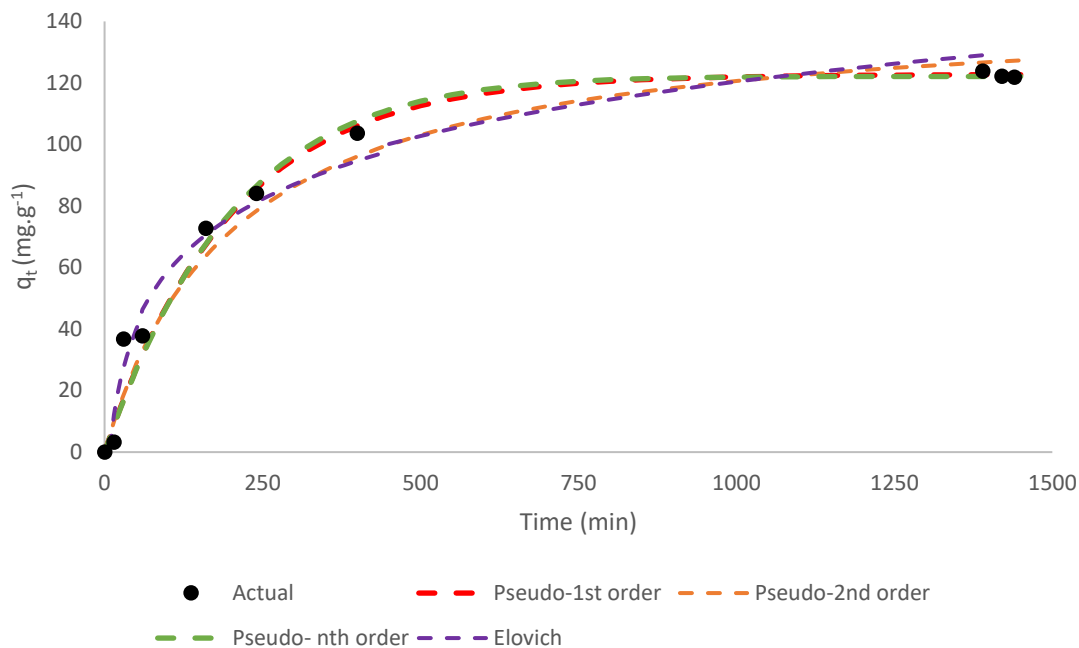


Figure 81 Kinetic model results for adsorption experiment performed on 3,7-DMO single component system at 25 °C and an initial concentration of 2 mass percentage.

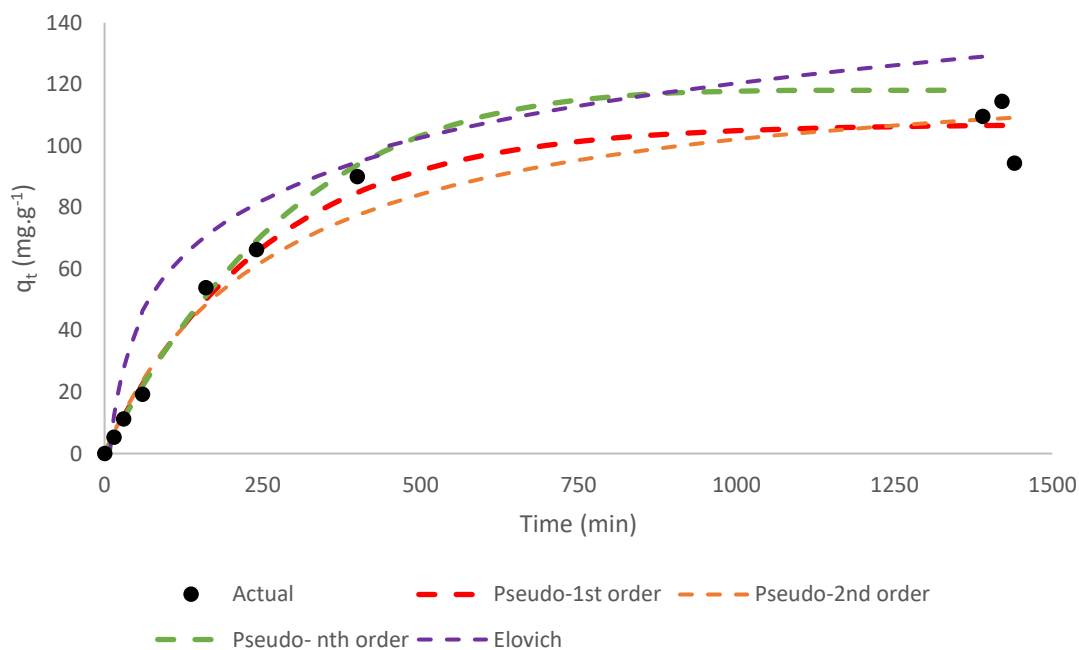


Figure 82 Kinetic model results for adsorption experiment performed on 3,7-DMO single component system at 25 °C and an initial concentration of 3 mass percentage.

D.1.2 Temperature of 35 °C

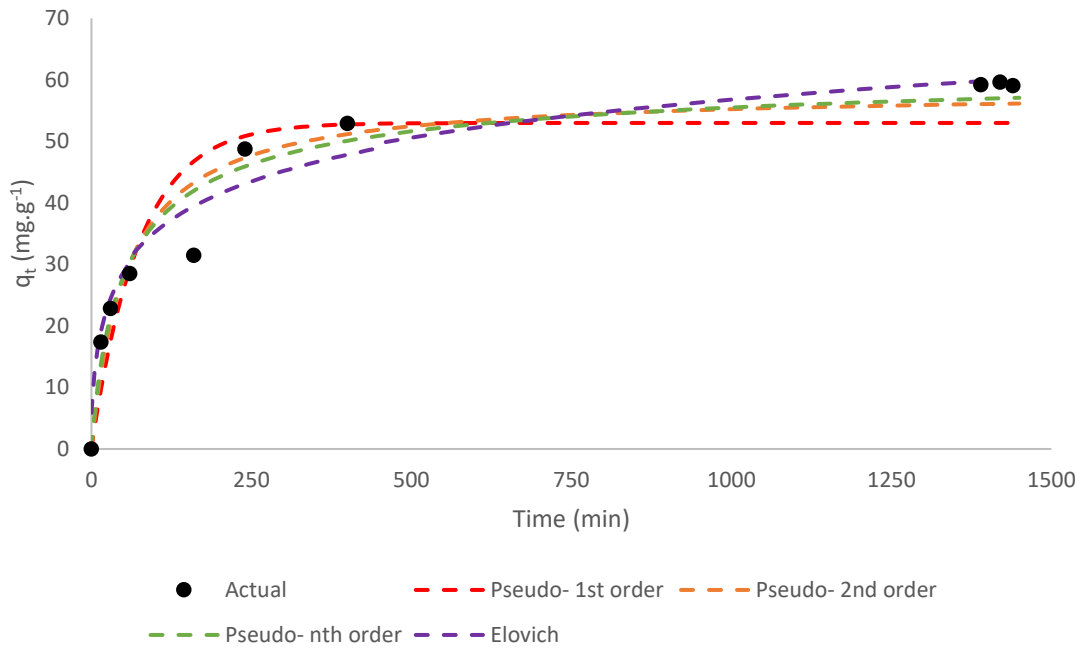


Figure 83 Kinetic model of single component 3,7-DMO system operated at 35 °C and an initial concentration of 0.47 mass percentage.

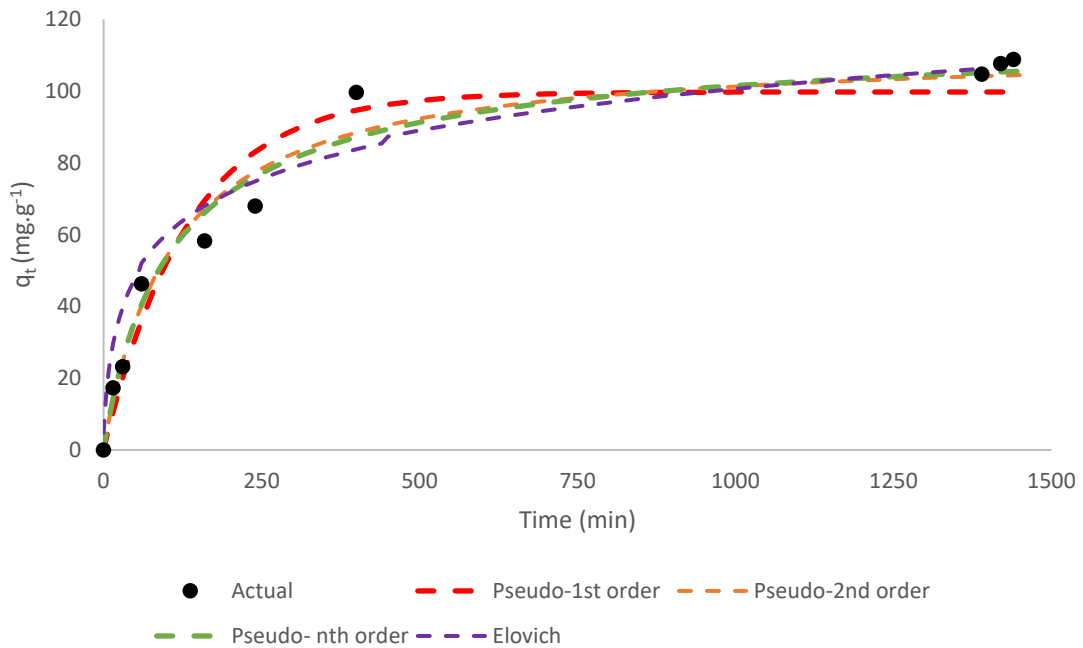


Figure 84 Kinetic model of single component 3,7-DMO system operated at 35 °C and an initial concentration of 1.51 mass percentage.

D.1.3 Temperature of 45 °C

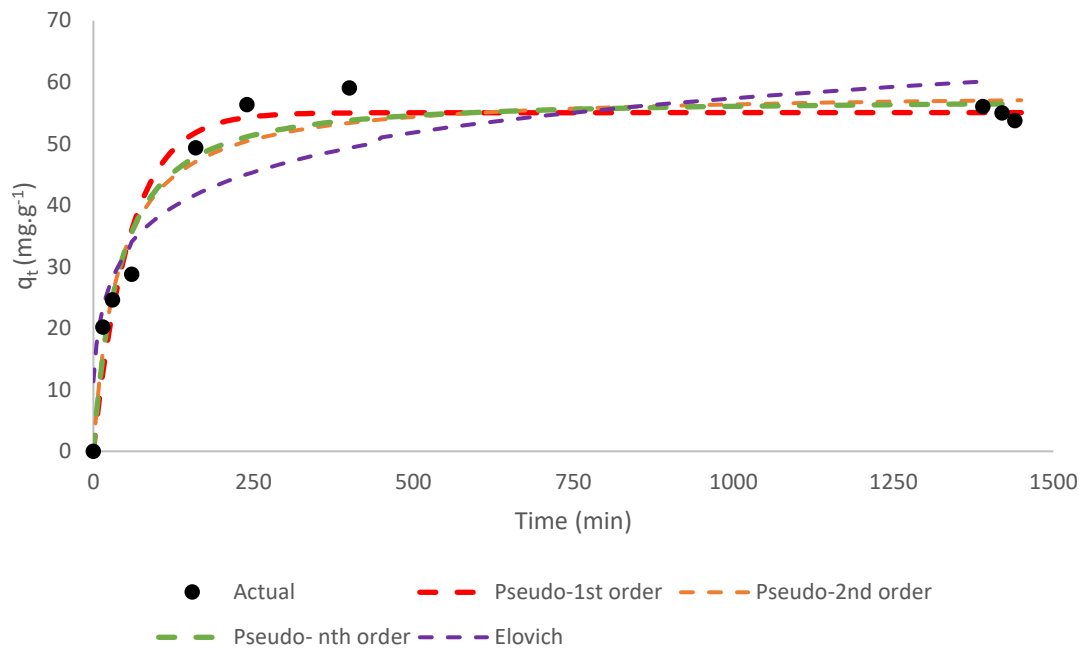


Figure 85 Kinetic model of single component 3,7-DMO system operated at 45 °C and an initial concentration of 0.50 mass percentage.

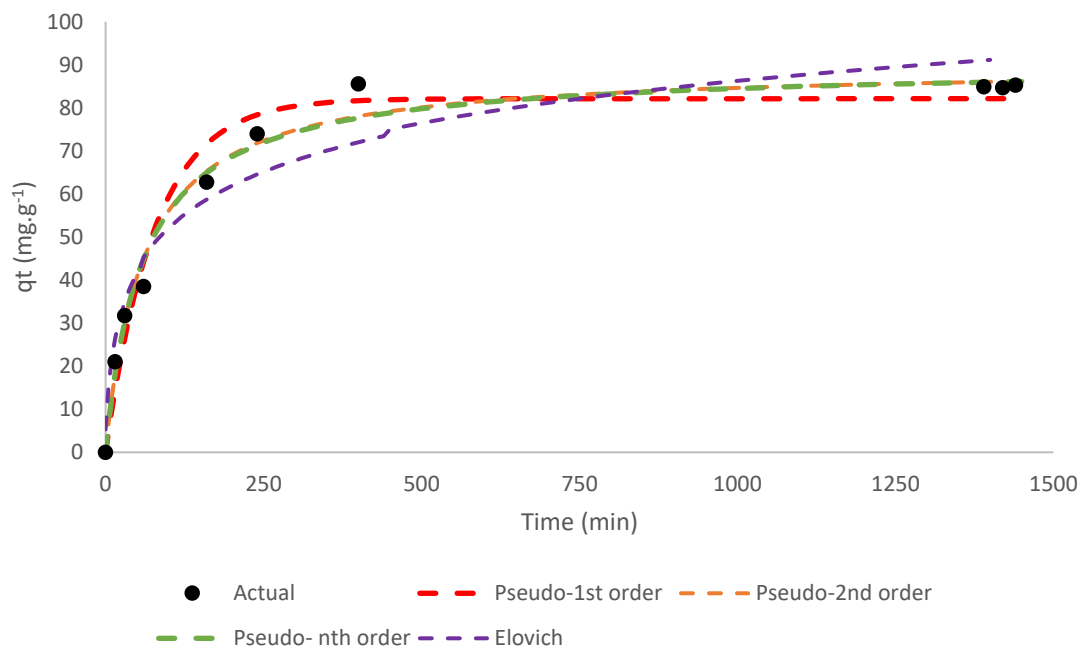


Figure 86 Kinetic model of single component 3,7-DMO system operated at 45 °C and an initial concentration of 1.52 mass percentage.